

Effect of carbonation on leachability and compressive strength of cement-solidified and geopolymersolidified synthetic metal wastes

by:

Bhishan Pandey

A thesis
presented to Lakehead University
in fulfillment of the
thesis requirement for the degree of
Master of Science
In
Environmental Engineering

Thunder Bay, Ontario, Canada, 2011

I hereby declare that I am the sole author of this thesis. This is the true copy of the thesis,
including any required final revisions, as accepted by my examiners.

I understand that my thesis may be made electronically available to the public.

Abstract

Stabilization/solidification (s/s) is a well-established technique for treating a variety of metal-containing hazardous waste streams prior to land disposal. Solidification refers to the improvement of the physical properties of the waste for easier handling, whereas stabilization refers to the reduction of contaminant mobility by various mechanisms such as precipitation, encapsulation, adsorption, and ion substitution. The s/s process consists of mixing the contaminants with binders and curing them over a period of time. At the disposal site, environmental carbon dioxide affects the s/s waste by a process known as carbonation. Carbonation brings about physical and chemical changes to the s/s waste. Thus, the study of the effect of carbonation on the s/s waste is important for assessing the long-term effectiveness of the s/s treatment process.

This research investigated the effect of carbonation on the leachability of toxic metals and the compressive strength of cement-solidified and geopolymers-solidified synthetic metal wastes. Synthetic sludges containing 0.1M copper nitrate, 0.1M lead nitrate, 0.1M chromium chloride, 0.1M zinc nitrate, 0.05M potassium dichromate and 0.1M cadmium chloride were mixed with ordinary portland cement (OPC) and fly-ash based geopolymers. After curing, the samples were crushed and subjected to accelerated carbonation for 21 days. Metal leachabilities were evaluated by the Toxicity Characteristic Leaching Procedure (TCLP) and the Synthetic Precipitation Leaching Procedure (SPLP) on both carbonated and non-carbonated samples. The compressive strengths of carbonated and non-carbonated monolith samples were compared. The effect of carbonation on microstructure and micromineralogy of cement and geopolymers samples

was investigated by scanning electron microscopy (SEM) and energy dispersive spectrometry (EDS).

Cement was effective at immobilizing Cd, Cr(III), Cu, Pb and Zn under both the SPLP and the TCLP, but ineffective for retaining Cr(VI). Carbonated cement maintained its ability to immobilize Cd, Cr(III), Pb and Zn, but, under acidic TCLP conditions, was much worse at retaining Cu. Geopolymer was effective at immobilizing Cr(III) and Cu, and, to a lesser degree, Cd, Pb and Zn in SPLP leaching tests. Only Cr(III) was immobilized under comparatively acidic TCLP testing conditions. Carbonation did not change the metal retention capacity of the geopolymer matrix. Metal doping caused compressive strengths of both geopolymer and cement to decrease. Carbonation increased the compressive strength of cement, but decreased that of the geopolymer. Geochemical equilibrium modeling provided insight on the mechanisms of metal immobilization. SEM-EDS analyses were not conclusive on the effect of carbonation on the fixation of metals in both cement and geopolymer samples because metals concentrations were generally below the EDS detection limit.

Acknowledgements

First and foremost, I want to thank my supervisor, Dr. Lionel J.J. Catalan. It has been an honor to be his M.Sc. student. His wisdom, I believe, has made the past few years a period of great professional growth. I appreciate all his contributions of his time, ideas and funding to make my M.Sc. experience productive and stimulating. I am certain my time under his supervision has been life-changing.

I gratefully acknowledge Dr. Stephen D. Kinrade, my co-supervisor, for his advice, supervision and crucial contribution to this research. He was instrumental in the completion of this thesis.

I would like to thank Mr. Ain Raitsakas for analysing the ICP samples for this research. To Mr. Allan MacKenzie and Dr. Shannon Zurevinski, I would like to express my gratitude for training me to operate the SEM. I would like to acknowledge Ms. Anne Hammond's excellent work preparing the SEM slides.

I would like to thank my colleagues Andrea Johnson, Hassan HajiEsmaeili and Ricardo Herrera for their help during this period.

I would also like to thank my family for playing an instrumental part in my education. Their patience, support and sacrifices are greatly appreciated.

Table of Contents

Declaration	ii
Abstract	iii
Acknowledgements	v
Table of Contents	vi
List of Figures	x
List of Tables	xii
Glossary	xiv
1. Introduction	1
2. Literature Review	2
2.1. Solidification/Stabilization	2
2.2. Portland Cement	6
2.2.1. Composition and Manufacture	6
2.2.2. Hydration	8
2.3. Cement Based S/S	11
2.3.1. S/S of Metal Wastes	12
2.3.1.1. Arsenic	14
2.3.1.2. Cadmium	15
2.3.1.3. Chromium (III)	16
2.3.1.4. Chromium (VI)	17

2.3.1.5. Copper	17
2.3.1.6. Nickel	18
2.3.1.7. Lead	18
2.3.1.8. Zinc	18
2.4. Geopolymers	19
2.4.1. Geopolymerization	20
2.4.2. Chemistry of Geopolymers	20
2.4.3. Structural Characteristics of Geopolymers	23
2.4.4. Compressive Strength of Geopolymer	24
2.4.5. S/S of Metal Wastes	25
2.5. Standard Testing Methods	27
2.5.1. Permeability (Hydraulic Conductivity) Testing	27
2.5.2. Compressive Strength Testing	27
2.5.3. Freezing and Thawing Testing	28
2.5.4. Leaching Tests	28
2.5.4.1. Toxicity Characteristic Leaching Procedure (TCLP)	29
2.5.4.2. Synthetic Precipitation Leaching Procedure (SPLP)	29
2.5.4.3. Flow Through Leaching Test	30
2.6. Cement-based S/S Waste in the Environment	33
2.6.1. Carbonation	34
2.6.1.1. Effect of Carbonation on Leachability	37
2.6.1.2. Effect of Carbonation on Strength	38
2.7. Carbonation of Geopolymer Based S/S	38

2.8. Research Opportunities	39
2.9. Research Objectives	40
3. Materials and Methods	41
3.1. Materials	41
3.1.1. Fly Ash	41
3.1.2. Cement	43
3.1.3. Sand	43
3.1.4. Mixing Water	44
3.1.5. Metal Salts and NaOH Solution	45
3.1.6. Sodium Silicate Solution	45
3.2. Methods	46
3.2.1. Mortar Preparation	46
3.2.2. Carbonation	48
3.2.3. Compressive Strength Testing	49
3.2.4. Leaching Tests	50
3.2.5. Microstructure and Micro-mineralogy Study	51
3.2.6. Geochemical Equilibrium Modeling of the Leachates	52
4. Results and Discussion	54
4.1. Leachability of Metals	54
4.2. Compressive Strength	71
4.3. Microstructure and Micro-mineralogy Study	73
5. Conclusion	80
6. Future Research	81

7. References	82
Appendix I	101
Appendix II	110
Appendix III	195

List of Figures

Figure 2-1	Technologies selected for source control treatment at Superfund remedial action sites	4
Figure 2-2	Solidification-Stabilization in situ schematic	6
Figure 2-3	Schematic models for the hydration and setting of portland cement. (a) Gel model (b) crystal model	11
Figure 2-4	Calculated solubilities of metal hydroxides at different pH	14
Figure 2-5	Cadmium solubility and TCLP data. Diamond: cadmium (2 days); triangle: cadmium (370 days); solid line: cadmium Solubility	16
Figure 2-6	Conceptual model for geopolymmerization	23
Figure 2-7	Percentage of toxic metals locked in geopolymeric matrix	26
Figure 2-8	Schematic of a packed column apparatus	31
Figure 2-9	Triaxial Cell Construction	32
Figure 2-10	Schematic of carbonation process	34
Figure 2-11	Proposed mechanism for accelerated carbonation	36
Figure 3-1	Fly Ash	42
Figure 3-2	Ordinary Portland Cement Type I manufactured by Lafarge	43
Figure 3-3	ASTM 20-30 sand manufactured by U.S. Silica Company	44
Figure 3-4	NANOpure Diamond, Barnstead D11911	45
Figure 3-5	Hobart 5-quart mixer	47
Figure 3-6	Cubes of cement and geopolymer were cut into eight sub-cubes (a), and the depth of carbonation measured at six locations for each sub-cube (b)	49

Figure 4-1	Leachate Cd concentration and calculated mineral solubilities as a function of pH	59
Figure 4-2	Leachate Cr(III) concentration and calculated mineral solubilities as a function of pH	61
Figure 4-3	Leachate Cr(VI) concentration and calculated mineral solubilities as a function of pH	63
Figure 4-4	Leachate Cu concentration and calculated mineral solubilities as a function of pH	65
Figure 4-5	Leachate Pb concentration and calculated mineral solubilities as a function of pH	67
Figure 4-6	Leachate Zn concentration and calculated mineral solubilities as a function of pH	69
Figure 4-7	Non-carbonated cement sample under SEM showing different phases	75
Figure 4-8	Carbonated cement sample under SEM showing different phases	75
Figure 4-9	Non-carbonated and carbonated (left to right) geopolymer samples under SEM showing the geopolymer matrix between sand grains	77
Figure 4-10	Non-carbonated geopolymer matrix in between sand grains	78
Figure 4-11	Carbonated geopolymer matrix in between sand grains	78

List of Tables

Table 2-1	Typical composition of portland cement in mass %	7
Table 2-2	Properties of major clinker phases	8
Table 2-3	Some past and present applications of cement-based s/s	12
	techniques to industrial wastes	
Table 2-4	Different Leaching Procedures	33
Table 3-1	Bulk composition of Atikokan fly ash	41
Table 3-2	Trace metal content of Atikokan fly ash	42
Table 3-3	Particle size distribution of ASTM 20/30 sand	44
	manufactured by U.S. Silica Company	
Table 3-4	Geopolymer composition	48
Table 4-1	TCLP and SPLP leaching results for carbonated and	55
	non-carbonated samples of metal-doped cement	
Table 4-2	Matrices that immobilize metals under SPLP and TCLP	56
	leaching conditions	
Table 4-3	Effect of carbonation on metal leachability from cement and	56
	geopolymer matrices	

Table 4-4	TCLP and SPLP leaching results for carbonated and non-carbonated samples of metal-doped geopolymers	57
Table 4-5	Phases controlling metal immobility in cement and geopolymers	70
Table 4-6	Aluminum concentration in TCLP and SPLP leachates for carbonated and non-carbonated geopolymers	71
Table 4-7	Compressive strength and extent of carbonation at 24 days for sample cubes of metal-doped cement and geopolymers	72
Table 4-8	Elemental composition of CSH, Ca(OH) ₂ and CaCO ₃ phases of carbonated and non-carbonated cement samples	79
Table 4-9	Elemental composition of the geopolymers matrix of carbonated and non-carbonated geopolymers	79

Glossary

Components of Ordinary Portland Cement

Tricalcium silicate	Ca_3SiO_5
Dicalcium silicate	Ca_2SiO_4
Tricalcium aluminate	$\text{Ca}_3\text{Al}_2\text{O}_6$
Calcium alumino ferrite	$\text{Ca}_2\text{AlFeO}_5$
Anhydrite or Gypsum	CaSO_4 , $\text{CaSO}_4 \cdot 2\text{H}_2\text{O}$
Periclase	MgO
Free lime	CaO

Components of Hydrated Ordinary Portland Cement

C-S-H	$x\text{CaO} \cdot \text{SiO}_2 \cdot n\text{H}_2\text{O}$
Portlandite	$\text{Ca}(\text{OH})_2$
Ettringite	$\text{Ca}_6\text{Al}_2\text{O}_6(\text{SO}_4)_3 \cdot 32\text{H}_2\text{O}$
Gypsum	$\text{CaSO}_4 \cdot 2\text{H}_2\text{O}$
Hydrogarnet	$\text{Ca}_3\text{Al}_2\text{O}_6 \cdot 6\text{H}_2\text{O}$

Other Terms

ASTM	American Society for Testing and Materials
------	--

ICP-AES	Inductively Coupled Plasma-Atomic Emission Spectroscopy
L/S	Liquid to Solid Ratio
NMR	Nuclear Magnetic Resonance
OPC	Ordinary Portland Cement
Pozzolan	High silica cement additive
RCRA	Resource Conservation and Recovery Act
SEM-EDS	Scanning Electron Microscope-Energy Dispersive Spectroscopy
SPLP	Synthetic Precipitation Leaching Procedure
S/S	Solidification/stabilization
TCLP	Toxicity Characteristic Leaching Procedure
USEPA	United States Environmental Protection Agency
w/c	Water/cement ratio
XAFS	X-ray Absorption Fine Structure Spectrometry

1. Introduction

Stabilization/solidification (s/s) is a well established technique for treating a variety of metal-containing hazardous waste streams prior to land disposal, including solutions, slurries, sludges, contaminated soils, dust and other particulate matter. In the s/s process, waste is mixed with a binder to decrease the mobility of the contaminant metals through mechanisms such as metal hydroxide precipitation, ion adsorption/substitution by hydration products, and physical encapsulation (Chen *et al.*, 2009a; Conner and Hoeffner, 1998b; Gougar *et al.*, 1996; Malviya and Chaudhary, 2006). Although OPC is the most commonly used s/s binder, geopolymers have also received recent attention (*e.g.*, Luna *et al.*, 2011; Pereira *et al.*, 2009; Zhang *et al.*, 2008). The term geopolymer refers to a synthetic alkali aluminosilicate produced by the activation of aluminosilicate particles with a concentrated alkaline solution (*e.g.*, sodium hydroxide, sodium silicate) (Davidovits, 1989; Davidovits, 1991). Fly-ash, blast furnace slag and metakaolin are among the most commonly used aluminosilicate solids. Geopolymers have been reported to exhibit better chemical and physical properties than cement for certain s/s applications, including diminished leachability of the treated waste metals, lower permeability, improved resistance to chloride attack, and higher compressive strength (Nugteren *et al.*, 2009; Pereira *et al.*, 2009; Shi & Fernandez-Jimenez, 2006; Zhang *et al.*, 2010).

Carbonation of s/s-treated waste by atmospheric carbon dioxide in the disposal environment results in physical and chemical transformations that can affect the long-term effectiveness of the s/s process (Garrabrants *et al.*, 2004; Klich *et al.*, 1999; Malviya and Chaudhary, 2006; Van Gerven *et al.*, 2006). Previous reports on the effects of carbonation on metal leachability from cement-stabilized wastes are contradictory, with the discrepancies being attributable to differences in waste characteristics, degree of carbonation and leaching test procedures that were employed (Alba *et al.*, 2001; Chen *et al.*, 2009a, 2009b; Johnson *et al.*, 2003; Lange *et al.*, 1996, 1997; Sanchez *et al.*, 2002; Walton *et al.*, 1997). Additionally, metal solubility is affected by the nature and concentration of

accompanying solute species through complexation, common-ion effect, ionic strength and/or redox potential (Chen *et al.*, 2009b). At this time, little is known about how carbonation affects metal immobilization by geopolymmer matrices. Luna *et al.* (2009) reported the effects of carbonation on leachability of lead, cadmium, total chromium and zinc from electric arc furnace dust that was stabilized in geopolymers made from different proportions of fly ash, blast furnace slag, metakaolin and potassium silicate. The effect varied for each metal in question and depended strongly on the composition of the geopolymers as well as on the conditions of the leaching test. No studies have yet been reported on how carbonation influences the effectiveness of geopolymers for s/s treatment of metals that are introduced as soluble salts or alkaline sludges typical of normal industrial/mining wastes.

In this work, the effects of carbonation on metal leachability and compressive strength were compared for ordinary portland cement (OPC) and a simple, fly ash-based geopolymers that were doped with synthetic alkaline waste sludge containing cadmium (II), chromium (III), chromium (VI), copper (II), lead (II) or zinc (II). In contrast to prior studies, the effects were determined for each metal individually at a uniform dosage of $0.029 \text{ mol kg}^{-1}$. Additional insight on the mechanisms of metal immobilization was achieved by comparing the leaching test findings with solubilities predicted from geochemical equilibrium modeling. Micro-structural changes in the carbonated s/s samples were studied using Scanning Electron Microscope - Energy Dispersive X-Ray spectroscopy (SEM-EDS).

2. Literature Review

2.1. Solidification/Stabilization

Solidification/Stabilization (s/s), a pre-landfill waste treatment process, has been accepted as one of the important methods for the treatment of hazardous and other wastes from metal industries, mining industries, petrochemical industries, inorganic chemical industries, incinerator

ash, municipal sewage, and others (Conner and Hoeffner, 1998b; Coolier *et al.*, 2006; Ligia *et al.*, 2004; Sophia and Swaminathan, 2005). Solidification refers to the encapsulation of the waste in a solid form to increase its structural integrity and thus prevents its exposure to the environment. Solidification involves complex chemical processes like the hydration reactions of cement or pozzolanic materials. Stabilization means the process which reduces the risk possessed by the waste to the environment by changing the waste into less soluble, mobile or toxic forms. Stabilization generally involves chemical processes (Poon *et al.*, 2004). Stabilization of metals is achieved by converting the metals into insoluble precipitates, or by the interaction (e.g., sorption and ion substitution) between metallic ions and cement hydration products such as ettringite and calcium silicate hydrate gel (Gougar *et al.*, 1996; Malviya and Chaudhary, 2006; Chen *et al.*, 2009b).

The wide use of s/s in waste treatment is due to the (a) availability of solidifying materials like lime and cement on a worldwide basis, (b) low cost, (c) ability to adjust the mixture for different wastes, and (d) high physical strength. The US Environmental Agency has identified s/s as the best demonstrated available technology for 57 RCRA (Resource Conservation and Recovery Act)-listed hazardous wastes, and s/s technology was selected in 24% of all source control treatments at Superfund remedial action sites in the United States (USEPA, 2004). Figure 2-1 shows the use of different technologies for source control treatment at Superfund remedial sites (USEPA, 2004). In Canada also, s/s has been selected in some major projects such as the Sydney Tar Ponds, Nova Scotia; Dockside Green Harbour, Victoria; Zinc Plating Plant, Vancouver; Rifle Range, Burnaby; Battery Breaking Site, Manitoba; and others (Paria and Yuet, 2006).

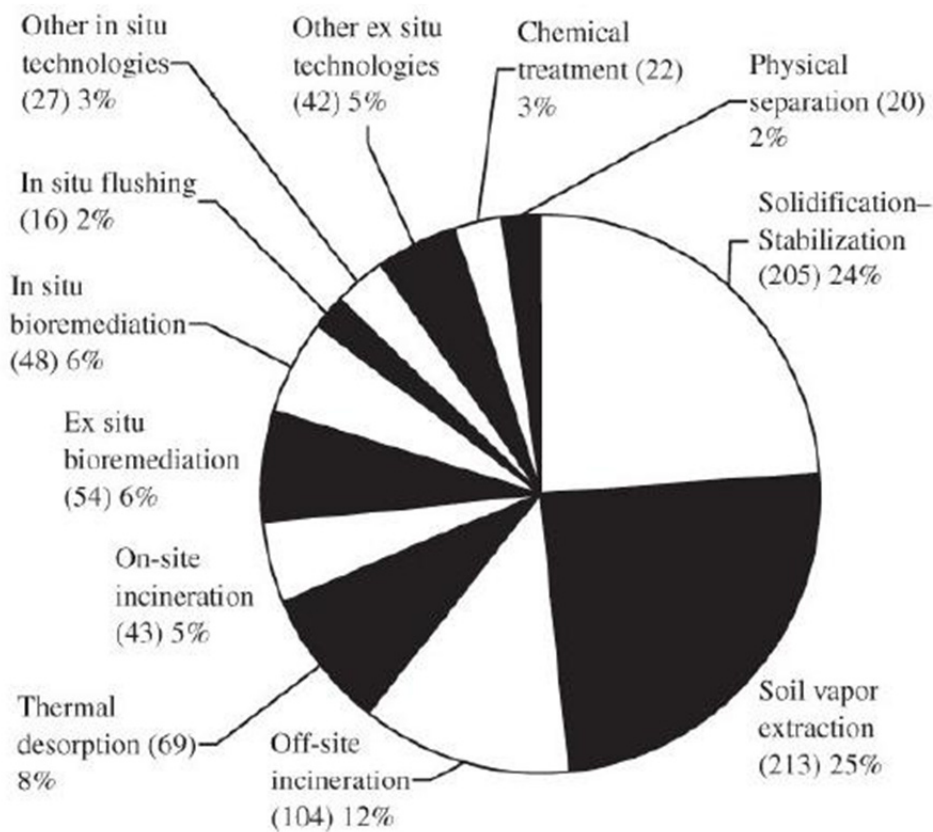


Fig. 2-1 Technologies selected for source control treatment at Superfund remedial action sites (USEPA, 2004)

Different types of s/s processes are developed and used in the field for waste treatment. Some of the commonly used processes are cement-based, pozzolan-based, and lime-based processes (Batchelor, 2006; Erdem and Özverdi, 2011). Of these processes, the portland cement based process has been the most widely used s/s process for more than 50 years because (a) it is cheap, (b) it is easy to use and process, (c) the reactions occurring in the cement while setting, hardening, and metal fixation are known, (d) it has good long-term stability, both physical and chemical, (e) it has good impact and compressive strength, (f) it has non-toxic chemical ingredients, (g) it has high resistance to biodegradation, (h) it has relatively low water permeability, and (e) regardless of the source, the composition of cement is same (Conner, 1990; Conner and Hoeffner,

1998a; Alba *et al.*, 2001; Shi and Spence, 2004; Malviya and Chaudhary, 2006). “Cement” generally refers to “Portland Cement” unless otherwise specified.

Recently, as a substitute for cement, geopolymeric materials have been investigated as a material for stabilizing various toxic and radioactive wastes (Van Deventer *et al.*, 2007; Milestone, 2006; Deja, 2002b; Palomo and Palacios, 2003). Geopolymeric materials are synthesized by alkaline activation of an aluminosilicate source, such as fly-ash, forming a compact gel binder phase (Duxson *et al.*, 2007). Because of its low permeability, resistance to acid attack and durability, the geopolymeric matrix provides an ideal binder for the immobilization of toxic wastes (Van Jaarsveld and Van Deventer, 1999a; Lee and Van Deventer, 2002; Duxson *et al.*, 2007). In certain situations where portland cement experiences problems, like chloride attack and freeze-thaw degradation, geopolymers have been found to fare better (Shi *et al.*, 2006).

In the field, s/s processes can be applied using different techniques (Conner and Hoeffner, 1998b):

- In-drum processing: s/s binder is added to the waste in a drum and is disposed off after setting.
- In-plant processing: a plant is specifically designed to solidify and stabilise bulk waste materials usually from a single or similar source.
- Mobile plant (ex situ) processing: mobile processing equipment is used wherever needed.
- In-situ processing: in this process, binder is directly mixed with the waste in in-situ condition (Fig. 2-2).

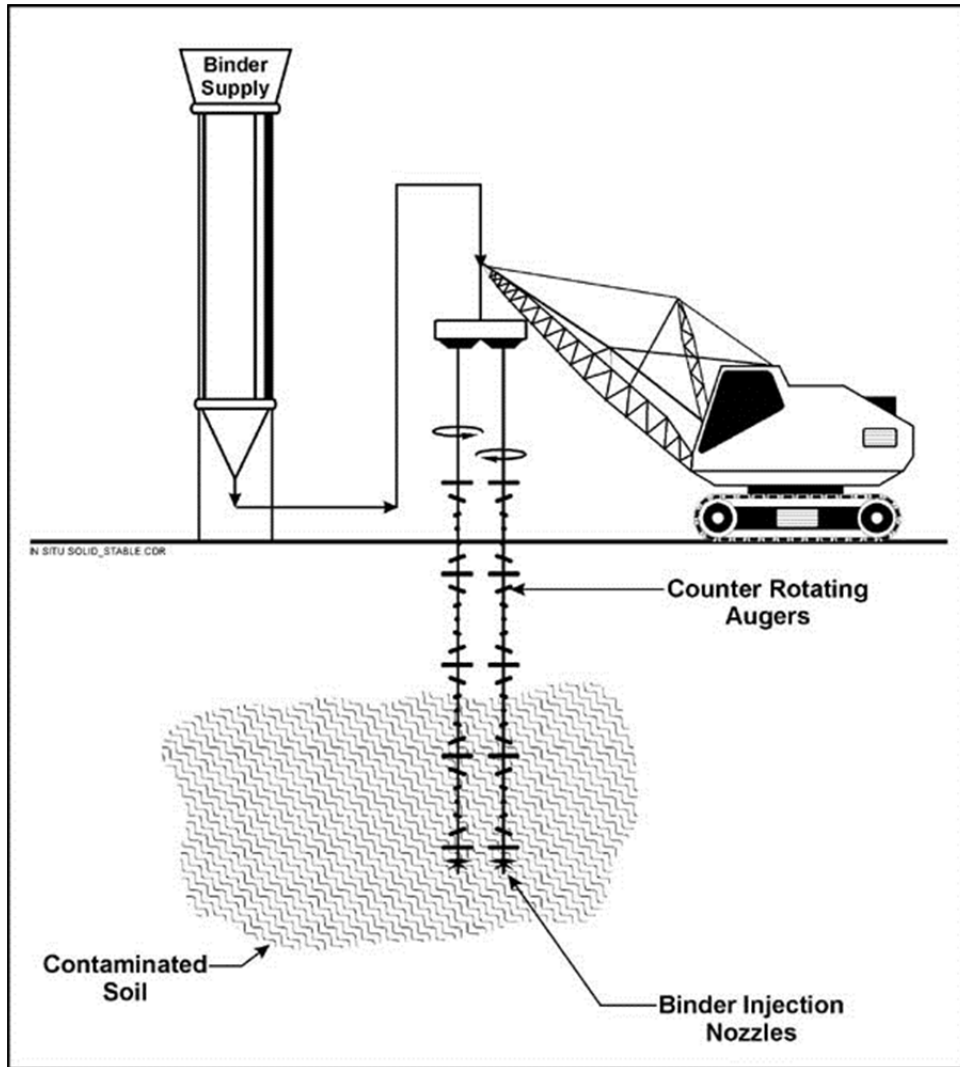


Fig. 2-2 Solidification-Stabilization in situ schematic (USEPA, 2001)

2.2. Portland Cement

2.2.1. Composition and Manufacture

In the cement manufacturing process, first the mixture of limestone (70%) and clay (30%) or other aluminosilicate materials is heated at a temperature of around 1450°C for 10 to 15 minutes, which results in partial fusion of the materials to form 3 to 20 mm nodules called clinker (Kosmatka *et al.*, 2002). Then, cement is formed by grinding the clinker with gypsum to a fine powder (Blasing and Hand, 2007). The clinker is mixed with gypsum to delay the initial

setting time (Paria and Yuet, 2006). The main crystalline phases in clinker are tricalcium silicate (Ca_3SiO_5 or C_3S), dicalcium silicate (Ca_2SiO_4 or C_2S), tricalcium aluminate ($\text{Ca}_3\text{Al}_2\text{O}_6$ or C_3A), and calcium alumino ferrite ($\text{Ca}_2\text{AlFeO}_5$ or C_4AF). In cement, the C/S (CaO/SiO_2) molar ratio is around 1.75 (Zhang *et al.*, 2000). Tricalcium silicate, dicalcium silicate, tricalcium aluminate, and calcium alumino ferrite constitute 50-70%, 15-30%, 5-10%, and 5-15% of the clinker mass, respectively (Gougar *et al.*, 1996). Tricalcium silicate is a solid solution of CaO in dicalcium silicate having the formula $\text{Ca}_2\text{SiO}_4 \cdot \text{CaO}$. Dicalcium silicate has more rounded grains than tricalcium silicate, and is darker when observed by optical microscopy in thin sections. Periclase (MgO), free lime (CaO), anhydrite (CaSO_4) or gypsum ($\text{CaSO}_4 \cdot \text{H}_2\text{O}$) – additives that slow OPC setting and alkali sulphates (Na_2SO_4 and K_2SO_4) are minor phases, usually less than 1 mass % (Taylor, 1997). The typical composition of Portland cement is given in Table 2-1, and the properties of different phases in cement are given in Table 2-2.

Table 2-1 Typical composition of portland cement in mass % (Lawrence, 1998)

Components	Minimum (%)	Average (%)	Maximum (%)
SiO_2	18.4	21.02	24.5
Fe_2O_3	0.16	2.85	5.78
Al_2O_3	3.1	5.04	7.56
CaO	58.1	64.18	68
MgO	0.02	1.67	7.1
Na_2O	0	0.24	0.78
K_2O	0.04	0.7	1.66
SO_3	0	2.58	5.35
Free Lime	0.03	1.24	3.68
Chloride	0	0.016	0.047

Table 2-2 Properties of major clinker phases (Dalton *et al.*, 2004)

Mineral Phase	Properties in cement
Tricalcium silicate	Rapid hydration, high initial and final strength
Dicalcium silicate	Slow hydration, good final strength, low heat of hydration
Tricalcium aluminate	Rapid hydration, high heat of hydration
Calcium alumino ferrite	Slow and moderate hydration, moderate heat of hydration

2.2.2. Hydration

In the solidification of cement, water is added to the cement powder to form hydrate phases. The hydration process is a complex, exothermic process which leads to the formation of hydrate phases of the constituents of the cements, along with the formation of new compounds.

The presence of CaO in the tricalcium silicate structure provides a favoured site for water attack. Tricalcium silicate reacts with water to form calcium silicate hydrate gel (C-S-H) and portlandite (CH, Ca(OH)₂). In the notation C-S-H, C represents CaO, S represents SiO₂, H represents H₂O, and the dashes represent an unspecified composition. The hydration of tricalcium silicate usually controls the setting and early strength development of portland cement pastes, mortars, and concretes. Equation (2-1) represents the hydrolysis of tricalcium silicate.



The hydrolysis reaction of dicalcium silicate, resulting in the formation of C-S-H gel and portlandite, is relatively slower than that of tricalcium silicate. The compressive strengths of tricalcium silicate and dicalcium silicate, however, after a year of hydration are comparable. Equation (2-2) represents the hydrolysis of dicalcium silicate.



For tricalcium silicate and dicalcium silicate, the hydration amount in the first day is

about 10 and 15%, respectively.

Tricalcium aluminate and calcium alumino ferrite are the most reactive major phases. The hydration amount for them in one day is 70% or more. The rapid hydration of tricalcium aluminate and calcium alumino ferrite, which results in flash set, is not desirable (Taylor, 1997). However, the addition of anhydrite or gypsum causes ettringite ($3\text{CaO}\cdot\text{Al}_2\text{O}_3\cdot3\text{CaSO}_4\cdot32\text{H}_2\text{O}$) to form, which laminates tricalcium aluminate, retarding further hydration. This lamination constantly ruptures and forms again until gypsum in the surrounding solution depletes. This enables the control of strength and durability of the cement (Gougar *et al.*, 1996). The reaction of tricalcium aluminate phase with water in the presence of gypsum forming ettringite is shown in reaction (2-3).



The calcium alumino ferrite phase shows variable reactivity with water. The hydration products of calcium alumino ferrite phase are similar to that of tricalcium aluminate phase, but the reactions are relatively slower and there is a substitution of Fe^{3+} for Al^{3+} . Calcium alumino ferrite also reacts with gypsum in the presence of water to form ettringite.

Calcium Silicate Hydrate (C-S-H), a mixture of poorly crystallized particles with different morphologies, is the principal hydration product of portland cement, comprising approximately 50 wt% of the cement paste (Gougar *et al.*, 1996). Based on their morphology, the four types of C-S-H reported are: (a) fibrous, (b) reticular network, (c) equate grain morphology, and (d) inner product morphology (Taylor, 1997; Famy *et al.*, 2002). The fibrous type is dominant in the early hydration stages. Type (b) is also an early hydration product, and is known to form reticular or honeycomb like networks. Type (c) and (d) form in the late hydration stages, and are relatively larger than type (a) and (b) (Taylor, 1997). C-S-H gel is also classified as high density (HD) and low density (LD) C-S-H. The HD C-S-H forms near the

cement grain boundaries, whereas the LD C-S-H forms away from the cement grain boundaries, filling the pores (Jennings, 2000). The detailed structure of C-S-H is not completely known, but Taylor (1997) proposed that the structure is most similar to tobermorite.

The cement hydration and setting phenomena have been explained using two models, the gel (or osmotic) model and the crystalline model (Mollah *et al.*, 1995). According to the gel model, upon hydration a C-S-H gel membrane is formed on the surface of the cement particle. Due to the osmotic potential on both sides, this membrane allows the inward movement of water, and outward movement of Ca^{2+} and silicate ions. This results in the precipitation and accumulation of portlandite on the fluid side of the membrane. The excess of silicate ions on the grain side of the membrane will create enough osmotic pressure over time and pushes through and ruptures the membrane periodically. The crystal model assumes the formation of charged calcium and silicate ions upon contact with water. This forms a concentrated thin layer of silicate ions on the cement particle surface. This retards the further release of calcium and silicate ions. Then, the hexagonal crystals of calcium hydroxide start forming and fills up the spaces between the cement grains. Also, C-S-H particles precipitate onto the silicate-rich layer of the cement grains and forms needles like structures. All the different needles from different cement grains come in contact to form sheets of tobermorite. Figure 2-3 shows schematics for the gel and crystal model.

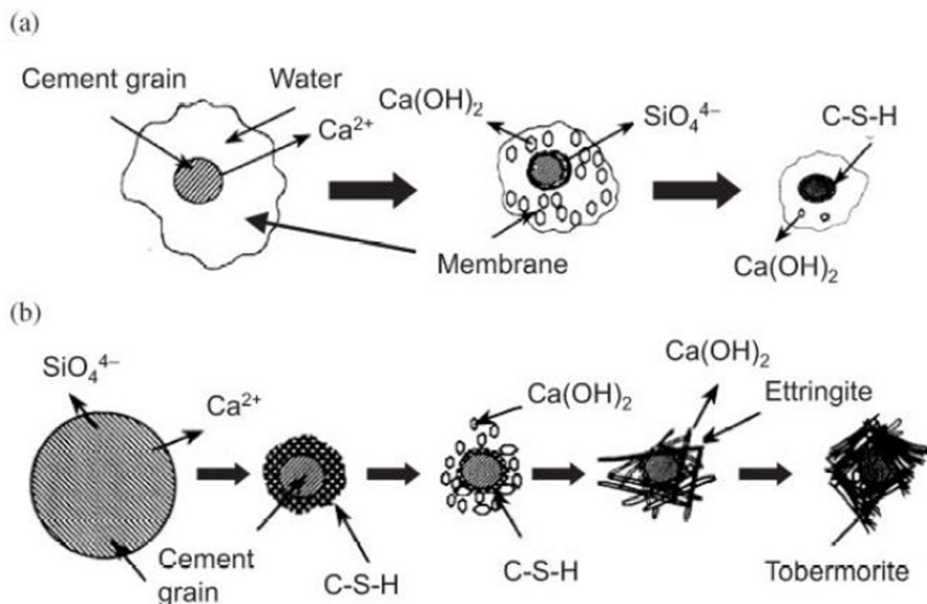


Fig. 2-3 Schematic models for the hydration and setting of portland cement. (a) Gel model (b) crystal model (Mollah et al., 1995)

2.3. Cement Based S/S

The cement based process is the most widely used s/s. It is usually preferred for treating liquids and sludges rich in heavy metals by precipitating the dissolved metals using alkaline and cementing agents (Catalan *et al.*, 2002). Application of s/s technology to organic wastes is found to be less successful than to metal containing wastes (Yilmaz *et al.*, 2003). In Canada, cement-based s/s is used by metal producing and processing industries for the treatment of sludges contaminated with heavy metals before land disposal (Seyer *et al.*, 2001; Catalan *et al.*, 2002). Some of the types of industrial wastes which have been treated by s/s cement-based process are shown in Table 2-3.

Table 2-3 Some past and present applications of cement-based s/s techniques to industrial wastes (Sollars et al., 1989)

Industry Type of waste	Pollutants
Electroplating Filter cakes/sludges	Cd, Cr, Pb, Cu, Ni, Zn, Cyanide
Galvanizing Filter cakes/sludges	Zn
Electrical component manufacture	Carbon, cyanide, Sn, Pb
Filter cakes/sludges	
Organic chemicals Liquids	Pb, Ti
Gas scrubbing Liquids	Alkaline sulphides
Petrochemical catalysts Solids	Co, Mo, Ni
Metal treatments Liquids	Cyanide, acids, alkalies, Zn, Mg, Ba
Pharmaceutical manufacture	Zn, Hg, Ba, Be
Filter	
Metal recovery plant Solids	Cu, Ni, Zn
Incineration wastes Solids	Mn, Fe, Pb, Zn, Fe
Acid Pickling Filter cakes/sludges	Acid, Cr, Zn, Fe
Aluminum finishing Filter	Alkalies, acids, Cr, Cu

2.3.1. S/S of Metal Wastes

Cement-based s/s has been used extensively with inorganic solid wastes containing heavy metals such as As, Cd, Cr, Cu, Ni, Pb, and Zn (Choi et al., 2009; Zhang et al., 2009), and numerous experimental modeling studies can be found in the literature (Islam *et al.*, 2004a, 2004b; Catalan *et al.*, 2002). Various types of waste ion interactions occur when waste ions are mixed with cement and water. Waste ions may be incorporated in cement by chemisorption, precipitation, surface compound formation, inclusions, chemical incorporation, or several of the above together. Sorption to surfaces and incorporation into cement minerals have been suggested as the main two mechanisms for metal uptake. Physical adsorption occurs when the contaminants present in the pore water are attracted to the surface of the particles because of their charge. Chemical adsorption, on the other hand, generally involves covalent bonding. These adsorption processes alter the binding capacity of cement gels for metals ions (Tamas *et*

al., 1992). Metals, during the hydration of cement, get adsorbed to the hydration products and alter their structure and solubility (Kitamura *et al.*, 2002). Ettringite is reported to immobilize heavy metals by substitution of Ca^{2+} , Al^{3+} , and SO_4^{2-} by metal ions (Gougar *et al.*, 1996). Chemical precipitation is also a dominant heavy metal immobilisation mechanism in cement-based s/s wastes. Some heavy metal compounds formed by chemical precipitation have amorphous structures and are not stable. Heavy metals can precipitate as hydroxides, carbonates, sulphates, and silicates. Hydroxides precipitate at an optimum pH of the solution. Different metals have different optimum pH for their hydroxide precipitation (Fig. 2-4). The variation of metal hydroxide solubility with pH is an important factor for the s/s process because the pore solution of hydrated cement paste is highly alkaline ($\text{pH} \approx 13$). Some metal carbonates are known to be more effective than corresponding metal hydroxides because of their low solubility (Asavapisit *et al.*, 1997). Kulik and Kersten (2001) reported that these heavy metal compounds generally precipitate readily on the surface of a solid rather than in the bulk solution.

Many researchers have reported that heavy metals are deleterious to the hydration reactions of cement and thus lower the s/s efficiency. Ca^{2+} has the highest efficiency of hydration acceleration (Kantro, 1975). Thus, inorganic compounds that form complexes with calcium act as hydration retarders.

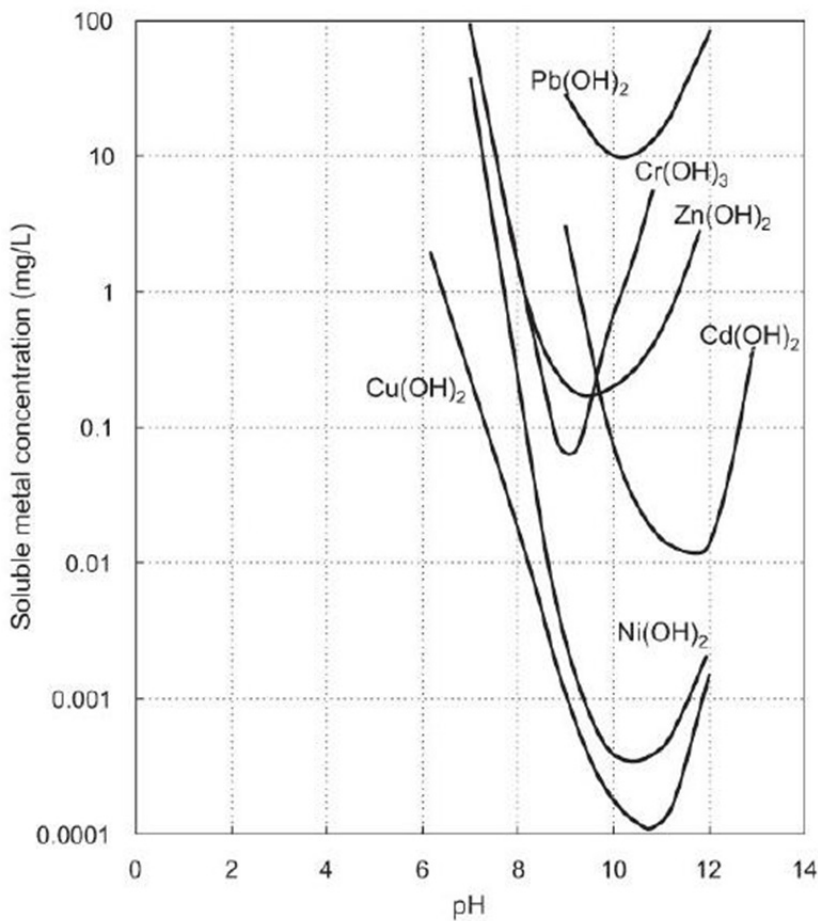


Fig. 2-4 Calculated solubilities of metal hydroxides at different pH (Cullinane *et al.*, 1986; Shi and Spence, 2004)

2.3.1.1. Arsenic

Arsenic is a toxic element and is a carcinogen to humans even in trace amounts (Karim, 2000). The USEPA reduced the maximum allowable concentration level (MCL) of arsenic in drinking water from 50 to 10 µg/L in January 2001 (Federal Register, 2001). As(III) and As(V) are the naturally occurring valence states of arsenic. As(III) is more mobile and 25-60 times more toxic than As(V) (Pantsar-Kallio and Manninen, 1997; Corwin *et al.*, 1999). Cement-based s/s technology currently provides the most promising solution for the disposal of arsenic wastes (Leist *et al.*, 2003). The main mechanism of

immobilization of As in solidified/stabilized contaminated soil is by the formation of $\text{Ca}_3(\text{AsO}_4)_2$ and CaHAsO_3 precipitates (Dutre *et al.*, 1999; Vandecasteele *et al.*, 2002). Since As(V) is easier to immobilize than As(III) with cement, many researchers have successfully oxidized As(III) to As(V) using H_2O_2 before s/s (Fuessle and Taylor, 2000; Vandecasteele *et al.*, 2002). It is also reported that arsenic can be chemically fixed into the cementitious environment of the s/s matrices by three important immobilization mechanisms, namely, sorption onto C-S-H surface, replacing SO_4^{2-} of ettringite, and reaction with cement components to form calcium arsenate compounds (Phenrat *et al.*, 2005). It is reported that the early hydration of cement is inhibited by the presence of AsO_4^{3-} , and that the inhibition is mainly caused by the formation of highly insoluble $\text{Ca}_3(\text{AsO}_4)_2$ on the surface of hydrating cement particles (Mollah *et al.*, 1998).

2.3.1.2. Cadmium

Due to its extensive use in steel plating, pigment stabilization, and nickel-cadmium battery industries, cadmium has become a pollutant of concern. Cadmium has been known to cause renal dysfunction and osteomalacia in humans (Burgatsacaze *et al.*, 1996). Fuessle and Taylor (2004) reported that the concentration of cadmium in the TCLP extracts increases with the increase in curing time (Fig. 2-5). This phenomenon has been attributed to pH variation. Other researchers also have reported the importance of pH (Halim *et al.*, 2004; Coz *et al.*, 2004). It has been reported that $\text{Cd}(\text{OH})_2$ precipitates were not homogenous in the cement matrix. Rather, they were found to be concentrated within the cement pores or adsorbed on the C-S-H matrix, with up to 30% concentration at various other locations (Paria and Yuet, 2006).

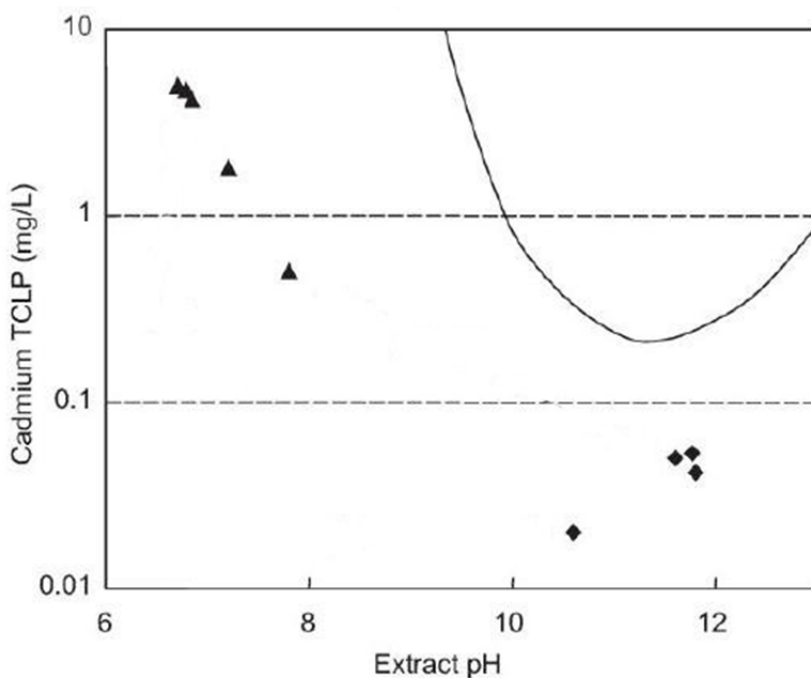


Fig. 2-5 Cadmium solubility and Toxicity Characteristic Leaching Procedure (TCLP) data. Diamond: cadmium (2 days); triangle: cadmium (370 days); solid line: cadmium solubility (Fuessle and Taylor, 2004)

2.3.1.3. Chromium (III)

Ettringite phase has been suggested to be involved in the stabilization of Cr(III) by the substitution with Al (Macias et al., 1997). Kindness *et al.* (1994) also reported that Cr(III) could be substituted for Al in most of the calcium aluminate hydrates forming $\text{Ca}_2\text{Cr}(\text{OH})_7 \cdot 3\text{H}_2\text{O}$, $\text{Ca}_2\text{Cr}_2\text{O}_5 \cdot 6\text{H}_2\text{O}$, and $\text{Ca}_2\text{Cr}_2\text{O}_5 \cdot 8\text{H}_2\text{O}$. Tashiro and Kawaguchi (1977) and Tashiro *et al.* (1977) reported that 10% or more of Cr_2O_3 (Cr(III)) could enter into solid solution with C-S-H. They suggested that 2Cr^{3+} substitutes both Ca^{2+} and Si^{4+} . Otomoso *et al.* (1995) concluded that the addition of chromium as Cr(III) accelerates the C_3S hydration. Also, Cr(III) improves the crystal growth of ettringite but reduces the strength of hardened ettringite (Katsioti *et al.*, 2005).

2.3.1.4. Chromium (VI)

Chromium (VI) compounds are highly soluble in basic environment. It is difficult, therefore, to apply cement-based s/s to this type of waste. Chromium (VI) is known to form Ca-Cr aluminates, $\text{Ca}_4\text{Al}_6\text{O}_{12}\text{CrO}_4$, and $\text{Ca}_6\text{Al}_4\text{Cr}_2\text{O}_5$ in the presence of cement phases (Stephan *et al.*, 1999). Ettringite phase has been suggested to be involved in the stabilization of Cr(VI) by the substitution of CrO_4^{2-} with SO_4^{2-} (Macias *et al.*, 1997). Mollah *et al.* (1992) confirmed the chemical interaction of chromium with C-S-H through EDS and FTIR examinations of Cr-OPC systems. However, no speculation as to the mechanism of Cr incorporation into the C-S-H was made. Otomoso *et al.* (1995) concluded that the addition of chromium as Cr(VI) shortens the C-S-H gel fibres formed at early ages and increases of the matrix porosity.

2.3.1.5. Copper

Due to its presence in fertilizers, pesticide sprays, building materials, rayon manufacture, agricultural and municipal wastes, and industrial emissions, the level of copper in soil has been a concern for the environment. S/s is known to safely stabilize copper containing waste (Zain *et al.*, 2004). The predominant stabilization mechanism for copper has been reported to be the precipitation reaction and is dependent on the pH of the leachant. For pH values higher than 7, copper hydroxide is the solubility controlling phase and for acidic conditions, attacamite ($\text{Cu}(\text{OH})_3\text{Cl}$) can be the solubility controlling phase (Polettini *et al.*, 2004).

2.3.1.6. Nickel

The s/s of nickel has been studied by several researchers (Fatta *et al.*, 2004; Fuessle and Taylor, 2004). Nickel is reported to retard the hydration of portland cement, although the final hydration products remain the same (Roy *et al.*, 1992). They suggested that the physical encapsulation of the metal hydroxide was reported to be the major stabilization mechanism.

2.3.1.7. Lead

Due to its extensive use in lead-zinc smelters, piping, insecticides, paints, and batteries, lead is a concern for the environment. The concentration of lead in the leachate of solidified stabilized waste has been reported to be dependent on the pH of the leachant (Halim *et al.*, 2003; Fuessle and Taylor, 2004). Between pH 9 and 11, almost all the lead present turns into insoluble lead hydroxide. At pH 12, lead forms amphoteric lead hydroxy ions, thus increasing the concentration of lead in the leachate again (Paria and Yuet, 2006). In addition to physical encapsulation, lead has also been reported to be immobilized by the formation of a new phase with Al and Si-rich species (Paria and Yuet, 2006). Halim *et al.* (2004), using X-ray analysis, report that lead is evenly distributed throughout the C-S-H of the cementitious matrix. It has been noted that lead ions retard the setting time of portland cement based materials by coating the cement particles with its insoluble salts, thus preventing hydration (Thomas *et al.*, 1981).

2.3.1.8. Zinc

The presence of zinc in the environment is attributed to the manufacture of brass and bronze alloys, galvanized products, cosmetics, pharmaceuticals, batteries, metal coatings,

glass, paint, and zinc-based alloys. Zinc is generally found as zinc chloride, zinc oxide, zinc sulfate, and zinc sulphide in the waste. Zinc precipitates mostly as zinc hydroxide at pH 8 (Mulligan *et al.*, 2001). The leaching of Zn is highly dependent on the pH of the leachate (Coz *et al.*, 2004). The hydroxy-complexes $Zn(OH)_4^{2-}$ and $Zn(OH)_5^{3-}$ can be present in a strong alkaline solution. Their anionic properties preclude their adsorption onto the negative surface of the C-S-H. Zinc is known to form hydrated complexes like $CaZn_2(OH)_6 \cdot H_2O$ (Yousuf *et al.*, 1992, Li *et al.*, 2001) and $Zn_4SiO_2O_7(OH)_2 \cdot H_2O$ (Ziegler *et al.*, 2001). These complexes may get adsorbed to C-S-H. Ziegler *et al.* (2001) found that Zn forms a solid solution with CSH using X-ray absorption fine structure (XAFS) spectrometry. However, it has been reported that zinc is immobilized by its precipitation as hydroxide and carbonate and no substitution in crystalline C-S-H form was found (Gougar *et al.*, 1996, Yousuf *et al.*, 1995). Gougar *et al.* (1996) reported substitution of calcium by zinc on ettringite minerals.

2.4. Geopolymers

Geopolymers are inorganic binders formed by the reaction between an alkaline solution and an aluminosilicate material. Hardened geopolymer is amorphous with a three-dimensional structure similar to that of aluminosilicate glass. The alkaline metal hydroxide/silicate solution needed to form a geopolymer is also referred as the chemical activator. The fine aluminosilicate material, which acts as the binder, needs to have considerable amount of silicon and aluminum ions in amorphous phase. Although fly ash, ground granulated slag and metakaolin are commonly used binders, any fine amorphous aluminosilicate material can be used. Geopolymer technology has been gaining popularity in mining, energy, construction and waste containment industries since it may help these industries address various sustainability issues currently experienced. Industrial by-products such as fly ash, bottom ash, ground granulated blast-furnace slags, bauxite processing

residues and kaolinitic clays used to be treated as waste but now can be used as a valuable ingredients for geopolymmer production. About 780 million tonnes of fly ash are produced each year (Hardjito *et al.*, 2004). Most of this ends up in landfills. This practice is costly and also will create problems to the environment in the long run. The most important benefit is the reduction of greenhouse gas emission in the concrete industry by substituting cement with geopolymers. Approximately 2.8 tons of raw materials, including fuel and other materials, are needed to produce one ton of portland cement. This process releases about 5 to 10% of dusts and about a ton of greenhouse gas CO₂ to the atmosphere (Buchwald and Schulz, 2005).

2.4.1. Geopolymerization

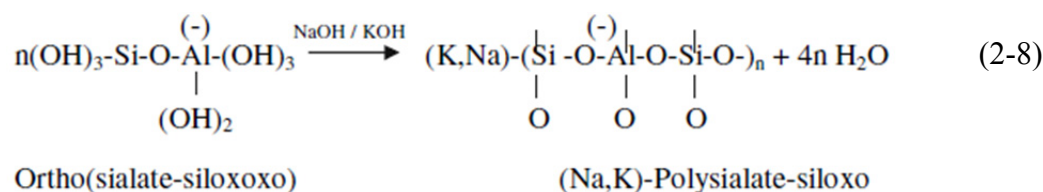
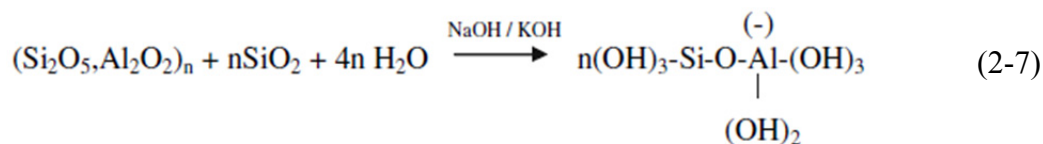
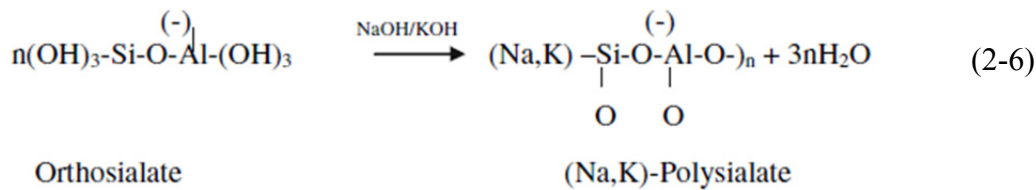
The process of geopolymers involves forming monomers in solution, then thermally triggering them to polymerise to form a solid. After mixing the binder with the alkaline solution, the silicon and aluminum ions from the binder dissolve in the alkaline solution. Then, the silicon and aluminum hydroxide ions undergo a condensation reaction where they form an oxygen bond between them, and a free molecule of water. Silicon and aluminum atoms react to form materials that are structurally and chemically similar to natural rocks (Hermann *et al.*, 1999). Then, under the application of heat, these monomers undergo polymerisation to form a matrix of oxygen bonded tetrahedrals, where the silica and aluminum tetrahedrals are interlinked alternately by sharing all the oxygen atoms.

2.4.2. Chemistry of Geopolymers

Geopolymerisation involves the polycondensation reaction of alumino-silicate oxide with alkali polysiliates to produce polymeric Si-O-Al bonds (Hardjito *et al.*, 2003):

$$M_n[-(Si-O_2)_z-Al-O]_n \cdot wH_2O \quad (2-4)$$

In equation (2-4), M denotes the alkaline element, z denotes 1, 2 or 3 and n denotes the degree of polycondensation (Hardjito *et al.*, 2003). For the formation of strong products, compositions lay in the range M_2O/SiO_2 0.2 to 0.48, SiO_2/Al_2O_3 3.3 to 4.5, H_2O/M_2O 10 to 25 and M_2O/Al_2O_3 0.8 to 1.6 (Van Jaarsveld *et al.*, 1997; Palomo and Glasser, 1992; Davidovits *et al.*, 1994). Depending on the atomic ratio Si/Al, which may be 1, 2 or 3, geopolymers have been grouped in three families (Davidovits *et al.*, 1994). Equations (2-5), (2-6), (2-7) and (2-8) are the reactions involved in geopolymerisation (Khale and Chaudhary, 2007).



In a geopolymers, the aluminum and silica atoms are tetrahedrally interlinked alternately by sharing the oxygen atoms. The alkali metal salts and/or hydroxide help in the dissolution of silica and alumina and also act as the catalyst for the condensation reaction. Since aluminum is four fold, some cations are present to keep the structure neutral. It is not clear whether these ions are bonded into the matrix via Al-O or Si-O bond or just present for charge-balance (Van Jaarsveld *et al.*, 1998). During the hardening of the matrix, some water and NaOH are expelled. It is reported that the alkali metal hydroxide acts as a catalyst and leaches out from the hardened geopolymers in approximately the same amount as was added (Van Jaarsveld *et al.*, 1998). Figure 2-6 presents a highly simplified reaction mechanism for geopolymers (Duxson *et al.*, 2007).

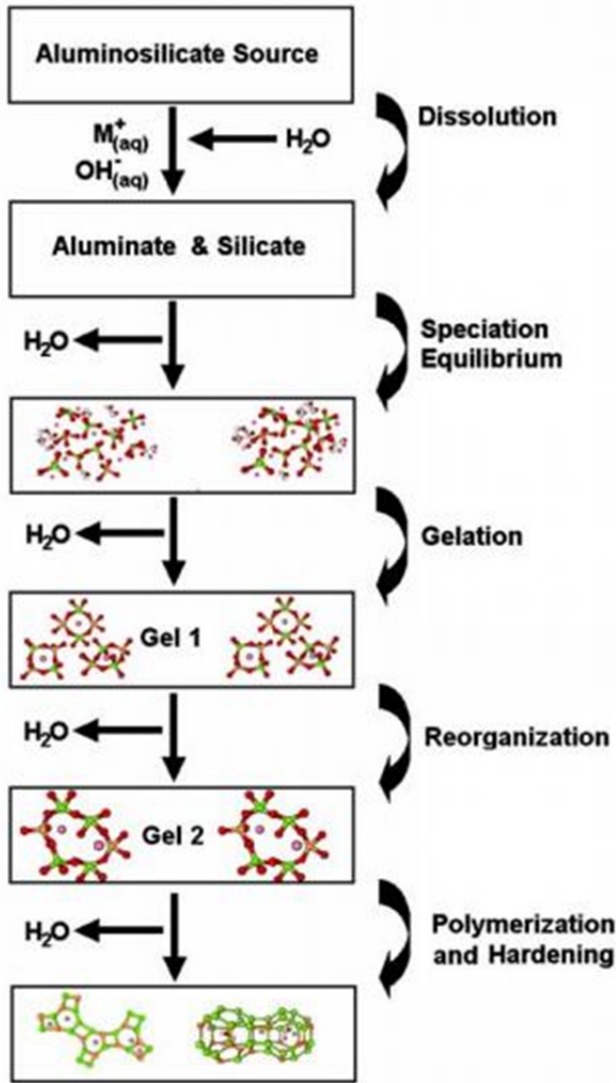


Fig. 2-6 Conceptual model for geopolymers (Duxson *et al.*, 2007)

2.4.3. Structural Characteristics of Geopolymers

The main product of the geopolymer system is semi crystalline aluminosilicate gel. Although this gel appears to be amorphous to X-rays, Nuclear Magnetic Resonance (NMR) studies have found a three-dimensional short-range structure in which silica is present in a variety of environments (Palomo *et al.*, 2004b; Fernández-Jiménez and Palomo, 2005a). The SiO_2/Al_2O_3 ratio of the hydration products depends on the characteristics of the aluminosilicate used, nature and concentration of activators, and curing temperature (Krivenko and Kovalchuk,

2002). With the use of different alkaline activators, different microstructures in the geopolymers have been noticed (Palomo *et al.*, 2004a; Fernández-Jiménez and Palomo, 2005b). The OH⁻ ion acts as a catalyst in the reaction, whereas the alkaline metal (Na⁺) and other ions take part in the reaction to form the structure. If NaOH solution is used as the alkali activator, the gel has a Si/Al ratio of 1.8-2.0 and a Na/Al ratio of 0.46-0.68. With the introduction of silicate ions, the Si content in the gel rises, giving a Si/Al ration of 2.7 and a Na/Al ratio of 1.5. This increases the mechanical strength of the structure (Palomo *et al.*, 2004a; Fernández-Jiménez and Palomo, 2005b).

2.4.4. Compressive Strength of Geopolymer

The strength of geopolymers depends on various factors. Source materials with high reactivity produce stronger geopolymers (Xu and Van Deventer, 2002). Calcined binder like fly ash is known to produce stronger geopolymers compared to non-calcined binder like kaolinite. Curing temperature is one of the most important factors affecting strength of geopolymers. Unlike cement, at ambient temperature the geopolymersation reaction is slow (Puertas *et al.*, 2000). For the same period of time, curing at 90°C increased the strength compared to curing at 30°C (Papadakis, 2000). Curing at higher temperatures for more than a couple of hours showed adverse effects on the development of the compressive strength (Papadakis, 2000). Kirschner and Harmuth reported that curing at ambient temperature had a delayed setting time, whereas curing at 75°C for 4h seemed to be enough for the major part of geopolymersation process (Kirschner and Harmuth, 2004). Curing temperature has been reported to have the most noticeable effect on the compressive strength during the first 2 hours to 5 hours of curing (Palomo *et al.*, 1999). Wang *et al.* also reported that strength of geopolymers increased at elevated temperature (Wang *et al.*, 2004). It has been seen that curing at elevated temperature in

the range of 30°C to 90°C is effective in increasing the strength of the geopolymer. Curing time up to 48 hours is reported to give significant increase in compressive strength (Hardjito *et al.*, 2004; Palomo *et al.*, 1999; Swanepoel and Syrdom, 2002; Martinez-Ramirez and Palomo, 2001). After 48 hours, the strength gain is not significant. Curing at higher temperature for longer period of time has adverse effects on the strength of the geopolymer. At higher temperature, the granular structure of the geopolymer structure breaks. Higher temperature also results in dehydration and shrinkage of the gel (Van Jaarsveld *et al.*, 2002). Alkaline metal silicate to alkaline metal hydroxide ratio is an important factor affecting the compressive strength of geopolymer. Higher value of this ratio is reported to give higher compressive strength (Hardjito *et al.*, 2004; Xu and Van Deventer, 2002; Sumajouw *et al.*, 2004). Excess alkaline metal silicate hindering the water evaporation and structural formation has been reported to be the reason for this behaviour (Cheng and Chin, 2003). $\text{SiO}_2/\text{Al}_2\text{O}_3$ ratio in the range of 3.16 to 3.46 has been reported to give better compressive strength (Cheng and Chin, 2003).

2.4.5. S/S of Metal Wastes

Presently, cement based stabilisation/solidification is the conventional method for the immobilization of toxic metals. This is a costly method because of the cost of cement (Van Jaarsveld *et al.*, 2002; Van Jaarsveld *et al.*, 1997). Geopolymer based stabilisation/solidification is a good alternative because of the small amount of additive and activators needed for the stabilisation/solidification of toxic metals. Jimenez and Palomo (2003) reported that about 90% of toxic metals get locked into the geopolymeric matrix (Fig. 2-7). Fly ash based geopolymers have been reported as effective binders for s/s of wastes (Palomo and Palacios, 2003; Palacio and Palomo, 2004; Fernández-Jiménez *et al.*, 2005b). Very little literature is available on the

stabilisation/solidification of toxic metals by geopolymers. Geopolymers have been reported to effectively immobilize lead as it is precipitated as a highly insoluble silicate Pb_3SiO_5 in the geopolymer matrix (Palomo and Palacios, 2003; Palacio and Palomo, 2004). The immobilization of copper was reported to be less effective than lead (Phair and Van Deventer, 2001). Cr(VI) in geopolymer matrix was found to form $Na_2CrO_4 \cdot 4H_2O$, which is highly soluble, thus leaches readily (Palomo and Palacios, 2003). The formation of $Na_2CrO_4 \cdot 4H_2O$ was also reported to have an adverse effect on the activation of fly ash. Physical micro-encapsulation is the dominant mechanism for immobilization of these metals because of the low permeability of the geopolymer matrices (Shi and Fernández-Jiménez, 2006). It has been reported that the matrices with smaller pore openings as well as high compressive strength immobilize the toxic metals best, leading to the assumption that physical encapsulation plays the major role in toxic metal immobilization (Van Jaarsveld *et al.*, 1998; Phair *et al.*, 2004).

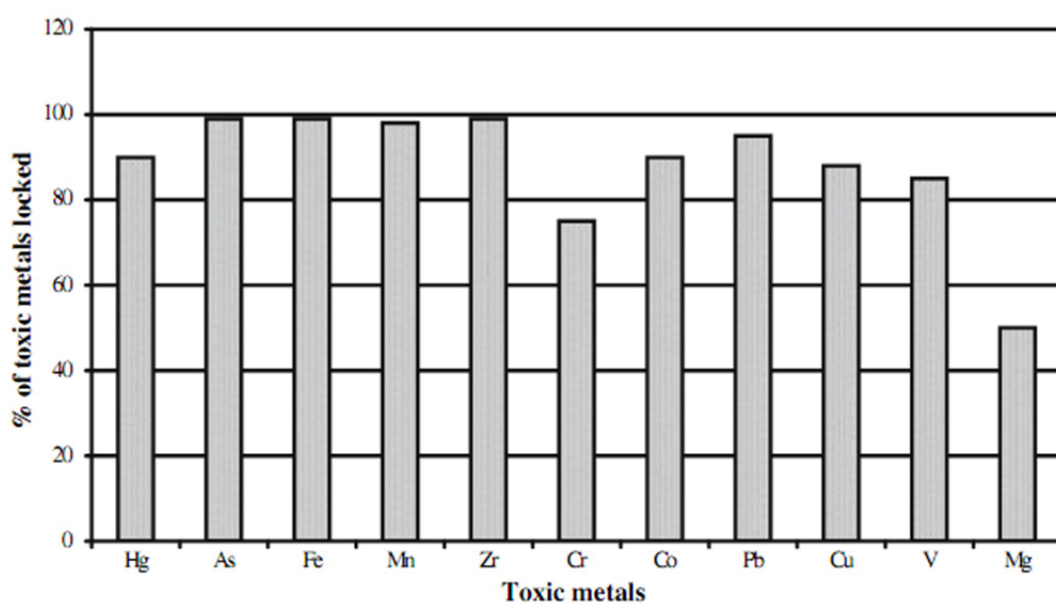


Fig. 2-7 Percentage of toxic metals locked in geopolymeric matrix (Jimenez and Palomo, 2003)

2.5. Standard Testing Methods

Some physical and chemical tests are performed to characterize s/s wastes. These physical and chemical testing of s/s waste helps demonstrate the relative success or failure of the s/s process.

2.5.1. Permeability (Hydraulic Conductivity) Testing

Permeability is the measure of the ability of a material to transmit water. It has a strong relationship with the leachability of contaminants from the s/s waste. Increase in permeability will increase the contact of contaminants with water, thus increasing the rate of leaching. Permeability tests are performed to estimate the amount and flow rate of water through the s/s waste. Two commonly used permeability tests are: constant-head and falling-head permeability tests (USEPA, 1989). The constant-head test is suitable for material with permeability greater than 10^{-6} cm/s and the falling-head test is suitable for material with permeability less than 10^{-6} cm/s (Isaacs and Carter, 1983). Both of these tests are laboratory methods and are only considered accurate to within one order of magnitude. Their general description can be found in USEPA/625/6-89/022 (USEPA, 1989). Permeability of less than 10^{-5} cm/s is recommended for s/s waste designed for land burial (USEPA, 1986). The permeability of s/s waste should be two orders of magnitude below that of the surrounding materials (USEPA, 1989).

2.5.2. Compressive Strength Testing

Compressive strength values are valuable indicators for how well the s/s waste material will hold up under mechanical stresses. ASTM D1633-84 test method is used to test the compressive strength of the s/s materials (ASTM, 2006a). The USEPA considers the s/s waste with unconfined compressive strength of 50 psi (0.35 MPa) to be satisfactory (USEPA, 1989). This minimum value of 50 psi is designed to provide a stable foundation for materials placed on

it, including construction equipment and impermeable caps and cover material.

2.5.3. Freezing and Thawing Testing

The ASTM D560 test method is used to determine the resistance of s/s waste to repeated cycles of freezing and thawing (ASTM, 2006b). Each cycle consists of freezing at -23°C for 24 hours, thawing at 21°C for 23 hours, and scraping the surface of the specimen with a wire brush. The loss in weight is measured after scraping to calculate the amount of specimen lost as a percentage of the original weight of the specimen. The cycles are repeated 12 times or until the weight loss of the material exceeds 30%. The number of cycles that a material can withstand without failing can be used to judge the mechanical integrity of the material. No standards have been established, but up to 15% weight loss after 12 cycles is considered acceptable (USEPA, 1989).

2.5.4. Leaching Tests

Leaching tests are some of the most important methods of measuring the effectiveness s/s waste treatment. Leaching tests help:

- classify a waste as hazardous or non-hazardous waste,
- evaluate the leaching potential of a waste at a specific environmental condition,
- produce leachate representative of the field leachate,
- measure the effectiveness of the waste treatment,
- determine effective waste disposal conditions, and
- model contaminant transport.

2.5.4.1. Toxicity Characteristic Leaching Procedure (TCLP)

The TCLP method (USEPA, 1992) is a regulatory leaching test in the United States developed by the USEPA. It is also widely used outside the United States. This test is a single extract batch test and is relatively easy to perform (Butcher *et al.*, 1993). The TCLP process involves extraction of contaminants from 100 g of ground waste material using a specified extraction fluid. Two types of extraction fluids can be used for TCLP. Extraction fluid 1 is prepared by mixing 5.7 ml glacial acetic acid, 500 ml of reagent water and 64.3 ml of 1N NaOH and diluting to a volume of 1 litre. The pH of this fluid will be 4.93 ± 0.05 . Extraction fluid 2 is prepared by diluting 5.7 ml glacial acetic acid with reagent water to a volume of 1 litre. When correctly prepared, the pH of this fluid will be 2.88 ± 0.05 . For the acceleration of the test, the TCLP requires the waste to be ground so that it passes through a standard 9.5 mm sieve. The L/S ratio of the mixture is maintained at 20:1. The mixture is rotated for 18 ± 2 hours at 30 rpm. The alkalinity of the waste material determines the type of extraction fluid to be used. The final pH is measured after the rotation, and the mixture is filtered using a glass fibre filter. Then, the filtrate is analysed for a number of constituents whose regulatory levels are provided in the Toxicity Characteristic (TC) list. If the constituents in the leachate exceed the limit, the waste material is considered to be hazardous. It is designed to evaluate the “worst-case” leachate scenario in the landfill.

2.5.4.2. Synthetic Precipitation Leaching Procedure (SPLP)

The synthetic precipitation leaching procedure (USEPA, 1994) is similar to TCLP, except that the extraction fluids are different. Instead of the landfill leachate simulating acetic acid mixture, nitric and sulphuric acids are utilized in an effort to simulate the acid rains resulting from airborne nitric oxides and sulfur dioxide. Two types of extraction fluids

can be used for SPLP. Extraction fluid 1 is made by adding the 60/40 weight percent mixture of sulphuric and nitric acids (or a suitable dilution) to reagent water until the pH is 4.20 ± 0.05 . Extraction fluid 2 is made by adding the 60/40 weight percent mixture of sulphuric and nitric acids (or a suitable dilution) to reagent water until the pH is 5.00 ± 0.05 (USEPA, 1994).

2.5.4.3. Flow Through Leaching Test

The TCLP test being a static leachant test cannot represent the real leaching in the field where there is a constant flow of groundwater. Thus, there is a need for a realistic assessment considering the flow of leachant through the material. Flow-through tests can be carried out on monolith samples using a modified triaxial testing method (Butcher *et al.*, 1993) or on crushed samples using packed column tests (Shackelford *et al.*, 1997).

Packed Column Test (Shackelford *et al.*, 1997)

A packed column test is another type of flow-through test used to study leaching process from waste material. In this test, the leaching solution is continuously flowed through a crushed waste sample placed in a column. This test may have problems with channelling and clogging of the sample, resulting in un-representative results. Figure 2-8 shows the schematic of a packed column apparatus.

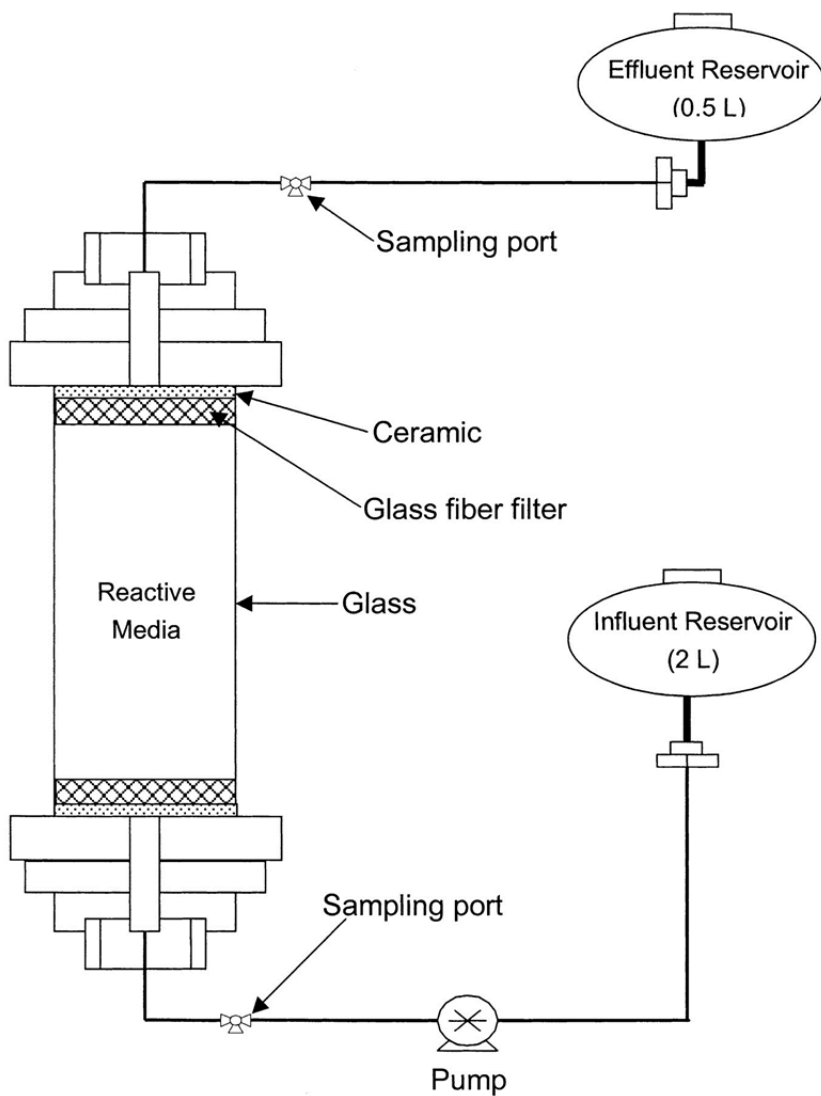


Fig. 2-8 Schematic of a packed column apparatus (Lee and Benson, 2004)

Modified Triaxial Testing Method (Butcher *et al.*, 1993)

The Modified Triaxial Test uses a monolith sample, which is more representative of the field conditions. The modified triaxial testing equipment enables the samples to be tested in variable confining and leachant pressures. This enables the acceleration of the leaching process without the need to crush the sample. This test enables the determination of the relation between release of contaminants and volume of leachant passed. A schematic diagram of the modified triaxial cell is shown in Figure 2-9.

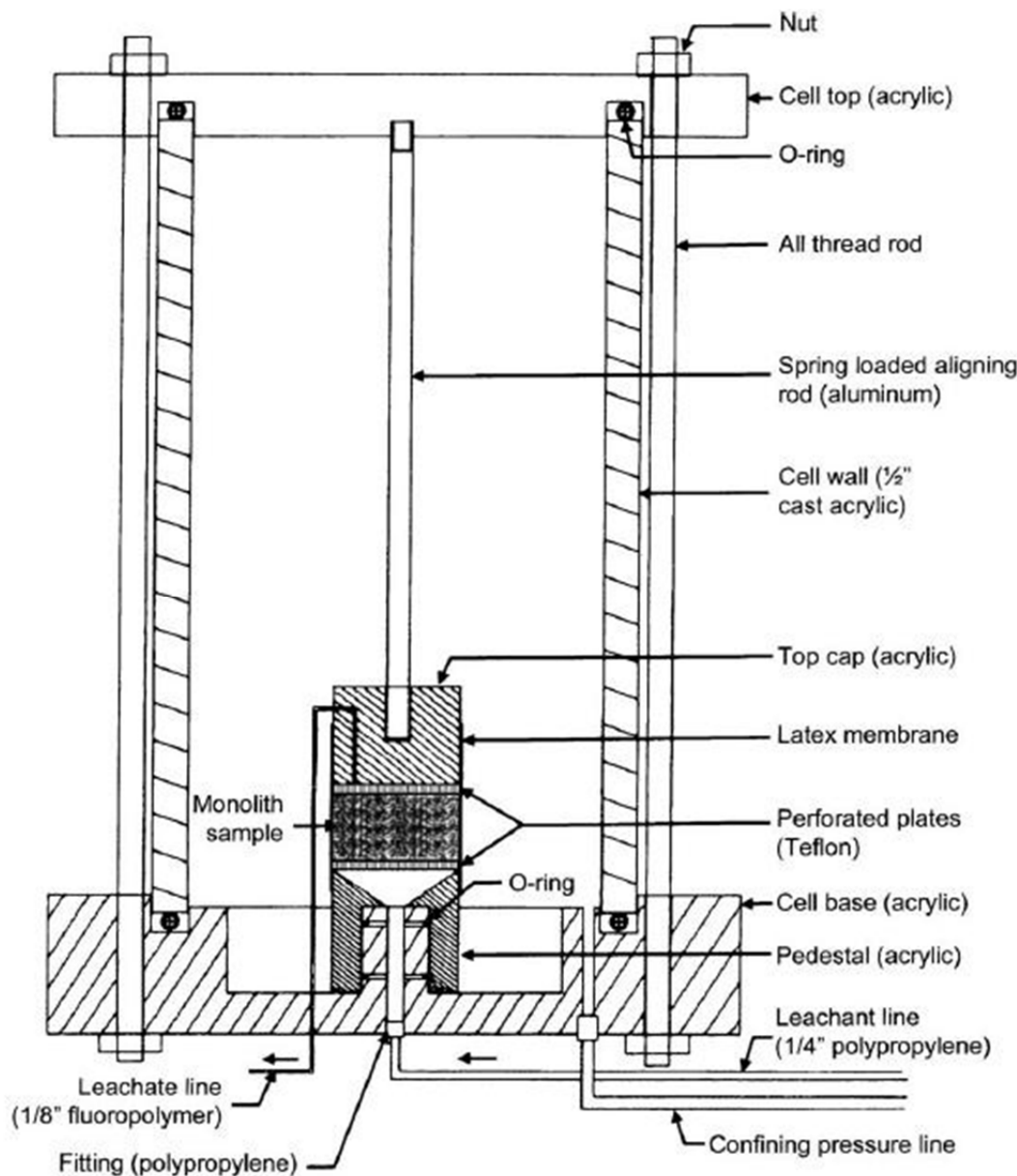


Fig. 2-9 Triaxial Cell Construction (Catalan *et al.*, 2002)

In addition to the test methods described above, several other test methods have been developed for contaminant leaching. Some of these methods are listed in Table 2-4.

Table 2-4 Different Leaching Procedures (USEPA, 1989; Paria and Yuet, 2006)

Test method	Leaching medium	Liquid/solid ratio by weight	Maximum particle size	Number of extractions	Time of extraction
TCLP	Acetic acid (pH ≈ 5 and 3)	20:1	9.5 mm	1	18 h
SPLP	Sulphuric/nitric acids (pH ≈ 4.2 and	20:1	9.5 mm	1	18 h
Semi-dynamic leaching test (ANS 16.1)	Water	V _L /S* = 10 cm	Intact sample	10	Fixed time intervals
Extraction procedure toxicity test (EP Tox)	0.4 M acetic acid (pH = 5)	16:1	9.5 mm	1	24 h
California waste extraction test	0.2 M sodium citrate (pH = 5)	10:1	2.0 mm	1	48 h
Multiple extraction procedure	Same as EP Tox, then sulfuric:nitric acid in 60:40 wt%	20:1	9.5 mm	9 (or more)	24 h per extraction
Modified waste extraction procedure	Distilled/deionised water	10:1 per extraction	9.5 mm	4	18 h per extraction
Equilibrium leach test	Distilled water	4:1	150 µm	1	7 days
Acid neutralization	HNO ₃ solution of increasing strength	3:1	150 µm	1	48 h per extraction
Sequential extraction tests	0.04 M acetic acid	50:1	9.5 mm	15	24 h per extraction
Sequential chemical extraction	5 leaching solutions increasing in acidity	Varies from 16:1 to 40:1	150 µm	5	Varies from 2 to 24 h

*Ratio of leachant volume (V_L) to specimen surface area (S).

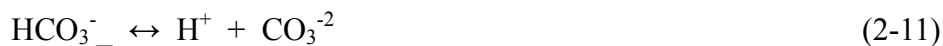
2.6. Cement-based S/S Waste in the Environment

After land disposal, the s/s treated wastes are exposed to various physical and chemical alteration processes like rain and groundwater leaching, freeze-thaw cycles, wet-dry cycles, carbonation, alkali-aggregate reaction, sulphate attack, and microbial actions. These alter the physical and chemical properties of the waste. The extent of these alterations depends on factors such as porosity, chemical composition, types of waste and micro-structure. Knowledge of these alterations is essential for the study of long term immobilization of the contaminants in the treated

waste.

2.6.1. Carbonation

Carbon dioxide is present in air and dissolved in surface and subsurface water. The calcium bearing phases of cement react with this carbon dioxide. This process is known as carbonation. It is the most common alteration mechanism in cement-based s/s waste (Macias *et al.*, 1997). The dissolution of CO₂ leads to the formation of aqueous carbonic acid (H₂CO₃), bicarbonate and carbonate ions (Eq. 2-9, 2-10, and 2-11). This solution dissolves the calcium ions from the solid phases, which then re-precipitate in the pore space of the matrix as CaCO₃.



This process is exothermic and diffusion-controlled. The gas diffuses into the solid, resulting in a carbonation front surrounding an inner zone of non-carbonated material. The conceptual model for the reaction of carbon dioxide with a waste form is presented in Figure 2-10.

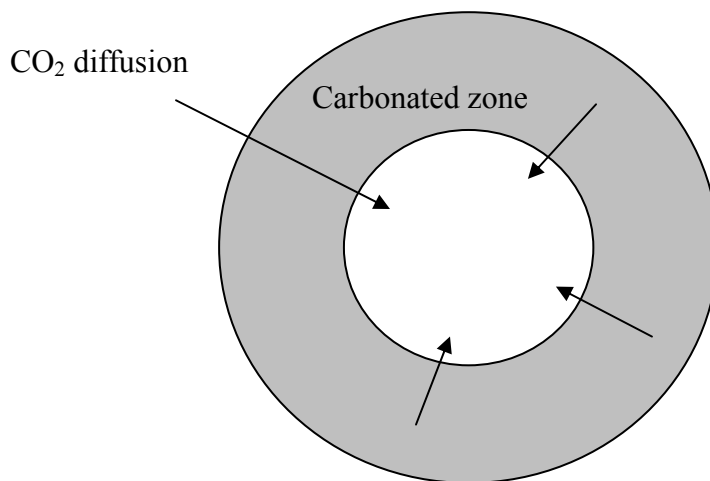
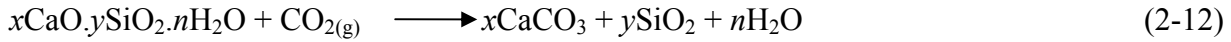


Fig. 2-10 Schematic of carbonation process (Bin-Shafique *et al.*, 1998)

The reactions representing the carbonation process are shown below:



The rates of carbonation depend on interrelated factors such as porosity, water-to-cement ratio, carbon dioxide concentration and carbon dioxide diffusivity (Houst and Wittman, 1994; Malami and Kaloidas, 1994; Loo *et al.*, 1994). Presence of water is an essential factor controlling the carbonation of cement. Carbonation is slow in water-saturated monoliths because carbon dioxide diffusion is hindered when the pores are filled with water. Completely dry pores will also slow down carbonation because the formation of calcium carbonate occurs in the liquid phase, often in water films within pores (Papadakis *et al.*, 1989). Relative humidity (RH) of 40% to 90% is favourable for carbonation. The overall effects of carbonation of cement are neutralization of pore water alkalinity, formation of calcium carbonate, and reduction in the Ca/Si ratio of the CSH gel.

Several laboratory carbonation techniques have been used by different researchers to simulate the carbonation of s/s wastes. A chamber at atmospheric pressure with elevated carbon dioxide concentration, regulated relative humidity (RH), and regulated temperature is commonly used (Lange *et al.*, 1996; Lange *et al.*, 1997). This process of carbonation is called accelerated carbonation. Figure 2-11 illustrates a proposed mechanism for accelerated carbonation. The numbered steps represent:

1. CO_2 diffusion in air.
2. CO_2 permeation in the solid.
3. Solvation of $\text{CO}_2(\text{g})$ to $\text{CO}_2(\text{aq})$.
4. Hydration of $\text{CO}_2(\text{aq})$ to H_2CO_3 .
5. Drop in pH due to the ionization of H_2CO_3 to H^+ , HCO_3^- and CO_3^{2-} .
6. Exothermic dissolution of C_3S and C_2S releasing Ca^{2+} and SiO_4^{4-} ions.
7. Nucleation of CaCO_3 , C-S-H.
8. Precipitation of CaCO_3 .
9. Secondary carbonation with the progressive decalcification of C-S-H gel ultimately converting to S-H and CaCO_3 .

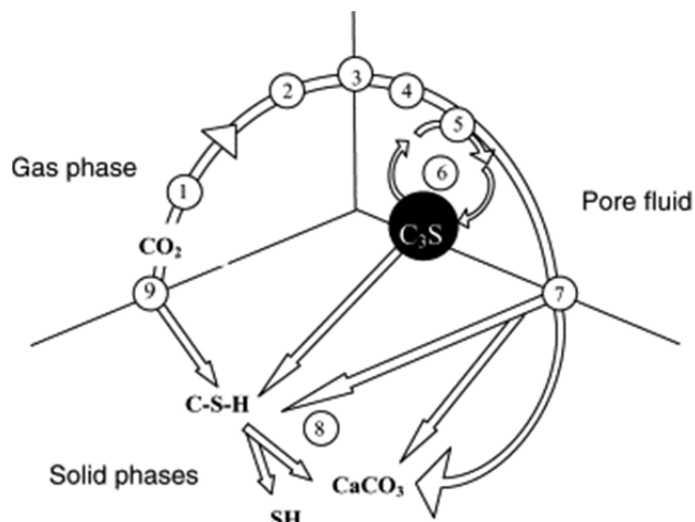


Fig. 2-11 Proposed mechanism for accelerated carbonation (Maries, 1985)

Another method is supercritical carbonation, where supercritical carbon dioxide (scCO_2) is used for carbonation. Supercritical carbonation involves exposing cement-based materials to carbon dioxide at slightly elevated temperature ($>31^\circ \text{ C}$) and pressure ($>71 \text{ bar}$).

Another method used for carbonation is vacuum carbonation. In this method, the s/s

waste is carbonated in a near vacuum condition. The supercritical carbonation and vacuum carbonation are relatively more expensive than the atmospheric carbonation process.

2.6.1.1. Effect of Carbonation on Leachability

As seen in reaction (2-12), carbon dioxide reacts with C-S-H gel to form calcite. C-S-H is known to play an important role in the fixation of toxic metals. Carbonation increases the binding capacity of metals such as As, Ba, Cr, Cu, Hg and Zn (Lange *et al.*, 1996; Sweeny *et al.*, 1998). Lange *et al.* (1997) reported that carbonation reduced the concentration of leachable metals like As, Cr, Cu and Zn up to 80%. Flitch and Cheeseman (2003) reported extensive carbonation and reduction in acid neutralisation capacity in the first 5 cm of a 10 year old s/s waste exposed to the environment. They also reported a significant reduction in the concentration of heavy metals like Zn, Fe, Pb and Cr in the surface region. Carbonation has been seen to decrease the pH of the leachate by 2 to 4 units (Lea, 1970; Lange *et al.*, 1997). Lange *et al.* (1997) reported lower concentration of the metals such as Zn, Cu, Cr and As in the leachate of carbonated waste and attributed these results to the modification of pore structure due to the formation of calcite. However, other researchers have reported the exact opposite; i.e. Alba *et al.* (2001) reported the increase in concentration of Cr and Zn in the leachate upon carbonation. Walton *et al.* (1997) have reported that nickel, cadmium, mercury, lead and cobalt were leached in greater amounts from carbonated waste forms. Chen *et al.* (2009a) reported that carbonation benefited chromium, copper and zinc immobilization, but demonstrated deteriorative nickel retention. These conflicting results could be caused by different operating conditions, leading to the differences in the degree of carbonation, waste characteristics and leaching methods (Chang *et al.*, 2001; Van der Sloot, 2002). Furthermore, the presence of other soluble species may

influence the actual solubility of heavy metals through common ion effect, complexation, ionic strength and redox potential (Chen *et al.*, 2009a).

2.6.1.2. Effect of Carbonation on Strength

The volume change accompanying reaction (2-13) helps fill the pore space, densifies the product, and improves the structural integrity of the s/s waste (Lange *et al.*, 1996). Experiments performed by Klich *et al.* (1999) revealed that carbonate material precipitated around areas of unmixed waste material and also along the vertical cracks. They also reported microcrystalline precipitates of calcite within the cement paste. Lange *et al.* (1997) reported that carbonation increased the mean strength of s/s waste by up to 70%. This result was related to the accelerated hydration of C₃S driven by the formation of calcium carbonate. The relationship between C₃S hydration and the formation of calcite, reported by Lange *et al.* (1996), suggested the existence of an optimum cement quantity for the beneficial effects of carbonation. This optimum was found to be cement specific and dependent on the type of waste material treated (Hills *et al.*, 1994). Metals originally present as hydroxides in the matrix are progressively converted to carbonates, thus changing their solubility (Garrabrants *et al.*, 2004; Van Gerven *et al.*, 2004; Gervais *et al.*, 2004). The increase in volume of the products compared to the reactants could either reduce porosity, strengthen the matrix or induce expansive stress, leading to micro cracking and an increase in porosity (Bin Shafique *et al.*, 1998).

2.7. Carbonation of Geopolymer based S/S

Luna *et al.* (2009) reported the effects of carbonation on the leachability of lead, cadmium, total chromium, and zinc from electric arc furnace dust stabilized in various complex geopolymeric

matrices made with different proportions of Class F fly ash, blast furnace slag, metakaolin, and potassium silicate. Their results reveal that the effects of carbonation strongly depend on the composition of the geopolymers matrix, the metal whose leachability is evaluated, and the type of leaching test used for the evaluation. At this time, little is known on how carbonation affects the mechanisms of metal immobilization in geopolymers matrices.

2.8. Research Opportunities

There are a lot of contradictory results in the literature on the effect of carbonation on the leachability of metals from solidified wastes (Lange *et al.*, 1996, 1997; Walton *et al.*, 1997; Alba *et al.*, 2001; Chen *et al.*, 2009a). These conflicting results could be caused by differences in the degree of carbonation, waste characteristics and leaching methods (Chang *et al.*, 2001; Van Der Sloot, 2002). Furthermore, the presence of other soluble species may influence the actual solubility of heavy metals through common ion effect, complexation, ionic strength and redox potential (Chen *et al.*, 2009a).

Most of the literature to date focuses on physical and chemical tests like leaching and compressive strength tests to study the effect of carbonation of s/s metal wastes. There is a need for micro-structural analysis of the carbonated s/s waste to understand the mechanisms of carbonation that affects the leachability of contaminants.

A lot of research has been done on the effect of carbonation on cement based s/s but no studies have yet been reported on how carbonation influences the effectiveness of geopolymers for s/s treatment of metals that are introduced as soluble salts or alkaline sludges typical of normal industrial/mining waste.

2.9. Research Objectives

The primary objective of this research is to study the effect of carbonation on leachability of Cd, Cr (III), Cr (VI), Cu, Pb and Zn from different cement-based and geopolymers-based s/s synthetic wastes. Various synthetic wastes, each containing only one type of metal, will be s/s-treated using portland cement and fly ash based geopolymers. These s/s samples will then be carbonated by the accelerated carbonation process. Then, the samples will be leached and the leaching results of the carbonated samples will be compared with those of the non-carbonated samples. The effect of carbonation on the strength of cement-based and geopolymers-based s/s wastes will also be studied. Another objective of this research is to explain the leaching and strength results by studying the micro-structural changes in the carbonated s/s samples using Scanning Electron Microscope/Energy Dispersive X-Ray spectroscopy (SEM-EDS).

3. Materials and Methods

3.1. Materials

3.1.1. Fly Ash

The fly ash used in this research was generated from the combustion of coal at the Atikokan Generating Station (AGS) in Northwestern Ontario. The coal was lignite from Saskatchewan. The composition and loss on ignition (LOI) of the fly ash are shown in Table 3-1. This is a class C fly ash due to its large calcium content (13.6% CaO) (ASTM, 2008b). Table 3-2 shows the concentrations of minor elements in the fly ash measured by ICP-AES after acid digestion. As seen in Table 3-2, the fly ash contains significant amounts of toxic metals such as Cu, Co, Pb, Mo, Ni and Zn. The specific gravity of the fly ash was 2.361 ± 0.072 (Johnson, 2009).

Table 3-1 Bulk composition of Atikokan fly ash

Oxides	Mass (%)
Total	97.11
SiO₂	45.2
Al₂O₃	21.5
Fe₂O₃	4.0
MgO	2.5
CaO	13.6
Na₂O	7.3
K₂O	0.7
TiO₂	1.0
P₂O₅	0.6
MnO	0.02
V₂O₅	0.03
S	0.26
SiO₂ + Al₂O₃ + Fe₂O₃	70.7
LOI	0.40

Table 3-2 Trace metal content of Atikokan fly ash (Johnson, 2009)

Elements	g/t
Ag	<2 ^a
As	<30
Ba	3900
Be	4.2
Bi	<20
Cd	<2
Co	16
Cu	41
Hg	<0.3
Li	16
Mo	10
Ni	27
Pb	48
Sb	<10
Se	<30
Sn	<20
Sr	3300
Tl	<30
U	<20
Y	45
Zn	53

^a Values following “<” represent the detection limit in the solid back-calculated from the ICP-AES detection limit on the solution from the acid digestion.



Fig. 3-1 Fly Ash

3.1.2. Cement

The cement used in this research was OPC Type I (Type 10 in Canada), as specified by ASTM C150/C150M-09 (2009). It was manufactured by Lafarge, Montreal, PQ.

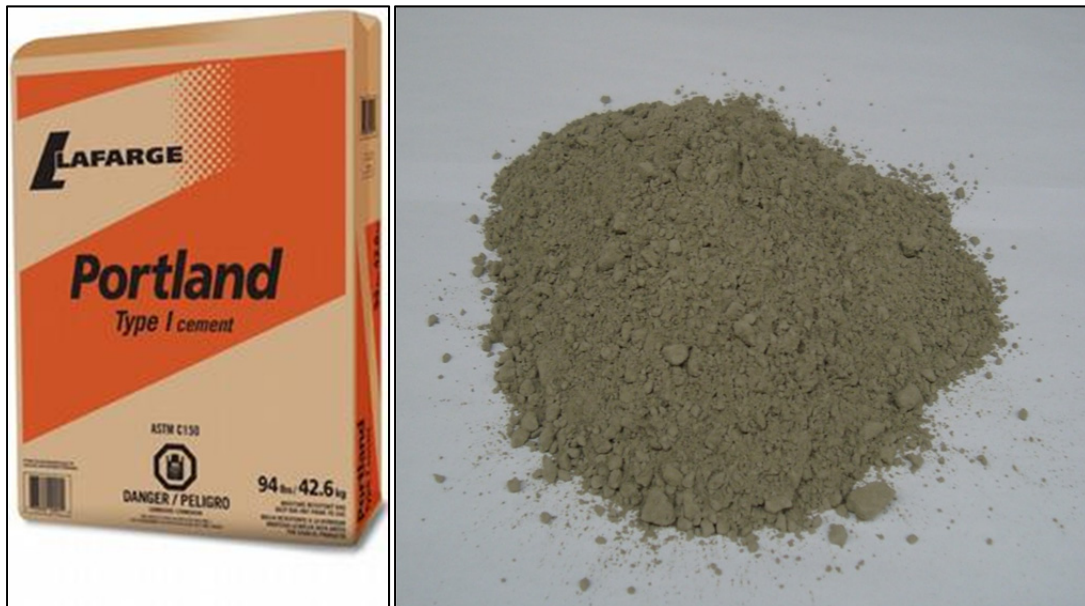


Fig. 3-2 Ordinary Portland Cement Type I manufactured by Lafarge

3.1.3. Sand

The sand used in this research was as specified by ASTM C778-06 (2006c). The manufacturer was U.S. Silica Company, Ottawa, Illinois, USA. Table 3-3 shows the particle size distribution of the sand as provided by the manufacturer. 97% of the sand particles are of size between 0.60 and 0.85 mm.

Table 3-3 Particle size distribution of ASTM 20/30 sand manufactured by U.S. Silica Company

Sieve Size mm	% Retained		% Passing Cumulative
	Individual	Cumulative	
1.18	0	0	100
0.85	1	1	99
0.60	97	98	2
PAN	2	100	0



Fig. 3-3 ASTM 20-30 sand manufactured by U.S. Silica Company

3.1.4. Mixing Water

The mixing water used for this research was de-ionized water prepared using a NANOpure Diamond, Barnstead D11911 treatment unit



Fig 3-4 NANOpure Diamond, Barnstead D11911

3.1.5. Metal Salts and NaOH Solution

All the metal salts used, cupric nitrate (98+%), lead(II) nitrate (99+%), chromium(III) chloride (99+%), zinc nitrate (98+%), potassium dichromate (99.5+%), and cadmium chloride (99+%), were shipped from Sigma-Aldrich Group, Oakville, Ontario. A 6.0M NaOH solution was used for the preparation of the metal sludge.

3.1.6. Sodium Silicate Solution

The sodium silicate solution was shipped from The Sigma-Aldrich Group, Oakville, Ontario. The solution is of reagent grade and contains ~10.6% Na₂O, ~26.5% SiO₂ and ~62.9% water.

3.2. Methods

3.2.1. Mortar Preparation

Cement Samples

Sludges of metal hydroxide synthetic sludge were prepared by alkalizing 0.100 mol L⁻¹ solutions of CdCl₂•2.5H₂O, Cu(NO₃)₂•2.5H₂O, CrCl₃•6H₂O, Pb(NO₃)₂, or Zn(NO₃)₂•6H₂O with 6 mol L⁻¹ NaOH to pH 9.0. A solution of K₂Cr₂O₇ was similarly treated, but did not precipitate hydroxide. The metal content of these mixtures was typical of wastes that are treated by s/s (US EPA/542-R00-010, 2000; Catalan *et al.*, 2002).

Sludge (or deionized water in the case of control batches) was mixed with OPC at a 0.40:1 mass ratio in a 5-L Hobart mixer according to ASTM C305-06 (2006d). The resulting waste metal content of the cement mixture was 0.029 mol kg⁻¹. It was poured in three successive layers into 2-in (5 cm) cubic molds that were fitted with polyethylene liners (ELE International, Loveland, CO, USA). Each layer was tamped 25 times with a rounded rod. Bubbles were eliminated by tapping the walls with a mallet. Samples were cured 3 days in an ESPEC-3CA environmental chamber (Espec North America Inc., Hudsonville, MI, USA) at 23.0 ± 0.5 °C and 99 ± 1% relative humidity. After the first day of the initial 3-day curing period, the specimens were removed from the liners and molds and kept in the above mentioned conditions for 2 more days.



Fig. 3-5 Hobart 5-quart (*ca.* 5 L) mixer

Geopolymer Samples

Geopolymer with the composition described in Table 3-4 (which falls in the region of optimum compressive strength reported by Provis *et al.*, 2009) was prepared by combining fly ash, sand (ASTM 20/30 Graded Sand, U.S. Silica Company, Berkeley Springs, WV, USA) and alkaline activator. The alkaline activator was a mixture of sodium silicate solution, sodium hydroxide (both reagent grade, Fisher Scientific), deionized water and, as required, a sufficient amount of metal salt (one of those listed above) to provide a concentration of 0.029 mol metal per kg geopolymer. Mixing was conducted in a Hobart mixer according to ASTM C 305-06 (2006d), that is, 30 s wetting, 30 s slow mixing, 15 second rest, and, finally, 60 s rapid mixing. 2-in cubes were prepared as described above and cured in an ESPEC-3CA environmental chamber for 3 days at 39.5 ± 0.5 °C and of $99 \pm 1\%$ humidity. After the first day of the initial 3-day curing period, the specimens were removed from the liners and molds and kept in the above mentioned conditions for 2 more days.

Table 3-4 Geopolymer composition

Component	Mass %
Fly ash	26.96
Sand	57.36
Activator: H₂O	9.98
SiO₂	3.35
Na₂O	2.34

3.2.2. Carbonation

After the initial 3 day curing period, cement and geopolymer cubes to be used for leaching tests were stored in sealed polyethylene bags at room temperature for 25 days, crushed and sieved. Samples (*ca.* 100 g) of the 850-2000 µm particle fraction were placed in an atmosphere of 50 ± 3 vol% CO₂ (monitored by gas chromatography), $55 \pm 2\%$ relative humidity and $T = 20 \pm 1$ °C for 3 days. A parallel set of samples was subjected to identical conditions, excluding carbonation.

Cement and geopolymer cubes designated for compressive strength testing were maintained for 21 days (after the initial 3-day curing period) at 37 ± 1 °C in an atmosphere with either zero or 90 ± 2 vol% CO₂ enrichment and $55 \pm 2\%$ humidity . To measure the extent of carbonation, representative cubes were cut with a diamond saw along three orthogonal planes intersecting at the centre, thus providing eight equally sized sub-cubes (Figure 3-6). The freshly cut surfaces were sprayed with phenolphthalein which turned pink where the pore solution exceeded *ca.* pH 9 (RILEM, 1988), that is, where the matrix had not yet become carbonated. The depth of carbonation *d* was measured at 6 different locations for each sub-cube (Figure 3-6), and the average value used to determine the extent of carbonation

$$\text{Carbonation (vol\%)} = 100\% \left[1 - \frac{\left(\frac{l}{2} - d\right)^3}{\left(\frac{l}{2}\right)^3} \right] \quad (1)$$

where l is the edge length of the cube (2-in).

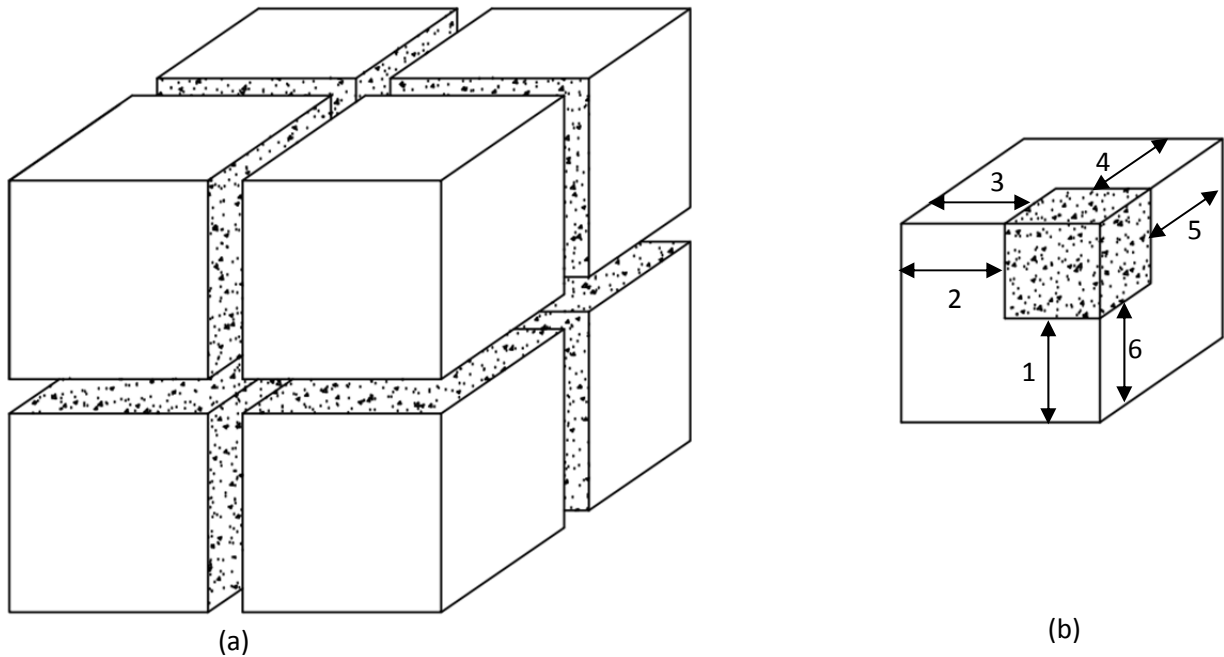


Fig. 3-6 Cubes of cement and geopolymers were cut into eight sub-cubes (a), and the depth of carbonation measured at six locations for each sub-cube (b)

3.2.3. Compressive Strength Testing

After a total of 24 days of curing, in accordance with ASTM C109/C109M (2008a), the carbonated and non-carbonated compressive strength samples were capped with polyurethane pads and retainers from American Cube Molds, and their compressive strength was measured using Compressive Strength Testing Machine, Model 311.21 manufactured by MTS Systems Corporation. Two different sets of polyurethane pads

were used depending on whether the expected maximum compressive load was less than (red pads) or greater than (yellow pads) 15,500 psi (*ca.* 107 MPa). These pads helped distribute the load uniformly on the surface of the sample being crushed. The cubes were wiped to a surface-dry condition, and loose grains and incrustations were removed from the faces which came into contact with the capping system. During testing, the capped cubes were placed on a spherically seated block which was free to tilt. The load was then applied at a rate of displacement of 0.1 in/min. The compressive strength was then determined by:

$$CS = \frac{P}{A}$$

Where CS = compressive strength of specimen

P = total maximum load

A = area of specimen

3.2.4. Leaching Tests

For the TCLP (US EPA, 1992) as well as SPLP (US EPA, 1994), 10 g crushed cement or geopolymer was combined with 200 g extraction fluid (1:20 solid to liquid ratio) in a polyethylene bottle and rotated for 18 h at 30 rpm. The same extraction fluids were used for cement and geopolymer samples to provide comparable results. The TCLP extraction fluid was 0.1 mol L⁻¹ acetic acid with a pH of 2.88 ± 0.05 and simulated a sanitary landfill environment. By contrast, the SPLP extraction fluid, which consisted of 0.024 mmol L⁻¹ H₂SO₄ and 0.018 mmol L⁻¹ HNO₃, was considerably less acidic (Catalan and Wettesking, 2002), had a pH of 4.20 ± 0.05, and simulated *in situ* leaching by infiltrating acid rain. The liquid extract was passed through a 0.45 µm nylon membrane

filter (Whatman GD/X), acidified to pH 2 with concentrated nitric acid, and analyzed by ICP-AES using a Varian Vista Pro ICAP Radial spectrometer. The detection limit was 0.02 mg L^{-1} for Cd, Cu, Cr(III), Cr(VI) and Zn, and 0.05 mg L^{-1} for Pb. The regulated TCLP limits for toxicity are 1 mg L^{-1} for Cd and 5 mg L^{-1} for Cr and Pb (US EPA, 1989). pH was measured at 23°C using a combination glass electrode (Fluka Analytical) calibrated at pH 4, 7, 10 and 13.

3.2.5. Microstructure and Micro-mineralogy Study

In order to examine the micro-mineralogy, polished sections were prepared from the carbonated and non-carbonated samples as well as the leached and dried carbonated and non-carbonated samples. While preparing a polished specimen for examination under the SEM, the porous space is first filled with a hard material such as epoxy resin, which stabilizes the microstructure and prevents damage during polishing. Filling the pores with epoxy was achieved using vacuum impregnation, in which the dried specimen is immersed in epoxy solution while under a vacuum and then is brought to atmospheric pressure while still immersed. The sections were lapped and polished using oil-based media so as not to alter the water-soluble minerals. After carbon-coating, the sections were imaged by SEM and quantitative elemental analysis of the samples were carried out by EDS with an Oxford Link ISIS system, using calibration standards: garnet for Al, Fe, Mg and Si; orthoclase for K; Jadeite for Na; wollastonite for Ca; chromite for Cr; chalcopyrite for Cu and S; zinc sulfide for Zn; lead sulfide for Pb; and cadmium sulfide for Cd. An accelerating voltage of 20kV, beam current of 0.475 mA, working distance of

10 mm, and a vacuum pressure of 5×10^{-5} torr (*ca.* 7×10^{-3} Pa) were consistently used for viewing of all samples.

3.2.6. Geochemical Equilibrium Modeling of the Leachates

Metal hydroxide, oxide and carbonate solubilities were modeled individually as a function of pH at 23 °C using Visual MINTEQ (Allison *et al.*, 1991; Gustafsson, 2011) and the default equilibrium constants provided therein. The input finite concentration of metal-containing solids ($0.00145 \text{ mol L}^{-1}$) was based on the total amount of metals present in the cement or geopolymer matrix ($0.029 \text{ mol kg}^{-1}$) divided by the 20:1 liquid-to-solid ratio used in the leaching tests. For example, $0.00145 \text{ mol L}^{-1} \text{ Cd(OH)}_2$ was introduced as a finite solid phase in Visual MINTEQ to calculate the concentration of Cd in solution in equilibrium with the solid as a function of pH in the range pH 4 – 13 using 0.5 pH increments. The leaching of calcium from non-carbonated cement and geopolymer matrices was simulated concurrently with the leaching of metals from individual metal-containing solids by assuming finite portlandite concentrations of 0.399 mol L^{-1} and $0.0327 \text{ mol L}^{-1}$, respectively, which were based on the assumption that the total CaO content in the solids was present as portlandite. This assumption was made because of the absence of solubility data for CSH and calcium-containing geopolymer phases in the Visual MINTEQ database. The amount of portlandite in the solids is thus overestimated, and simulations provide an upper limit on calcium leachability from non-carbonated matrices. Carbonation was assumed to completely convert portlandite into calcium carbonate owing to the severe carbonating conditions that were employed for the

leaching tests. Hence, the leachability of calcium and carbonate ions from the carbonated cement and geopolymer matrices was assumed to be controlled by the solubility of calcium carbonate. For example, for modeling the solubility of otavite in carbonated cement, $0.00145 \text{ mol L}^{-1}$ otavite and 0.399 mol L^{-1} calcium carbonate were introduced as finite solid phases in Visual MINTEQ. However, for modeling the solubility of otavite in carbonated geopolymer, $0.00145 \text{ mol L}^{-1}$ otavite and only $0.0327 \text{ mol L}^{-1}$ calcium carbonate were introduced as finite solid phases. The total dissolved metal concentrations predicted by the model were compared with measured leachate concentrations in order to identify the solid phases responsible for immobilizing the metal ions. Because of the uncertainties in solubility calculations, control by a given solid was considered feasible when the experimental and modeled concentrations were within an order of magnitude of one another.

4. Results and Discussion

4.1. Leachability of metals

Table 4-1 shows the leaching results which were obtained for the cement-based s/s samples. The TCLP and SPLP leachates of non-carbonated cement were highly alkaline, whereas those of carbonated cement exhibited lower pH values owing to the conversion of CO₂ of portlandite and CSH to CaCO₃. The drop in pH was especially pronounced for the TCLP leaching solution because of its high acid content. Non-carbonated cement matrix was very effective at immobilizing Cd, Cr(III), Cu and Zn under both SPLP and TCLP testing conditions, reasonably effective at retaining Pb, especially under TCLP conditions, and not at all effective for Cr(VI). When carbonated, the cement matrix maintained its efficiency at holding Cd, Cr(III) and Zn, and performed much better in the case of Pb. A comparative summary of the leaching test results is provided in Table 4-2 and 4-3.

Table 4-1 TCLP and SPLP leaching results for carbonated and non-carbonated samples of metal-doped cement

Metal	Curing condition	TCLP leachate			SPLP leachate		
		/mg L ⁻¹	/μmol L ⁻¹	final pH	/mg L ⁻¹	/μmol L ⁻¹	final pH
Cd	carbonated	0.03 ± 0.05 ^a	0.27 ± 0.44	6.62	<i>b</i>	<i>b</i>	11.47
	non-carbonated	<i>b</i>	<i>b</i>	12.43	<i>b</i>	<i>b</i>	12.65
Cr(III)	carbonated	0.07 ± 0.04	1.35 ± 0.77	10.91	0.03 ± 0.01	0.58 ± 0.19	12.04
	non-carbonated	<i>b</i>	<i>b</i>	12.47	0.039 ± 0.001	0.77 ± 0.02	12.76
Cr(VI)	carbonated	9.44 ± 0.45	181.6 ± 8.7	6.84	11.48 ± 0.42	220.8 ± 8.1	11.51
	non-carbonated	2.61 ± 0.19	50.2 ± 3.7	12.06	4.05 ± 0.40	77.9 ± 7.7	12.40
Cu	carbonated	0.35 ± 0.03	5.51 ± 0.47	6.75	<i>b</i>	<i>b</i>	11.57
	non-carbonated	<i>b</i>	<i>b</i>	12.39	<i>b</i>	<i>b</i>	12.64
Pb	carbonated	0.15 ± 0.01	0.72 ± 0.05	6.86	0.18 ± 0.01	0.87 ± 0.05	11.62
	non-carbonated	0.24 ± 0.03	1.16 ± 0.14	12.27	1.36 ± 0.07	6.56 ± 0.34	12.35
Zn	carbonated	0.13 ± 0.08	2.0 ± 1.2	6.66	0.032 ± 0.003	0.46 ± 0.04	11.62
	non-carbonated	<i>b</i>	<i>b</i>	12.29	0.024 ± 0.002	0.31 ± 0.03	12.53

^a Standard deviation were calculated from quadruplicate measurements

^b Below the detection limit (0.02 mg L⁻¹ for Cd, Cu, Cr(III), Cr(VI), Zn; 0.05 mg L⁻¹ for Pb).

Table 4-2 Matrices that immobilized metals under SPLP and TCLP leaching conditions (*i.e.*, maintain leachate concentrations $\leq 10^{-6}$ mol L⁻¹)

Metal	Non-carbonated		Carbonated	
	SPLP	TCLP	SPLP	TCLP
Cd	C	C	C, G	C
Cr(III)	C, G	C, G	C, G	C
Cr(VI)	--	-	-	-
Cu	C, G	-	C	C
Pb	-	C	C, G	C
Zn	C	C	C	C

C = cement, G = geopolymer

Table 4-3 Effect of carbonation on metal leachability from cement and geopolymer matrices

Metal	Cement		Geopolymer	
	SPLP	TCLP	SPLP	TCLP
Cd	NC	↑	↓	NC
Cr(III)	↓	↑	↓	↑
Cr(VI)	↑	↑	↓	↓
Cu	NC	↑↑↑	↑	↑
Pb	↓	↓	↓	NC
Zn	↑	↑	NC	NC

↑↑↑ = large (>10 fold) leachability increase. ↑ = small leachability increase. ↓ = small leachability decrease. ↓↓↓ = large leachability decrease. NC = no change (within limit of detection).

Leaching results for the geopolymer s/s samples are displayed in Table 4-4 and also summarized in Tables 4-2 and 4-3. Due to low alkalinity of geopolymer compared with cement,

the pH of each leachate solution was lower than that of the corresponding cement leachates (Table 4-1). Under alkaline SPLP extraction conditions, non-carbonated geopolymers were quite effective at immobilizing Cr(III) and Cu, and, to a lesser degree, Cd, Pb, Zn. Only Cr (III) was immobilized under the acidic TCLP extraction conditions, however. Carbonation did not significantly change the overall metal retention characteristics of the geopolymer matrix.

The leachability of each doping metal is examined individually below, and compared with solid phase solubilities that were generated from geochemical equilibrium modeling. The resulting conclusions are summarized in Table 4-5.

Table 4-4 TCLP and SPLP leaching results for carbonated and non-carbonated samples of metal-doped geopolymer

Metal	Curing condition	TCLP leachate			SPLP leachate		
		/mg L ⁻¹	/μmol L ⁻¹	final pH	/mg L ⁻¹	/μmol L ⁻¹	final pH
Cd	carbonated	101 ± 12 ^a	900 ± 100	4.81	0.141 ± 0.006	1.25 ± 0.05	9.92
	non-carbonated	104 ± 16	920 ± 140	4.78	0.25 ± 0.02	2.22 ± 0.18	12.10
Cr(III)	carbonated	0.130 ± 0.001	2.50 ± 0.02	4.76	0.033 ± 0.005	0.58 ± 0.01	9.76
	non-carbonated	0.07 ± 0.01	1.35 ± 0.19	4.70	0.04 ± 0.01	0.77 ± 0.19	11.64
Cr(VI)	carbonated	70.9 ± 3.1	1363 ± 59	4.88	88.8 ± 1.6	1708 ± 31	9.85
	non-carbonated	77.7 ± 2.2	1494 ± 42	4.71	94.9 ± 4.2	1825 ± 81	11.89
Cu	carbonated	21.18 ± 0.58	333.3 ± 9.1	4.69	0.22 ± 0.07	3.5 ± 1.1	9.73
	non-carbonated	18.30 ± 0.28	288.0 ± 4.4	4.59	0.09 ± 0.03	1.41 ± 0.47	11.53
Pb	carbonated	33.55 ± 0.63	161.9 ± 3.0	4.50	0.27 ± 0.04	1.30 ± 0.19	9.59
	non-carbonated	32.4 ± 2.8	156 ± 13	4.62	0.49 ± 0.03	2.36 ± 0.14	11.70
Zn	carbonated	44.26 ± 0.80	677 ± 12	4.73	0.30 ± 0.04	4.59 ± 0.61	9.77
	non-carbonated	44.41 ± 0.36	679.3 ± 5.5	4.64	0.38 ± 0.08	5.8 ± 1.2	11.65

^a Standard deviation calculated from quadruplicate measurements.

Cadmium

TCLP and SPLP leachates of non-carbonated cadmium-doped cement contained no detectable Cd, in accordance with the reported effectiveness of cement at immobilizing this particular metal (Bishop, 1988; Cartledge *et al.*, 1990; Herrera *et al.*, 1992; Lange *et al.*, 1996a; Díez *et al.*, 1997; Li *et al.*, 2007; Erdem and Özverdi, 2011). This finding is also consistent with the low modeled solubility of Cd(OH)₂ (Fig. 4-1) and thus corroborates Cartledge *et al.*'s (1990) conclusion that cadmium is immobilized in the form of Cd(OH)₂ which is encapsulated on a microscopic scale with CSH and/or portlandite. Carbonation caused the pH of TCLP cement leachate to drop to 6.6, and yet the Cd concentration did not rise in accordance with the increased solubility of Cd(OH)₂. Cadmium availability in carbonated cement, therefore, was apparently controlled by otavite CdCO₃ (Fig. 4-1). Additionally, the fact that SPLP leachate contained no detectable Cd at pH 11.5 would suggest that otavite dissolved under alkaline leaching conditions and reprecipitated as cadmium hydroxide.

The SPLP leachate extracted from non-carbonated geopolymer contained 2.22 µmol L⁻¹ Cd at pH 12.1, close to that calculated solubility of Cd(OH)₂, which would suggest that Cd was again immobilized in the form of hydroxide. The leachate of carbonated geopolymer contained 1.3 µmol L⁻¹ at pH 9.9, which is compatible with Cd being held as the carbonate. The TCLP leachates of carbonated and non-carbonated geopolymer contained nearly 100% of the originally added Cd, which is consistent with the high solubility of both Cd(OH)₂ and CdCO₃ in acidic solution.

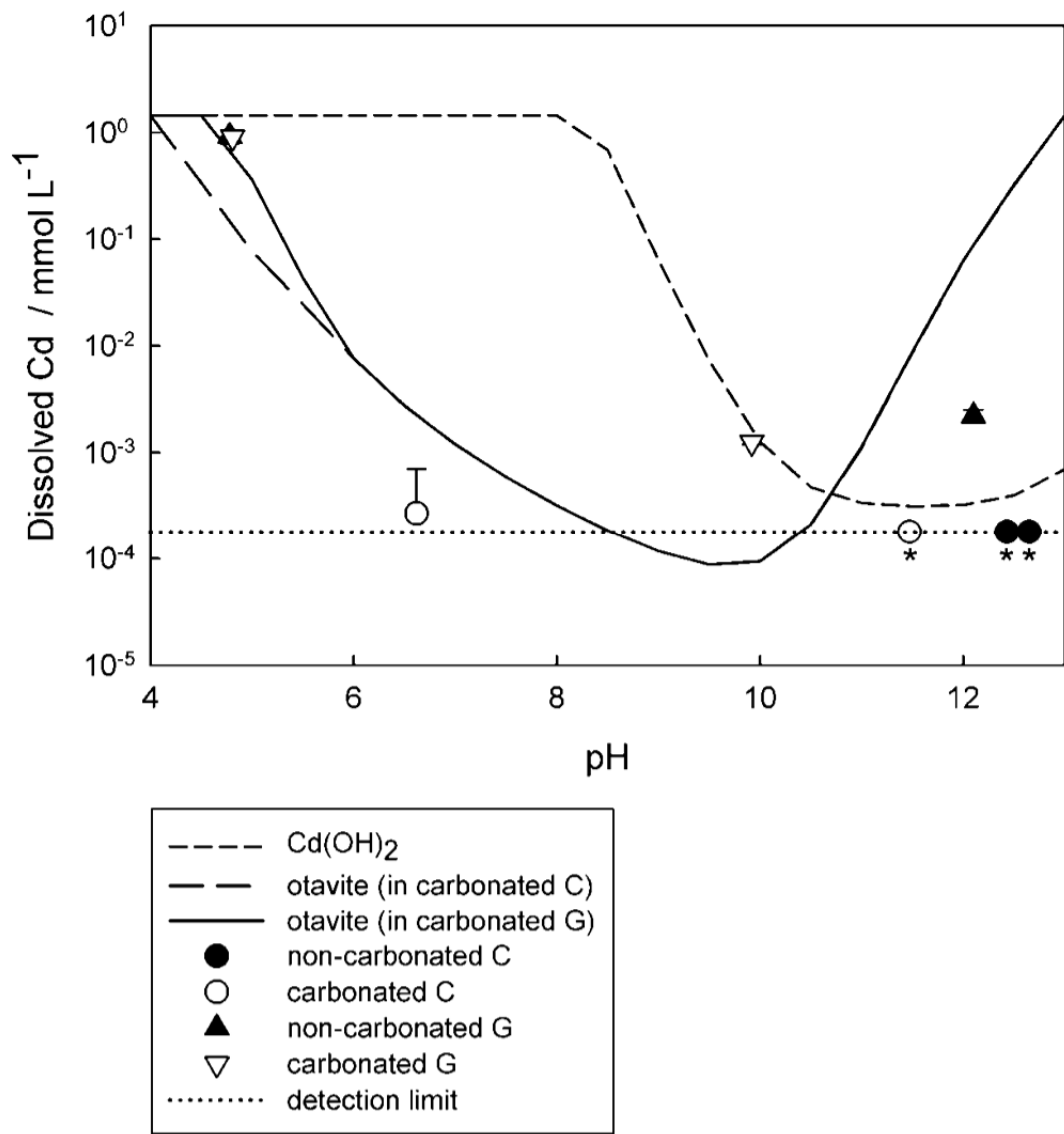


Fig. 4-1 Leachate Cd concentration and calculated mineral solubilities as a function of pH. The maximum concentration level shown corresponds to 100% extraction of the originally doped metal. Solubility curves for otavite diverge at pH<6 because the solubility of otavite (CdCO_3) is affected by the amount of CaCO_3 present in geopolymer or cement through the common-ion effect. Thus, the lower CaCO_3 content in carbonated geopolymer compared to carbonated cement results in higher otavite solubility for carbonated geopolymer at $\text{pH} < 6$. C = cement. G = geopolymer. * = below detection limit.

Chromium III

The TCLP and SPLP leachates of non-carbonated cement contained very little Cr(III) at pH 12.5 and 12.8 respectively, which is in accordance with the low predicted solubility of Cr(OH)₃ under such alkaline conditions (Figure 4-2). Other workers have proposed that Cr(III) may also substitutes for Si, Ca & Al in CSH and for Al & Fe in calcium aluminoferrite hydrates (Ivey *et al.*, 1990; Mollah *et al.*, 1992; Kindness *et al.*, 1994; Lin *et al.*, 1997; Sophia *et al.*, 2010). Carbonation had no major effect on the amount of Cr(III) that was leached from cement. The Visual MINTEQ database did not include Cr(III) carbonate solubility data, but Cr(OH)₃ would have been capable anyway of controlling Cr(III) availability under the present test conditions (Figure 4-2).

Geopolymer proved to be remarkably effective immobilizing Cr(III) over a wide range of pH values and carbonation conditions. Cr(OH)₃ appears to have controlled Cr(III) in the SPLP leachates of both non-carbonated and carbonated geopolymer. By contrast, the levels observed in acidic TCLP leachates were well below the predicted solubility of Cr(OH)₃, which indicates that another immobilization mechanism was active in carbonated and non-carbonated geopolymer.

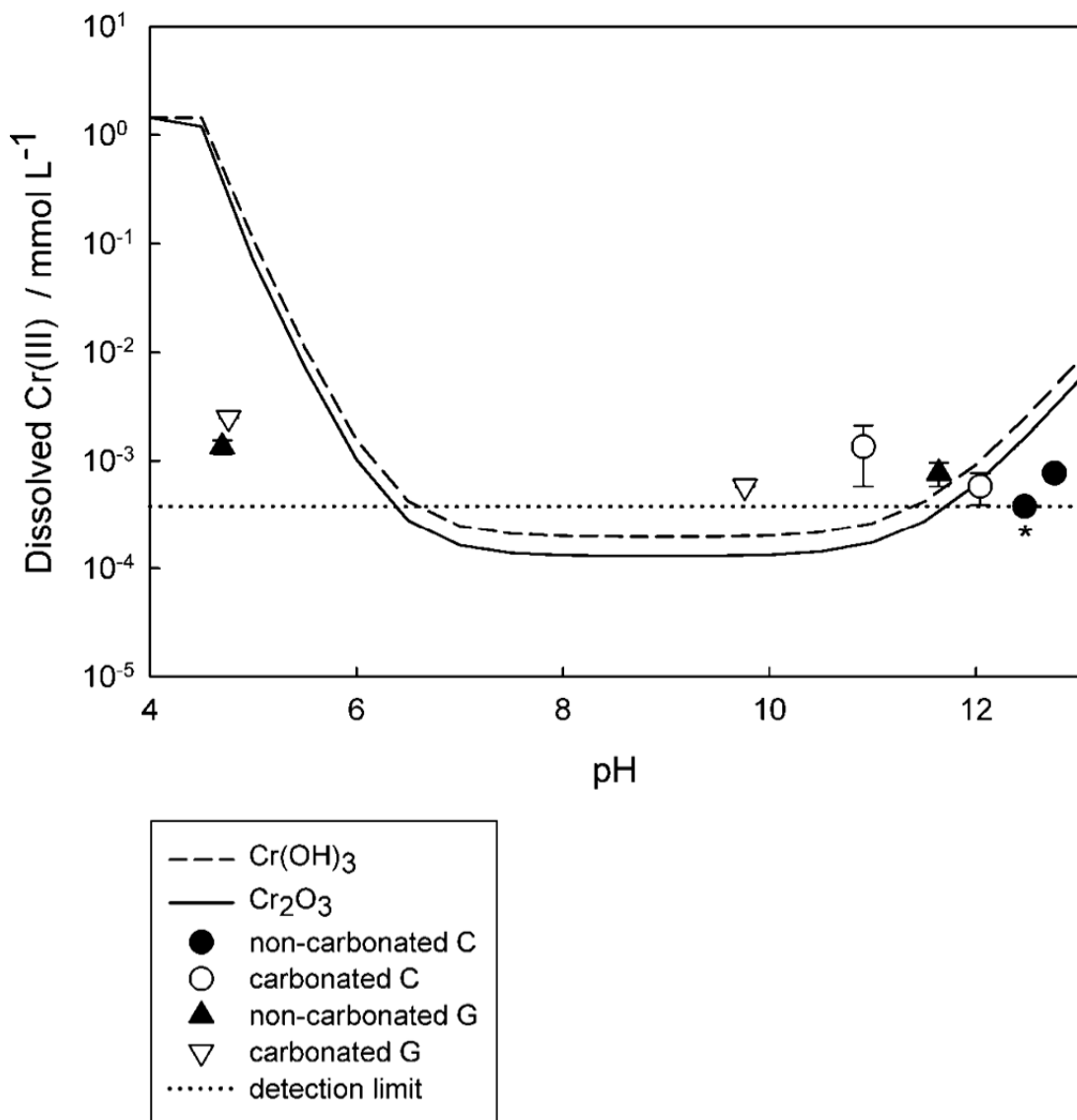


Fig. 4-2 Leachate Cr(III) concentration and calculated mineral solubilities as a function of pH.

The maximum concentration level shown corresponds to 100% extraction of the originally doped metal. C = cement. G = geopolymer. * = below detection limit.

Chromium VI

Cr(VI) was much more leachable than all the other metal ions in both non-carbonated and carbonated cement (Fig. 4-3) because it can not be precipitated by either hydroxide or carbonate ions (Zamorani *et al.*, 1988; Ivey *et al.*, 1990; Mollah *et al.*, 1992; Kindness *et al.*, 1994). The oxide CrO₃ is also fully soluble. Wang and Vipulanandan (2000) reported that Cr(VI) can react with dissolved calcium at high pH to form CaCrO₄. Geochemical modeling, however, indicates that it was Cr(VI)-ettringite ($\text{Ca}_6[\text{Al}(\text{OH})_6]_2(\text{CrO}_4)_3 \cdot 26\text{H}_2\text{O}$), the chromate analog of the sulfate mineral ettringite (Perkins and Palmer, 2000), and not CaCrO₄ that was responsible for controlling the leachability of Cr(VI) in non-carbonated cement under TCLP and SPLP test conditions (Fig. 4-3). Carbonation increased SPLP and TCLP leachate level three fold, but in neither case did the Cr(VI) concentration rise to the predicted level, which indicates that another, yet unknown, immobilization mechanism may be active for Cr(VI) in carbonated cement.

Cr (VI) was almost fully mobilized from geopolymer samples, non-carbonated and carbonated alike, in TCLP and SPLP tests spanning pH 4.7 to 11.9. Unable to be taken up as Cr(VI)-ettringite, it apparently remains within the pores of the geopolymer matrix as readily leachable CrO₄²⁻ (Zhang *et al.*, 2008b).

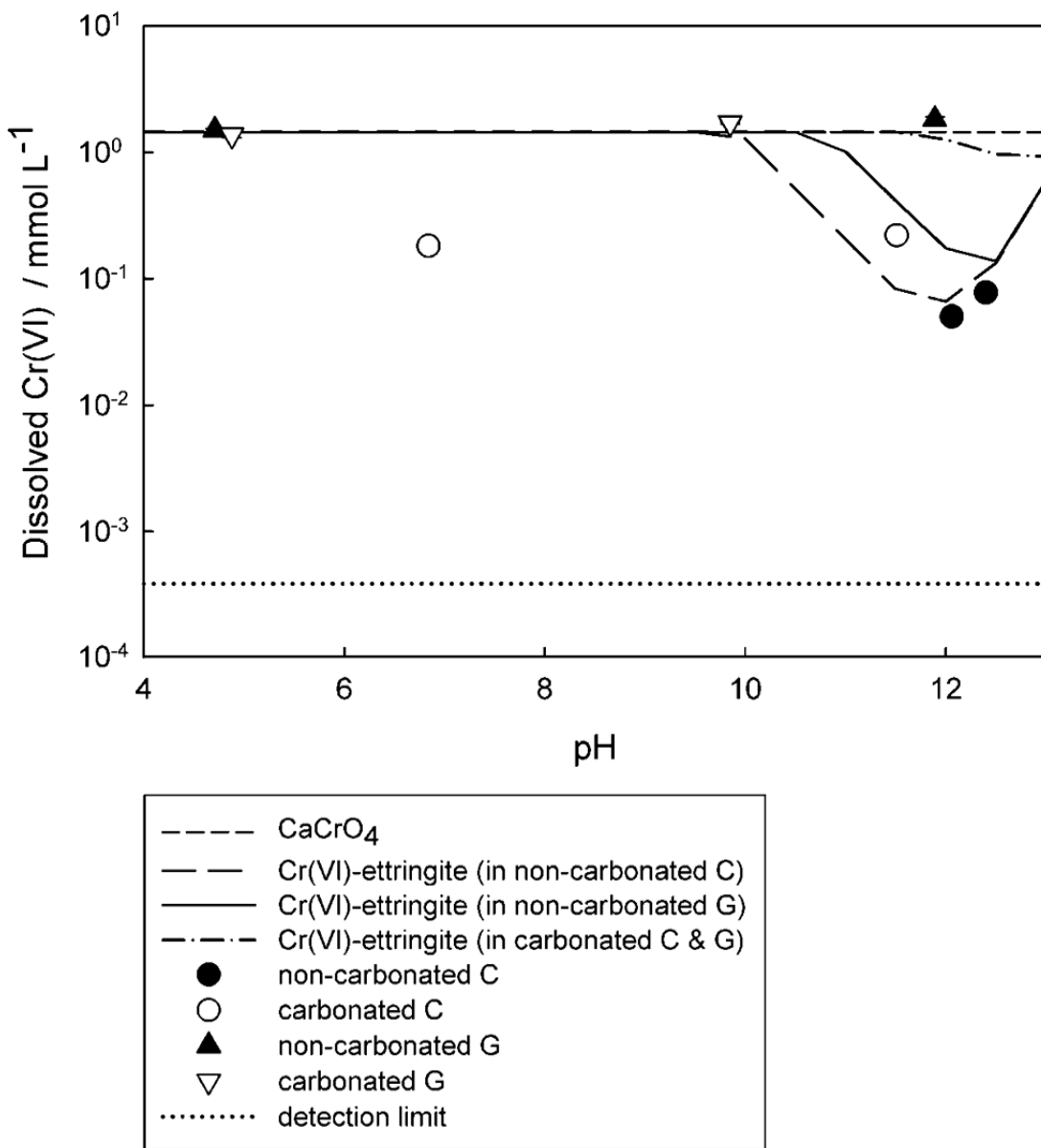


Fig. 4-3 Leachate Cr(VI) concentration and calculated mineral solubilities as a function of pH.

The maximum concentration level shown corresponds to 100% extraction of the originally doped metal. Solubility curves for Cr(VI)-ettringite diverge because the solubility of Cr(VI)-ettringite is affected by the amount of $\text{Ca}(\text{OH})_2$ present in geopolymer or cement through the common-ion effect. Thus, the lower $\text{Ca}(\text{OH})_2$ content in geopolymer compared to cement results in higher Cr(VI)-ettringite solubility for geopolymer at $\text{pH} > 10$. C = cement. G = geopolymer.

Copper

The highly alkaline TCLP and SPLP leachates of non-carbonated Cu-doped cement contained no detectable copper. Geochemical modeling (Fig. 4-4) indicated that the metal was immobilized as tenorite (CuO), consistent with the findings of Li *et al.* (2001). TCLP leachate of carbonated cement contained nearly $6 \mu\text{mol L}^{-1}$ Cu at $\text{pH} = 6.8$ which, being close to the solubility of both malachite ($\text{Cu}_2(\text{OH})_2\text{CO}_3$) and tenorite (CuO), would suggest that one or both phases controlled Cu leachability. SPLP leachate contained no detectable Cu at $\text{pH} 11.6$, however, which indicates that tenorite and not malachite controlled availability of Cu in carbonated cement.

Geopolymer was less effective at immobilizing copper. The SPLP leachate of the non-carbonated matrix contained $1.4 \mu\text{mol L}^{-1}$ Cu, indicating that it was more likely trapped in the form of Cu(OH)_2 than as tenirite (Fig. 4-4). Carbonation increased the SPLP leachate concentration to $3.5 \mu\text{mol L}^{-1}$, which is above the solubility of both Cu(OH)_2 and malachite, but below that of CuCO_3 . Under acidic TCLP test conditions, Cu was not effectively immobilized in either the non-carbonated or carbonated matrix due to the high solubility of both the hydroxide and carbonate phases.

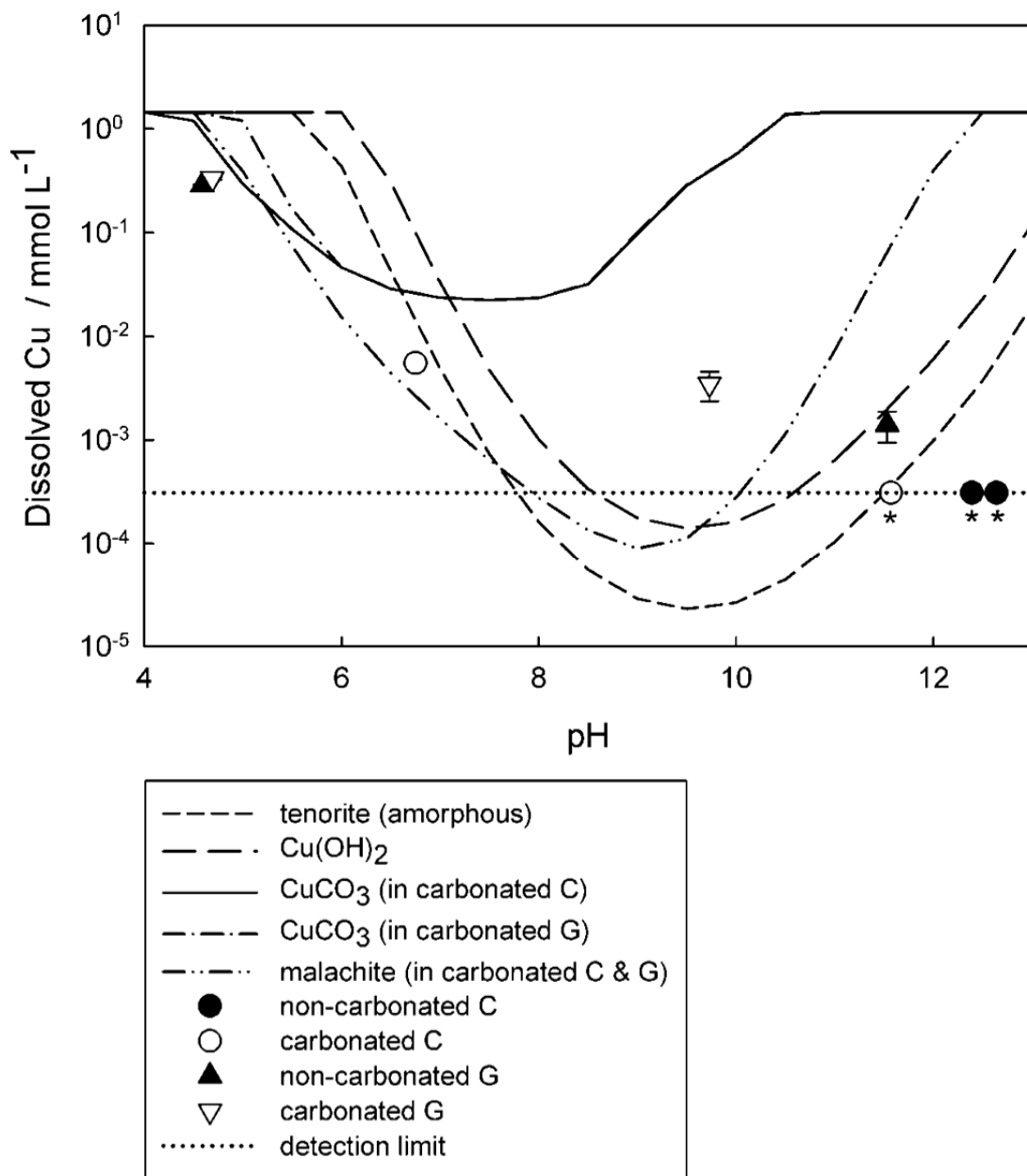


Fig. 4-4 Leachate Cu concentration and calculated mineral solubilities as a function of pH. The maximum concentration level shown corresponds to 100% extraction of the original doped metal. Solubility curves for CuCO_3 as well as for malachite ($\text{Cu}_2(\text{OH})_2\text{CO}_3$) diverge because of the high CaCO_3 content of carbonated cement compared with carbonated geopolymers. C = cement. G = geopolymers. * = below detection limit.

Lead

The lead concentrations in the TCLP and SPLP leachates of non-carbonated cement were higher than those obtained for all other metals except Cr(VI) and was similar to the calculated solubility of $\text{Pb}(\text{OH})_2$ (Fig. 4-5). Several other lead hydroxide and oxide phases were modeled (e.g. $\text{Pb}_2\text{O}(\text{OH})_2$, PbO , $\text{PbO}\cdot 0.3\text{H}_2\text{O}$, Pb_2OCO_3 , $\text{Pb}_{10}(\text{OH})_6\text{O}(\text{CO}_3)_6$, $\text{Pb}_3\text{O}_2\text{CO}_3$), but all were significantly more soluble than $\text{Pb}(\text{OH})_2$ over the tested pH range. Lead was the only metal tested whose TCLP and SPLP leachate levels consistently decreased as a result of cement carbonation. The TCLP leachate level ($0.15 \mu\text{mol L}^{-1}$ at pH 6.9) approached the calculated solubilities of both cerrusite (PbCO_3) and hydrocerrusite ($\text{Pb}_3(\text{OH})_2(\text{CO}_3)_2$), indicating that either carbonate phase could be responsible for controlling Pb availability. The SPLP leachate level ($0.9 \mu\text{mol L}^{-1}$ at pH 11.6) was much lower than the solubility of either cerrusite or hydrocerrusite, and was similar to the solubility of $\text{Pb}(\text{OH})_2$.

Non-carbonated geopolymer was slightly more effective than non-carbonated cement at immobilizing Pb during the SPLP test. Geochemical modeling indicates that the controlling phase in both matrices was probably $\text{Pb}(\text{OH})_2$, with the small disparity in leachate concentrations being attributable to the small pH differences (Figure 4-5). Carbonation reduced the SPLP leachate concentration to $1.3 \mu\text{mol L}^{-1}$ at pH 9.6, which was similar to the solubility of cerrusite. Geopolymers, whether non-carbonated or carbonated, were poor at immobilizing Pb under the TCLP test conditions due to high solubility of the hydroxide and carbonate phases at low pH.

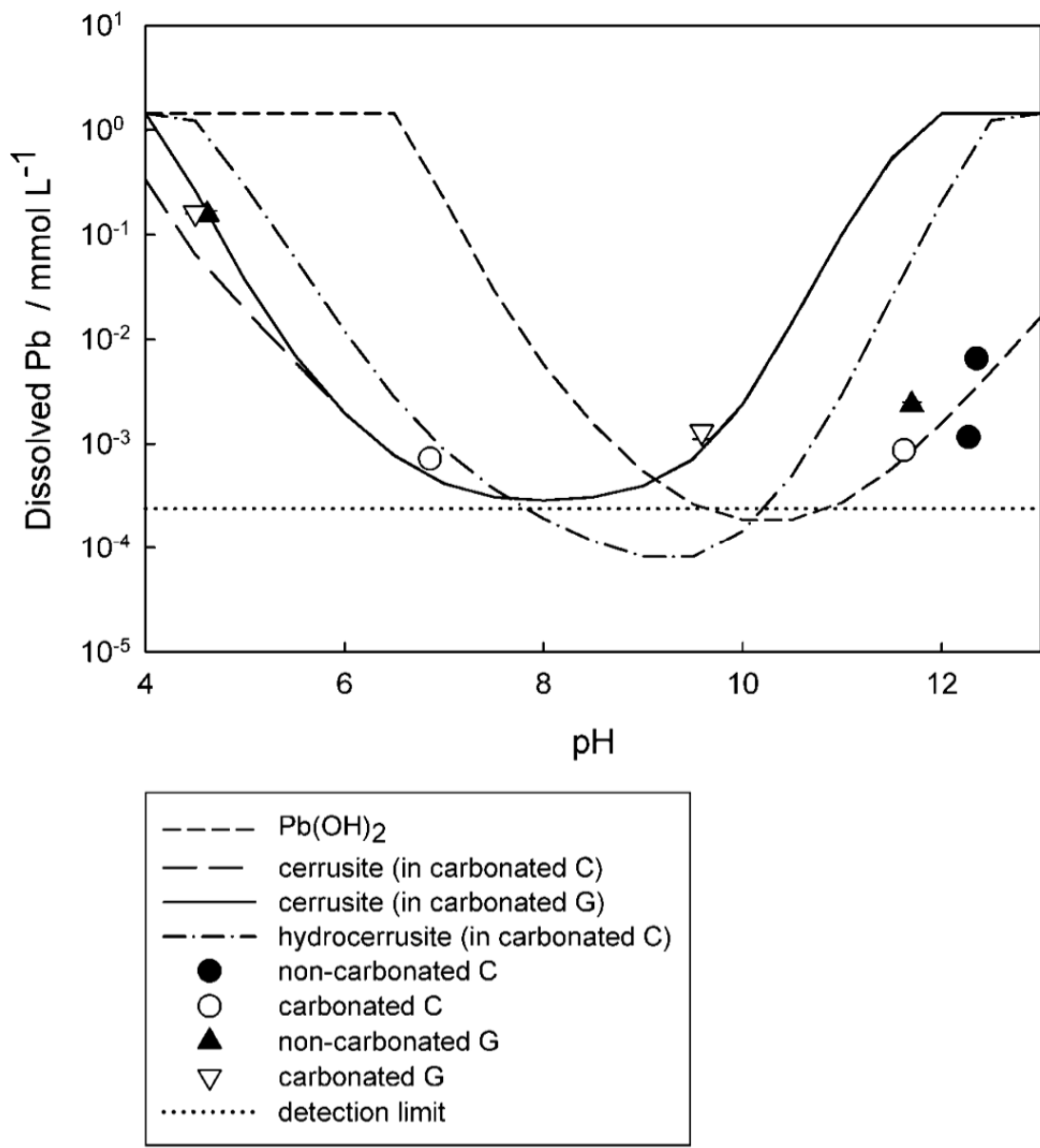


Fig. 4-5 Leachate Pb concentration and calculated mineral solubilities as a function of pH. The maximum concentration level shown corresponds to 100% extraction of the originally doped metal. Solubility curves for cerrusite (PbCO_3) diverge because of the high CaCO_3 content of carbonated cement compared with geopolymer. C = cement. G = geopolymer.

Zinc

Zn concentrations in the TCLP and SPLP leachates of non-carbonated cement were significantly below the solubility of either amorphous or crystalline Zn(OH)₂ (Figure 4-6), in accordance with previous reports of Zn forming a solid solution with CSH (Tommaseo and Kersten (2002); Ziegler *et al.*, 2001). The TCLP and SPLP leachate concentration for carbonated cement were somewhat higher, but well below the solubility of Zn carbonates. Using a Gibbs energy minimization model, Kulik and Kersten (2001) predicted that carbonation causes re-partitioning of Ca and Zn into a carbonate solid solution that coexist with amorphous silica.

Geopolymer was much less effective than cement at immobilizing zinc, presumably owing to differences in the amount and chemical/physical nature of the silicate content. The SPLP zinc concentration was similar to the zincite (ZnO) solubility in non-carbonated geopolymer and to the hydrozincite Zn₅(CO₃)₂(OH)₆ solubility in the carbonated matrix (Figure 4-6). As with most other metals tested, geopolymer was ineffective at immobilizing zinc under TCLP leaching conditions owing to the high solubility of hydroxide and carbonate phases at low pH.

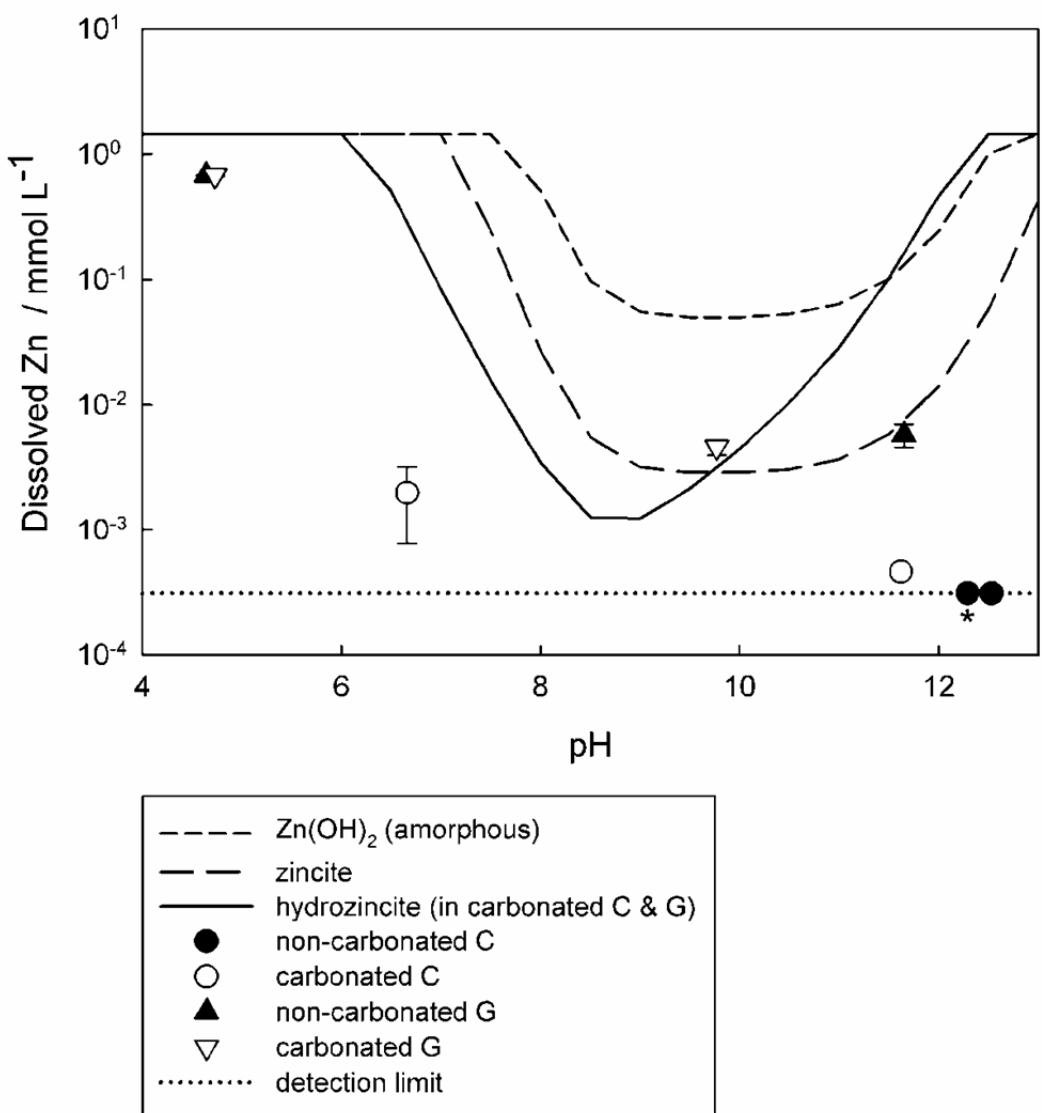


Fig. 4-6 Leachate Zn concentration and calculated mineral solubilities as a function of pH. The maximum concentration level shown corresponds to 100% extraction of the originally doped metal. Solubility curves for hydrozincite ($\text{ZnS}(\text{CO}_3)_2(\text{OH})_6$) diverge because of the high CaCO_3 content of carbonated cement compared with carbonated geopolymers. The solubility curves for ZnCO_3 , $\text{ZnCO}_3 \cdot \text{H}_2\text{O}$ and crystalline Zn(OH)_2 have been excluded from the figure for clarity and because they offered no additional insight. C = cement. G = geopolymer. * = below detection limit.

Table 4-5 Phases controlling metal immobility in cement and geopolymers matrices (in accordance with geochemical equilibrium modeling)

Metal	Cement		Geopolymer	
	non-carbonated	carbonated	non-carbonated	carbonated
Cd	Cd(OH) ₂	CdCO ₃ ^a	Cd(OH) ₂ ^c	CdCO ₃ ^c
Cr(III)	Cr(OH) ₃	Cr(OH) ₃ ^b	unidentified solid	unidentified solid ^b
Cr(VI)	Cr(VI)-ettringite	unidentified solid	pore water	pore water
Cu	CuO	CuO	Cu(OH) ₂ ^c	CuCO ₃ ^c
Pb	Pb(OH) ₂	PbCO ₃ or Pb ₃ (OH) ₂ (CO ₃) ₂ ^a	Pb(OH) ₂ ^d	PbCO ₃ ^{a,d}
Zn	unidentified solid	unidentified solid	ZnO ^c	Zn ₅ (CO ₃) ₂ (OH) ₆ ^c

^a Reprecipitates as hydroxide in SPLP test. ^b No data for carbonate phase. ^c Freely soluble in TCLP test. ^d Partially soluble in TCLP test.

Aluminum

Although aluminum was not added as a dopant in any of our samples, leaching of aluminum from geopolymers is a potential concern because the fly ash used to produce geopolymers contained large quantities of this element (Table 3-1). The toxicity of Al to fish and other aquatic organisms at levels as low as 25 µg/L and in a range of pH values from acidic to alkaline is well established (World Health Organization, 1997). Penney *et al.*, 2009 found that Al concentrations in the effluent of a column containing 100% fly ash permeated with pure water ranged from 10 to 50 mg L⁻¹. Table 4-6 reports that the concentrations of Al in the TCLP and SPLP leachates of our carbonated and non-carbonated geopolymers samples ranged from 0.3 to

39.6 mg L^{-1} . The largest Al concentrations was obtained at the lowest leachate pH values ($\text{pH} = 4.60$). Overall, the results suggest that geopolymers reduced the leachability of Al from fly ash.

Table 4-6 Aluminum concentration in TCLP and SPLP leachates for carbonated and non-carbonated geopolymers samples

Curing condition	TCLP leachate			SPLP leachate		
	/mg L ⁻¹	/μmol L ⁻¹	final pH	/mg L ⁻¹	/μmol L ⁻¹	final pH
carbonated	10.65 ± 0.73^a	394 ± 27	4.78	0.30 ± 0.02	11.1 ± 7.4	10.01
non-carbonated	39.6 ± 3.4	1460 ± 130	4.60	8.8 ± 2.4	326 ± 89	11.91

^a Standard deviation calculated from quadruplicate measurements.

4.2. Compressive strength

Table 4-7 shows compressive strength and extent of carbonation for cubes of metal-doped cement and geopolymers following 24 days of curing. All samples greatly exceeded the generally required compressive strength for s/s wasteforms which is ca. 0.7 MPa (Hills and Pollard, 1997).

Table 4-7 Compressive strength and extent of carbonation at 24 days for sample cubes of metal-doped cement and geopolymers

Metal	Compressive strength /MPa			
	Cement		Geopolymer	
	non-carbonated	carbonated (vol% carbonation)	non-carbonated	carbonated (vol% carbonation)
none	58.8 ± 4.6 ^a	74.0 ± 3.6 (93.1 ± 3.2)	52.4 ± 1.7	46.3 ± 2.1 (81.4 ± 2.5)
Cd	53.2 ± 2.7	66.6 ± 2.5 (92.6 ± 2.1)	44.3 ± 0.0	39.4 ± 2.7 (84.8 ± 3.0)
Cr(III)	48.8 ± 3.1	58.6 ± 1.5 (92.1 ± 2.1)	39.4 ± 4.4	34.2 ± 8.0 (80.0 ± 0.1)
Cr(VI)	42.1 ± 2.6	49.5 ± 4.9 (91.3 ± 2.3)	43.1 ± 1.6	41.5 ± 1.1 (82.4 ± 3.6)
Cu	40.7 ± 2.3	53.4 ± 1.6 (93.0 ± 2.4)	46.9 ± 5.0	40.7 ± 3.7 (84.8 ± 2.0)
Pb	42.7 ± 3.2	55.1 ± 4.0 (94.2 ± 2.2)	52.1 ± 9.9	45.6 ± 2.7 (85.6 ± 3.5)
Zn	45.9 ± 4.6	57.4 ± 2.8 (92.0 ± 3.9)	44.3 ± 5.0	41.7 ± 1.7 (85.8 ± 2.9)

^a Standard deviations are calculated from quadruplicate measurements.

Depending on the doping metal they contained, the cement samples which had been cured under CO₂ exhibited 91-94 vol% carbonation and yielded compressive strengths that were 18-31% higher than those of corresponding non-carbonated cements. Other researchers have reported similar strength gains caused by carbonation during curing and attributed these increases to the transformation of calcium hydroxide (the most abundant cement hydration product after CSH) to lower density calcium carbonate which grows into and fills the cement matrix pores (Chen *et al.*, 2009a; Bertos *et al.*, 2004). The literature is contradictory concerning the effects of metal doping on strength development in cement, however, due to the use of widely varying experimental conditions (Olmo *et al.*, 2001;

Gineys *et al.*, 2010). In the present study each metal was applied separately at a fixed molar dosage (0.029 mol per kg matrix) as alkaline waste sludge. For non-carbonated cement, doping caused compressive strength to decrease by 10-31% depending on the metal. The magnitude of the effect increased as: Cd ≤ Cr(III) ≤ Zn ≤ Pb ~ Cr(VI) ≤ Cu. The influence of metal doping was similar for carbonated cement, with copper again having the largest effect in keeping with its well documented retarding properties (Zain *et al.*, 2004).

Geopolymer cubes cured under CO₂ exhibited 80-86 vol% carbonation. In contrast to the effect observed for cement, carbonation caused the compressive strength of geopolymers samples to drop by 4-13%, depending on the type of metal added. In the absence of Ca(OH)₂ and CSH, CO₂ is thought to react with the geopolymer matrix to form Na₂CO₃, thus decreasing its alkalinity and, in turn, suppressing fly ash activation and development of strength (Davidovits, 2005).

Metal doping caused strength of non-carbonated geopolymers to decrease by 10-25% as in the case of cement. The influence increased as: Cu ≤ Cd ~ Zn ≤ Cr(VI) ≤ Cr(III). The exception was lead, which had no apparent effect on strength. The trend was similar albeit not identical for carbonated cement, with Cr(III) having the greatest detrimental effect and Pb having none.

4.3. Microstructure and Micro-mineralogy Study

Figure 4-7, and 4-8 show non-carbonated and carbonated cement samples under SEM (Scanning Electron Microscope). There were no noticeable visual differences in the control and the metal doped samples. This could be due to the low concentration of doped metals. As

seen in Figure 4-7 and 4-8, the pore volume of non-carbonated sample may be greater than that of the carbonated sample. This is consistent with the studies using image analysis on cement stabilized wastes which have shown a decrease of up to 26% in the observable pore volume in carbonated samples (Johannesson and Utgenannt, 2001). Carbonation causes precipitation of calcite in the pores, decalcification of C-S-H gel and the production of gypsum from the decomposition of ettringite. Several EDS readings were taken from various points in the carbonated and non-carbonated samples. The readings were taken at C-S-H gel, $\text{Ca}(\text{OH})_2$, unreacted cement particles and CaCO_3 phases. Except for the case of Cr(VI) doped samples, metal ions were under the detection limit of EDS. The elemental percentages of various phases of the carbonated and non-carbonated cement samples are shown in Table 4-8. The elemental percentages of Cd, Cu, Cr(III), Cr(VI), Pb and Zn provided in Table 4-8 are the average values from the respective metal doped samples.

SEM/EDS analysis could not be used to corroborate whether Cr(VI) was present as Cr(VI)-ettringite in non-carbonated cement samples. This is because ettringite was likely inter-dispersed within the C-S-H phase (Scrivener and Taylor, 1993; Yang *et al.*, 1996), thus the two phases could not be distinguished from each other.

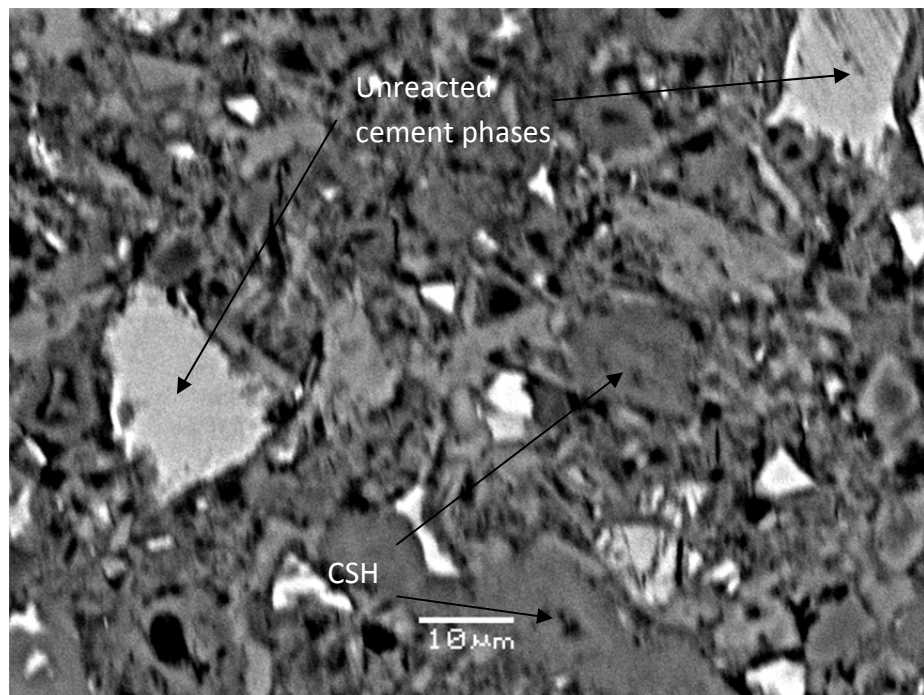


Fig. 4-7 Non-carbonated cement sample under SEM showing different phases

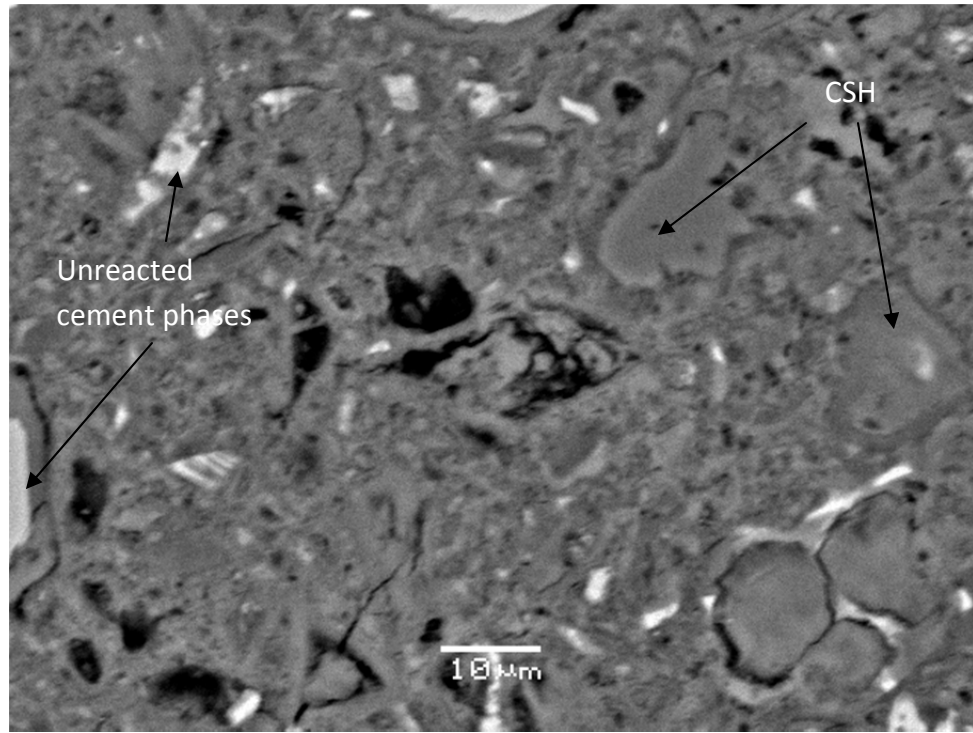


Fig. 4-8 Carbonated cement sample under SEM showing different phases

Figure 4-9, 4-10 and 4-11 show non-carbonated and carbonated geopolymers samples under SEM. There were no noticeable visual differences in the control and the metal doped samples. This could be due to the low concentration of doped metals. There are no noticeable visual differences between the carbonated as well as non-carbonated samples. The matrix consists of many cracks fine running through them. These cracks are likely to be caused during the compressive strength tests, from which the samples were taken to prepare the SEM slides. Zhang et al. (2008) also reported microcracks in fly ash-geopolymers, which they reported to be due to mechanical damage during sample preparation or due to the drying process. The samples contain both unreacted fly ash and sand particles. Unreacted components of fly ash based geopolymer binder make up a significant proportion of the total volume of the binder (Stevenson and Sagoe-Crentsil, 2005; Chindaprasirt et al., 2009). These components are composites, thus the strength of the unreacted particles, the interface between them and geopolymer matrix all have significant roles in the final strength of the material. The elemental percentages in the geopolymer matrix of the carbonated and non-carbonated samples are shown in Table 4-9. The composition of the all doped metals was below the detection limit of the instrument. This may be due to the low concentration of the metals mixed in the samples. The major components found in all specimens were Si, Al, Na and Ca. Other elements such as Mg, K and Fe were found in lower quantities. This confirms that the matrix of geopolymer concrete mainly comprises Si-Al-O. Na comes from the sodium silicate and NaOH in the activating solution. The large amount of Ca is due to the high amount of CaO in the fly ash (13.6%). The elemental percentages of all components in both carbonated as well as non-carbonated samples were virtually the same. Thus, no

conclusion could be reached from SEM-EDS studies on the causes for the decrease in compressive strength in the carbonated samples.

Our study has focused on the effects of the solubility of metal precipitates on metal leachability. However, metal leachability also depends on the permeability of the matrix, which is the function of pore structure and the size distribution of pore openings (Conner, 1990; Van Jaarsveld & Van Deventer, 1999b). Matrix permeability has also been reported as one of the important physical properties linking the strength of the matrix to contaminant leachability (Davis et al., 1994).

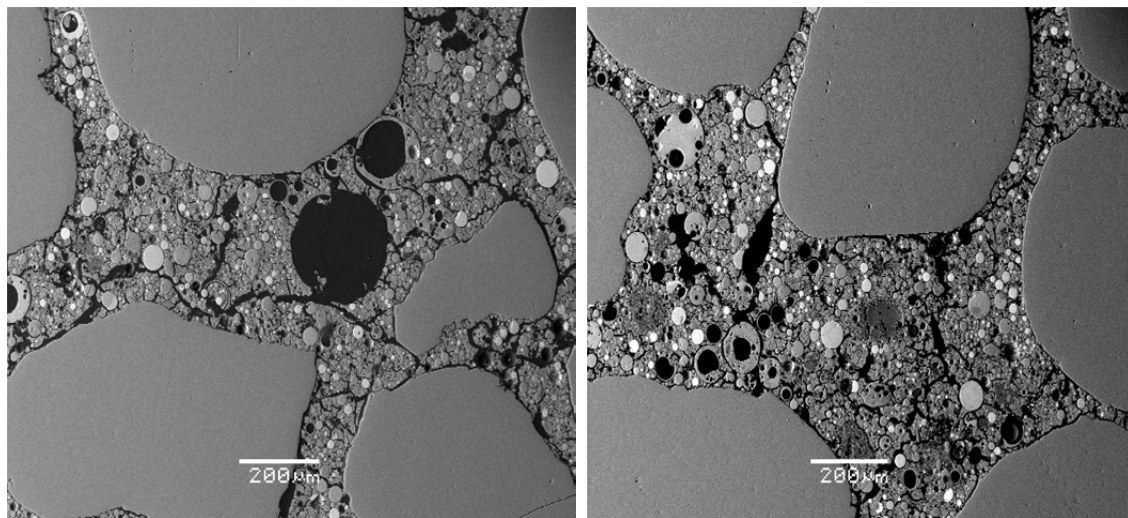


Fig. 4-9 Non-carbonated and carbonated (left to right) geopolymer samples under SEM showing the geopolymer matrix between sand grains

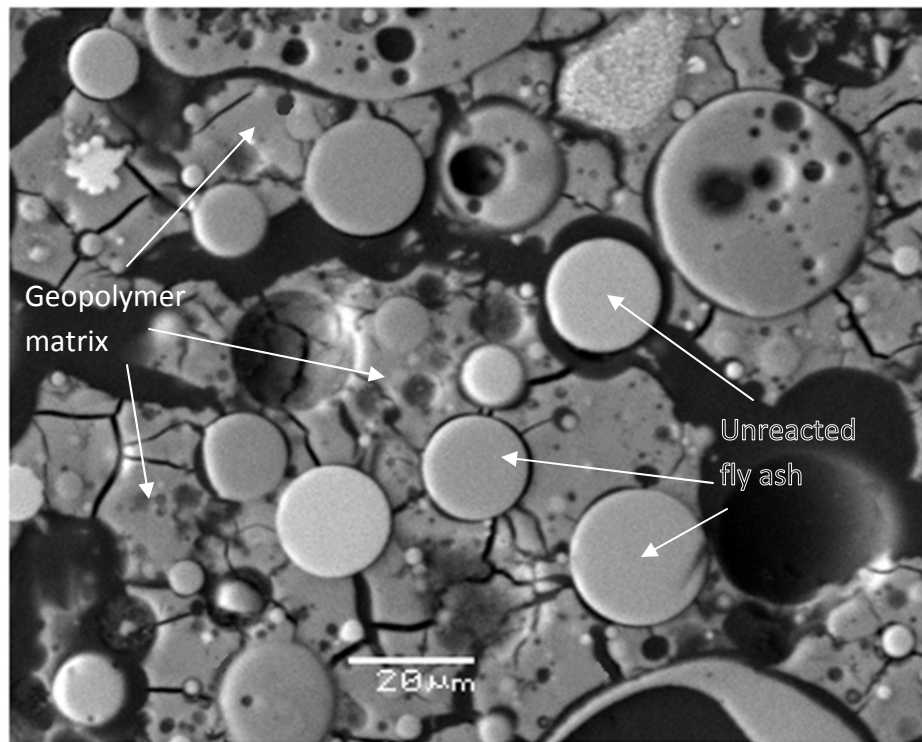


Fig. 4-10 Non-carbonated geopolymer matrix in between sand grains

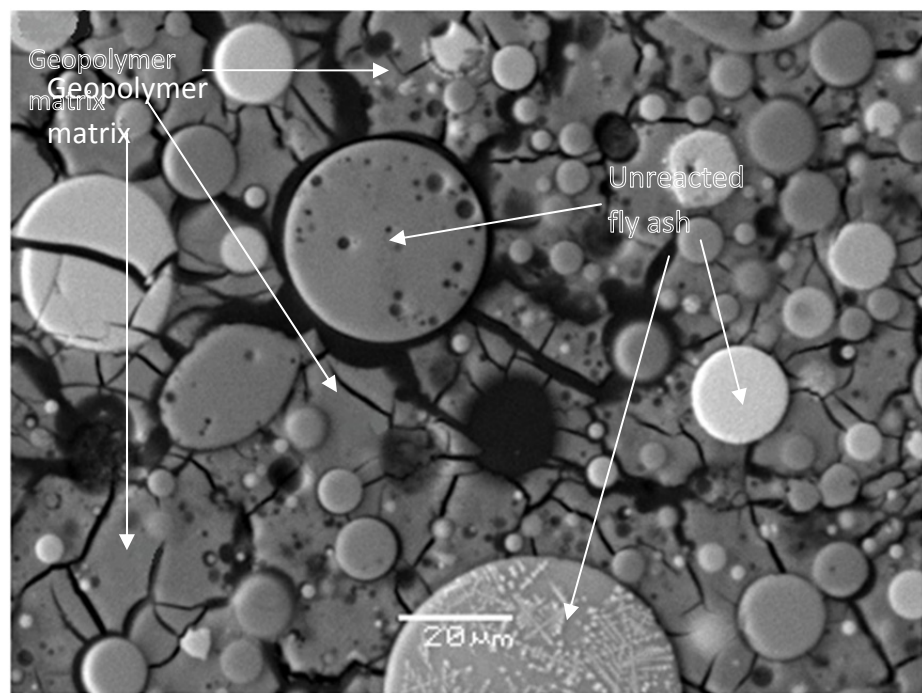


Fig. 4-11 Carbonated geopolymer matrix in between sand grains

Table 4-8 Elemental composition of CSH, Ca(OH)₂ and CaCO₃ phases of carbonated and non-carbonated cement samples

Elements (wt%)	Non-carbonated		Carbonated	
	CSH	Ca(OH) ₂	CSH	CaCO ₃
Na	<DL ^a	<DL	<DL	<DL
Mg	0.31 ± 0.04	<DL	0.38 ± 0.05	<DL
Al	0.98 ± 0.06	<DL	1.09 ± 0.07	<DL
Si	9.24 ± 0.42	1.13	9.31 ± 0.31	0.38 ± 0.04
S	1.08 ± 0.08	<DL	0.61 ± 0.10	<DL
K	0.33 ± 0.03	<DL	<DL	<DL
Ca	28.42 ± 0.81	36.79 ± 0.76	30.82 ± 0.92	38.54 ± 1.03
Fe	0.67 ± 0.07	<DL	0.78 ± 0.06	<DL
Cd	<DL	<DL	<DL	<DL
Cu	<DL	<DL	<DL	<DL
Cr(III)	<DL	<DL	<DL	<DL
Cr(VI)	0.35 ± 0.02	<DL	0.34 ± 0.04	<DL
Pb	<DL	<DL	<DL	<DL
Zn	<DL	<DL	<DL	<DL

^a Standard deviation were calculated from more than 20 measurements

Table 4-9 Elemental composition of the geopolymer matrix of carbonated and non-carbonated geopolymer samples

Element (wt%)	Non-carbonated	Carbonated
Na	8.43 ± 0.42 ^a	7.10 ± 0.39
Mg	0.86 ± 0.66	0.86 ± 0.54
Al	6.32 ± 0.86	6.56 ± 0.43
Si	21.23 ± 1.54	19.61 ± 0.96
K	0.35 ± 0.05	0.26 ± 0.08
Ca	7.79 ± 0.14	7.55 ± 0.49
Fe	1.70 ± 0.09	1.48 ± 0.15
Cd	<DL	<DL
Cu	<DL	<DL
Cr(III)	<DL	<DL
Cr(VI)	<DL	<DL
Pb	<DL	<DL
Zn	<DL	<DL

^a Standard deviation were calculated from more than 20 measurements

5. Conclusions

1. Cement (OPC) s/s matrix that was doped with $0.029 \text{ mol kg}^{-1}$ alkaline metal sludge during mixing, and cured 28 days, was effective at immobilizing Cd, Cr(III), Cu and Zn under both SPLP and TCLP testing conditions, reasonably effective at retaining Pb, and ineffective for retaining Cr(VI). When aggressively carbonated during the curing period, the cement maintained its ability to immobilize Cd, Cr(III) and Zn, performed much better at retaining Pb, and, under acidic TCLP conditions, was much worse at retaining Cu.
2. Similarly prepared fly ash-based geopolymer matrix was effective at immobilizing Cr(III) and Cu, and, to a lesser degree, Cd, Pb and Zn in SPLP leaching tests. Only Cr(III) was immobilized under comparatively acidic TCLP testing conditions. Carbonation did not significantly change the metal retention characteristics of the geopolymer matrix.
3. For non-carbonated cement, metal doping caused compressive strengths to decrease by 10-31%, depending on the metal, (Cu had the largest impact and Cd the smallest). Carbonated cement samples exhibited compressive strengths that were 18-31% higher than those of corresponding non-carbonated cements.
4. Metal doping caused similar declines in the compressive strength of non-carbonated geopolymer, ranging from 0% for Pb to 25% for Cr(III). In contrast to cement, however, geopolymer matrices exhibited 4-13% additional loss in strength upon carbonation. Nevertheless, all samples greatly exceeded the strength requirements for s/s wasteforms.
5. Geochemical equilibrium modeling was effective at providing insight on the mechanisms of metal immobilization.

6. SEM-EDS analyses were not conclusive on the effect of carbonation on the fixation of metals in both cement and geopolymer samples because metals concentrations were generally below the EDS detection limit.

6. Recommendations For Future Research

Further research into the effects of carbonation on compressive strength and leachability of geopolymer-based s/s-treated wastes should address the following aspects:

- Testing the leachability of geopolymer treated s/s-waste samples at several systematic pH values between 2 and 13 using a parallel extraction procedure similar to TCLP 1313. This would allow a more precise determination of controlling solid phases.
- Using aluminosilicate precursors other than Type C fly ash (e.g. blast furnace slag or Type F fly ash) for the preparation of geopolymer.
- Test actual industrial wastes in addition to synthetic metal hydroxide sludges.

7. References

- Alba N., Vázquez E., Gassó S., Baldasano J.M., Stabilization/solidification of MSW incineration residues from facilities with different air pollution control systems. Durability of matrices versus carbonation, *Waste Management*, 21(4):313-323, 2001.
- Allison J.D., Brown D.S., Novo-Gradac K.J., MINTEQA2/PRODEFA2, A geochemical assessment model for environmental systems: Version 3.0 User's Manual. Environmental Research Laboratory, Georgia, USA, 1991.
- Asavapisit S., Fowler G., Cheeseman C.R., Solution chemistry during cement hydration in the presence of metal hydroxide wastes, *Cement and Concrete Research*, 27(8):1249-1260, 1997.
- ASTM D1633, Standard test methods for compressive strength of molded soil-cement cylinders, American Society for Testing and Materials, West Conshohocken, PA, 2006a.
- ASTM D560, Standard test methods for freezing and thawing compacted soil-cement mixtures, American Society for Testing and Materials, West Conshohocken, PA, 2006b.
- ASTM C778-06, Standard specification for standard sand, American Society for Testing and Materials, West Conshohocken, PA, 2006c.
- ASTM C305-06, Standard practice for mechanical mixing of hydraulic cement pastes and mortars of plastic consistency, American Society for Testing and Materials, West Conshohocken, PA, 2006d.
- ASTM C109/C109M-08, Standard Test Method for Compressive Strength of Hydraulic Cement Mortars (Using 2-in. or [50-mm] Cube Specimens), American Society for Testing and Materials, West Conshohocken, PA, 2008a.
- ASTM C618-08a, Standard specification for coal fly ash and raw or calcined natural pozzolan for use in concrete, American Society for Testing and Materials, West Conshohocken, PA, 2008b.
- ASTM C150/C150M-09, Standard specification for portland cement, American Society for Testing and Materials, West Conshohocken, PA, 2009.
- Batchelor B., Overview of waste stabilization with cement, *Waste Management*, 26:689-698, 2006.

Bertos M.F., Simons S.J.R., Hills C.D., Carey P.J., A review of accelerated carbonation technology in the treatment of cement-based materials and sequestration of CO₂, Journal of Hazardous Materials, 112(3):193-205, 2004.

Bin Shafique M.S., Walton J.C., Gutierrez N., Smith R.W., Tarquin A.J., Influence of carbonation on leaching of cementitious wasteforms, Journal of Environmental Engineering, 124(5):463-467, 1998.

Bishop P.L., Leaching of inorganic hazardous constituents from stabilized/ solidified hazardous wastes, Hazardous Waste and Hazardous Materials, 5:129-143, 1988.

Blasing T.J., Hand K., Monthly carbon emissions from natural-gas flaring and cement manufacture in the United States, Tellus, 59(1):15-21, 2007.

Buchwald A., Schulz M., Alkali-activated binders by use of industrial by-products, Cement Concrete Research, 35(5):968-973, 2005.

Burgatsacaze V., Craste L., Guerre P., Cadmium in the food chain : a review, Revue de Medecine Veterinaire, 147(10):671-680, 1996.

Butcher E.J., Cheeseman C.R., Sollars C.J., Perry R., Flow-through leach testing of solidified waste using a modified triaxial cell, Environmental Technology, 14(2):113-124, 1993.

Cartledge F.K., Butler L.G., Chalasani D., Eaton H.C., Frey F.P., Herrera E., Tittlebaum M.E., Yang S., Immobilization Mechanisms in Solidification/Stabilization of Cd and Pb Salts Using Portland Cement Fixing Agents, Environmental Science and Technology, 24:867-873, 1990.

Catalan L.J.J., Merlière E., Chezick C., Study of the physical and chemical mechanisms influencing the long-term environmental stability of natrojarosite waste treated by stabilization/solidification, Journal of Hazardous Materials, 94(1):63-98, 2002.

Catalan L.J.J., K.L. Wetteskind, Alkalinity Depletion by Flow-Through Leaching in Stabilized/Solidified Natrojarosite Waste, Proceedings of Waste Management 2002, Cadiz, Spain,

4 – 6 September, Wessex Institute of Technology, 2002.

Chang E.E., Chang P.C., Lu P.H., Ko Y.W., Comparison of metal leachability for various wastes by extraction and leaching methods, *Chemosphere*, 45(1):91-99, 2001.

Chen Q.Y., Zhang L., Ke Y., Hills C.D., Kang Y., Influence of carbonation on the acid neutralizing capacity of cements and cement-solidified/stabilized electroplating sludge, *Chemosphere*, 74(6):758-764, 2009a.

Chen Q.Y., Tyrer, M, Hills, C.D., Yang, X.M., Carey, P., Immobilization of heavy metal in cement-based solidification/stabilisation: A review, *Waste Management*, 29(1):390-403, 2009b.

Chen Q.Y., Ke Y., Zhang L., Tyrer M., Hills C.D., Xue G., Application of accelerated carbonation with a combination of Na_2CO_3 and CO_2 in cement-based solidification/stabilization of heavy metal-bearing sediment, *Journal of Hazardous Materials*, 166(1):421-427, 2009c.

Cheng T.W., Chin J.P., Minerals Engineering, Fire-resistant geopolymer produced by granulated blast furnace slag, 16(3):205-211, 2003.

Chindaprasirt P., Jaturapitakkul C., Chalee W., Rattanasak U., Comparative study on the characteristics of fly ash and bottom ash geopolymers, *Waste Management*, 29(2):539-543, 2009.

Choi W.-H., Lee S.-R., Park J.-Y., Cement based solidification/stabilization of arsenic-contaminated mine tailings, *Waste Management*, 29(5):1766-1771, 2009.

Conner J.R., Chemical Fixation and Solidification of Hazardous Waste, Van Nostrand-Reinhold, New York, USA, 1990.

Conner J.R., Hoeffner S.L., The history of stabilization/solidification technology, *Critical Reviews in Environmental Science and Technology*, 28(4):325-396, 1998a.

Conner J.R., Hoeffner S.L., The critical review of stabilization/solidification technology, *Critical Reviews in Environmental Science and Technology*, 28(4):397-462, 1998b.

Coolier N.C., Milestone N.B., Hill I.M., Godfrey I.M., The disposal of radioactive ferric floc, *Waste*

- Management, 26(7):769-775, 2006.
- Corwin D.L., David A., Goldberg S., Mobility of arsenic in soil from the Rocky Mountain Arsenal area, Journal of Contaminant Hydrology, 39(1-2):35-58, 1999.
- Coz A., Andres A., Soriano S., Irabien A., Environmental behavior of stabilised foundry sludge, Journal of Hazardous Materials, 109(1-3):95-104, 2004.
- Cullinane M.J., Jones L.W., Malone P.G., 1986, Handbook for stabilization/stabilization of hazardous wastes, EPA/540/2-86/001, US Environmental Protection Agency, 1986.
- Dalton J.L., Gardner K.H., Seager T.P., Weimer M.L., Spear J.C.M., Magee B.J., Properties of portland cement made from contaminated sediments, Resources Conservation and Recycling, 41(3):227-241, 2004.
- Davidovits J., Geopolymers and geopolymeric materials. Journal of Thermal Analysis and Calorimetry, 35:429-441, 1989.
- Davidovits J., Geopolymers Inorganic polymeric new materials. Journal of Thermal Analysis and Calorimetry, 37:1633-1656, 1991.
- Davidovits J., Davidovits M., Davidovits N., Process for obtaining a geopolymeric alumino-silicate and products thus obtained, US Patent No. 5342595, 1994.
- Davidovits J., Geopolymer chemistry and sustainable development. The poly(sialate) terminology : A very useful and simple model for the promotion and understanding of green-chemistry. In J. Davidovits (Ed.), Geopolymer, Green Chemistry and Sustainable Development Solutions, pp:9-15, Saint-Quentin, France: Institut Géopolymère, 2005.
- Davis P.J., Deshpande R., Smith W.M., Brinker C.J., Assink R.A., Pore structure evolution in silica gel during aging/drying iv. Varying pore fluid pH, Journal of Non-crystalline Solids, 167:295-306, 1994.
- Deja J., Immobilization of Cr⁶⁺, Cd²⁺, Zn²⁺ and Pb²⁺ in alkali-activated slag binders, Cement Concrete

- and Research, 32(12):1971-1979, 2002.
- Díez J.M., Madrid J., Macías A., Characterization of cement-stabilized Cd wastes, Cement and Concrete Research, 27(3):337-343, 1997.
- Dutre V., Vandecasteele C., Opdenakker S., Oxidation of arsenic bearing fly ash as pretreatment before solidification, Journal of Hazardous Materials, 68(3):205-215, 1999.
- Duxson P., Fernández-Jiménez A., Provis J.L., Lukey G.C., Palomo A., van Deventer J.S.J., Geopolymer technology: the current state of the art, Journal of Materials Science, 42(9):2917-2933, 2007.
- Erdem M., Özverdi A., Environmental risk assessment and stabilization/solidification of zinc extraction residue: II. Stabilization/solidification, Hydrometallurgy, 105(3-4):270-276, 2011.
- Famy C., Scrivener K.L., Crumbie A.K., What causes differences of C-S-H gel grey levels in backscattered electron images, Cement and Concrete Research, 32(9):1465-1471, 2002.
- Fatta D., Papadopoulos A., Stefanakis N., Loizidou M., Savvides C., An alternative method for the treatment of waste produced at a dye and metal-plating industry using natural and/or waste materials, Waste Management and Research, 22(4):234-239, 2004.
- Federal Register, Vol. 66, Issue 14, Rules and Regulations, National Oceanic and Atmospheric Administration, 22 January 2001.
- Fernández-Jiménez A., Palomo A., Alkali activation of fly ashes: mechanisms of reaction, In: Bilek V., Kersner Z. (Eds.), Proceedings of the Second Congress on Non-Traditional Cement and Concrete, Brno University of Technology, Brno, Czech Republic, 13-24, 2005a.
- Fernández-Jiménez A., Palomo A., Corrosion resistance in activated fly ash mortars, Cement and Concrete Research, 35:1984-1992, 2005b.
- Fitch J.R., Cheeseman C.R., Characterisation of environmentally exposed cement-based stabilised/solidified industrial waste, Journal of Hazardous Materials, 101(3):239-255, 2003.

Fuessle R.W., Taylor M.A., Stabilisation of arsenic- and barium-rich glass manufacturing waste, Journal of Environmental Engineering, 126(3):272-278, 2000.

Fuessle R.W., Taylor M.A., Long term solidification/stabilization and toxicity characteristic leaching procedure for and electric arc furnace dust, Journal of Environmental Engineering, 130(5):492-498, 2004.

Garrabrants A.C., Sanchez F., Kosson D.S., Changes in constituent equilibrium leaching and pore water characteristics of a portland cement mortar as a result of carbonation, Waste Management, 24(1):19-36, 2004.

Gervais C., Garrabrants A.C., Sanchez F., Barna R., Moszkowicz P., Kosson D.S., The effect of carbonation and drying during intermittent leaching on the release of inorganic constituents from a cement-based matrix, Cement and Concrete Research, 34(1):119-131, 2004.

Gineys N., Aouad G., Damidot D., Managing trace elements in portland cement – Part I: Interactions between cement paste and heavy metals added during mixing as soluble salts, Cement and Concrete Composites, 32:563-570, 2010.

Gougar M.L.D., Scheetz B.E., Roy D.M., Ettringite and C-S-H portland cement phases for waste ion-immobilization: A review, Waste Management, 16(4):295-303, 1996.

Gustafsson J.P., Visual MINTEQ ver 3.0. <<http://www2.lwr.kth.se/English/OurSoftware/vminteq/>>, 2011.

Halim C.E., Amal R., Beydoun D., Scott J.A., Low G., Evaluating the applicability of a modified toxicity characteristic leaching procedure (TCLP) for the classification of cementitious wastes containing lead and cadmium, Journal of Hazardous Materials, 103(1-2):125-140, 2003.

Halim C.E., Amal R., Beydoun D., Scott J.A., Low G., Implications of the structure of cementitious wastes containing Pb(II), Cd(II), As(V), and Cr(VI) on the leaching of metals, Cement and Concrete Research, 34(7):1093-1102, 2004.

Hardjito D., Wallah S.E., Sumajouw D.M.J., Rangan B.V., In: George Hoff Symposium, ACI, Las Vegas USA, 2003.

Hardjito D., Wallah S.E., Sumajouw D.M.J., Rangan B.V., On the development of fly ash-based geopolymers concrete, ACI Materials Journal, 101(6):467-472, 2004.

Hermann E., Kunze C., Gatzweiler R., Kiebig G., Davidovits J., Solidification of various radioactive residues by geopolymers with special emphasis on long term stability, In: Proceedings of Geopolymers, 1999.

Herrera E., Tittlebaum M., Cartledge F., Eaton H., Evaluation of the leaching properties of solidified heavy metal wastes, Journal of Environmental Science and Health, 27(4):983-998, 1992.

Hills C.D., Sollars C.J., Perry R., A calorimetric and microstructural study of solidified toxic wastes – Part 1: A classification of OPC/waste interference effects, Waste Management, 14(7):589-599, 1994.

Houst Y.F., Wittman F.H., Influence of porosity and water content on the diffusivity of CO₂ and O₂ through hydrated cement paste, Cement and Concrete Research, 24(6):1165-1176, 1994.

Isaacs L.T., Carter J.P., Theoretical study of pore water pressures developed in hydraulic fill in mine slopes, Transactions of the Institution of Mining and Metallurgy, Section A: Mining Technology, 92:93-102, 1983.

Islam M.Z., Catalan L.J.J., Yanful E.K., A two-front leach model for cement-stabilized heavy metal waste, Environmental Science and Technology, 38(5):1522-1528, 2004a.

Islam M.Z., Catalan L.J.J., Yanful E.K., Effect of remineralization of heavy-metal leaching from cement-stabilized/solidified waste, Environmental Science and Technology, 38(5):1561-1568, 2004b.

Ivey D.G., Heimann R.B., Neuwirth N., Shumborski S., Conrad D., Mikula R.J., Lam W.W., Electron microscopy of heavy metal waste in cement matrices, Journal of Materials Science, 25:5055-5062,

1990.

Jennings H.M., Model for the microstructure of calcium silicate hydrate in cement paste, Cement and Concrete Research, 30(1):101-116, 2000.

Jimenez AF, Palomo A., Characterization of fly ashes. Potential reactivity as alkaline cements, Fuel, 82(18):2259-2265, 2003.

Johannesson B., Utgenannt P., Microstructural changes caused by carbonation of cement mortar, Cement and Concrete Research 31(6):925-931, 2001.

Johnson D.C., MacLeod C.L., Hills C.D., Accelerated carbonation of stainless steel slag, In: Sebastian (Ed.), Proceedings of the 5th international conference on the environmental and technical implications of construction with alternative materials, Spain, pp. 543-551, 2003.

Johnson A., Thesis: Characterization and utilization of fly ash derived from the co-combustion of biomass and coal as a mineral admixture for ordinary portland cement, Lakehead University, Ontario, 2009.

Kantro D.L., Tricalcium silicate hydration in the presence of various salts, Journal of Testing and evaluation, 3(4):312-321, 1975.

Karim M., Arsenic in groundwater and health problems in Bangladesh, Water Research, 34(1):304-310, 2000.

Katsioti M., Boura P., Aqatzinia S., Tsakiridis P.E., Oustadakis P., Use of jarosite/alunite as a substitute for gypsum in portland cement, Cement and Concrete Composites, 27(1):3-9, 2005.

Khale D., Chaudhary R., Mechanism of geopolymserisation and factors influencing its development: A review, Journal of Materials Science, 42(3):729-746, 2007.

Kindness A., Macias A., Glasser F.P., Immobilization of chromium in cement matrices, Waste Management, 14(1):3-11, 1994.

Kirschner A., Harmuth H., Investigation of geopolymer binders with respect to their application for

- building materials, Ceramics-Silikaty, 48(3):117-120, 2004.
- Kitamura M., Konno H., Yasui A., Masuoka H., Controlling factors and mechanism of reactive crystallization of calcium carbonate polymorphs from calcium hydroxide suspensions, Journal of Crystal Growth, 236(1-3):323-332, 2002.
- Klich I., Batchelor B., Wilding L.P., Drees L.R., Mineralogical alterations that affect the durability and metals containment of aged solidified and stabilized wastes, Cement and Concrete Research, 29(9):1433-1440, 1999.
- Kosmatka S.H., Kerkhoff B., Panarese W.C., MacLeod N.F., McGrath R.J., Design and control of concrete mixtures, EB101, 7th ed., Cement Association of Canada, Ottawa, Ont., 2002.
- Kulik D.A., Kersten M., Aqueous solubility diagrams for cementitious waste stabilization systems. II, end-member stoichiometries of ideal calcium silicate hydrate solid solutions, Journal of American Ceramic Society, 84(12):3017-3026, 2001.
- Kulik D.A., Kersten M., Aqueous solubility diagrams for cementitious waste stabilization systems. 4. A carbonation model for Zn-doped calcium silicate hydrate by Gibbs energy minimization, Environmental Science & Technology, 36(13): 2926-2931, 2002.
- Lange L.C., Hills C.D., Poole A.B., Preliminary investigation into the effects of carbonation on cement-solidified hazardous wastes, Environmental Science and Technology, 30(1):25-30, 1996.
- Lange L.C., Hills C.D., Poole A.B., Effect of carbonation on properties of blended and non-blended cement solidified waste forms, Journal of Hazardous Materials, 52(2-3):193-212, 1997.
- Lawrence C.D., The constitution and specification of portland cement. In: Leas's chemistry of cement and concrete, 4th ed. Ed. P.C. Hewlett. Butterworth-Heinemann, UK, 131-193, 1998.
- Lea F.M., The Chemistry of Cement and Concrete, Edwards Arnold, London, 1970.
- Lee T., Benson C.H., Sorption and degradation of alachlor and metolachlor in groundwater using green sands, Journal of Environmental Quality, 33(5):1682-1693, 2004.

- Lee W.K.W., Van Deventer J.S.J., The effect of ionic contaminants on the early-age properties of alkali-activated fly-ash based cements, *Cement Concrete Research*, 32(4):577-584, 2002.
- Leist M., Casey J.R., Caridi D., Evaluation of leaching tests for cement based immobilization of hazardous compounds, *Journal of Environmental Engineering, ASCE*, 129(7):637-641, 2003.
- Li X.D., Poon C.S., Sun H., Lo I.M.C., Kirk D.W., Heavy metal speciation and leaching behaviors and in cement based solidified/stabilized waste materials, *Journal of Hazardous Materials*, 82(3):215-230, 2001.
- Li X., Bertos M.F., Hills C.D., Carey P.J., Simon S., Accelerated carbonation of municipal solid waste incineration fly ashes, *Waste Management*, 27(9):1200-1206, 2007.
- Ligia T.-B., Apichat I., Radu B., Long term prediction of the leaching behavior of pollutants from solidified wastes, *Advances in Environmental Research*, 8(3-4):697-711, 2004.
- Lin C., Chen J., Lin C., An NMR, XRD and EDS study of solidification/stabilization of chromium with Portland cement and C₃S, *Journal of Hazardous Materials*, 56:21-34, 1997.
- Loo Y.H., Chin M.S., Tam C.T., Ong K.C.G., Carbonation prediction model for accelerated carbonated testing of concrete, *Magazine of Concrete Research*, 46(168):191-200, 1994.
- Luna Y., Fernandez-Pereira C., Vale J., Waste s/s using fly ash-based geopolymers. Influence of carbonation on the s/s of an EAF dust, *Proceedings of the 3rd WOCA Conference*, Lexington, KY, USA, May 4-7, 2009.
- Luna G.Y., Fernández P.C., Vale J., Stabilization/solidification of a municipal solid waste incineration residue using fly ash-based geopolymers. *Journal of Hazardous Materials*, 185:373-381, 2011.
- Macias A., Kindness A., Glasser F.P., Impact of carbonation on the immobilization potential of cemented wastes: chromium, *Cement and Concrete Research*, 27(2):215-225, 1997.
- Malami C.H., Kaloidas V., Carbonation and porosity of mortar specimens with pozzolanic and hydraulic cement admixtures, *Cement and Concrete Research*, 24(8):1444-1456, 1994.

Malviya R., Chaudhary R., Factors affecting hazardous waste solidification/stabilization: a review, Journal of Hazardous Materials, 137(1):267-276, 2006.

Maries A., The activation of portland cement by carbon dioxide, In: Proceedings of Conference in Cement and Concrete Science, Oxford, UK, 1985.

Martinez-Ramirez S., Palomo A., Microstructure studies on portland cement pastes obtained in highly alkaline environments, Cement and Concrete Research, 31(11):1581-1585, 2001.

Milestone N.B., Reactions in cement encapsulated nuclear wastes: Need for toolbox of different cement types, Advances in Applied Ceramics, 105(1):13-20, 2006.

Mollah M.Y.A., Tsai Y.N., Hess T.R., Cocke D.L., An FTIR, SEM and EDS investigation of solidification/stabilization of chromium using portland cement type V and type IP, Journal of Hazardous Materials, 30(3):273-283, 1992.

Mollah M.Y.A., Vempati R.K., Lin T.C., Cocke D.L., The interfacial chemistry of solidification/stabilization of metals in cement and pozzolanic material systems, Waste Management, 15(2):137-148, 1995.

Mollah M.Y.A., Lu F., Cocke D.L., An X-Ray Diffraction (XRD) and Fourier transform infrared spectroscopic (FT-IR) characterization of the speciation of arsenic (V) in portland cement type-V, Science of the Total Environment, 224(1-3):57-68, 1998.

Mulligan C.N., Yong R.N., Gibbs B.F., Remediation technologies for metal-contaminated soils and groundwater; an evaluation, Engineering Geology, 60(1-4):193-207, 2001.

Nugteren H.W., Butselaar-Orthlieb V.C.L., Izquierdo M., High strength geopolymers produced from coal combustion fly ash, Global NEST Journal, 11:155-161, 2009.

Olmo I.F., Chacon E., Irabien A., Influence of lead, zinc, iron (II) and chromium (III) oxides on the setting time and strength development of portland cement, Cement and Concrete Research, 31:1213-1219, 2001.

Otomoso O.E., Ivey D.G., Mikula R., Electron microscopic and ^{29}Si -nuclear magnetic resonance spectroscopic studies of chromium doped tricalcium silicate, In: Hager J.P., Mishra B., Davidson C.F., Litz J.L. (Eds.), Treatment and Minimisation of Heavy Metal-Containing Wastes, 129-141, 1995.

Palacios M., Palomo A., Alkali-activated fly ash matrices for lead immobilisation: a comparision of different leaching tests, *Advances in Cement Research*, 16(4):137-144, 2004.

Palomo A., Glasser F.P., Chemically-bonded cementitious materials. Based on metakaolin, *British Ceramic Transactions Journal*, 91:107-113, 1992.

Palomo A., Grutzeck M.W., Blanco M.T., Alkali-activated fly ashes: A cement for the future, *Cement and Concrete Research*, 29(8):1323-1329, 1999.

Palomo A., Palacios M., Alkali-activated cementitious materials: alternative matrices for the immobilisation of hazardous wastes – Part II. Stabilisation of chromium and lead, *Cement Concrete Research*, 33(2):289-295, 2003.

Palomo A., Alonso S., Fernández-Jiménez A., Criado M., Geopolymers: one only chemical basis, some different microstructures, *Materiales de Construcción*, 54(275):77-91, 2004a.

Palomo A., Alonso S., Fernández-Jiménez A., Sobrados I., Sanz J., *Journal of American Ceramic Society*, 87(6):1141-1145, 2004b.

Pantsar-Kallio M., Manninen P.K.G., Speciation of mobile arsenic in soil samples as a function of pH, *Science of the Total Environment*, 204(2):193-200, 1997.

Papadakis V.G., Vayenas C.G., Fardis M.N., Reaction engineering approach to the problem of concrete carbonation, *AIChE Journal*, 35(10):1639-1650, 1989.

Papadakis V.G., Effect of fly ash on portland cement systems. Part II. High-calcium fly ash, *Cement and Concrete Research*, 30(10):1647-58, 2000.

Paria S., Yuet P.K., Solidification/stabilization of organic and inorganic contaminants using portland

- cement: a literature review, Environmental Reviews, 14(4):217-255, 2006.
- Penney K., Mohamedelhassen E., Catalan L.J.J., Utilization of coal/biomass fly ash in reactive barriers for treating acid mine drainage, Proceedings of the International Association of Science and Technology for Development Environmental Management and Engineering Conference, Banff, AB, July 6-8, 2009.
- Pereira C.F., Luna Y., Querol X., Antenucci D., Vale J., Waste stabilization/solidification of an electric arc furnace dust using fly-ash based geopolymers, Fuel, 88:1185-1193, 2009.
- Perkins, R.B, Palmer, C.D., Solubility of $\text{Ca}_6[\text{Al}(\text{OH})_6]_2(\text{CrO}_4)_3 \cdot 26\text{H}_2\text{O}$, the chromate analog of ettringite at 5 – 75 °C, App. Geochem., 15:1203-1218, 2000.
- Phair J.W., Van Deventer J.S.J., Effect of silicate activator pH on the leaching and material characteristics of waste-based inorganic polymers, Minerals Engineering, 14(3):289-304, 2001.
- Phair J.W., Van Deventer J.S.J., Smith J.D., Effect of Al source and alkali activation on Pb and Cu immobilization in fly-ash based geopolymers, Applied Geochemistry, 19(3):432-434, 2004.
- Phenrat T., Marhaba F.T., Rachakornkij M., A SEM and X-Ray study for investigation of solidified/stabilized arsenic-iron hydroxide sludge, Journal of Hazardous Materials, 118(1-3):185-195, 2005.
- Polettini A., Pomi R., Valente M., Remediation of a heavy metal-contaminated soil by means of agglomeration, Journal of Environmental Science and Health, 39(4):999-1010, 2004.
- Poon C.S., Qiao X.C., Lin Z.S., Effects of flue gas desulphurization sludge on the pozzolanic reaction of reject-fly-ash-blended cement pastes, Cement and Concrete Research, 34(10):1907-1918, 2004.
- Provis J.L., Yong C.Z., Duxson P., Van Deventer J.S.J., Correlating mechanical and thermal properties of sodium silicate-fly ash geopolymers, Colloids and Surfaces A: Physicochemical and Engineering Aspects, 336:57-63, 2009.
- Puertas F., Martinez-Ramirez S., Alonso S., Vazquez T., Alkali activated fly ash-slag cement. Strength

- behavior and hydration products, Cement and Concrete Research, 30(10):1625-1632, 2000.
- RILEM, Measurement of hardened concrete carbonation depth, Materials and Structures, 21(6): 453-455, 1988.
- Roy A., Eaton H.C., Cartledge F.K., Tittlebaum M.E., Solidification/stabilization of hazardous waste: evidence of physical encapsulation, Environmental Science Technology, 26:1349-1353, 1992.
- Sanchez F., Gervais C., Garrabrants A.C., Barna R., Kosson D.S., Leaching of inorganic contaminants from cement-based waste materials as a results of carbonation during intermittent wetting, Waste Management, 22:249-260, 2002.
- Scrivener K.L., Taylor H.F.W., Delayed ettringite formation: a microstructural and microanalytical study, Advances in Cement Research, 5(20):139-146, 1993.
- Seyer S., Chen T.T., Dutrizac J.E., Jarofix: addressing iron disposal in the zinc industry, JOM-Journal of the Minerals Metals and Materials Society, 53(12):32-35, 2001.
- Shackelford C.D., Glade M.J., Analytical mass leaching model for contaminated soil and soil stabilized waste, Ground Water, 35(2):233-242, 1997.
- Shi C., Fernández-Jiménez A., Stabilization/solidification of hazardous and radioactive wastes with alkali-activated cements, Journal of Hazardous Materials, 137(3):1656-1663, 2006.
- Shi C., Krivenko P.V., Roy D.M., Alkali-Activated Cements and Concretes, Taylor and Francis, Abingdon, UK, 2006.
- Shi C., Spence R., Designing of cement-based formula for solidification/stabilization of hazardous, radioactive, and mixed wastes, Critical Reviews in Environmental Science and Technology, 34(4):391-417, 2004.
- Sollars C.J., Perry R., Cement based solidification of wastes: practical and theoretical considerations, J. IWEM, 3:125-134, 1989.
- Sophia A.C., Swaminathan K., Assessment of the mechanical stability and chemical leachability of

- immobilized electroplating waste, Chemosphere, 58(1):75-82, 2005.
- Sophia A.C., Sandhya S., Swaminathan K., Solidification and stabilization of chromium laden wastes in cementitious binders, Current Science, 99:365-369, 2010.
- Stephan D., Maleki H., Knofel D., Eber B., Hardtl R., Influence of Cr, Ni, and Zn on the properties of pure clinker phases: Part II. C₃A and C₄AF, Cement and Concrete Research, 29(5):651-657, 1999.
- Steveson M., Sagoe-Crentsil K., Relationships between composition, structure and strength of inorganic polymers: PPPart 2 fly ash-derived inorganic polymers, Journal of Materials Science, 40(16):4247-4259, 2005.
- Sumajouw D.M.J., Hardjito D., Wallah S.E., Rangan B.V., Geopolymer concrete for a sustainable future, In: Green Processing, The Australian Institute of Mining and Metallurgy Publication Series, 2:237-240, 2004.
- Swanepoel J.C., Strydom C.A., Utilisation of fly ash in a geopolymeric material, Applied Geochemistry, 17(8):1143-1148, 2002.
- Sweeney R.E.H., Hills C.D., Investigation into the carbonation of stabilized/solidified synthetic waste, Buenfeld N.R., Environmental Technology, 19:893-902, 1998.
- Tamas F.D., Csetenyi L., Tritthart E., Effect of adsorbents on the leachability of cement bonded electroplating wastes, Cement and Concrete Research, 22(2-3):399-404, 1992.
- Tashiro C., Kawaguchi K., Effects of the CaO/SiO₂ ratio and Cr₂O₃ on the hydrothermal synthesis of xonotlite, Cement and Concrete Research, 7(1):69-76, 1977.
- Tashiro C., Takahashi H., Kanaya M., Hirakida I., Yoshida R., Hardening property of cement mortar adding heavy metal compound and solubility of heavy metal from hardened mortar, Cement and Concrete Research, 7(3):283-290, 1977.
- Taylor H.F.W., Cement Chemistry, Second Edition, Thomas Telford Press, London, 1997.
- Thomas N.L., Jameson D.A., Double D.D., Effect of lead nitrate on the early hydration of portland

- cement, Cement and Concrete Research, 11(1):143-153, 1981.
- Tommaseo C.E., Kersten M., Aqueous solubility diagrams for cementitious waste stabilization systems. 3. Mechanism of zinc immobilization by calcium silicate hydrate, Environmental Science & Technology, 36(13): 2919-2925, 2002.
- US EPA, Handbook for stabilization/solidification of hazardous waste, EPA/540/2-86/001, 1986.
- US EPA, Stabilization/Solidification of CERCLA and RCRA wastes: Physical tests, chemical testing procedures, technology screening, and field activities, EPA/625/6-89/022, 1989.
- US EPA, Method 1311: Toxicity Characteristic Leaching Procedure, In EPA SW-846: test methods for evaluating solid waste, physical/chemical methods, 1992.
- US EPA, Method 1312: Synthetic Precipitation Leaching Procedure, In EPA SW-846: test methods for evaluating solid waste, physical/chemical methods, 1994.
- US EPA, EPA/542-R-00-010, Solidification/stabilization use at Superfund sites, Office of Solid Waste and Emergency Response, Washington D.C., 2000.
- US EPA, A citizen's guide to solidification/stabilization, Office of Solid Waste and Response, EPA 542-F-01-024, 2001.
- US EPA, Treatment technologies for site cleanup: annual status report (eleventh edition), EPA-542-R-03-009, 2004.
- Vandecasteele C., Dutre V., Geysen D., Wauters G., Solidification/stabilization of arsenic bearing fly ash from the metallurgical industry. Immobilization mechanism of arsenic, Waste Management, 22(2):143-146, 2002.
- Van der Sloot H.A., Characterization of the leaching behavior of concrete mortars and of cement-stabilized wasted with different waste loading for long term environmental assessment, Waste Management, 22(2):181-186, 2002.
- Van Deventer J.S.J., Provis J.L., Duxson P., Lukey G.C., Reaction mechanisms in the geopolymERIC

conversion of inorganic waste to useful products, Journal of Hazardous Materials, 139(3):506-513, 2007.

Van Gerven T., Van Baelen D., Dutre V., Vandecasteele C., Influence of carbonation and carbonation methods on leaching of metals from mortars, Cement and Concrete Research, 34(1):149-156, 2004.

Van Gerven T., Cornelis G., Vandoren E., Vandecasteele C., Garrabrants A.C., Sanchez F., Kosson D.S., Effects of progressive carbonation on heavy metal leaching from cement-bound waste, AIChE Journal, 52:826–837, 2006.

Van Jaarsveld J.G.S., Van Deventer J.S.J., Lorenzen L., Potential use of geopolymeric materials to immobilize toxic metals: Part I. Theory and applications, Minerals Engineering, 10(7):659-669, 1997.

Van Jaarsveld J.G.S., Van Deventer J.S.J., Lorenzen L., Factors affecting the immobilization of metals in geopolymersized flyash, Metallurgical and Materials Transactions B: Process Metallurgy and Materials Processing Science, 29(1):283-291, 1998.

Van Jaarsveld J.G.S., Van Deventer J.S.J., Effect of metal contaminants on the formation and properties of waste-based geopolymers, Cement Concrete Research, 29(8):1189-1200, 1999a.

Van Jaarsveld J.G.S., Van Deventer J.S.J., Effect of alkali metal activator on the properties of fly-ash based geopolymers, Industrial and Engineering Chemistry Research, 38:3932-3941, 1999b.

Van Jaarsveld J.G.S., Van Deventer J.S.J., Lukey G.C., The effect of composition and temperature on the properties of fly ash- and kaolinite-based geopolymers, Chemical Engineering Journal, 89(1-3):63-73, 2002.

Walton J.C., Bin-Shafique S., Smith R.W., Guitierrez N., Tarquin A., Role of carbonation in transient leaching of cementitious wasteforms, Environmental Science and Technology, 31(8):2345-2349, 1997.

Wang S., Vipulanandan C., Solidification/stabilization of Cr(VI) with cement leachability and XRD analysis, Cement and Concrete Research, 30(3):385-389, 2000.

Wang K., Shah S.P., Mishulovich A., Effects of curing temperature and NaOH addition on hydration and strength development of clinker-free CKD-fly ash binders, Cement and Concrete Research, 34(2):299-309, 2004.

World Health Organization, Environmental Health Criteria 194, Aluminum, Geneva, 1997.
<http://www.inchem.org/documents/ehc/ehc/ehc194.htm#SubSectionNumber:9.2.2> (accessed July 2011)

Xu H., Van Deventer J.S.J., Geopolymerisation of multiple minerals, Minerals Engineering, 15(12):1131-1139, 2002.

Yang R., Lawrence C.D., Sharp J.H., Delayed ettringite formation in 4-yr old cement pastes, Cement and concrete research, 26(11):1649-1659, 1996.

Yilmaz O., Ünlü K., Cokca E., Solidification/stabilization of hazardous wastes containing metals and organic contaminants, Journal of Environmental Engineering, 129(4):366-376, 2003.

Yousuf M., Mollah M.Y.A., Parga J.R., Cocke D.L., An infrared spectroscopic examination of cement-based solidification/stabilization systems – portland types V and IP with zinc, Journal of Environmental Science and Health, Part A: Toxic/Hazardous Substances and Environmental Engineering, 27(6):1503-1519, 1992.

Yousuf M., Mollah A., Vempati R.K., Lin T.C., Cocke D.L., The interfacial chemistry of solidification/stabilization of metals in cement and pozzolanic material systems, Waste Management, 15(2):137-148, 1995.

Zain M.F.M., Islam M.N., Radin S.S., Yap S.G., Cement-based solidification for the safe disposal of blasted copper slag, Cement and Concrete Composites, 26(7):845-851, 2004.

Zamorani E., Sheikh I.A., Serrini G., Physical properties measurements and leaching behavior of

chromium compounds solidified in a cement matrix, Nuclear and Chemical Waste Management, 8:239-245, 1988.

Ziegler F., Scheidegger A.M., Johnson C.A., Dahn R., Wieland E., Sorption mechanisms of zinc to calcium silicate hydrate: X-ray Absorption Fine Structure (XAFS) investigation, Environmental Science and Technology, 35(7):1550-1555, 2001.

Zhang X.Z., Chang W.Y., Zhang T.J., Ong C.K., Nanostructure of calcium silicate hydrate gels in cement paste, Journal of the American Ceramic Society, 83(10):2600-2604, 2000.

Zhang J., Provis J.L., Feng D., van Deventer J.S.J., Geopolymers for immobilization of Cr^{6+} , Cd^{2+} , and Pb^{2+} , Journal of hazardous materials, 157(2-3):587-598, 2008.

Zhang J., Liu J., Li C., Jin Y., Nie Y., Li J., Comparision of the fixation effects of heavy metlals by cement rotary kiln co-processing and cement-based solidification/stabilization, Journal of Hazardous Materials, 165(1-3):1179-1185, 2009.

Zhang Z., Yao X., Zhu H., Potential uses of geopolymers as protection coatings for marine concrete: I. Basic properties, Applied Clay Science, 49:1-6, 2010.

Ziegler F., Scheidegger A.M., Johnson C.A., Dahn R., Wieland E., Sorption mechanisms of zinc to calcium silicate hydrate: X-ray absorption fine structure (XAFS) investigation, Environmental Science & Technology, 35(7):1550-1555, 2001.

Appendix I - ICP-AES analysis of the TCLP and SPLP leachates

The following tables contain the results of the ICP-AES analysis of the TCLP and SPLP leachates of carbonated and non-carbonated cement-based and geopolymers-based stabilized/solidified synthetic metal wastes. The concentrations are provided in mol L⁻¹. The equipment used was a Varian Vista Pro CCD Simultaneous ICP-OES CETAC ASX-510 Auto Sampler. The detection limits for Al, B, Ba, Cd, Cr, Cu, Fe, Mg, S, Si, Sr, and Zn are 0.02 mg L⁻¹ and the detection limits for Ca, K, and Pb are 0.05 mg L⁻¹. The empty cells represent concentrations that were not analysed.

ICP-AES analysis results for TCLP leachates of non-carbonated cement samples

Sample	#	Concentration (mg L ⁻¹)															
		Al	B	Ba	Ca	Cd	Cr	Cu	Fe	K	Mg	Na	Pb	S	Si	Sr	Zn
Control	1	0.584		2.694	1436	0.001	0.024	0.000	0.000	15.67	0.035		0.131		0.509		0.023
	2	0.509		2.175	15855	0.000	0.031	0.000	0.000	15.90	0.027		0.137		0.478		0.025
	3	0.416		3.957	1603	0.000	0.026	0.000	0.000	15.52	0.085		0.129		0.493		0.023
	4	0.649		2.306	1618	0.000	0.020	0.000	0.000	15.09	0.034		0.132		0.501		0.015
Cadmium	1	0.338		2.847	1441	0.000	0.034	0.000	0.000	15.347	0.023		0.154			12.107	0.137
	2	0.305		2.885	1438	0.001	0.033	0.000	0.000	15.360	0.023		0.157			12.210	0.140
	3	0.582		2.697	1839	0.000	0.033	0.000	0.000	14.960	0.030		0.147			12.920	0.127
	4	0.126		2.960	1048	0.000	0.034	0.001	0.000	15.720	0.017		0.159			11.190	0.146
Chromium III	1	0.688		2.132	2035	0.002	0.054	0.006	0.000		0.092					11.660	0.408
	2	0.385		2.220	1515	0.018	0.045	0.006	0.000		0.040					9.922	0.221
	3	0.505		2.248	1524	0.001	0.046	0.006	0.000		0.028					10.080	0.178
	4	0.528		2.201	1693	0.009	0.046	0.006	0.000		0.050					10.542	0.265
Chromium VI	1		1.609	1737	0.001	2.627	0.000	0.000	184	0.015	51.3		0.495	0.4749		10.83	
	2		1.520	1708	0.000	2.490	0.000	0.000	182	0.020	49.3		0.587	0.5814		9.979	
	3		1.662	1735	0.000	2.569	0.000	0.000	183	0.014	50.7		0.486	0.4926		10.97	
	4		1.545	1690	0.000	2.939	0.000	0.000	178	0.037	51.6		1.503	0.5031		10.92	
Copper	1	1.126	4.164	1809	0.000	0.100	0.009	0.003	73.210	0.021	104.5		1.152	0.409		15.090	0.007
	2	0.732	3.949	1940	0.001	0.097	0.003	0.003	71.805	0.013	102.2		0.311	0.489		14.850	0.004
	3	0.849	3.969	1503	0.000	0.046	0.001	0.001	72.300	0.007	103.0		0.303	0.373		14.360	0.002
	4	0.415	4.142	1559	0.000	0.051	0.001	0.002	73.404	0.009	103.4		0.331	0.473		14.580	0.002
Lead	1	0.690	2.697	1726	0.001	0.023	0.001	0.000	15.513	0.062		0.239				12.330	0.192
	2	0.759	2.388	1722	0.001	0.027	0.000	0.000	15.070	0.093		0.201				11.710	0.198
	3	0.663	2.940	1790	0.001	0.020	0.002	0.000	15.540	0.045		0.273				12.600	0.204
	4	0.647	2.762	1668	0.001	0.020	0.000	0.000	15.930	0.048		0.244				12.680	0.174
Zinc	1	0.593	2.374	1645	0.001	0.024	0.001	0.000		0.042			0.347				0.022
	2	0.489	2.064	1598	0.001	0.021	0.001	0.000		0.039			0.374				0.024
	3	0.678	2.845	1612	0.001	0.026	0.001	0.000		0.035			0.376				0.029
	4	0.564	2.091	1634	0.001	0.024	0.000	0.000		0.045			0.365				0.026

ICP-AES analysis results for SPLP leachates of non-carbonated cement samples

Sample	#	Concentration (mg L^{-1})															
		Al	B	Ba	Ca	Cd	Cr	Cu	Fe	K	Mg	Na	Pb	S	Si	Sr	Zn
Control	1	0.22	0.000	1.94	604	0.000	0.019	0.000	0.00	78.40	0.001	52.21	0.000	1.544	0.1956	7.373	0.000
	2	0.15	0.000	1.90	657	0.000	0.023	0.000	0.00	78.30	0.001	52.03	0.000	2.419	0.2514	7.415	0.000
	3	0.23	0.000	1.97	663	0.000	0.020	0.000	0.00	78.93	0.000	52.44	0.000	1.614	0.2369	7.446	0.000
	4	0.19	0.000	1.87	659	0.000	0.023	0.000	0.00	77.47	0.001	51.42	0.000	2.374	0.2654	7.364	0.000
Cadmium	1	0.05		1.80	663	0.001	0.062	0.000	0.00	16.25	0.015		0.002			10.700	0.053
	2	0.05		1.85	666	0.001	0.062	0.001	0.00	15.88	0.016		0.006			10.980	0.057
	3	0.04		1.76	663	0.002	0.063	0.000	0.00	16.11	0.014		0.005			10.770	0.052
	4	0.07		1.79	659	0.001	0.060	0.000	0.00	16.77	0.014		0.005			10.350	0.050
Chromium III	1	0.13		1.84	663	0.000	0.060	0.004	0.00		0.012		0.000			8.941	0.087
	2	0.11		1.93	675	0.000	0.062	0.005	0.00		0.012		0.000			9.643	0.053
	3	0.11		1.87	663	0.000	0.059	0.005	0.00		0.009		0.000			9.005	0.067
	4	0.02		1.88	667	0.000	0.059	0.005	0.00		0.012		0.000			9.201	0.066
Chromium VI	1			0.98	632	0.000	4.675	0.000	0.00	176	0.018	51.14	0.000	6.213	0.314	7.350	0.000
	2			1.19	662	0.000	3.815	0.000	0.00	180	0.005	48.87	0.000	3.506	0.246	7.220	0.000
	3			1.14	656	0.000	3.894	0.000	0.00	181	0.004	49.18	0.000	3.821	0.250	7.075	0.000
	4			1.09	661	0.000	3.932	0.000	0.00	171	0.004	45.52	0.000	4.167	0.244	6.577	0.000
Copper	1	0.74		3.06	673	0.000	0.045	0.001	0.00	74.73	0.003	106.60	0.000	1.671	0.304	11.950	0.001
	2	1.70		2.99	664	0.000	0.053	0.010	0.01	74.63	0.008	107.13	0.000	2.328	0.405	11.693	0.004
	3	3.73		2.89	642	0.000	0.070	0.028	0.02	75.74	0.018	110.30	0.000	4.108	0.592	11.530	0.011
	4	0.62		3.01	676	0.000	0.045	0.001	0.00	73.42	0.002	104.50	0.000	1.205	0.318	11.600	0.001
Lead	1	0.14		2.30	646	0.000	0.029	0.000	0.00	15.420	0.050		1.613			8.339	0.025
	2	0.17		2.52	658	0.000	0.028	0.002	0.00	15.740	0.028		1.591			9.031	0.004
	3	0.20		2.23	568	0.000	0.023	0.000	0.00	16.050	0.007		1.098			8.084	0.002
	4	0.23		2.30	623	0.000	0.024	0.002	0.00	15.150	0.012		1.612			8.194	0.107
Zinc	1	0.12	0.003	1.84	651	0.000	0.028	0.000	0.00	68.05	0.021	99.30	0.000	18.440	0.359	7.826	0.019
	2	0.11	0.002	1.88	654	0.000	0.026	0.000	0.00	69.82	0.010	101.70	0.000	4.534	0.285	7.936	0.020
	3	0.12	0.002	1.87	647	0.000	0.025	0.000	0.00	69.63	0.005	101.50	0.000	2.986	0.264	7.747	0.020
	4	0.13	0.002	1.76	641	0.000	0.025	0.000	0.00	68.20	0.005	98.81	0.000	3.021	0.266	7.309	0.019

ICP-AES analysis results for TPLP leachates of carbonated cement samples

Sample	#	Concentration (mg L^{-1})															
		Al	B	Ba	Ca	Cd	Cr	Cu	Fe	K	Mg	Na	Pb	S	Si	Sr	Zn
Control	1	0.41	0.17	0.706	1630	0.000	0.386	0.008	0.193	26.79	7.552	18.62	0.000	47.96	41.98	4.530	0.036
	2	0.60	0.17	0.709	1627	0.000	0.493	0.030	0.218	26.76	7.587	20.31	0.000	48.54	41.66	4.532	0.049
	3	0.24	0.18	0.704	1686	0.000	0.429	0.014	0.066	24.33	7.870	16.97	0.000	51.25	40.58	4.341	0.075
	4	0.66	0.19	0.707	1684	0.000	0.611	0.067	0.100	24.54	7.971	21.81	0.000	53.57	40.18	4.365	0.114
Cadmium	1	0.03	0.29	0.511	1626	0.324	0.494	0.015	0.003	24.22	10.050	40.48	0.000	66.830	45.110	4.660	0.325
	2	0.03	0.28	0.505	1614	0.347	0.477	0.016	0.003	23.37	9.782	39.19	0.000	65.043	44.597	4.569	0.334
	3	0.03	0.26	0.512	1603	0.304	0.466	0.014	0.003	22.74	9.601	38.39	0.000	63.580	45.100	4.541	0.321
	4	0.03	0.30	0.492	1615	0.414	0.472	0.019	0.002	23.17	9.694	38.71	0.000	64.720	43.580	4.507	0.357
Chromium III	1	0.11		0.709	2953	0.000	0.613		0.010	44.51	3.117	101.7	0.000	40.82	6.059	12.11	0.035
	2	0.10		0.703	2921	0.000	0.553		0.005	46.60	1.768	103.0	0.000	36.22	4.825	12.22	0.018
	3	0.12		0.712	2913	0.000	0.509		0.006	46.72	1.002	104.9	0.000	34.54	3.916	12.40	0.038
	4	0.11		0.709	2931	0.000	0.561		0.007	46.01	1.951	103.4	0.000	37.02	4.904	12.23	0.032
Chromium VI	1			0.488	2031	0.000	18.850		0.359		0.777	29.51	0.001	52.910	15.280		
	2			0.477	1564	0.000	11.990		0.107		0.344	32.05	0.001	37.490	8.435		
	3			0.894	1100	0.000	4.261		0.241		0.160	39.75	0.001	4.236	4.447		
	4			0.529	622	0.000	4.630		0.384		0.094	30.61	0.001	4.104	2.998		
Copper	1	0.02		0.719	1807	0.001	0.470	0.349	0.011	4.81	9.597		0.001			5.161	0.306
	2	0.04		0.737	1825	0.001	0.423	0.316	0.011	4.68	9.544		0.001			5.220	0.241
	3	0.01		0.700	1757	0.001	0.505	0.347	0.000	4.68	9.310		0.001			5.000	0.293
	4	0.01		0.719	1840	0.000	0.482	0.384	0.000	5.08	9.936		0.001			5.262	0.382
Lead	1	0.33	0.15	0.714	1656	0.000	0.611	0.003	0.138	28.56	8.198	39.90	0.000	45.55	43.56	4.434	0.021
	2	0.43	0.15	0.719	1640	0.000	0.342	0.005	0.203	26.77	8.033	39.22	0.000	44.43	43.22	4.533	0.020
	3	0.41	0.14	0.711	1603	0.000	0.333	0.003	0.187	26.50	7.622	38.66	0.000	42.90	43.57	4.435	0.015
	4	0.77	0.14	0.695	1588	0.000	0.488	0.033	0.246	28.57	7.670	44.07	0.000	44.55	44.13	4.323	0.057
Zinc	1	0.05	0.22	0.608	1668	0.000	0.389		0.004	27.0	7.412	42.17	0.000	54.21	47.46	4.605	0.055
	2	0.30	0.18	0.650	1799	0.000	0.394		0.128	26.0	7.970	39.63	0.000	59.81	46.10	4.523	0.393
	3	0.17	0.10	0.467	1602	0.000	0.302		0.025	28.3	5.087	47.22	0.000	46.23	37.97	4.724	0.011
	4	0.06	0.12	0.470	1605	0.000	0.301		0.000	28.2	4.446	46.20	0.000	46.68	38.61	4.731	0.153

ICP-AES analysis results for SPLP leachates of carbonated cement samples

Sample	#	Concentration (mg L ⁻¹)															
		Al	B	Ba	Ca	Cd	Cr	Cu	Fe	K	Mg	Na	Pb	S	Si	Sr	Zn
Control	1	2.742	0.011	0.080	141		0.215	0.001	0.004	6.898	0.047	5.553		18.93	8.758	0.427	0.000
	2	2.735	0.013	0.083	148		0.214	0.001	0.011	6.980	0.080	5.561		18.96	8.878	0.445	0.003
	3	2.043	0.013	0.066	143		0.479	0.001	0.007	5.856	0.071	4.439		28.16	10.780	0.345	0.000
	4	2.040	0.013	0.065	141		0.479	0.001	0.005	5.791	0.062	4.401		28.07	10.750	0.338	0.000
Cadmium	1	0.844		0.085	144	0.001	0.366	0.004			0.180						0.277
	2	1.045		0.084	141	0.000	0.362	0.003			0.146						0.137
	3	0.954		0.080	140	0.000	0.379	0.003			0.156						0.090
	4	0.947		0.083	142	0.000	0.369	0.003			0.160						0.168
Chromium III	1	1.872		0.105	114	0.000	0.070	0.000	0.006	35.760	0.043	82.650		7.050	2.236	1.099	0.101
	2	1.881		0.110	114	0.000	0.078	0.001	0.006	33.610	0.046	79.257		7.794	2.254	1.018	0.102
	3	1.964		0.123	128	0.000	0.093	0.001	0.003	30.120	0.046	73.990		8.466	1.937	0.975	0.098
	4	1.808		0.102	99	0.000	0.070	0.001	0.009	34.950	0.048	81.130		7.866	2.589	0.981	0.106
Chromium VI	1			0.235	282		11.21	0.001			0.032	17.88	0.166	14.89	1.14	0.451	0.056
	2			0.371	464		11.76	0.001			0.007	29.12	0.145	15.72	0.48	0.416	0.054
	3			0.448	549		12.02	0.001			0.005	38.21	0.134	17.94	0.30	0.410	0.052
	4			0.386	480		11.12	0.000			0.005	31.51	0.151	16.35	0.40	0.362	0.046
Copper	1	1.220		0.107	162	0.001	0.284	0.001	0.000	1.148	0.083		0.158			0.451	0.056
	2	0.481		0.078	142	0.001	0.304	0.000	0.032	1.300	0.099		0.160			0.416	0.054
	3	0.761		0.083	147	0.001	0.278	0.000	0.000	1.244	0.095		0.163			0.410	0.052
	4	0.582		0.065	137	0.001	0.247	0.001	0.002	1.285	0.104		0.171			0.362	0.046
Lead	1	1.638	0.014	0.063	155		0.148	0.001	0.009	12.260	0.074	23.53		22.86	12.14	0.389	0.001
	2	1.564	0.014	0.055	149		0.583	0.001	0.006	10.310	0.057	19.82		22.65	12.42	0.331	0.000
	3	1.995	0.011	0.072	160		0.139	0.001	0.003	9.630	0.040	18.84		21.91	10.07	0.414	0.000
	4	1.967	0.011	0.068	147		0.131	0.001	0.002	8.129	0.030	17.08		12.23	10.43	0.377	0.000
Zinc	1	2.031	0.015	0.047	145		0.141	0.001	0.121	5.07	0.119	13.12		32.57	12.86	0.306	0.025
	2	3.605	0.016	0.055	151		0.122	0.001	0.105	12.00	0.065	24.48		29.02	10.3	0.342	0.025
	3	2.054	0.018	0.050	144		0.105	0.001	0.100	8.34	0.064	18.76		30.48	11.72	0.314	0.020
	4	2.290	0.010	0.052	156		0.099	0.000	0.087	13.20	0.043	26.89		29.33	11.12	0.340	0.020

ICP-AES analysis results for TCLP leachates of non-carbonated geopolимер samples

Sample	#	Concentration (mg L ⁻¹)															
		Al	B	Ba	Ca	Cd	Cr	Cu	Fe	K	Mg	Na	Pb	S	Si	Sr	Zn
Control	1	44.07		1.90	405.1	0.001	0.033	0.022	4.36	11.46	40.41			11.14	42.19	13.43	0.101
	2	34.39		1.79	451.4	0.001	0.032	0.016	3.35	12.58	44.00			13.08	39.30	14.35	0.089
	3	39.93		2.36	428.1	0.001	0.033	0.462	3.92	11.66	41.85			11.98	41.06	14.13	0.115
	4	40.06		1.99	425.9	0.001	0.033	0.142	3.90	11.82	41.97			11.92	40.96	14.02	0.106
Cadmium	1	15.37		2.59	405.5	91.72	0.019	0.027	1.61	10.91	41.45	632.6		11.53	35.08	13.31	0.150
	2	10.45		2.08	439.4	125.70	0.015	0.024	0.81	11.31	43.79	719.3		13.14	33.14	14.02	0.144
	3	9.71		2.62	448.6	93.94	0.014	0.022	0.82	11.59	43.88	742.1		14.25	32.01	14.19	0.132
	4	11.76		2.43	432.6	99.86	0.015	0.025	0.89	11.32	43.24	701.6		13.12	33.23	13.98	0.145
Chromium III	1	7.53	6.47	1.64	370.1	0.006	0.110	0.011	0.80	10.86	41.55	655.5		15.78	234.3	10.010	0.078
	2	7.11	6.50	1.68	378.8	0.010	0.089	0.013	0.90	11.01	41.96	654.7		15.73	235.2	10.170	0.126
	3	7.85	6.52	1.54	367.8	0.013	0.092	0.012	0.84	10.95	39.96	650.9		16.48	240.1	9.884	0.088
	4	7.60	6.50	1.63	371.9	0.011	0.095	0.011	0.82	10.97	41.26	653.2		15.87	235.3	10.067	0.091
Chromium VI	1	6.73	6.77	1.06	386.3	0.000	78.03	0.003	0.44	77.17	37.12	661.2		17.34	237.2	11.68	0.029
	2	7.61	6.60	1.08	389.4	0.002	75.48	0.004	0.50	76.21	36.34	644.6		16.73	238.2	11.64	0.031
	3	5.79	7.03	0.99	408.2	0.000	80.59	0.003	0.39	80.01	37.94	692.0		18.17	228.3	11.91	0.026
	4	6.69	6.79	1.04	390.4	0.000	78.49	0.003	0.42	77.42	37.63	654.7		17.43	236.6	11.70	0.031
Copper	1	8.68	5.74	2.37	379.1	0.003	0.729	0.000	0.72	10.680	31.99	612.0	0.007	11.08	133.6	10.48	0.280
	2	7.84	5.87	2.37	382.4	0.002	0.263	0.000	0.53	10.710	32.66	624.4	0.004	11.09	134.2	10.62	0.280
	3	8.40	5.78	2.36	378.8	0.002	0.377	0.000	0.56	10.637	32.32	615.2	0.003	10.97	134.5	10.54	0.276
	4	8.69	5.73	2.33	375.0	0.002	0.137	0.000	0.59	10.520	32.31	609.2	0.000	10.76	135.7	10.54	0.270
Lead	1	7.93	6.00	2.89	373.3	0.002	0.021	0.030	0.66	9.130	33.52	597.7	30.870	10.39	124.0	10.85	0.117
	2	9.77	5.71	2.94	361.4	0.002	0.020	0.029	0.81	8.889	32.66	567.0	32.977	9.44	126.7	10.74	0.114
	3	12.50	5.21	3.09	338.2	0.002	0.022	0.035	1.03	8.455	31.34	510.5	36.660	8.04	132.8	10.38	0.123
	4	8.80	5.90	2.84	372.8	0.002	0.017	0.021	0.75	9.082	33.14	593.0	31.400	9.89	123.5	11.00	0.100
Zinc	1	9.05	5.87	2.38	391.1	0.002	0.017	0.061	1.26	9.134	34.69	606.4	0.027	11.51	144.1	10.95	44.870
	2	9.54	5.83	2.33	385.7	0.003	0.016	0.049	1.29	9.076	34.25	602.3	0.014	11.50	144.6	10.86	44.460
	3	9.75	5.80	2.34	384.6	0.004	0.016	0.045	1.27	9.007	34.07	598.4	0.016	11.48	144.7	10.80	44.470
	4	9.83	5.83	2.26	381.6	0.002	0.015	0.042	1.33	9.088	34.01	602.3	0.000	11.53	145.0	10.84	44.040

ICP-AES analysis results for SPLP leachates of non-carbonated geopolymers samples

Sample	#	Concentration (mg L^{-1})															
		Al	B	Ba	Ca	Cd	Cr	Cu	Fe	K	Mg	Na	Pb	S	Si	Sr	Zn
Control	1	11.42		0.345	9.065	0.000	0.026	0.125	1.155	3.015	1.072	394.0	0.000	25.35	22.92	0.183	0.014
	2	10.06		0.160	7.809	0.000	0.025	0.135	0.879	2.953	1.177	396.6	0.000	25.81	22.34	0.133	0.009
	3	4.89		0.085	3.837	0.000	0.020	0.002	0.295	2.503	0.257	384.4	0.000	23.58	17.81	0.067	0.002
	4	8.80		0.192	7.121	0.000	0.025	0.098	0.829	2.913	0.986	392.4	0.000	25.06	21.43	0.131	0.010
Cadmium	1	0.33		0.022	3.570	0.229	0.024	0.002	0.249	2.731	0.256	413.6	0.000	23.46	22.29	0.055	0.002
	2	0.28		0.022	3.478	0.260	0.026	0.003	0.253	2.963	0.222	448.9	0.000	24.97	22.88	0.050	0.002
	3	0.28		0.025	3.954	0.273	0.026	0.001	0.285	3.089	0.238	465.8	0.000	26.47	23.79	0.049	0.002
	4	0.29		0.022	3.643	0.256	0.26	0.003	0.259	2.956	0.241	430.7	0.000	24.89	22.96	0.050	0.002
Chromium III	1	7.20	5.346	0.049	1.118	0.000	0.082	0.002	0.242	2.779	0.146	402.5	0.000	26.62	133.5	0.034	0.009
	2	7.27	5.185	0.055	1.168	0.000	0.069	0.002	0.272	2.707	0.159	392.1	0.010	26.07	131.0	0.035	0.013
	3	6.91	5.393	0.050	1.123	0.000	0.061	0.002	0.248	2.820	0.141	406.9	0.003	27.42	127.8	0.033	0.010
	4	7.24	5.324	0.054	1.133	0.001	0.068	0.002	0.251	2.701	0.145	401.9	0.003	26.58	132.6	0.033	0.012
Chromium VI	1	11.50	5.980	0.047	0.816	0.001	94.96	0.003	0.234	29.73	0.154	454.9	0.009	23.89	171.3	0.032	0.010
	2	11.47	5.642	0.046	0.812	0.000	89.07	0.003	0.234	28.41	0.156	432.0	0.000	22.64	164.4	0.031	0.010
	3	11.67	6.279	0.040	0.781	0.000	98.79	0.002	0.206	31.15	0.134	473.0	0.000	24.72	172.6	0.030	0.009
	4	11.52	5.922	0.046	0.813	0.000	94.49	0.003	0.229	29.16	0.150	453.8	0.000	23.92	170.4	0.032	0.010
Copper	1	7.68	4.822	0.059	3.274	0.001	0.144	0.233	0.214	2.457	0.360	360.8	0.005	20.72	82.5	0.098	0.011
	2	7.80	4.883	0.053	2.412	0.001	0.105	0.192	0.213	2.440	0.276	362.7	0.000	20.95	84.0	0.072	0.011
	3	7.89	5.006	0.055	2.438	0.001	0.095	0.195	0.221	2.469	0.281	368.5	0.000	21.38	85.7	0.074	0.011
	4	7.84	4.821	0.046	1.525	0.000	0.075	0.147	0.205	2.395	0.188	359.0	0.000	20.76	83.8	0.045	0.010
Lead	1	8.42	5.37	0.057	2.984	0.000	0.022	0.014	0.218	2.567	0.356	394.8	0.539	21.73	91.8	0.093	0.016
	2	8.26	5.08	0.056	2.337	0.000	0.021	0.007	0.260	2.441	0.296	375.7	0.511	20.91	88.9	0.072	0.012
	3	8.24	4.93	0.057	2.373	0.001	0.021	0.004	0.309	2.386	0.305	365.4	0.523	20.34	87.7	0.074	0.010
	4	8.12	4.96	0.053	1.654	0.000	0.022	0.004	0.254	2.371	0.226	367.1	0.473	20.67	87.1	0.049	0.010
Zinc	1	8.76	4.74	0.067	2.490	0.001	0.026	0.003	0.256	2.155	0.292	367.0	0.000	21.28	82.2	0.075	0.366
	2	8.71	4.95	0.075	3.266	0.000	0.031	0.003	0.269	2.261	0.364	381.7	0.000	21.84	83.1	0.099	0.454
	3	8.53	4.60	0.064	2.468	0.001	0.024	0.003	0.250	2.065	0.299	350.8	0.000	20.93	82.1	0.075	0.376
	4	9.02	4.66	0.063	1.737	0.002	0.024	0.005	0.250	2.140	0.212	368.5	0.000	21.08	81.4	0.052	0.269

ICP-AES analysis results for TPLP leachates of carbonated geopolимер samples

Sample	#	Concentration (mg L^{-1})															
		Al	B	Ba	Ca	Cd	Cr	Cu	Fe	K	Mg	Na	Pb	S	Si	Sr	Zn
Control	1	11.87		2.07	397	0.008	0.030	0.010	0.90	8.51	37.80		0.000	14.80	25.0	11.82	0.050
	2	10.10		1.97	414	0.001	0.027	0.009	0.77	8.62	39.23		0.000	15.66	24.2	11.91	0.046
	3	10.06		2.18	413	0.002	0.027	0.008	0.85	8.74	38.77		0.000	15.39	23.9	12.02	0.049
	4	10.58		2.06	409	0.002	0.027	0.009	0.84	8.64	38.74		0.000	15.31	24.3	11.94	0.049
Cadmium	1	3.35	7.49	1.58	452	98.47	0.011	0.014	0.27	8.53	50.70	657.9	0.002	13.30	155.2	11.74	0.415
	2	2.61	7.88	1.53	469	118.60	0.009	0.014	0.22	8.67	52.43	689.2	0.000	14.46	147.8	11.93	0.478
	3	4.81	7.01	1.58	423	93.01	0.016	0.019	0.43	8.66	47.03	610.3	0.017	12.68	168.7	11.34	0.555
	4	3.67	7.48	1.57	450	99.25	0.010	0.015	0.29	8.70	51.06	664.9	0.004	12.93	154.3	11.55	0.471
Chromium III	1	7.78	6.75	1.14	383	0.004	0.156	0.008	0.67	8.89	35.30	703.5	0.000	19.40	98.5	8.90	0.065
	2	7.41	6.81	1.17	392	0.003	0.157	0.008	0.65	8.23	36.12	706.2	0.000	18.95	98.3	9.15	0.063
	3	7.15	6.82	1.18	397	0.003	0.156	0.007	0.62	8.21	36.71	705.0	0.000	18.73	98.3	9.30	0.061
	4	7.31	6.86	1.21	395	0.002	0.160	0.008	0.65	8.20	36.33	710.3	0.000	18.66	98.0	9.26	0.063
Chromium VI	1	6.32	7.06	1.04	423	0.001	73.170	0.003	0.42	67.25	32.77	704.3	0.000	18.98	102.7	11.48	0.027
	2	7.35	6.84	1.08	414	0.001	71.700	0.003	0.48	65.91	31.95	680.1	0.000	18.27	103.7	11.38	0.028
	3	7.77	6.77	1.10	410	0.001	70.413	0.003	0.50	65.62	31.74	673.2	0.000	17.97	104.6	11.33	0.029
	4	9.66	6.40	1.17	393	0.001	66.370	0.004	0.62	63.72	30.51	635.2	0.000	16.66	107.4	11.13	0.032
Copper	1	8.09	6.59	2.26	413	0.002	0.031	20.390	0.46	8.44	34.34	628.2	0.020	12.04	98.1	10.54	0.307
	2	8.81	6.42	2.17	403	0.001	0.027	21.750	0.49	8.58	33.49	632.5	0.008	12.52	100.7	10.42	0.315
	3	8.75	6.48	2.16	406	0.001	0.029	21.093	0.51	8.53	33.55	628.9	0.011	12.34	99.5	10.44	0.310
	4	9.35	6.43	2.07	402	0.001	0.027	21.140	0.56	8.55	32.83	626.1	0.006	12.45	99.8	10.35	0.309
Lead	1	11.01	5.83	2.48	365	0.002	0.024	0.015	0.71	7.32	30.70	556.8	33.453	10.56	88.3	10.45	0.105
	2	12.02	5.55	2.43	349	0.003	0.026	0.016	0.80	7.11	30.01	526.9	34.160	10.09	88.0	10.10	0.121
	3	11.06	5.85	2.48	367	0.001	0.025	0.015	0.71	7.47	30.83	557.2	33.510	10.30	88.6	10.54	0.100
	4	9.95	6.08	2.54	377	0.001	0.022	0.013	0.62	7.38	31.28	586.2	32.690	11.28	88.3	10.71	0.094
Zinc	1	9.15	6.24	1.92	397	0.002	0.028	0.091	0.903	6.90	34.18	596.9	0.003	12.59	94.3	10.39	45.490
	2	9.40	6.24	1.91	392	0.002	0.028	0.066	0.889	6.90	33.96	597.8	0.007	12.61	93.7	10.24	44.440
	3	9.16	6.32	1.91	394	0.002	0.028	0.057	0.863	6.90	34.33	602.7	0.012	12.71	93.4	10.21	44.080
	4	9.89	6.17	1.91	384	0.001	0.027	0.050	0.900	6.90	33.37	593.8	0.006	12.54	93.4	10.13	43.750

ICP-AES analysis results for SPLP leachates of carbonated geopolymers samples

Sample	#	Concentration (mg L^{-1})															
		Al	B	Ba	Ca	Cd	Cr	Cu	Fe	K	Mg	Na	Pb	S	Si	Sr	Zn
Control	1	0.33		0.022	3.570	0.000	0.006	0.000	0.03	1.861	0.719	425.0	0.000	24.81	2.874	0.089	0.001
	2	0.28		0.022	3.478	0.000	0.007	0.000	0.02	1.769	0.765	413.5	0.000	24.02	2.875	0.084	0.000
	3	0.28		0.025	3.954	0.000	0.008	0.001	0.03	1.727	0.766	404.2	0.000	22.41	2.957	0.093	0.000
	4	0.29		0.022	3.658	0.000	0.008	0.000	0.03	1.775	0.758	416.4	0.000	23.86	2.892	0.089	0.000
Cadmium	1	0.99	5.350	0.046	2.494	0.154	0.010	0.002	0.25	1.675	0.442	379.2	0.009	22.74	30.94	0.042	0.018
	2	0.69	6.096	0.033	2.260	0.174	0.011	0.001	0.13	1.815	0.393	426.8	0.000	25.08	30.64	0.035	0.020
	3	0.66	5.918	0.031	2.238	0.092	0.009	0.001	0.12	1.760	0.379	412.0	0.000	24.82	31.32	0.034	0.010
	4	0.74	5.875	0.034	2.302	0.152	0.009	0.001	0.14	1.764	0.391	414.8	0.000	24.43	30.87	0.034	0.018
Chromium III	1	0.68	4.484	0.050	4.690	0.001	0.028	0.002	0.15	1.771	0.712	428.9	0.000	26.88	11.17	0.102	0.008
	2	0.64	4.636	0.045	3.838	0.001	0.028	0.002	0.11	1.773	0.616	438.3	0.000	27.57	11.10	0.081	0.012
	3	0.65	4.755	0.046	3.823	0.001	0.031	0.003	0.12	1.792	0.625	444.3	0.000	28.32	10.96	0.081	0.021
	4	0.59	4.670	0.039	3.001	0.001	0.026	0.002	0.10	1.757	0.511	441.8	0.000	27.51	11.17	0.059	0.007
Chromium VI	1	0.42	5.454	0.046	5.433	0.000	89.200	0.002	0.08	20.090	0.610	481.5	0.000	24.13	12.08	0.151	0.008
	2	0.45	5.413	0.044	4.581	0.000	88.557	0.002	0.08	19.807	0.504	477.5	0.000	24.14	12.38	0.126	0.008
	3	0.46	5.291	0.045	4.631	0.001	86.470	0.003	0.08	19.540	0.500	470.5	0.000	23.79	12.24	0.126	0.008
	4	0.44	5.494	0.042	3.678	0.000	90.000	0.001	0.08	19.790	0.403	480.5	0.000	24.51	12.82	0.099	0.008
Copper	1	0.95	4.68	0.07	5.463	0.000	0.013	0.225	0.176	1.720	0.790	397.8	0.001	21.37	11.7	0.11	0.008
	2	0.52	4.63	0.04	6.276	0.000	0.016	0.196	0.082	1.691	0.816	387.3	0.002	20.71	10.4	0.11	0.009
	3	0.48	4.69	0.04	5.032	0.000	0.012	0.160	0.072	1.711	0.711	403.7	0.004	21.62	10.9	0.09	0.008
	4	1.86	4.73	0.13	6.175	0.000	0.012	0.319	0.375	1.757	0.841	402.5	0.000	21.77	14.0	0.12	0.009
Lead	1	0.43	4.23	0.04	6.789	0.000	0.004	0.002	0.071	1.530	0.822	371.9	0.327	19.52	11.0	0.16	0.010
	2	0.36	4.34	0.04	5.153	0.000	0.003	0.002	0.062	1.559	0.734	384.6	0.272	20.02	11.0	0.14	0.009
	3	0.34	4.51	0.04	5.097	0.000	0.003	0.002	0.055	1.591	0.743	388.2	0.249	20.64	11.0	0.14	0.008
	4	0.32	4.27	0.03	5.645	0.000	0.003	0.002	0.059	1.555	0.638	393.8	0.241	19.90	11.1	0.13	0.008
Zinc	1	0.58	4.80	0.05	6.301	0.001	0.006	0.006	0.095	1.489	0.897	413.0	0.000	21.88	10.6	0.11	0.305
	2	0.58	4.37	0.05	6.452	0.002	0.006	0.003	0.094	1.383	0.884	378.4	0.000	20.51	11.2	0.12	0.347
	3	0.58	4.80	0.05	6.301	0.001	0.006	0.006	0.095	1.489	0.897	413.0	0.000	21.88	10.6	0.11	0.305
	4	0.58	5.22	0.05	6.150	0.000	0.006	0.008	0.096	1.595	0.910	447.5	0.000	23.25	10.1	0.11	0.262

Appendix II – SEM Images and EDS Analyses

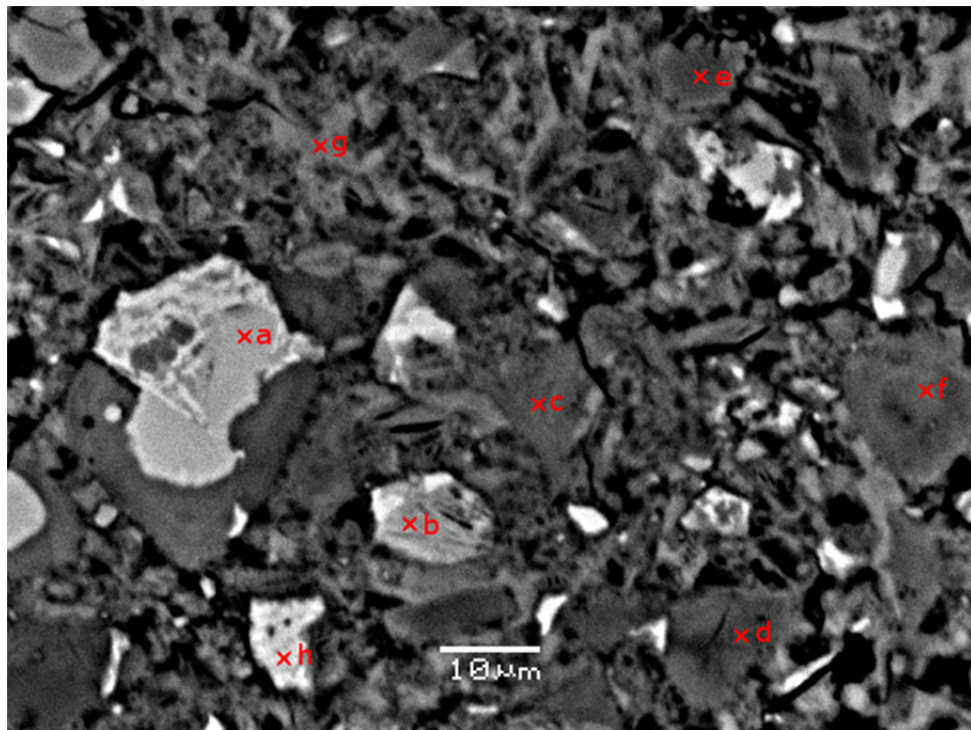
The following pages contain SEM images of carbonated and non-carbonated cement-based and geopolymers-based stabilized/solidified synthetic metal wastes along with their EDS analysis at various points marked in the images. The equipment used was a JEOL JSM-5900LV Variable Pressure SEM with 4"x5" Analytical Stage. If the element % (i.e., weight %) of any element is less than twice the sigma value, the element is under the detection limit. The standards used for calibration and their composition are shown in the table below.

Standards used for calibration and their composition

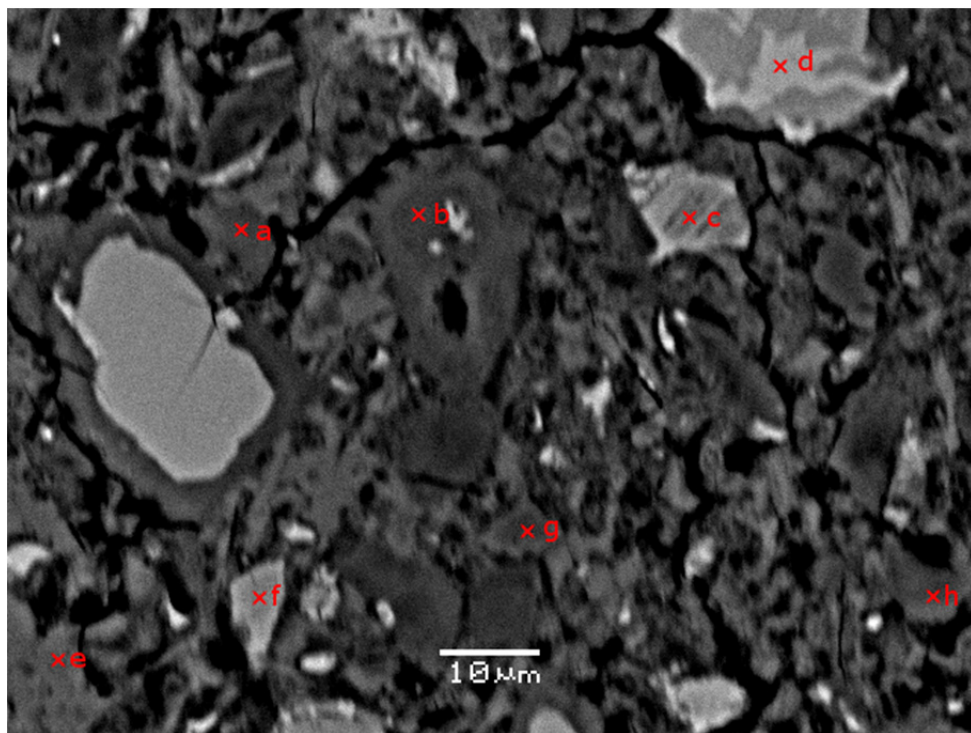
Mineral (wt %)	MgO	Al₂O₃	SiO₂	CaO	Cr₂O₃	FeO	Na₂O	TiO₂	MnO
Garnet	21.16	21.08	42.02	4.98	3.53	6.65			
Orthoclase	12.10	8.82	56.89	16.83			5.36		
Jadeite		25.10	58.50				15.10		
Wollastonite			51.70	48.30		0.80			
Chromite	12.30	19.40			44.50	22.09		0.47	0.19

SEM-EDS analysis of non-carbonated cement-based s/s control sample

Sample a



Sample b



Sample a

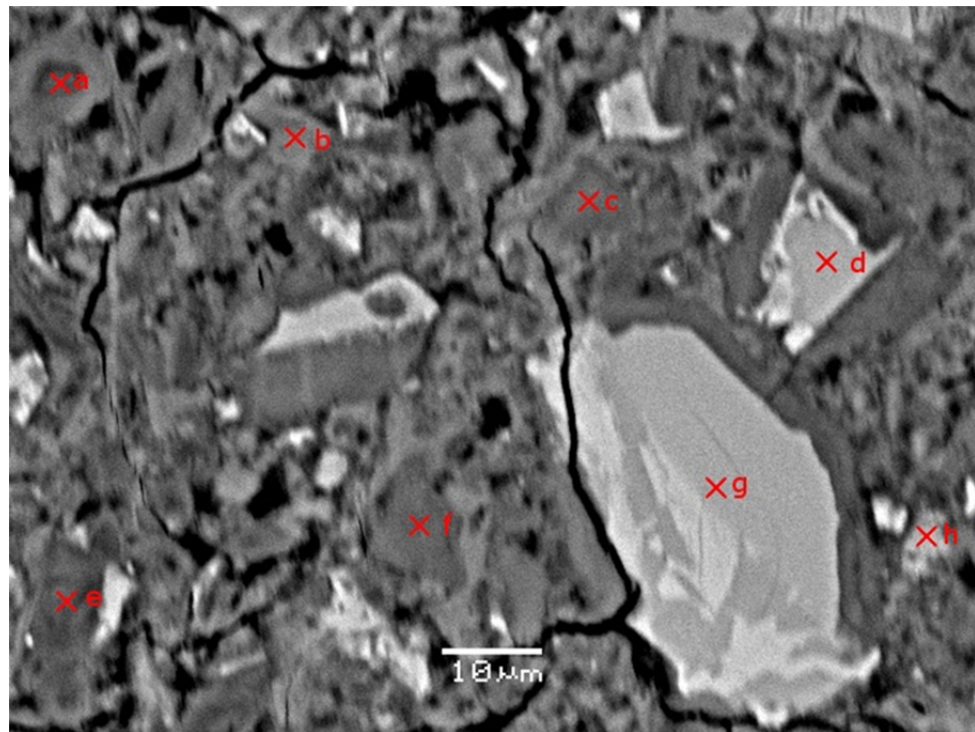
	a		b		c		d		e		f		g		h	
	Element %	σ	Element %	σ	Element %	σ	Element %	σ	Element %	σ	Element %	σ	Element %	σ	Element %	σ
O	24.79	0.13	25.54	0.15	40.95	0.14	41.87	0.12	48.54	0.17	41.33	0.12	39.43	0.18	27.36	0.13
Na	0.00	0.10	0.19	0.10	-0.08	0.09	0.03	0.09	-0.07	0.10	0.14	0.09	-0.09	0.10	0.52	0.13
Mg	0.42	0.08	0.29	0.08	0.42	0.08	0.25	0.08	0.14	0.07	0.30	0.07	-0.04	0.08	1.09	0.11
Al	0.78	0.08	1.46	0.08	0.94	0.07	1.87	0.08	0.03	0.06	1.39	0.08	0.50	0.07	6.71	0.13
Si	11.17	0.13	11.97	0.13	10.81	0.13	8.37	0.12	0.14	0.05	10.51	0.12	2.63	0.08	3.96	0.11
S	-0.01	0.06	0.25	0.07	0.87	0.08	1.40	0.08	0.08	0.05	1.26	0.08	0.56	0.06	1.42	0.08
K	0.10	0.07	0.09	0.05	-0.02	0.06	0.09	0.07	-0.03	0.05	0.02	0.05	-0.02	0.05	0.04	0.04
Ca	46.74	0.30	37.74	0.28	31.92	0.25	25.61	0.23	33.04	0.25	27.91	0.24	38.92	0.27	31.07	0.25
Cd	0.28	0.19	-0.07	0.15	-0.26	0.14	-0.31	0.14	0.18	0.17	-0.04	0.18	-0.05	0.18	0.09	0.16
Cu	-0.11	0.13	-0.04	0.15	-0.03	0.13	-0.02	0.12	-0.02	0.13	-0.07	0.14	-0.04	0.14	-0.02	0.12
Cr	0.09	0.07	0.07	0.07	0.03	0.07	0.03	0.06	-0.01	0.07	0.03	0.06	0.09	0.07	0.06	0.06
Pb	0.24	0.17	0.23	0.17	0.14	0.17	0.18	0.19	0.10	0.20	0.04	0.18	0.17	0.20	0.11	0.18
Zn	-0.48	0.50	0.01	0.63	0.06	0.56	0.26	0.37	0.69	0.35	0.36	0.37	-0.63	0.56	0.66	0.38
Fe	0.63	0.13	2.07	0.16	0.57	0.13	0.87	0.13	-0.05	0.10	0.58	0.12	0.48	0.12	6.59	0.23
TOT	84.64		79.80		86.32		80.50		82.76		83.76		81.91		79.66	
	Unreacted cement phases		Unreacted cement phases		CSH		CSH		Ca(OH) ₂		CSH		Ca(OH) ₂		Unreacted cement phases	

Sample b

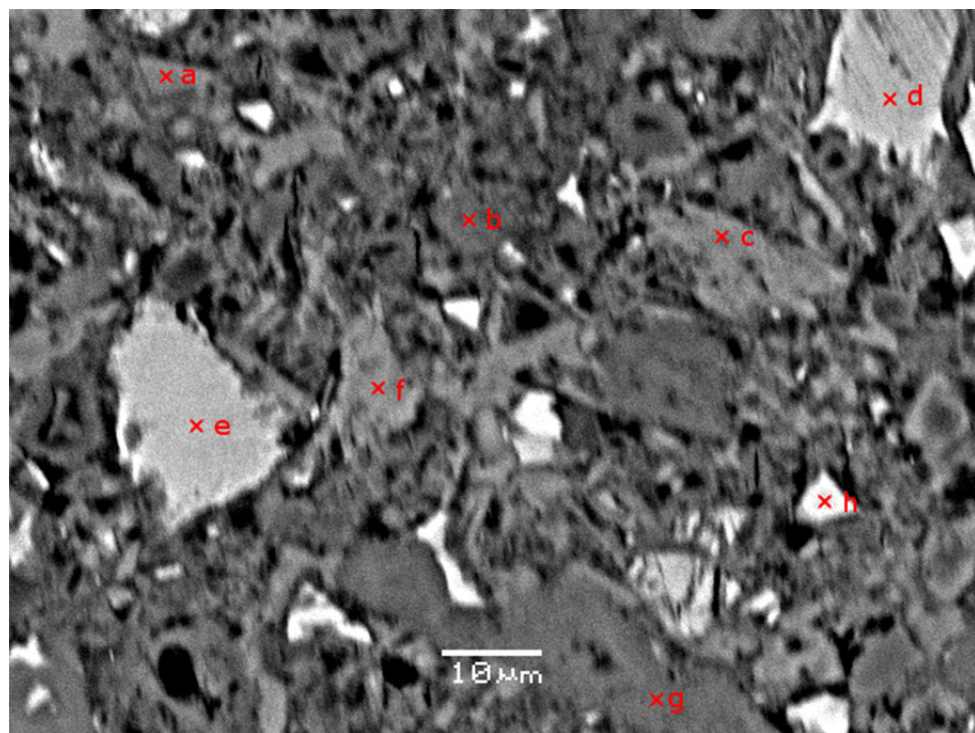
	a		b		c		d		e		f		g		h	
	Element %	σ	Element %	σ	Element %	σ	Element %	σ	Element %	σ	Element %	σ	Element %	σ	Element %	σ
O	43.08	0.14	39.42	0.18	26.14	0.16	25.73	0.17	39.18	0.15	25.20	0.19	37.69	0.16	40.15	0.14
Na	-0.09	0.07	0.01	0.07	0.08	0.08	0.87	0.10	-0.03	0.07	0.09	0.07	-0.08	0.07	-0.18	0.08
Mg	0.09	0.05	0.18	0.05	0.27	0.06	1.48	0.08	0.28	0.05	0.04	0.06	0.32	0.05	-0.01	0.06
Al	0.03	0.04	0.77	0.06	0.66	0.06	10.94	0.12	0.63	0.05	0.86	0.06	0.65	0.06	0.17	0.05
Si	0.09	0.04	10.67	0.10	11.85	0.11	2.55	0.08	10.52	0.10	14.27	0.11	10.47	0.10	1.19	0.05
S	0.02	0.04	1.18	0.06	0.11	0.05	0.06	0.05	1.17	0.06	0.29	0.05	1.43	0.06	0.27	0.04
K	0.03	0.04	0.09	0.05	0.06	0.05	0.07	0.07	0.05	0.04	0.06	0.06	0.04	0.04	0.05	0.04
Ca	37.40	0.21	35.08	0.22	49.71	0.25	34.52	0.21	34.70	0.22	45.00	0.24	34.16	0.21	46.79	0.24
Cd	-0.26	0.14	0.02	0.18	0.08	0.16	-0.12	0.17	-0.13	0.15	0.35	0.19	0.35	0.16	-0.07	0.14
Cu	-0.07	0.12	-0.02	0.13	-0.04	0.13	-0.05	0.15	-0.09	0.13	-0.01	0.15	-0.12	0.15	-0.11	0.13
Cr	0.01	0.06	0.00	0.06	0.00	0.06	0.05	0.06	0.06	0.06	0.02	0.06	0.03	0.06	0.05	0.07
Pb	0.20	0.20	0.32	0.17	0.13	0.17	0.37	0.19	0.06	0.18	0.20	0.20	0.34	0.19	0.13	0.18
Zn	-0.71	0.50	-0.01	0.49	0.23	0.69	0.20	0.35	-0.74	0.44	0.12	0.37	-0.49	0.65	0.02	0.51
Fe	-0.01	0.10	0.56	0.10	0.55	0.11	12.36	0.25	0.74	0.11	0.75	0.12	0.85	0.11	0.03	0.10
TOT	79.81		88.27		89.83		89.03		86.40		87.24		85.64		88.48	
	Ca(OH)2		CSH		Unreacted cement phases		Unreacted cement phases		CSH		Unreacted cement phases		CSH		Ca(OH)2	

SEM-EDS analysis of non-carbonated cement-based s/s cadmium doped sample

Sample a



Sample b



Sample a

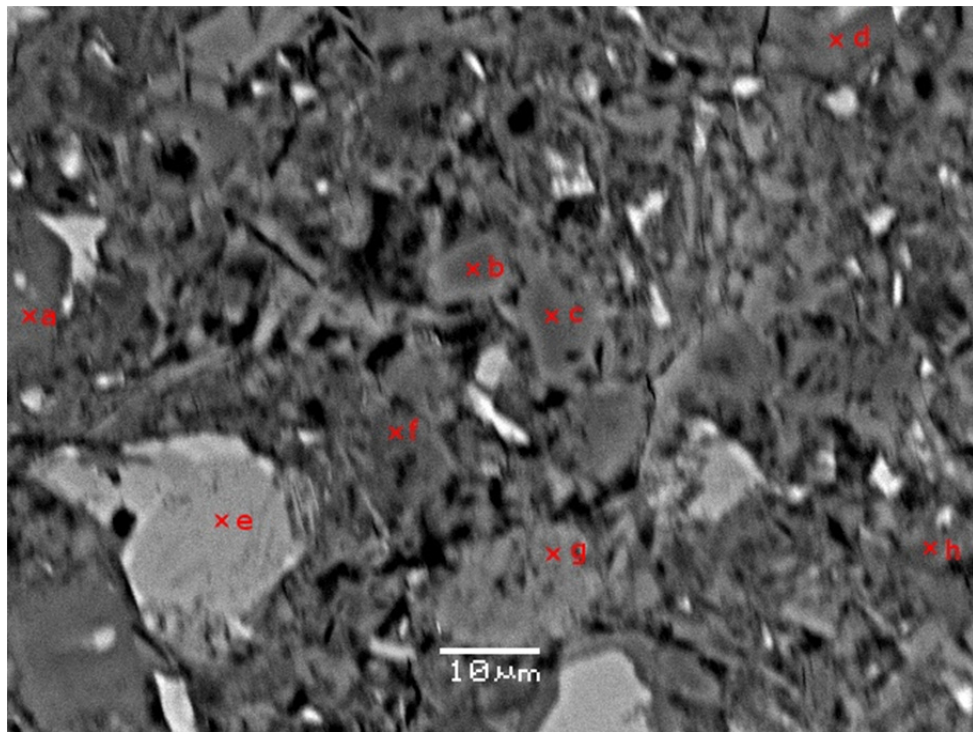
	a		b		c		d		e		f		g		h	
	Element %	σ	Element %	σ	Element %	σ	Element %	σ	Element %	σ	Element %	σ	Element %	σ	Element %	σ
O	40.69	0.15	38.74	0.14	40.90	0.14	27.35	0.17	41.30	0.19	38.41	0.15	25.85	0.18	27.45	0.18
Na	0.35	0.08	-0.09	0.08	0.04	0.08	0.70	0.09	0.27	0.07	-0.09	0.07	0.14	0.09	0.08	0.08
Mg	0.25	0.06	-0.03	0.06	0.06	0.06	0.54	0.08	0.37	0.06	0.41	0.06	0.59	0.07	0.17	0.06
Al	1.91	0.07	0.09	0.05	0.67	0.06	12.34	0.12	1.99	0.07	0.80	0.06	3.05	0.08	0.59	0.06
Si	8.08	0.10	0.56	0.05	9.39	0.10	1.81	0.08	6.95	0.09	9.94	0.10	8.81	0.10	12.62	0.11
S	1.32	0.06	0.06	0.04	1.06	0.06	0.03	0.05	1.44	0.07	1.31	0.07	0.09	0.05	0.26	0.05
K	0.09	0.05	0.07	0.04	0.08	0.07	0.00	0.07	0.00	0.04	0.01	0.04	0.04	0.04	-0.01	0.07
Ca	27.11	0.20	40.68	0.24	29.57	0.21	33.49	0.22	24.40	0.19	27.38	0.20	39.41	0.24	37.08	0.23
Cd	-0.25	0.15	-0.09	0.14	0.04	0.14	-0.01	0.17	0.12	0.16	-0.14	0.15	-0.09	0.18	0.26	0.18
Cu	-0.12	0.15	-0.10	0.13	-0.06	0.12	-0.04	0.15	-0.04	0.14	-0.03	0.13	-0.08	0.13	-0.01	0.12
Cr	0.08	0.06	0.03	0.06	0.03	0.07	0.07	0.06	0.05	0.07	0.03	0.07	0.07	0.07	0.01	0.07
Pb	0.01	0.17	0.22	0.20	0.17	0.17	0.26	0.17	0.13	0.18	0.17	0.18	0.30	0.18	0.31	0.17
Zn	0.44	0.59	-0.69	0.56	0.17	0.68	0.16	0.51	0.54	0.61	0.38	0.50	0.68	0.53	-0.18	0.38
Fe	0.57	0.10	0.22	0.10	0.66	0.10	6.27	0.20	1.48	0.12	0.54	0.10	3.88	0.17	0.71	0.11
TOT	79.53		79.67		82.78		82.97		79.00		79.12		82.74		79.34	
	CSH		Ca(OH)2		CSH		Unreacted cement phases		CSH		CSH		Unreacted cement phases		Unreacted cement phases	

Sample b

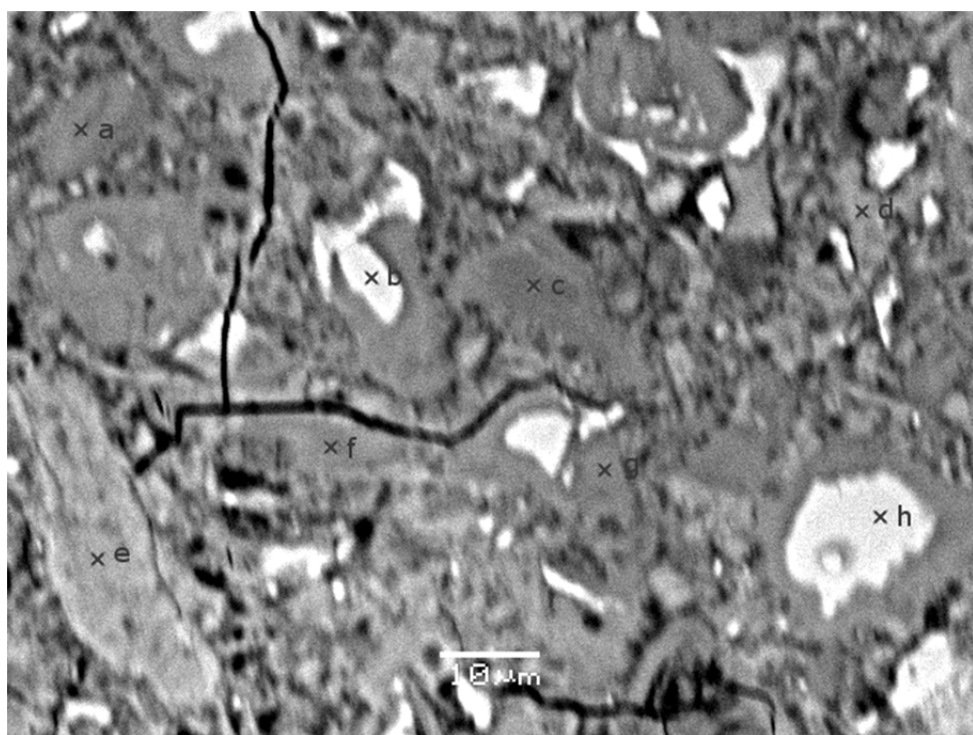
	a		b		c		d		e		f		g		h	
	Element %	σ	Element %	σ	Element %	σ	Element %	σ	Element %	σ	Element %	σ	Element %	σ	Element %	σ
O	39.55	0.17	40.91	0.14	40.29	0.15	30.42	0.19	26.44	0.18	41.10	0.18	41.63	0.19	46.33	0.17
Na	0.12	0.08	0.02	0.08	0.00	0.08	0.10	0.08	-0.09	0.08	0.10	0.07	0.10	0.07	0.01	0.08
Mg	0.20	0.06	0.58	0.06	0.10	0.06	0.21	0.06	0.10	0.06	0.18	0.06	0.17	0.06	0.17	0.06
Al	1.54	0.06	1.03	0.06	0.23	0.05	1.10	0.06	0.26	0.06	0.72	0.06	0.80	0.06	1.02	0.06
Si	3.11	0.07	8.80	0.10	1.48	0.06	11.43	0.11	13.46	0.11	4.36	0.07	9.48	0.10	5.00	0.08
S	0.51	0.05	1.00	0.06	0.24	0.05	0.37	0.05	0.02	0.05	0.54	0.05	1.03	0.06	0.71	0.06
K	0.08	0.05	0.07	0.05	0.01	0.04	0.03	0.07	-0.03	0.06	0.04	0.05	0.05	0.07	0.04	0.05
Ca	33.51	0.22	25.70	0.20	38.47	0.23	34.96	0.23	37.76	0.24	32.91	0.22	27.88	0.20	31.07	0.21
Cd	0.26	0.17	-0.25	0.14	0.14	0.15	-0.30	0.19	0.32	0.18	0.15	0.19	-0.04	0.19	-0.07	0.14
Cu	-0.08	0.13	-0.03	0.13	-0.09	0.13	-0.06	0.15	-0.11	0.13	-0.01	0.15	-0.10	0.12	-0.04	0.14
Cr	0.06	0.06	0.05	0.06	0.06	0.07	0.02	0.07	0.09	0.07	0.07	0.07	-0.01	0.06	0.02	0.06
Pb	0.14	0.18	0.38	0.18	0.05	0.18	0.23	0.20	0.06	0.18	0.26	0.18	0.13	0.20	0.05	0.17
Zn	0.56	0.45	0.43	0.55	-0.39	0.41	-0.14	0.34	0.51	0.39	-0.68	0.60	-0.70	0.41	-0.58	0.46
Fe	0.39	0.10	0.52	0.10	0.25	0.10	0.89	0.12	0.48	0.11	0.09	0.10	0.48	0.10	0.50	0.10
TOT	79.95		79.21		80.84		79.26		79.27		79.83		80.90		84.23	
	Ca(OH)2		CSH		Ca(OH)2		Unreacted cement phases		Unreacted cement phases		Ca(OH)2		CSH		Unreacted cement phases	

SEM-EDS analysis of non-carbonated cement-based s/s chromium (III) doped sample

Sample a



Sample b



Sample a

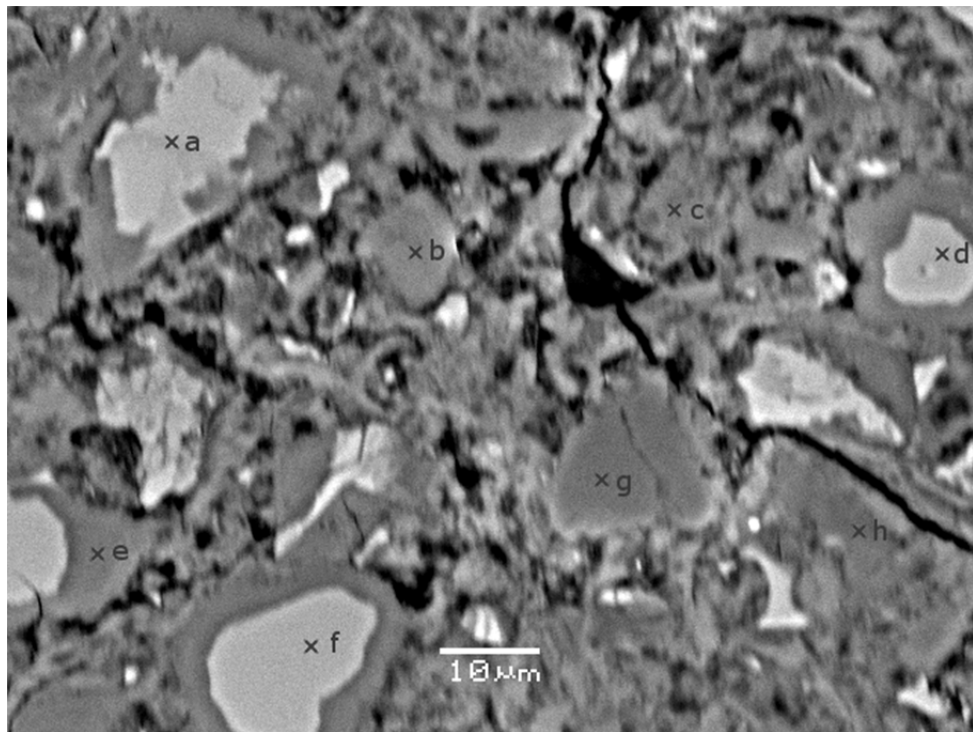
	a		b		c		d		e		f		g		h	
	Element %	σ	Element %	σ	Element %	σ	Element %	σ	Element %	σ						
O	38.42	0.18	51.52	0.18	48.00	0.15	38.59	0.19	29.34	0.11	42.00	0.19	41.81	0.15	47.43	0.12
Na	0.02	0.07	0.04	0.08	-0.07	0.08	-0.11	0.08	0.41	0.08	0.20	0.07	-0.10	0.09	0.88	0.09
Mg	0.38	0.06	0.14	0.06	0.10	0.06	0.48	0.06	0.15	0.06	0.29	0.06	-0.20	0.06	0.05	0.07
Al	0.73	0.06	0.12	0.05	0.03	0.05	0.57	0.06	0.88	0.06	1.53	0.06	0.14	0.05	5.81	0.09
Si	9.65	0.10	0.29	0.04	0.46	0.05	9.56	0.10	12.45	0.11	8.11	0.09	0.41	0.05	2.40	0.07
S	0.88	0.06	-0.02	0.04	0.08	0.04	0.91	0.06	0.24	0.05	1.18	0.06	0.16	0.04	1.92	0.07
K	-0.01	0.06	0.06	0.04	0.03	0.06	0.01	0.05	0.06	0.04	0.04	0.06	0.05	0.06	0.07	0.04
Ca	29.93	0.21	29.10	0.20	31.49	0.21	28.85	0.21	36.33	0.23	26.27	0.20	37.16	0.23	21.79	0.18
Cd	-0.11	0.18	0.23	0.17	-0.13	0.15	0.14	0.16	0.27	0.16	-0.08	0.18	0.15	0.15	0.19	0.19
Cu	-0.07	0.13	-0.04	0.15	-0.08	0.14	-0.12	0.12	-0.07	0.12	-0.07	0.15	-0.10	0.14	-0.01	0.12
Cr	0.07	0.06	0.07	0.07	0.07	0.07	0.01	0.07	-0.01	0.06	0.06	0.06	0.06	0.07	0.04	0.06
Pb	0.04	0.18	0.06	0.18	0.14	0.20	0.16	0.19	0.11	0.17	0.38	0.19	0.27	0.20	0.28	0.20
Zn	-0.42	0.57	0.33	0.69	0.57	0.63	0.25	0.58	-0.22	0.59	0.47	0.61	0.67	0.70	-0.57	0.41
Fe	0.61	0.11	0.03	0.09	0.09	0.09	0.57	0.10	0.74	0.12	0.52	0.10	0.15	0.09	0.30	0.10
TOT	80.12		81.93		80.78		79.87		80.68		80.90		80.63		80.58	
	CSH		Ca(OH)2		Ca(OH)2		CSH		Unreacted cement phases		CSH		Ca(OH)2		Unreacted cement phases	

Sample b

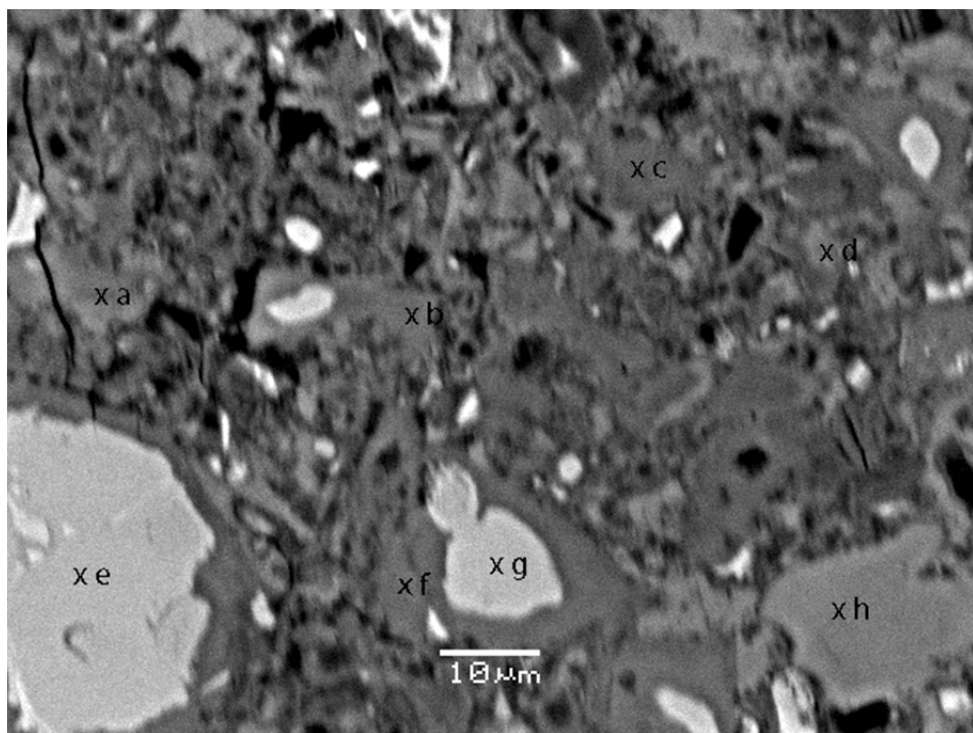
	a		b		c		d		e		f		g		h	
	Element %	σ	Element %	σ	Element %	σ	Element %	σ	Element %	σ	Element %	σ	Element %	σ	Element %	σ
O	39.45	0.15	26.67	0.18	42.65	0.18	40.93	0.17	45.31	0.18	40.60	0.18	42.84	0.16	30.20	0.18
Na	-0.01	0.07	0.08	0.08	0.02	0.07	0.02	0.08	-0.11	0.08	0.07	0.07	0.09	0.07	0.00	0.08
Mg	0.20	0.06	0.34	0.06	0.19	0.06	0.13	0.06	0.02	0.06	0.30	0.06	0.39	0.06	0.27	0.06
Al	0.49	0.06	0.50	0.06	0.48	0.05	0.34	0.05	0.03	0.05	0.61	0.06	0.83	0.06	0.74	0.06
Si	9.19	0.10	10.43	0.10	9.61	0.10	3.21	0.07	0.16	0.04	9.54	0.10	9.68	0.10	10.62	0.11
S	0.91	0.06	0.05	0.05	0.88	0.06	0.32	0.05	0.03	0.04	0.89	0.06	0.86	0.06	0.22	0.05
K	0.03	0.04	0.02	0.06	0.04	0.07	0.01	0.04	0.06	0.05	-0.03	0.07	0.00	0.07	0.05	0.05
Ca	27.48	0.21	41.71	0.24	26.74	0.20	35.14	0.22	36.79	0.22	26.73	0.20	26.35	0.20	40.85	0.24
Cd	0.20	0.15	-0.24	0.19	0.04	0.18	0.26	0.18	-0.33	0.18	-0.02	0.16	-0.15	0.16	-0.09	0.19
Cu	-0.01	0.15	-0.07	0.13	-0.07	0.12	-0.07	0.15	-0.01	0.15	-0.08	0.15	-0.05	0.15	-0.11	0.12
Cr	0.02	0.07	0.08	0.06	0.06	0.06	0.08	0.07	0.04	0.07	0.03	0.06	0.04	0.07	0.01	0.06
Pb	0.14	0.19	0.19	0.18	0.31	0.17	0.38	0.17	0.10	0.20	0.34	0.18	0.28	0.17	0.05	0.18
Zn	0.54	0.60	-0.58	0.56	-0.60	0.59	-0.02	0.51	-0.24	0.35	0.70	0.34	0.14	0.46	-0.01	0.59
Fe	0.58	0.10	0.33	0.10	0.55	0.10	0.26	0.10	0.08	0.09	0.36	0.10	0.76	0.11	0.45	0.11
TOT	79.21		79.51		80.90		80.99		81.93		80.04		82.06		83.25	
	CSH		Unreacted cement phases		CSH		Ca(OH)2		Ca(OH)2		CSH		CSH		Unreacted cement phases	

SEM-EDS analysis of non-carbonated cement-based s/s chromium (VI) doped sample

Sample a



Sample b



Sample a

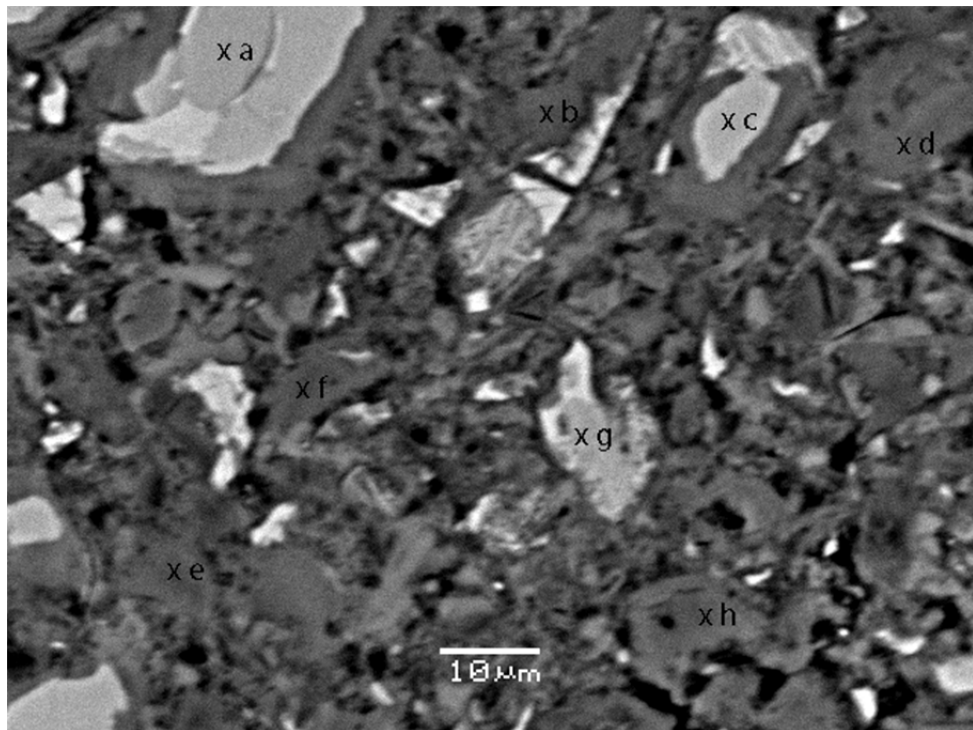
	a		b		c		d		e		f		g		h	
	Element %	σ	Element %	σ	Element %	σ	Element %	σ	Element %	σ	Element %	σ	Element %	σ	Element %	σ
O	32.17	0.11	44.93	0.18	50.60	0.14	33.82	0.12	45.11	0.10	27.54	0.16	57.90	0.13	42.03	0.18
Na	-0.04	0.08	0.06	0.08	0.10	0.07	0.15	0.09	-0.09	0.07	0.09	0.08	-0.07	0.08	0.04	0.08
Mg	0.22	0.06	0.23	0.06	0.34	0.06	0.43	0.07	0.45	0.06	0.26	0.06	0.10	0.06	0.42	0.06
Al	0.64	0.06	1.78	0.07	1.38	0.06	1.54	0.07	0.60	0.06	0.46	0.06	0.01	0.05	0.77	0.06
Si	10.55	0.11	6.75	0.09	5.74	0.08	9.24	0.10	9.33	0.10	10.10	0.10	0.07	0.04	8.69	0.10
S	0.26	0.05	1.16	0.06	1.13	0.06	0.09	0.05	1.05	0.06	0.09	0.05	0.04	0.04	1.03	0.06
K	0.11	0.06	0.47	0.06	0.43	0.05	0.15	0.06	0.15	0.05	0.06	0.05	0.05	0.04	0.27	0.06
Ca	39.26	0.24	22.95	0.19	21.35	0.18	37.05	0.23	26.23	0.20	39.98	0.24	25.20	0.19	26.24	0.21
Cd	-0.18	0.17	0.32	0.18	0.07	0.14	-0.21	0.15	0.24	0.19	-0.23	0.16	-0.03	0.17	0.03	0.14
Cu	-0.05	0.14	-0.01	0.14	-0.07	0.14	-0.04	0.14	-0.05	0.14	-0.05	0.12	-0.01	0.13	-0.01	0.14
Cr	0.07	0.08	0.44	0.08	0.26	0.08	0.04	0.08	0.28	0.08	0.10	0.08	0.05	0.07	0.30	0.09
Pb	0.33	0.20	0.36	0.17	0.30	0.17	0.04	0.17	0.06	0.20	0.07	0.17	0.27	0.17	0.18	0.18
Zn	0.37	0.50	-0.29	0.36	-0.28	0.63	-0.72	0.55	-0.22	0.58	0.64	0.70	0.46	0.50	-0.18	0.56
Fe	0.60	0.11	0.98	0.11	0.61	0.10	1.05	0.12	0.82	0.11	0.35	0.10	0.04	0.09	0.65	0.12
TOT	84.31		80.13		81.96		82.63		83.96		79.46		84.08		80.46	
	Unreacted cement phases		CSH		CSH		Unreacted cement phases		CSH		Unreacted cement phases		Ca(OH)2		CSH	

Sample b

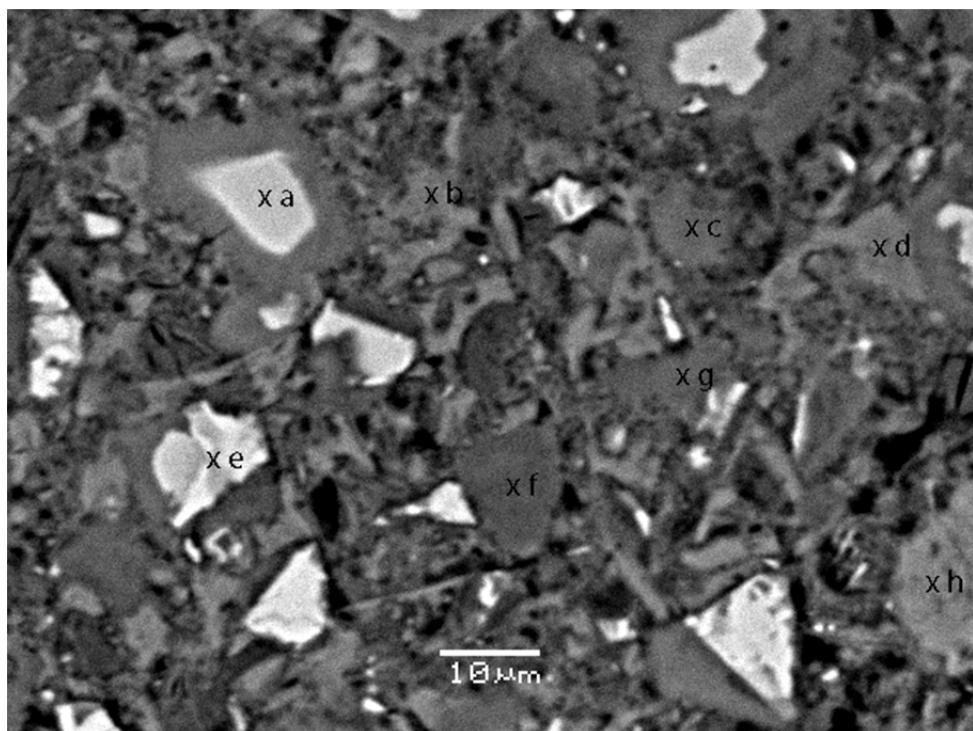
	a		b		c		d		e		f		g		h	
	Element %	σ	Element %	σ	Element %	σ	Element %	σ	Element %	σ						
O	38.14	0.17	42.84	0.17	40.40	0.13	43.97	0.12	27.85	0.14	48.00	0.17	36.29	0.11	38.62	0.14
Na	0.23	0.09	-0.09	0.05	0.11	0.09	0.30	0.07	0.02	0.11	-0.16	0.08	0.45	0.11	0.06	0.08
Mg	0.26	0.07	0.33	0.05	0.34	0.05	0.47	0.07	1.28	0.06	-0.04	0.07	0.64	0.11	-0.01	0.08
Al	1.68	0.06	0.96	0.06	1.29	0.05	1.42	0.06	11.54	0.12	0.05	0.07	1.17	0.12	1.03	0.04
Si	7.92	0.08	6.20	0.10	6.22	0.11	8.31	0.11	13.22	0.12	2.23	0.04	5.75	0.05	3.22	0.04
S	1.15	0.06	0.86	0.07	1.06	0.07	1.12	0.08	0.52	0.08	0.43	0.05	0.93	0.07	0.35	0.06
K	0.32	0.05	0.47	0.06	0.13	0.05	0.27	0.06	0.11	0.06	0.26	0.05	0.24	0.06	0.38	0.05
Ca	30.41	0.17	30.27	0.17	34.28	0.24	25.12	0.12	25.93	0.29	30.99	0.23	32.77	0.29	44.93	0.19
Cd	-0.28	0.14	-0.04	0.17	0.16	0.19	0.11	0.18	0.24	0.15	-0.25	0.17	0.33	0.14	-0.23	0.19
Cu	-0.04	0.13	-0.07	0.14	-0.04	0.13	-0.01	0.12	-0.02	0.14	-0.08	0.15	-0.12	0.15	-0.01	0.14
Cr	0.38	0.08	0.03	0.09	0.24	0.08	0.40	0.08	0.02	0.08	0.33	0.08	0.24	0.08	0.07	0.08
Pb	0.19	0.17	0.01	0.20	0.34	0.19	0.34	0.20	0.01	0.17	0.12	0.20	0.26	0.20	0.28	0.20
Zn	-0.75	0.50	-0.63	0.50	0.04	0.37	-0.28	0.69	0.40	0.56	-0.41	0.48	-0.30	0.52	-0.61	0.68
Fe	0.48	0.12	0.40	0.13	0.86	0.10	0.84	0.12	8.98	0.24	0.41	0.09	5.86	0.19	0.28	0.10
TOT	80.09		81.54		85.43		82.48		90.10		83.88		84.51		88.36	
	CSH		CSH		CSH		CSH		Unreacted cement phases		Ca(OH)2		Unreacted cement phases		Ca(OH)2	

SEM-EDS analysis of non-carbonated cement-based s/s copper doped sample

Sample a



Sample b



Sample a

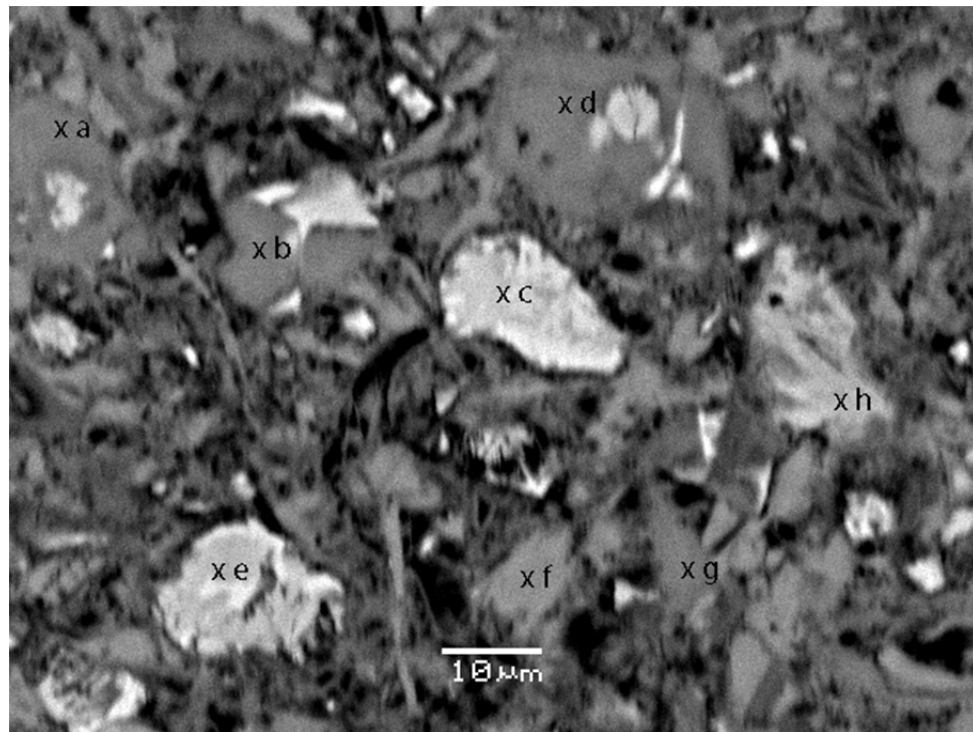
	a		b		c		d		e		f		g		h	
	Element %	σ	Element %	σ	Element %	σ	Element %	σ	Element %	σ	Element %	σ	Element %	σ	Element %	σ
O	17.23	0.19	42.27	0.19	14.42	0.10	38.12	0.17	42.39	0.12	39.70	0.13	31.39	0.10	41.09	0.16
Na	-0.04	0.08	0.21	0.08	0.48	0.12	0.00	0.07	0.04	0.09	0.02	0.09	0.87	0.07	0.14	0.05
Mg	0.26	0.05	0.49	0.06	1.30	0.11	0.04	0.05	0.34	0.08	0.37	0.07	0.19	0.10	0.26	0.07
Al	11.98	0.07	0.68	0.06	9.60	0.10	0.41	0.05	1.83	0.06	1.28	0.06	9.33	0.06	0.68	0.08
Si	11.70	0.07	7.52	0.08	12.56	0.10	3.69	0.05	6.53	0.11	6.43	0.13	8.18	0.10	8.05	0.08
S	1.35	0.05	1.24	0.07	0.38	0.05	0.28	0.06	0.91	0.07	0.93	0.07	0.04	0.08	1.13	0.06
K	0.07	0.06	0.00	0.04	0.07	0.06	0.04	0.05	0.07	0.04	0.06	0.05	0.04	0.06	0.06	0.07
Ca	39.40	0.29	26.89	0.18	36.69	0.26	43.79	0.21	28.73	0.13	33.80	0.24	25.66	0.30	28.88	0.19
Cd	-0.25	0.19	-0.27	0.19	0.17	0.19	0.32	0.15	0.11	0.15	-0.31	0.19	-0.11	0.19	-0.02	0.16
Cu	-0.01	0.13	-0.01	0.12	-0.12	0.14	-0.12	0.12	-0.06	0.14	-0.08	0.12	-0.05	0.13	-0.03	0.13
Cr	-0.01	0.07	0.05	0.07	-0.01	0.06	0.05	0.07	0.04	0.06	0.06	0.07	0.00	0.06	0.08	0.07
Pb	0.03	0.17	0.37	0.20	0.04	0.19	0.31	0.17	0.24	0.20	0.25	0.20	0.32	0.19	0.19	0.20
Zn	0.15	0.40	0.64	0.61	0.06	0.64	0.09	0.49	-0.30	0.49	0.00	0.64	0.56	0.63	-0.49	0.62
Fe	7.50	0.11	0.40	0.11	10.30	0.14	0.45	0.12	0.96	0.12	0.93	0.12	6.13	0.18	0.95	0.13
TOT	89.39		80.48		85.94		87.47		81.83		83.44		76.55		80.97	
	Unreacted Cement phases		CSH		Unreacted Cement phases		Ca(OH)2		CSH		CSH		Unreacted Cement phases		CSH	

Sample b

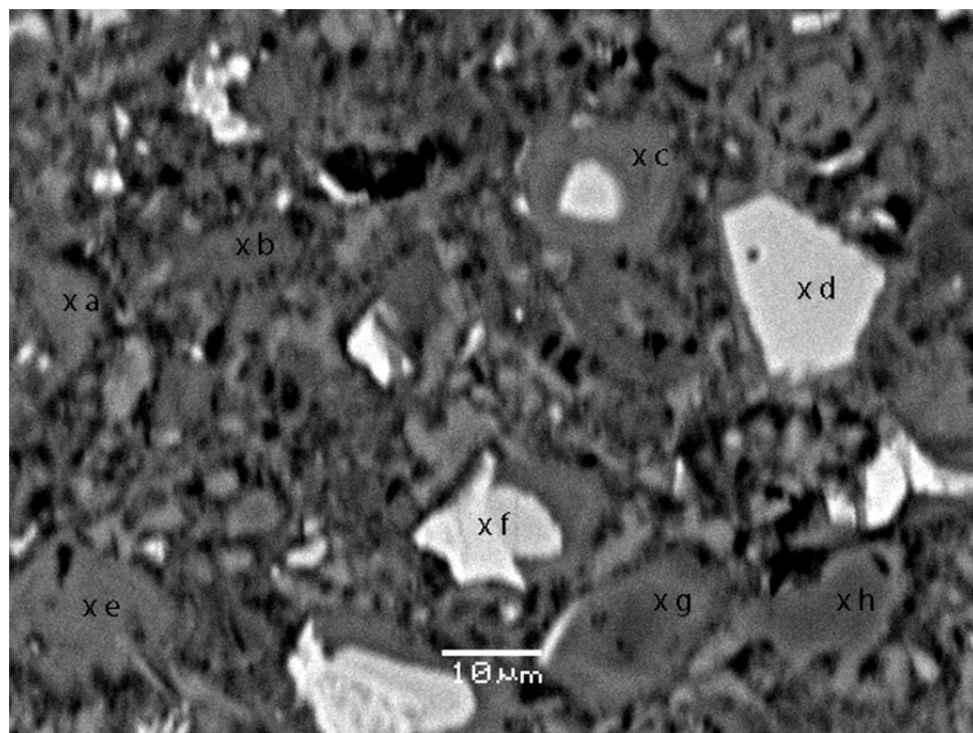
	a		b		c		d		e		f		g		h	
	Element %	σ	Element %	σ	Element %	σ	Element %	σ	Element %	σ	Element %	σ	Element %	σ	Element %	σ
O	22.86	0.12	39.07	0.15	40.26	0.19	49.56	0.10	25.92	0.18	38.92	0.18	49.85	0.14	50.69	0.14
Na	0.41	0.12	-0.03	0.05	0.22	0.05	0.05	0.09	0.55	0.11	-0.17	0.07	0.17	0.09	0.01	0.10
Mg	0.33	0.10	0.33	0.06	0.40	0.07	0.39	0.07	0.69	0.09	-0.12	0.06	0.11	0.06	0.12	0.06
Al	11.89	0.06	1.67	0.06	0.78	0.05	1.90	0.05	5.59	0.12	1.15	0.05	1.13	0.07	0.69	0.05
Si	6.91	0.10	8.99	0.08	5.82	0.13	8.85	0.08	6.09	0.05	2.52	0.04	7.87	0.13	2.08	0.04
S	1.33	0.08	0.90	0.07	1.21	0.08	1.19	0.08	1.36	0.05	0.40	0.04	0.93	0.08	0.35	0.05
K	0.03	0.04	-0.01	0.04	0.05	0.07	-0.01	0.06	-0.02	0.05	0.05	0.07	0.04	0.06	0.02	0.07
Ca	37.50	0.26	34.29	0.24	31.56	0.12	21.55	0.16	44.21	0.23	45.30	0.22	25.67	0.25	26.30	0.20
Cd	0.04	0.17	0.06	0.16	-0.31	0.19	0.15	0.15	-0.08	0.19	0.26	0.18	-0.13	0.14	-0.24	0.16
Cu	-0.10	0.14	-0.12	0.15	-0.04	0.15	-0.02	0.12	-0.12	0.14	-0.03	0.13	-0.05	0.15	-0.07	0.14
Cr	0.01	0.07	0.04	0.07	0.02	0.07	0.03	0.07	0.01	0.07	0.05	0.06	0.07	0.07	0.00	0.07
Pb	0.13	0.17	0.15	0.20	0.16	0.19	0.18	0.20	0.32	0.18	0.36	0.20	0.06	0.17	0.37	0.20
Zn	-0.19	0.55	0.60	0.50	0.66	0.66	0.20	0.63	0.64	0.46	-0.69	0.66	0.65	0.58	-0.74	0.37
Fe	7.90	0.13	0.39	0.11	0.66	0.12	0.92	0.10	3.96	0.24	0.14	0.11	0.62	0.10	0.15	0.12
TOT	89.05		86.33		81.45		84.94		89.12		88.14		86.99		79.73	
	Unreacted cement phases		CSH		CSH		CSH		Unreacted cement phases		Ca(OH)2		CSH		Ca(OH)2	

SEM-EDS analysis of non-carbonated cement-based s/s lead doped sample

Sample a



Sample b



Sample a

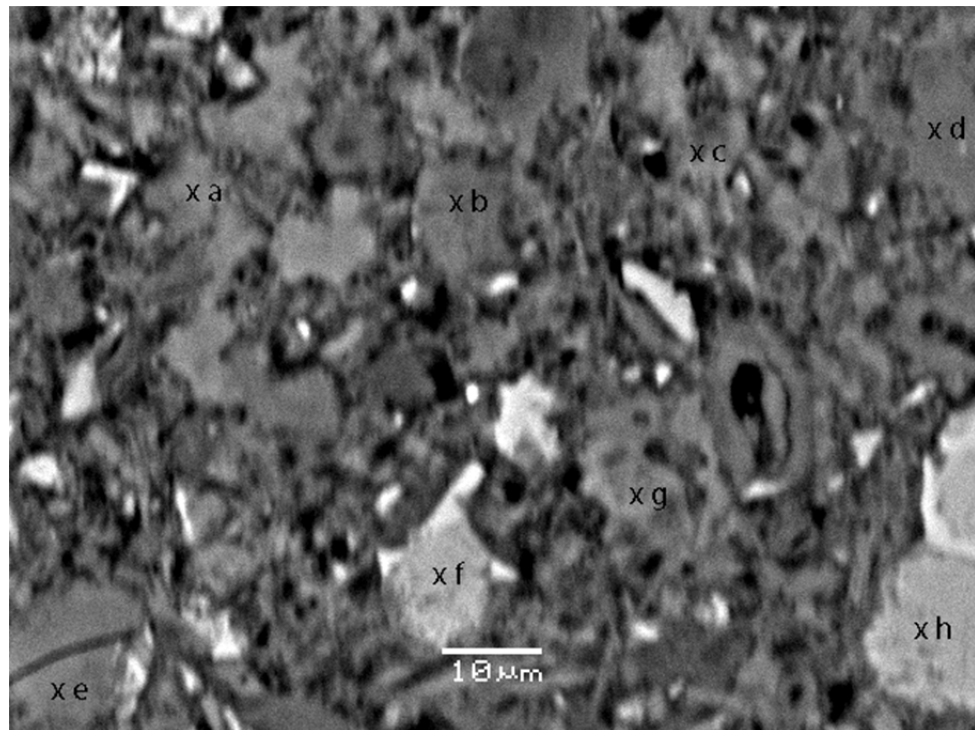
	a		b		c		d		e		f		g		h	
	Element %	σ	Element %	σ	Element %	σ	Element %	σ	Element %	σ	Element %	σ	Element %	σ	Element %	σ
O	38.20	0.10	38.88	0.14	24.71	0.15	50.52	0.11	16.27	0.11	48.58	0.19	42.98	0.18	26.93	0.13
Na	0.09	0.10	-0.10	0.09	0.45	0.09	0.03	0.07	0.61	0.11	0.10	0.09	0.15	0.07	0.54	0.09
Mg	0.12	0.06	0.06	0.05	1.23	0.08	0.19	0.08	0.60	0.06	0.14	0.07	0.29	0.08	1.30	0.06
Al	0.10	0.04	0.77	0.04	3.87	0.11	1.24	0.04	12.16	0.06	1.77	0.06	0.99	0.06	3.40	0.10
Si	3.32	0.05	0.39	0.04	14.21	0.06	3.91	0.06	2.29	0.08	7.15	0.10	7.99	0.12	12.21	0.10
S	0.31	0.05	0.33	0.06	1.77	0.07	0.24	0.05	1.21	0.05	0.96	0.08	1.21	0.06	1.10	0.05
K	0.04	0.05	-0.03	0.07	0.07	0.05	0.04	0.04	0.03	0.04	0.03	0.07	0.01	0.07	-0.02	0.07
Ca	45.50	0.20	40.23	0.19	30.54	0.29	25.91	0.20	41.65	0.21	22.62	0.19	27.95	0.13	37.70	0.23
Cd	0.13	0.19	0.06	0.14	-0.29	0.18	-0.12	0.16	-0.21	0.19	0.19	0.18	-0.30	0.18	-0.10	0.16
Cu	-0.10	0.15	-0.12	0.12	-0.01	0.15	-0.09	0.13	-0.09	0.15	-0.03	0.14	-0.06	0.13	-0.01	0.13
Cr	0.06	0.06	0.09	0.06	0.05	0.07	0.09	0.06	0.02	0.07	0.07	0.06	0.01	0.07	0.07	0.07
Pb	0.01	0.19	0.26	0.18	0.33	0.20	0.37	0.17	0.37	0.18	0.22	0.20	0.02	0.17	0.12	0.19
Zn	0.58	0.54	-0.53	0.39	0.62	0.39	-0.16	0.35	0.46	0.67	0.14	0.60	0.09	0.45	-0.69	0.61
Fe	0.44	0.11	0.31	0.11	12.09	0.20	0.14	0.11	10.73	0.10	0.49	0.12	0.61	0.13	4.23	0.23
TOT	88.80		80.60		89.64		82.31		86.10		82.43		81.94		86.78	
	Ca(OH)2		Ca(OH)2		Unreacted cement phases		Ca(OH)2		Unreacted cement phases		CSH		CSH		Unreacted cement phases	

Sample b

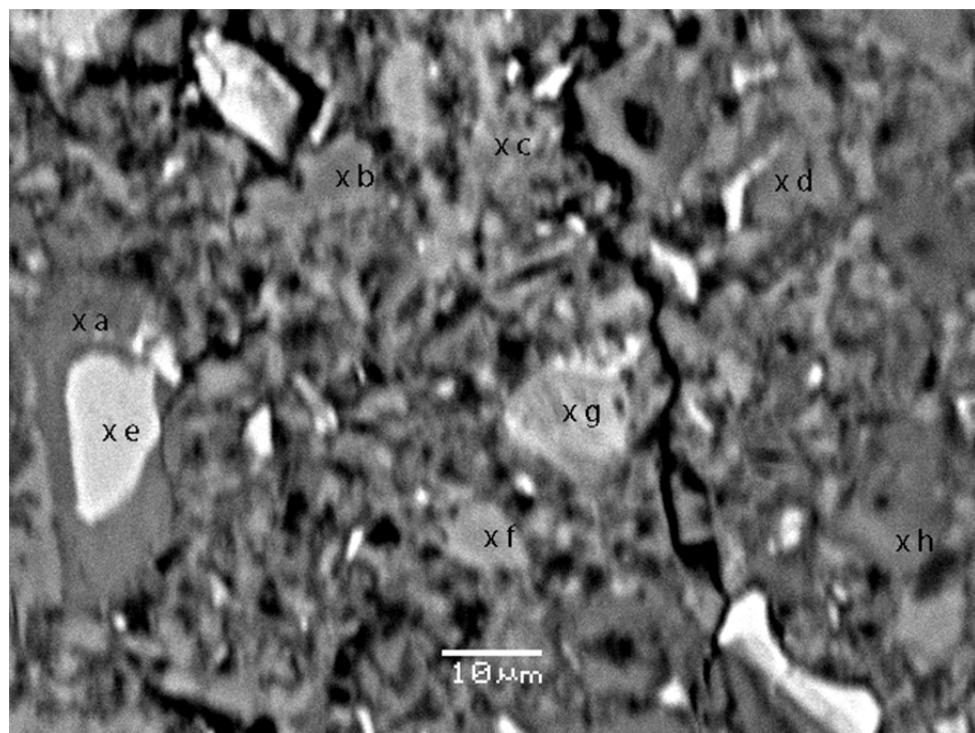
	a		b		c		d		e		f		g		h	
	Element %	σ	Element %	σ	Element %	σ	Element %	σ	Element %	σ	Element %	σ	Element %	σ	Element %	σ
O	50.43	0.13	38.53	0.15	50.16	0.12	22.50	0.11	45.47	0.12	27.19	0.18	38.71	0.12	49.51	0.16
Na	0.03	0.08	-0.11	0.08	-0.11	0.09	0.68	0.07	-0.09	0.07	0.57	0.13	-0.10	0.08	0.07	0.08
Mg	0.38	0.08	0.20	0.08	0.06	0.05	0.49	0.05	0.49	0.06	0.41	0.09	-0.14	0.07	-0.19	0.07
Al	0.51	0.08	0.72	0.05	1.33	0.07	4.52	0.06	1.31	0.07	7.40	0.07	1.00	0.06	0.53	0.06
Si	8.28	0.13	8.15	0.08	1.74	0.08	2.67	0.07	7.00	0.12	5.25	0.05	3.82	0.04	0.82	0.05
S	1.31	0.07	1.31	0.08	0.14	0.05	1.45	0.08	0.92	0.06	0.95	0.08	0.38	0.05	0.02	0.04
K	0.00	0.07	-0.02	0.05	0.00	0.07	-0.02	0.06	0.00	0.07	0.07	0.07	0.08	0.05	0.05	0.04
Ca	22.13	0.22	34.18	0.19	28.93	0.23	45.16	0.22	25.40	0.19	42.79	0.23	46.15	0.19	27.73	0.27
Cd	0.21	0.19	0.01	0.15	0.03	0.19	-0.32	0.17	-0.11	0.19	-0.30	0.18	-0.23	0.14	0.12	0.16
Cu	-0.04	0.13	-0.08	0.13	-0.04	0.14	-0.02	0.15	-0.10	0.14	-0.07	0.15	-0.02	0.12	-0.11	0.15
Cr	0.03	0.06	0.01	0.07	0.00	0.06	0.05	0.07	0.09	0.06	-0.01	0.06	0.07	0.07	0.03	0.07
Pb	0.37	0.19	0.10	0.19	0.26	0.20	0.30	0.19	0.03	0.18	0.17	0.20	0.01	0.20	0.15	0.18
Zn	-0.04	0.34	-0.38	0.54	0.10	0.39	0.10	0.47	0.45	0.59	-0.40	0.34	-0.22	0.50	0.68	0.43
Fe	0.66	0.12	0.86	0.11	0.40	0.12	8.80	0.11	0.87	0.10	0.54	0.23	0.25	0.10	0.31	0.09
TOT	84.26		83.48		83.00		86.36		81.75		84.56		89.76		79.72	
	CSH		CSH		Ca(OH)2		Unreacted cement phases		CSH		Unreacted cement phases		Ca(OH)2		Ca(OH)2	

SEM-EDS analysis of non-carbonated cement-based s/s zinc doped sample

Sample a



Sample b



Sample a

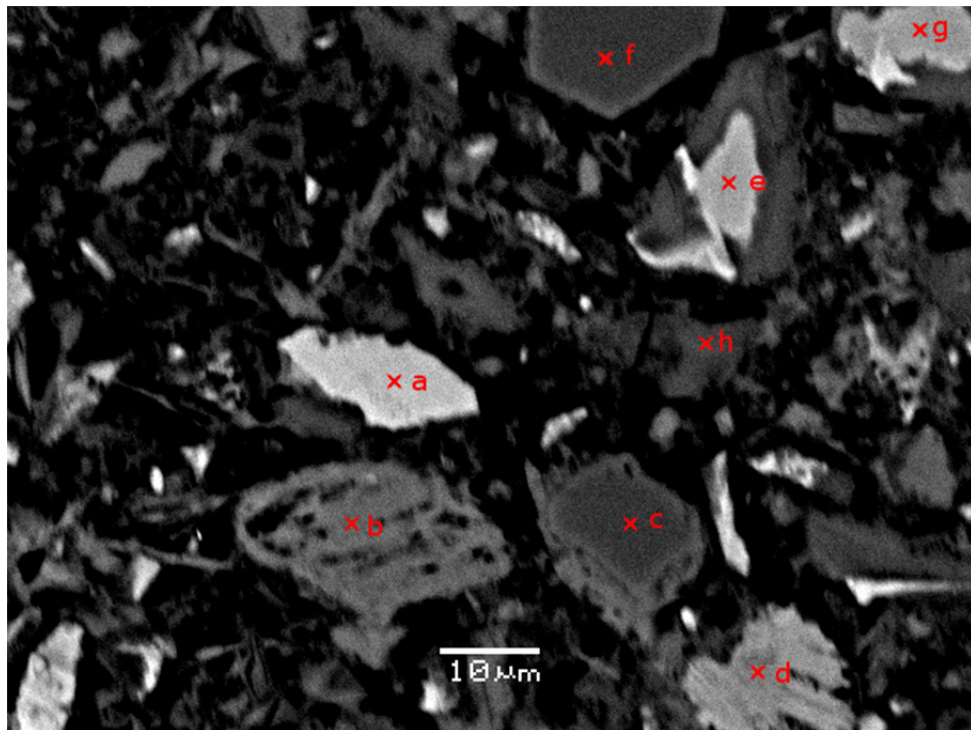
	a		b		c		d		e		f		g		h	
	Element %	σ	Element %	σ	Element %	σ	Element %	σ								
O	43.33	0.13	40.20	0.16	37.57	0.14	38.30	0.13	40.58	0.15	31.90	0.16	49.90	0.16	21.58	0.14
Na	0.20	0.06	0.28	0.08	0.23	0.09	0.07	0.05	-0.16	0.08	0.54	0.07	0.11	0.06	0.65	0.10
Mg	0.37	0.05	0.09	0.06	0.35	0.05	0.15	0.06	0.01	0.05	0.48	0.07	0.51	0.05	1.30	0.06
Al	0.64	0.05	1.43	0.07	1.61	0.07	1.77	0.07	0.24	0.04	3.13	0.09	1.51	0.06	12.30	0.08
Si	10.59	0.13	8.24	0.11	8.17	0.10	10.43	0.11	1.92	0.08	10.13	0.10	5.92	0.11	5.22	0.06
S	0.88	0.07	1.38	0.08	1.32	0.06	1.00	0.08	0.26	0.04	1.66	0.08	1.20	0.07	1.48	0.05
K	-0.01	0.06	0.04	0.07	0.00	0.05	0.03	0.06	0.06	0.06	0.03	0.07	-0.02	0.04	0.09	0.07
Ca	24.98	0.18	33.64	0.16	29.70	0.17	31.24	0.19	36.74	0.24	24.61	0.30	22.37	0.10	38.52	0.26
Cd	-0.27	0.17	-0.24	0.19	0.10	0.14	-0.33	0.18	-0.31	0.15	0.29	0.16	-0.07	0.16	0.05	0.14
Cu	-0.02	0.15	-0.12	0.15	-0.12	0.15	-0.03	0.13	-0.01	0.12	-0.06	0.15	-0.04	0.15	-0.11	0.13
Cr	0.02	0.06	0.05	0.06	0.08	0.06	0.00	0.06	0.04	0.06	0.04	0.07	0.07	0.07	0.07	0.07
Pb	0.15	0.17	0.14	0.20	0.00	0.17	0.36	0.20	0.10	0.18	0.15	0.20	0.28	0.18	0.38	0.20
Zn	0.54	0.47	-0.71	0.61	0.26	0.56	-0.40	0.64	-0.37	0.37	-0.46	0.39	0.53	0.56	0.52	0.63
Fe	0.62	0.13	0.98	0.12	0.65	0.13	0.84	0.10	0.33	0.10	8.60	0.25	0.42	0.12	8.73	0.24
TOT	82.05		85.40		79.92		83.43		79.43		81.04		82.69		90.78	
	CSH		CSH		CSH		CSH		Ca(OH)2		Unreacted cement phases		CSH		Unreacted cement phases	

Sample b

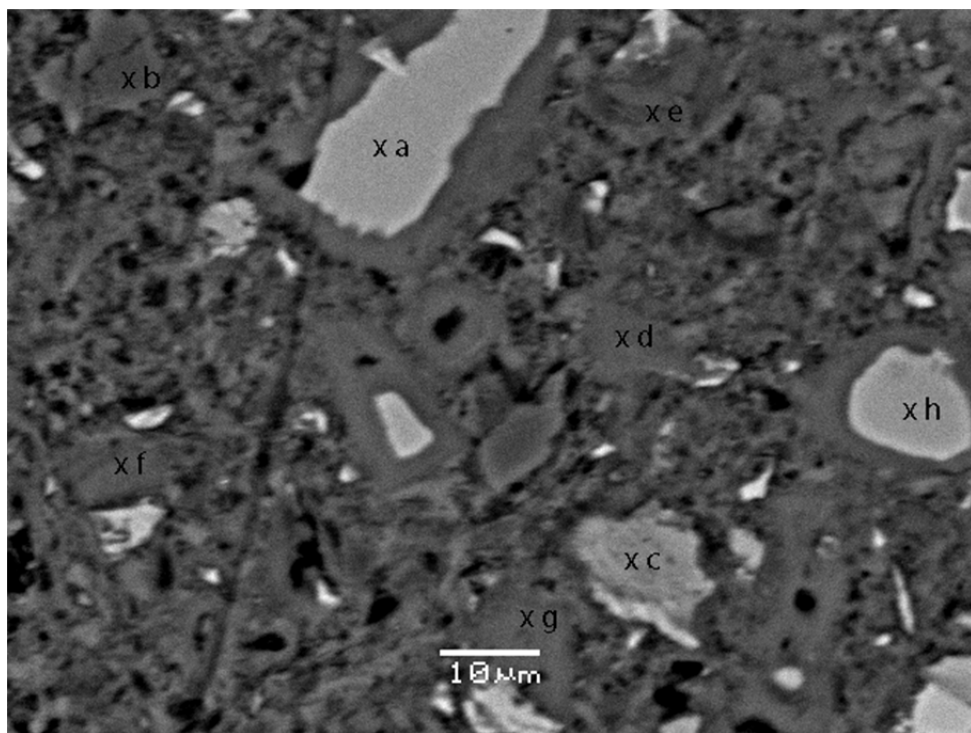
	a		b		c		d		e		f		g		h	
	Element %	σ	Element %	σ	Element %	σ	Element %	σ	Element %	σ						
O	59.12	0.15	39.85	0.16	40.72	0.14	39.88	0.15	26.50	0.12	34.04	0.12	16.36	0.14	39.31	0.16
Na	-0.16	0.08	0.18	0.09	0.14	0.08	0.07	0.05	0.82	0.07	0.74	0.12	0.48	0.08	-0.10	0.08
Mg	-0.16	0.07	0.56	0.07	0.23	0.08	0.47	0.05	0.82	0.09	0.20	0.07	0.18	0.07	0.03	0.07
Al	0.09	0.05	0.80	0.08	1.46	0.08	0.73	0.08	3.70	0.11	8.61	0.11	11.96	0.07	0.64	0.05
Si	1.38	0.04	10.14	0.08	9.15	0.11	8.79	0.12	7.20	0.07	13.00	0.11	14.25	0.07	2.98	0.08
S	0.36	0.04	1.08	0.06	1.06	0.08	1.29	0.08	1.62	0.08	0.79	0.08	1.46	0.05	0.00	0.05
K	0.01	0.06	0.02	0.07	-0.01	0.05	0.06	0.07	-0.02	0.07	0.03	0.05	0.02	0.06	-0.02	0.04
Ca	24.65	0.24	32.92	0.17	28.02	0.16	24.59	0.16	40.77	0.28	25.52	0.23	44.85	0.24	41.19	0.23
Cd	0.34	0.15	-0.29	0.16	-0.33	0.14	-0.35	0.16	-0.33	0.17	-0.11	0.14	0.16	0.15	-0.06	0.16
Cu	-0.04	0.13	-0.08	0.15	-0.01	0.14	-0.05	0.15	-0.08	0.15	-0.04	0.12	-0.03	0.14	-0.03	0.15
Cr	0.02	0.07	0.04	0.07	0.03	0.06	0.04	0.06	0.01	0.06	0.08	0.06	0.03	0.07	0.01	0.07
Pb	0.20	0.19	0.32	0.18	0.26	0.19	0.09	0.19	0.23	0.18	0.26	0.19	0.14	0.20	0.08	0.20
Zn	0.63	0.55	0.54	0.49	-0.64	0.67	0.46	0.40	-0.53	0.53	0.63	0.56	-0.76	0.67	-0.45	0.48
Fe	0.28	0.09	0.74	0.13	0.86	0.12	0.36	0.12	9.64	0.12	4.64	0.12	0.88	0.25	-0.01	0.09
TOT	86.72		86.82		80.94		76.43		90.35		88.39		89.98		83.57	
	Ca(OH)2		CSH		CSH		CSH		Unreacted cement phases		Unreacted cement phases		Unreacted cement phases		Ca(OH)2	

SEM-EDS analysis of carbonated cement-based s/s control sample

Sample a



Sample b



Sample a

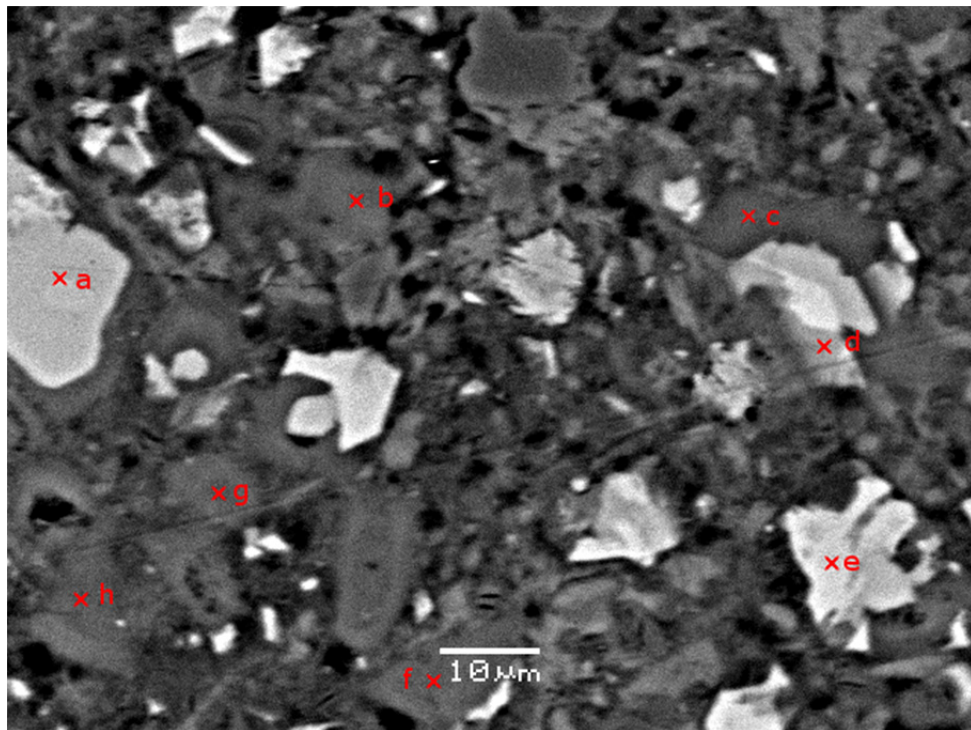
	a		b		c		d		e		f		g		h	
	Element %	σ	Element %	σ	Element %	σ	Element %	σ	Element %	σ	Element %	σ	Element %	σ	Element %	σ
O	25.97	0.13	38.48	0.18	48.29	0.13	26.31	0.12	26.50	0.17	51.24	0.10	25.05	0.13	38.58	0.14
Na	0.08	0.13	-0.06	0.11	-0.06	0.10	0.22	0.10	0.11	0.11	-0.08	0.10	0.03	0.11	-0.08	0.09
Mg	1.24	0.11	0.06	0.08	0.21	0.08	0.18	0.08	0.34	0.08	0.00	0.07	0.43	0.08	0.25	0.07
Al	7.86	0.14	0.13	0.06	0.06	0.06	0.74	0.08	0.57	0.08	0.04	0.06	0.74	0.08	0.71	0.07
Si	3.03	0.11	0.19	0.05	0.05	0.05	14.15	0.14	11.39	0.13	0.10	0.05	11.56	0.13	10.44	0.12
S	0.19	0.07	0.05	0.05	0.02	0.05	0.29	0.07	0.08	0.07	-0.03	0.05	0.10	0.07	0.75	0.07
K	-0.02	0.06	0.01	0.06	0.03	0.05	0.02	0.07	-0.02	0.07	0.05	0.05	0.02	0.06	0.06	0.07
Ca	32.48	0.26	46.22	0.29	34.57	0.26	40.33	0.29	47.94	0.31	35.04	0.26	47.51	0.31	30.82	0.25
Cd	0.05	0.19	-0.10	0.18	-0.09	0.19	-0.15	0.15	0.06	0.16	0.29	0.16	-0.27	0.16	-0.22	0.16
Cu	-0.01	0.15	-0.10	0.12	-0.01	0.13	-0.05	0.12	-0.03	0.13	-0.03	0.15	-0.09	0.15	-0.03	0.14
Cr	0.08	0.06	0.04	0.06	0.08	0.07	0.06	0.07	0.00	0.07	0.04	0.07	0.02	0.06	-0.01	0.06
Pb	0.10	0.19	0.06	0.20	0.24	0.17	0.27	0.20	0.26	0.17	0.24	0.18	0.20	0.17	0.25	0.20
Zn	-0.70	0.53	0.18	0.43	-0.53	0.66	-0.71	0.50	-0.72	0.55	0.55	0.35	-0.74	0.56	0.58	0.57
Fe	13.07	0.29	0.18	0.12	-0.13	0.10	1.02	0.14	0.61	0.13	-0.06	0.10	0.64	0.13	0.32	0.11
TOT	83.42		85.34		82.73		82.68		87.09		87.39		85.20		82.42	
	Unreacted cement phases		CaCO_3		CaCO_3		Unreacted cement phases		Unreacted cement phases		CaCO_3		Unreacted cement phases		CSH	

Sample b

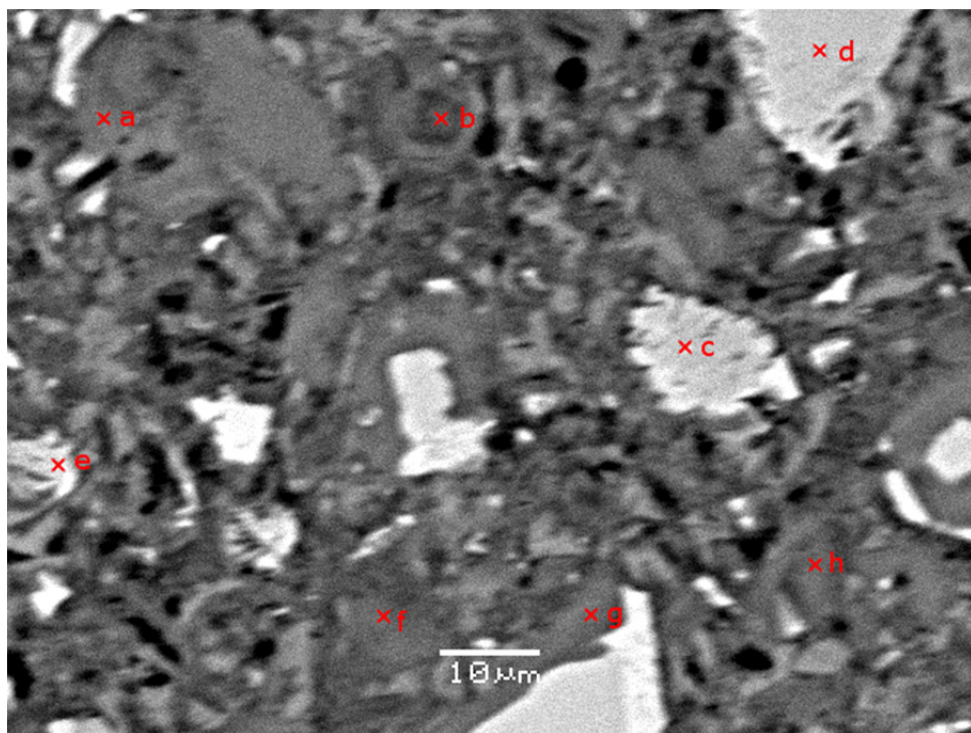
	a		b		c		d		e		f		g		h	
	Element %	σ	Element %	σ	Element %	σ	Element %	σ	Element %	σ	Element %	σ	Element %	σ	Element %	σ
O	24.20	0.11	39.85	0.16	44.68	0.14	38.80	0.18	37.98	0.19	40.58	0.12	40.16	0.12	24.03	0.19
Na	0.08	0.08	0.01	0.07	0.16	0.10	0.03	0.07	-0.08	0.08	-0.10	0.08	0.02	0.07	0.04	0.08
Mg	0.19	0.06	0.21	0.05	1.08	0.08	0.19	0.05	0.07	0.06	0.04	0.05	0.43	0.06	0.36	0.06
Al	0.80	0.06	0.67	0.06	1.67	0.08	0.97	0.06	0.12	0.05	0.24	0.05	0.80	0.06	0.58	0.06
Si	12.94	0.11	10.04	0.10	4.96	0.09	9.91	0.10	0.93	0.05	2.08	0.06	9.33	0.10	11.53	0.11
S	0.29	0.05	1.03	0.06	0.52	0.06	0.99	0.06	0.33	0.05	0.26	0.04	0.92	0.06	0.06	0.05
K	0.05	0.05	-0.01	0.07	0.05	0.04	0.03	0.07	0.08	0.05	0.07	0.07	0.04	0.06	0.10	0.06
Ca	46.04	0.25	32.11	0.20	10.37	0.12	31.12	0.20	46.85	0.24	39.79	0.22	32.78	0.21	50.89	0.26
Cd	-0.06	0.17	-0.15	0.16	0.31	0.14	0.08	0.16	0.31	0.19	-0.03	0.16	-0.16	0.18	0.17	0.18
Cu	-0.03	0.14	-0.04	0.15	-0.02	0.13	-0.07	0.14	-0.07	0.12	-0.12	0.12	-0.01	0.12	-0.04	0.12
Cr	0.03	0.07	0.09	0.06	0.02	0.07	0.01	0.06	0.01	0.07	0.00	0.07	0.03	0.06	0.03	0.06
Pb	0.05	0.19	0.07	0.18	0.02	0.18	0.32	0.18	0.08	0.19	0.01	0.17	0.37	0.17	0.26	0.19
Zn	-0.24	0.58	-0.26	0.52	-0.27	0.62	-0.04	0.69	-0.20	0.47	0.12	0.69	0.57	0.38	-0.37	0.43
Fe	0.64	0.11	0.75	0.11	22.26	0.30	0.89	0.11	0.20	0.10	0.31	0.10	0.81	0.11	0.82	0.12
TOT	84.98		84.37		85.81		83.23		86.61		83.25		86.09		88.46	
	Unreacted cement phases		CSH		Unreacted cement phases		CSH		CaCO ₃		CaCO ₃		CSH		Unreacted cement phases	

SEM-EDS analysis of carbonated cement-based s/s cadmium doped sample

Sample a



Sample b



Sample a

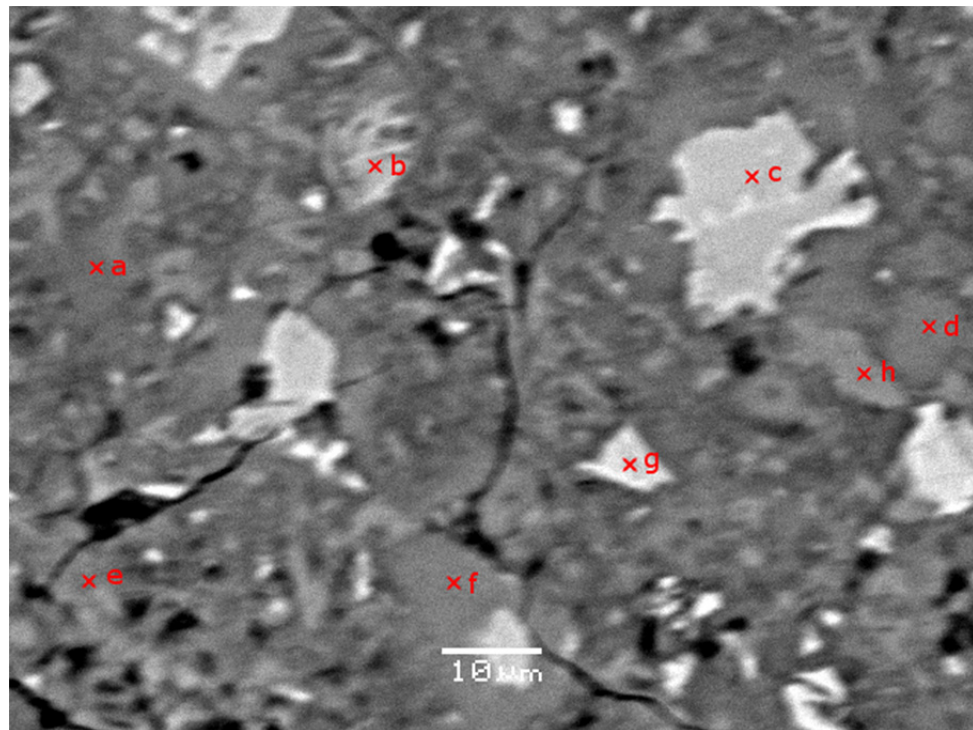
	a		b		c		d		e		f		g		h	
	Element %	σ	Element %	σ	Element %	σ	Element %	σ	Element %	σ	Element %	σ	Element %	σ	Element %	σ
O	19.65	0.13	37.99	0.11	36.16	0.15	27.20	0.12	21.23	0.16	40.00	0.14	39.72	0.13	40.32	0.17
Na	0.75	0.13	-0.08	0.10	0.03	0.10	0.71	0.12	0.27	0.13	-0.12	0.10	-0.07	0.09	-0.05	0.09
Mg	0.95	0.11	0.13	0.08	0.62	0.09	0.49	0.10	1.41	0.12	0.57	0.08	0.50	0.08	0.40	0.08
Al	7.13	0.13	0.49	0.07	1.20	0.08	9.99	0.14	10.97	0.16	1.15	0.08	0.80	0.08	0.94	0.08
Si	7.78	0.14	7.70	0.11	10.59	0.13	4.22	0.12	1.75	0.10	11.00	0.13	11.41	0.13	11.07	0.13
S	0.11	0.07	0.50	0.07	0.78	0.08	0.42	0.07	0.02	0.07	0.90	0.08	0.65	0.08	0.31	0.07
K	0.02	0.06	0.03	0.07	0.04	0.06	0.09	0.07	0.15	0.08	0.07	0.07	0.07	0.07	0.05	0.07
Ca	46.52	0.31	41.54	0.30	35.27	0.28	36.82	0.28	36.18	0.28	35.57	0.28	35.87	0.28	35.56	0.28
Cd	-0.12	0.15	0.09	0.19	0.27	0.15	0.08	0.15	0.24	0.16	0.08	0.17	0.34	0.18	0.24	0.17
Cu	-0.04	0.13	-0.08	0.14	-0.08	0.13	-0.10	0.14	-0.03	0.14	-0.12	0.12	-0.06	0.15	-0.04	0.15
Cr	0.09	0.07	0.04	0.07	0.01	0.06	0.04	0.07	0.00	0.06	0.01	0.06	0.03	0.06	0.03	0.06
Pb	0.10	0.19	0.06	0.19	0.13	0.20	0.27	0.18	0.35	0.19	0.28	0.18	0.19	0.20	0.27	0.18
Zn	0.01	0.56	0.64	0.56	0.17	0.53	-0.57	0.35	-0.51	0.45	0.40	0.45	0.65	0.42	-0.27	0.36
Fe	5.58	0.23	0.39	0.13	1.14	0.15	3.63	0.20	15.29	0.33	0.91	0.14	0.75	0.14	1.42	0.15
TOT	88.53		89.44		86.33		83.29		87.32		90.70		90.85		90.25	
	Unreacted cement phases		CSH		CSH		Unreacted cement phases		Unreacted cement phases		CSH		CSH		CSH	

Sample b

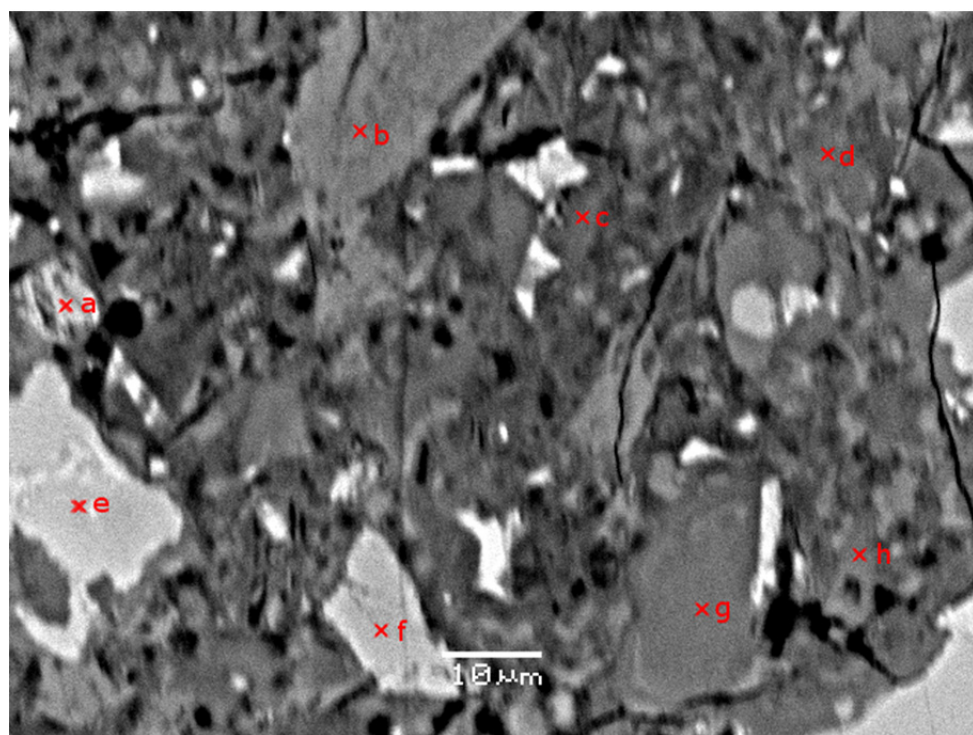
	a		b		c		d		e		f		g		h	
	Element %	σ	Element %	σ	Element %	σ	Element %	σ	Element %	σ	Element %	σ	Element %	σ	Element %	σ
O	40.13	0.10	50.19	0.18	25.96	0.14	26.89	0.19	34.20	0.17	40.79	0.10	41.16	0.16	47.99	0.19
Na	-0.01	0.08	0.12	0.08	0.13	0.09	0.05	0.09	0.09	0.09	-0.09	0.08	0.01	0.08	0.00	0.08
Mg	0.47	0.07	0.17	0.06	0.29	0.07	0.08	0.06	0.32	0.07	0.15	0.06	0.51	0.06	0.60	0.07
Al	1.82	0.07	3.80	0.08	1.33	0.07	0.50	0.06	3.11	0.09	1.82	0.07	0.68	0.06	1.32	0.07
Si	8.47	0.10	6.54	0.10	12.82	0.12	13.65	0.12	10.77	0.12	8.96	0.10	10.80	0.11	9.78	0.11
S	0.67	0.06	0.38	0.06	0.12	0.06	0.09	0.06	0.22	0.06	0.30	0.06	0.49	0.06	0.34	0.06
K	0.09	0.06	0.06	0.04	0.06	0.07	0.01	0.07	-0.02	0.04	0.07	0.05	0.10	0.06	0.11	0.06
Ca	29.42	0.22	26.34	0.21	39.48	0.25	40.00	0.25	37.28	0.24	27.57	0.21	29.74	0.22	27.26	0.21
Cd	-0.27	0.17	0.06	0.18	0.33	0.16	-0.24	0.19	0.27	0.18	-0.18	0.16	0.15	0.16	0.17	0.14
Cu	-0.12	0.14	-0.09	0.13	-0.02	0.14	-0.08	0.13	-0.05	0.13	-0.05	0.13	-0.05	0.14	-0.07	0.15
Cr	0.03	0.07	0.04	0.07	-0.01	0.06	0.02	0.06	0.06	0.07	0.09	0.07	0.01	0.07	0.05	0.07
Pb	0.12	0.20	0.31	0.20	0.25	0.20	0.29	0.19	0.18	0.18	0.36	0.19	0.31	0.17	0.21	0.19
Zn	-0.04	0.48	0.04	0.50	0.49	0.44	0.09	0.41	-0.02	0.43	-0.45	0.50	-0.01	0.61	0.20	0.50
Fe	2.30	0.15	0.64	0.12	1.17	0.13	0.49	0.12	3.29	0.17	0.88	0.12	0.60	0.12	0.61	0.11
TOT	83.08		88.60		82.40		81.84		89.70		80.22		84.50		88.57	
	CSH		CSH		Unreacted cement phases		Unreacted cement phases		Unreacted cement phases		CSH		CSH		CSH	

SEM-EDS analysis of carbonated cement-based s/s chromium (III) doped sample

Sample a



Sample b



Sample a

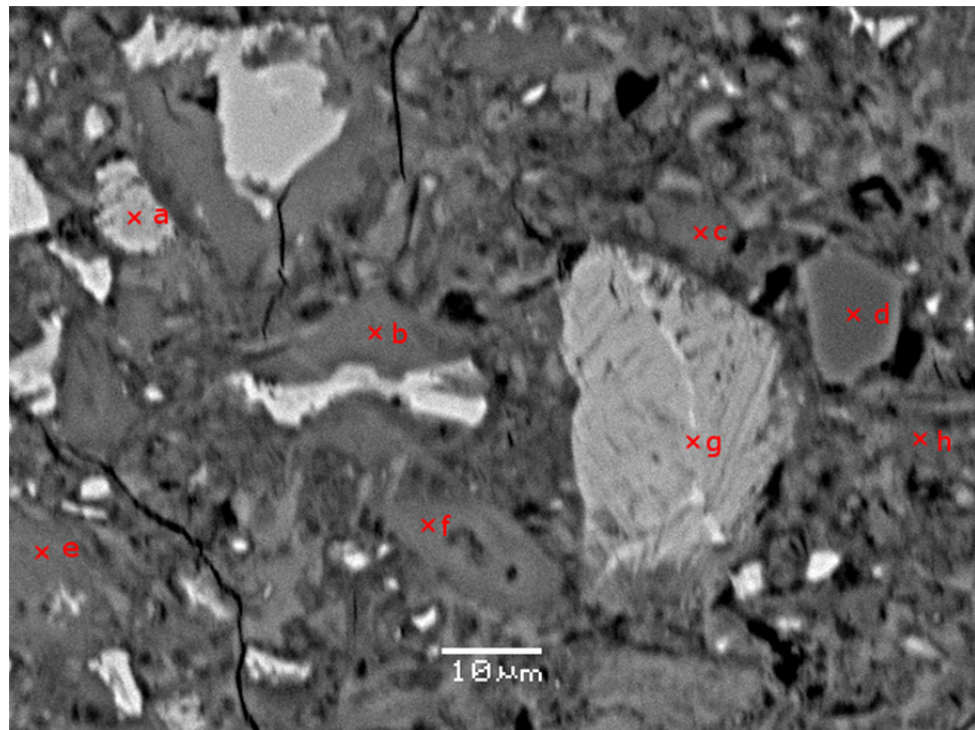
	a		b		c		d		e		f		g		h	
	Element %	σ	Element %	σ	Element %	σ	Element %	σ	Element %	σ	Element %	σ	Element %	σ	Element %	σ
O	47.72	0.10	34.47	0.14	34.60	0.15	47.48	0.17	48.32	0.15	39.91	0.18	27.37	0.15	41.30	0.19
Na	0.05	0.08	0.05	0.09	0.13	0.09	-0.07	0.08	-0.04	0.08	-0.05	0.08	0.55	0.10	-0.05	0.09
Mg	0.14	0.06	0.09	0.06	0.32	0.07	0.49	0.07	0.17	0.06	0.60	0.07	0.86	0.09	0.03	0.06
Al	0.50	0.06	0.74	0.06	0.81	0.07	0.78	0.06	0.74	0.06	0.60	0.06	11.28	0.13	0.66	0.06
Si	8.81	0.10	12.44	0.12	10.56	0.11	9.39	0.10	6.82	0.09	10.24	0.11	1.96	0.09	0.91	0.05
S	0.59	0.06	0.30	0.06	0.01	0.05	0.64	0.06	0.89	0.06	0.43	0.06	0.09	0.06	0.27	0.05
K	0.01	0.04	-0.03	0.07	0.10	0.06	0.02	0.05	0.00	0.05	0.06	0.06	0.01	0.05	0.09	0.05
Ca	30.69	0.22	36.19	0.24	43.87	0.26	29.35	0.22	31.31	0.22	29.83	0.22	31.72	0.23	39.65	0.24
Cd	0.10	0.16	-0.02	0.14	0.04	0.15	-0.14	0.15	-0.25	0.15	-0.02	0.18	0.21	0.15	-0.01	0.18
Cu	-0.10	0.12	-0.07	0.13	-0.06	0.15	-0.09	0.13	-0.10	0.14	-0.12	0.15	-0.03	0.12	-0.07	0.14
Cr	-0.01	0.07	0.05	0.06	0.03	0.07	0.08	0.07	-0.01	0.07	0.05	0.06	0.03	0.07	0.07	0.06
Pb	0.14	0.20	0.12	0.17	0.25	0.18	0.30	0.17	0.09	0.20	0.20	0.18	0.09	0.19	0.05	0.19
Zn	0.69	0.49	0.05	0.64	-0.77	0.68	-0.66	0.37	-0.59	0.51	0.18	0.41	0.51	0.40	-0.17	0.52
Fe	0.45	0.11	0.91	0.12	0.65	0.12	0.92	0.12	0.35	0.11	0.46	0.11	9.06	0.24	0.09	0.09
TOT	89.78		85.29		90.54		88.49		87.70		82.37		83.71		82.82	
	CSH		Unreacted cement phases		Unreacted cement phases		CSH		CSH		CSH		Unreacted cement phases		CaCO ₃	

Sample b

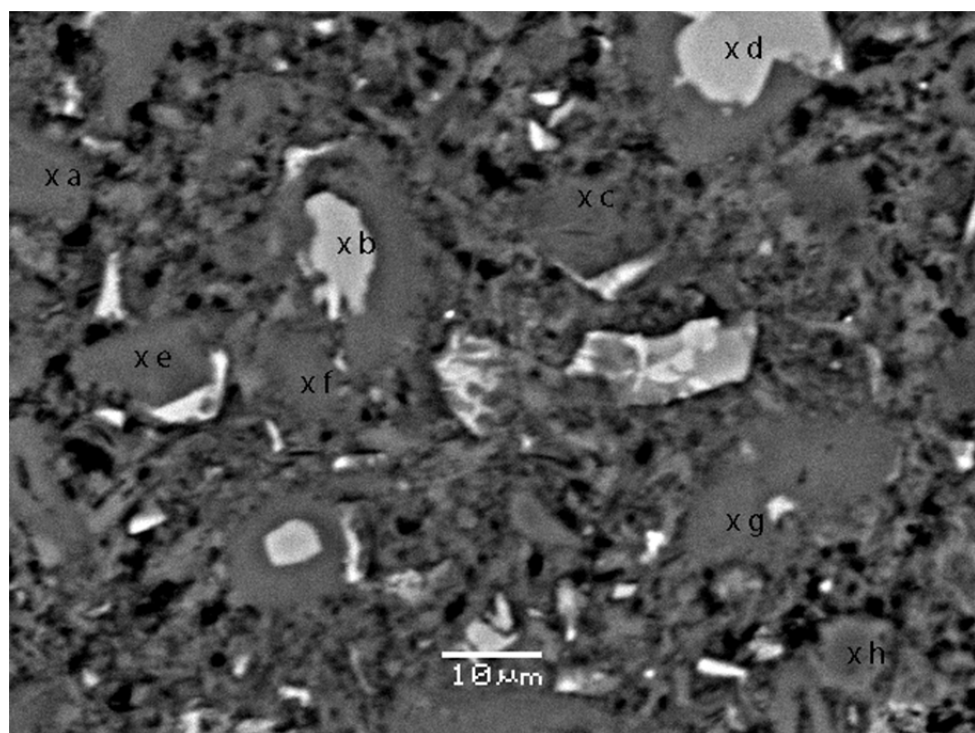
	a		b		c		d		e		f		g		h	
	Element %	σ	Element %	σ	Element %	σ	Element %	σ	Element %	σ	Element %	σ	Element %	σ	Element %	σ
O	26.16	0.12	38.42	0.15	48.08	0.17	39.89	0.19	25.86	0.13	27.89	0.12	38.45	0.19	48.47	0.18
Na	0.02	0.09	-0.05	0.09	0.01	0.08	-0.06	0.08	0.14	0.09	0.14	0.08	0.07	0.08	-0.09	0.08
Mg	0.17	0.07	-0.06	0.06	0.35	0.06	0.29	0.06	0.54	0.07	0.11	0.06	0.29	0.06	0.10	0.06
Al	0.90	0.07	0.00	0.05	2.11	0.07	1.35	0.07	1.55	0.07	0.22	0.06	0.48	0.06	0.49	0.06
Si	12.98	0.12	0.09	0.05	7.82	0.10	9.28	0.10	9.57	0.11	14.30	0.12	10.77	0.11	7.44	0.09
S	0.26	0.06	0.03	0.05	0.38	0.06	0.68	0.06	0.06	0.05	0.12	0.06	0.53	0.06	0.65	0.06
K	0.04	0.05	0.04	0.04	0.01	0.07	0.06	0.04	0.04	0.05	0.09	0.05	0.05	0.06	0.05	0.04
Ca	39.33	0.25	43.80	0.25	27.16	0.21	28.74	0.22	42.86	0.26	40.39	0.25	30.00	0.22	32.31	0.23
Cd	0.31	0.18	-0.16	0.14	0.24	0.17	-0.24	0.19	-0.23	0.16	0.08	0.16	0.12	0.19	0.12	0.15
Cu	-0.06	0.15	-0.07	0.15	-0.01	0.14	-0.01	0.15	-0.04	0.13	-0.01	0.14	-0.02	0.15	-0.04	0.12
Cr	-0.01	0.07	0.07	0.06	0.04	0.06	0.08	0.06	0.01	0.06	0.00	0.06	-0.01	0.06	0.03	0.07
Pb	0.33	0.17	0.37	0.19	0.30	0.18	0.05	0.19	0.31	0.17	0.12	0.18	0.05	0.17	0.21	0.18
Zn	0.61	0.59	-0.62	0.58	0.24	0.34	0.31	0.45	-0.73	0.53	-0.24	0.39	-0.41	0.62	0.64	0.47
Fe	0.90	0.13	-0.08	0.11	0.98	0.12	0.52	0.12	1.13	0.13	0.22	0.11	0.63	0.11	0.33	0.11
TOT	81.94		81.78		87.71		80.94		81.07		83.43		81.00		90.71	
	Unreacted cement phases		CaCO ₃		CSH		CSH		Unreacted cement phases		Unreacted cement phases		CSH		CSH	

SEM-EDS analysis of carbonated cement-based s/s chromium (VI) doped sample

Sample a



Sample b



Sample a

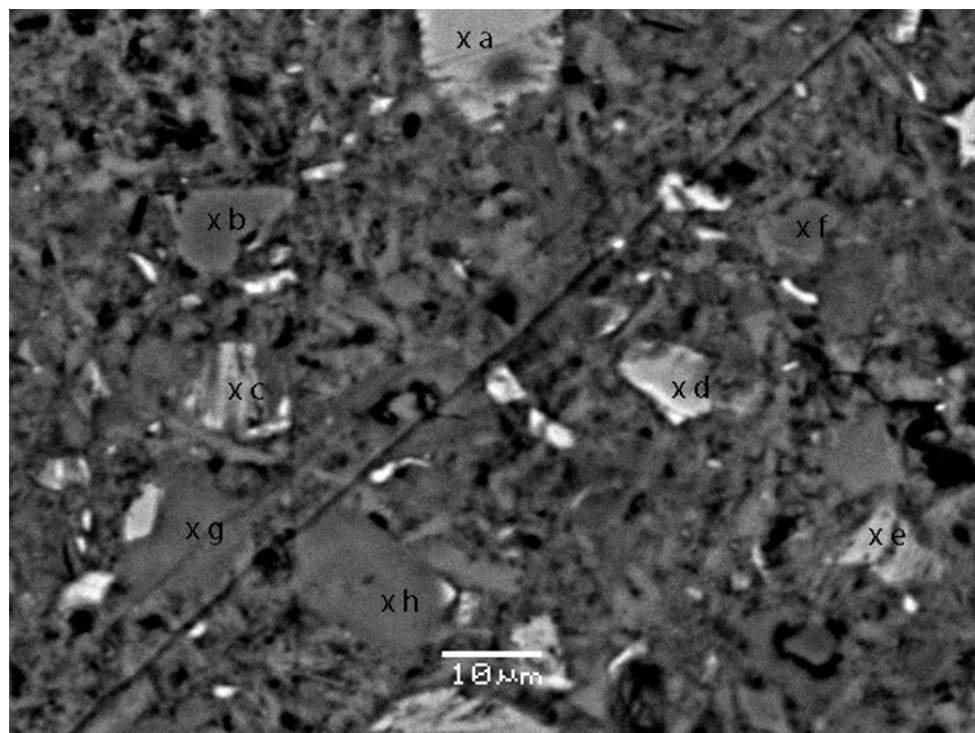
	a		b		c		d		e		f		g		h	
	Element %	σ	Element %	σ	Element %	σ	Element %	σ	Element %	σ	Element %	σ	Element %	σ	Element %	σ
O	27.97	0.12	38.65	0.19	48.36	0.13	48.98	0.17	40.66	0.12	47.42	0.15	26.63	0.14	49.10	0.19
Na	0.31	0.09	0.06	0.08	-0.13	0.08	-0.18	0.08	-0.03	0.08	-0.01	0.08	0.20	0.09	0.05	0.08
Mg	0.20	0.06	0.56	0.06	0.69	0.06	0.19	0.06	0.20	0.06	0.50	0.06	0.15	0.07	0.32	0.06
Al	0.79	0.07	0.60	0.06	0.69	0.06	0.03	0.05	0.57	0.06	0.62	0.06	2.48	0.08	1.50	0.07
Si	13.63	0.12	10.09	0.11	9.87	0.10	0.15	0.05	10.64	0.11	10.34	0.11	12.26	0.12	6.29	0.09
S	0.28	0.06	0.79	0.06	0.44	0.06	0.08	0.05	0.83	0.06	0.88	0.06	0.23	0.06	0.91	0.06
K	0.41	0.06	0.06	0.06	0.20	0.06	0.04	0.05	0.07	0.06	0.09	0.06	0.26	0.06	0.28	0.06
Ca	39.33	0.25	29.38	0.22	27.79	0.21	32.18	0.22	30.05	0.22	29.29	0.22	39.27	0.25	28.90	0.22
Cd	0.12	0.18	-0.31	0.19	-0.33	0.16	-0.20	0.16	-0.03	0.17	0.27	0.15	-0.23	0.17	-0.16	0.15
Cu	-0.12	0.12	-0.02	0.14	-0.10	0.13	-0.06	0.14	-0.12	0.14	-0.06	0.14	-0.07	0.14	-0.05	0.14
Cr	0.01	0.10	0.45	0.11	0.25	0.10	0.24	0.10	-0.03	0.09	0.54	0.11	0.20	0.10	0.17	0.10
Pb	0.13	0.19	0.09	0.18	0.17	0.17	0.01	0.17	0.32	0.17	0.02	0.18	0.05	0.17	0.05	0.19
Zn	0.47	0.40	0.02	0.65	-0.50	0.59	0.10	0.41	0.40	0.70	-0.04	0.58	-0.03	0.52	-0.62	0.49
Fe	0.93	0.13	0.95	0.12	0.65	0.12	0.10	0.09	0.64	0.12	0.82	0.12	0.90	0.12	0.64	0.12
TOT	84.46		81.37		88.05		81.66		84.17		90.68		82.30		87.38	
	Unreacted cement phases		CSH		CSH		CaCO ₃		CSH		CSH		Unreacted cement phases		CSH	

Sample b

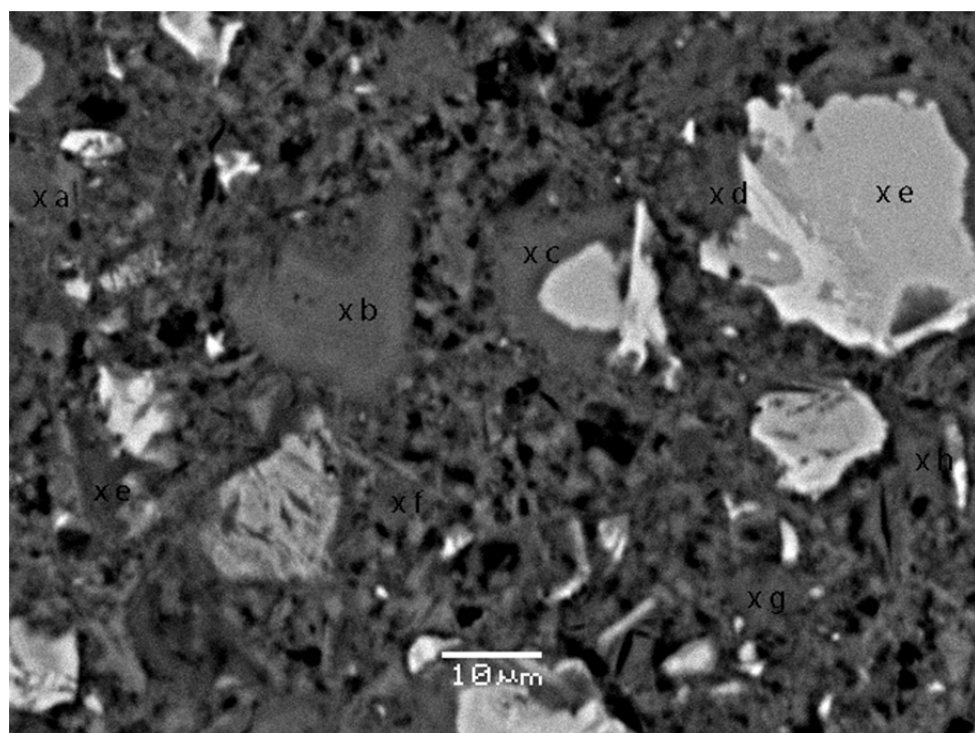
	a		b		c		d		e		f		g		h	
	Element %	σ	Element %	σ	Element %	σ	Element %	σ	Element %	σ	Element %	σ	Element %	σ	Element %	σ
O	24.53	0.10	28.20	0.14	37.43	0.12	28.56	0.12	39.57	0.14	40.12	0.13	34.26	0.12	38.85	0.14
Na	0.01	0.10	0.20	0.12	-0.01	0.09	-0.10	0.12	-0.10	0.12	-0.04	0.11	-0.09	0.12	-0.08	0.11
Mg	0.13	0.08	0.43	0.09	0.23	0.08	0.25	0.09	0.41	0.10	0.51	0.09	0.25	0.09	0.22	0.09
Al	1.12	0.08	0.72	0.09	0.58	0.08	0.61	0.09	2.31	0.10	0.77	0.09	0.82	0.09	0.78	0.09
Si	9.42	0.13	12.25	0.14	10.34	0.13	11.54	0.14	9.31	0.14	11.93	0.15	11.54	0.14	10.73	0.14
S	0.92	0.08	0.18	0.07	0.52	0.07	0.07	0.07	1.11	0.09	0.63	0.08	0.77	0.08	0.98	0.09
K	0.31	0.07	0.20	0.08	0.10	0.07	0.23	0.08	0.19	0.08	0.10	0.08	0.13	0.07	0.07	0.08
Ca	33.98	0.28	49.67	0.34	43.18	0.32	52.79	0.35	33.56	0.29	35.94	0.30	34.74	0.30	34.61	0.30
Cd	-0.18	0.19	-0.16	0.19	0.25	0.19	0.02	0.19	0.11	0.14	-0.23	0.14	0.20	0.19	-0.18	0.19
Cu	-0.04	0.15	-0.02	0.13	-0.02	0.12	-0.06	0.12	-0.10	0.15	-0.07	0.15	-0.12	0.12	-0.10	0.15
Cr	0.43	0.09	0.30	0.09	0.03	0.09	0.09	0.09	0.01	0.09	0.26	0.09	0.31	0.09	0.39	0.09
Pb	0.17	0.19	0.25	0.19	0.05	0.17	0.06	0.20	0.25	0.18	0.18	0.17	0.29	0.18	0.21	0.18
Zn	0.65	0.64	-0.56	0.61	0.15	0.37	-0.26	0.57	-0.72	0.39	-0.32	0.48	-0.21	0.47	-0.42	0.62
Fe	0.62	0.12	0.48	0.11	0.74	0.14	0.11	0.10	0.84	0.09	0.92	0.13	0.59	0.12	0.94	0.14
TOT	82.07		92.14		93.57		93.91		86.75		90.77		83.48		87.00	
	Unreacted cement phases		CSH		CSH		CaCO ₃		CSH		CSH		Unreacted cement phases		CSH	

SEM-EDS analysis of carbonated cement-based s/s copper doped sample

Sample a



Sample b



Sample a

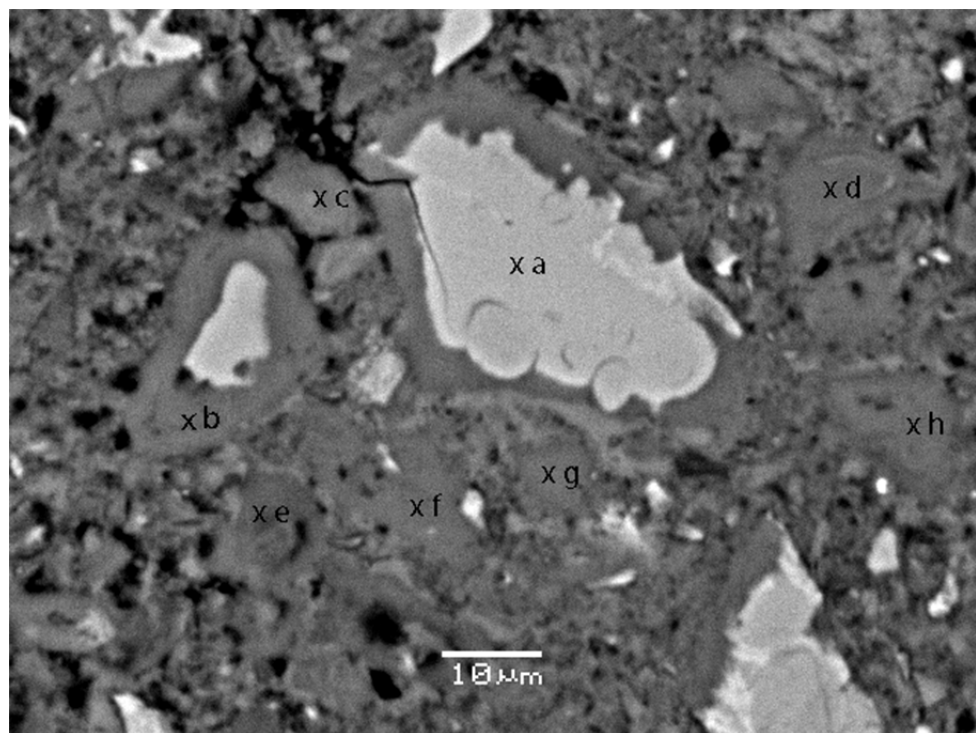
	a		b		c		d		e		f		g		h	
	Element %	σ	Element %	σ	Element %	σ	Element %	σ	Element %	σ	Element %	σ	Element %	σ	Element %	σ
O	24.65	0.13	39.41	0.14	38.13	0.17	26.41	0.13	26.58	0.17	49.28	0.11	38.62	0.13	38.75	0.14
Na	0.13	0.13	-0.16	0.11	-0.21	0.11	-0.05	0.11	0.68	0.14	-0.21	0.11	0.00	0.10	-0.04	0.10
Mg	0.10	0.10	0.23	0.09	0.45	0.09	0.05	0.08	1.14	0.12	0.01	0.08	0.18	0.07	0.32	0.08
Al	1.11	0.10	0.69	0.09	0.74	0.09	0.47	0.08	12.17	0.16	0.07	0.06	0.93	0.08	1.12	0.08
Si	13.81	0.16	11.41	0.14	10.90	0.14	15.42	0.15	2.10	0.11	0.15	0.05	10.10	0.13	10.51	0.13
S	0.22	0.08	0.92	0.08	0.82	0.08	0.11	0.07	0.02	0.07	0.06	0.05	1.12	0.08	1.11	0.08
K	0.06	0.06	0.05	0.07	0.11	0.08	-0.02	0.06	0.03	0.04	0.04	0.06	-0.01	0.05	0.04	0.07
Ca	45.29	0.34	35.45	0.30	35.55	0.30	47.33	0.32	38.51	0.29	39.59	0.28	33.97	0.27	33.39	0.27
Cd	0.34	0.17	-0.15	0.15	-0.12	0.17	0.22	0.17	0.23	0.17	-0.23	0.16	0.17	0.18	-0.34	0.14
Cu	-0.12	0.14	-0.01	0.15	-0.09	0.15	-0.07	0.13	-0.04	0.12	-0.11	0.13	-0.09	0.15	-0.10	0.15
Cr	0.09	0.07	0.03	0.06	0.02	0.07	0.02	0.07	0.02	0.07	0.07	0.06	0.05	0.07	0.01	0.06
Pb	0.02	0.20	0.21	0.20	0.13	0.17	0.01	0.18	0.04	0.19	0.25	0.17	0.21	0.17	0.27	0.19
Zn	-0.49	0.45	0.18	0.45	-0.64	0.56	-0.71	0.67	-0.48	0.41	0.65	0.38	0.59	0.67	0.57	0.66
Fe	0.53	0.15	1.22	0.18	0.89	0.16	0.47	0.15	11.34	0.30	0.03	0.12	0.71	0.14	0.82	0.14
TOT	85.74		89.48		86.68		89.66		92.34		89.65		86.55		86.43	
	Unreacted cement phases		CSH		CSH		Unreacted cement phases		Unreacted cement phases		CaCO ₃		CSH		CSH	

Sample b

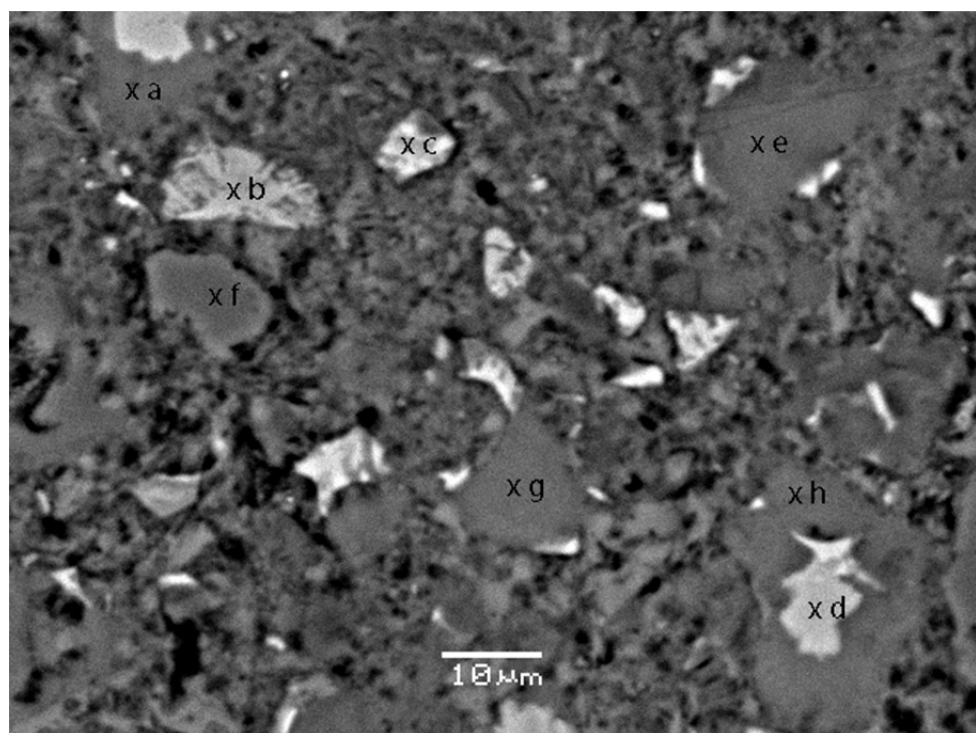
	a		b		c		d		e		f		g		h	
	Element %	σ	Element %	σ	Element %	σ	Element %	σ	Element %	σ						
O	49.41	0.10	38.13	0.13	38.62	0.16	38.75	0.14	24.65	0.19	37.58	0.18	39.00	0.14	38.24	0.11
Na	0.01	0.10	-0.10	0.10	-0.05	0.11	-0.18	0.11	0.58	0.15	0.02	0.11	0.03	0.11	-0.19	0.11
Mg	0.60	0.09	0.24	0.08	0.47	0.09	0.29	0.08	0.67	0.13	0.64	0.09	0.20	0.09	0.32	0.08
Al	7.12	0.12	0.72	0.08	1.13	0.09	1.04	0.09	12.53	0.17	1.36	0.09	1.26	0.09	0.83	0.08
Si	1.10	0.08	11.27	0.13	9.91	0.14	11.26	0.14	2.07	0.11	9.94	0.14	8.91	0.13	11.27	0.14
S	1.02	0.07	1.00	0.08	1.12	0.09	1.17	0.09	0.11	0.07	1.59	0.09	1.30	0.09	1.21	0.09
K	0.09	0.06	0.08	0.07	0.09	0.06	0.06	0.06	0.02	0.07	0.01	0.07	0.05	0.04	0.10	0.07
Ca	29.02	0.25	33.84	0.27	32.01	0.28	33.57	0.29	40.12	0.31	32.17	0.28	32.84	0.28	35.22	0.29
Cd	-0.25	0.19	0.25	0.17	0.18	0.16	-0.10	0.15	0.08	0.19	0.02	0.18	0.21	0.15	-0.19	0.14
Cu	-0.07	0.15	-0.02	0.12	-0.05	0.12	-0.08	0.14	-0.05	0.12	-0.04	0.12	-0.06	0.14	-0.07	0.14
Cr	0.07	0.07	0.07	0.07	0.02	0.06	-0.01	0.06	0.02	0.07	0.04	0.07	0.02	0.07	0.07	0.06
Pb	0.07	0.19	0.07	0.20	0.29	0.19	0.00	0.18	0.17	0.18	0.16	0.18	0.35	0.18	0.19	0.20
Zn	-0.34	0.67	0.12	0.51	-0.38	0.59	0.48	0.35	0.36	0.69	0.25	0.53	-0.46	0.44	-0.56	0.41
Fe	1.82	0.16	0.92	0.15	1.06	0.16	0.89	0.14	9.09	0.28	1.13	0.15	0.86	0.14	0.82	0.15
TOT	89.67		86.59		84.42		87.14		90.42		84.87		84.51		87.26	
	CSH		CSH		CSH		CSH		Unreacted cement phases		CSH		CSH		CSH	

SEM-EDS analysis of carbonated cement-based s/s lead doped sample

Sample a



Sample b



Sample a

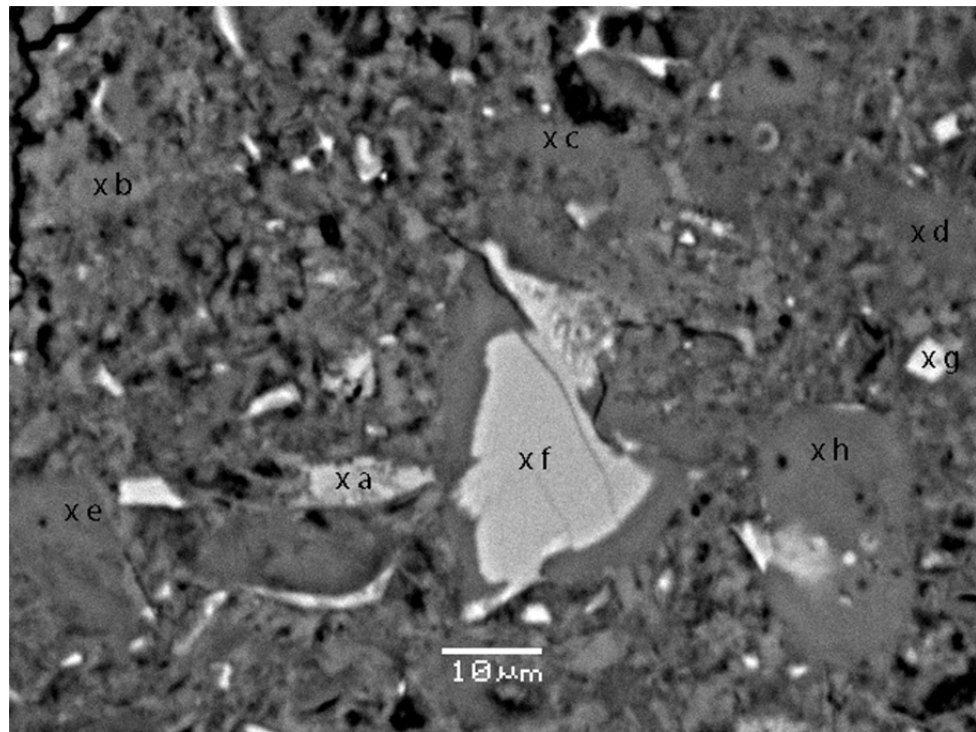
	a		b		c		d		e		f		g		h	
	Element %	σ	Element %	σ	Element %	σ	Element %	σ	Element %	σ	Element %	σ	Element %	σ	Element %	σ
O	26.43	0.13	40.13	0.14	38.48	0.17	41.03	0.14	39.12	0.17	40.12	0.13	37.54	0.10	41.37	0.14
Na	-0.08	0.13	-0.32	0.11	0.01	0.10	-0.08	0.11	-0.12	0.10	-0.11	0.10	-0.15	0.10	-0.12	0.11
Mg	0.29	0.09	0.26	0.08	0.29	0.08	0.14	0.08	0.14	0.07	0.09	0.07	0.42	0.08	0.31	0.08
Al	0.86	0.09	0.96	0.08	0.89	0.08	0.78	0.08	0.91	0.08	0.75	0.07	0.99	0.08	0.98	0.09
Si	11.28	0.14	10.48	0.14	9.96	0.13	10.27	0.13	6.99	0.11	10.30	0.12	10.41	0.13	12.22	0.14
S	0.07	0.07	1.06	0.09	0.78	0.08	1.01	0.08	0.99	0.07	0.71	0.07	0.68	0.07	0.65	0.08
K	0.04	0.07	0.05	0.06	0.10	0.07	0.10	0.07	0.00	0.06	0.00	0.07	0.07	0.07	0.07	0.07
Ca	52.69	0.35	33.51	0.29	35.39	0.29	34.69	0.29	37.62	0.28	33.05	0.26	34.21	0.27	33.81	0.29
Cd	-0.03	0.14	-0.06	0.15	-0.22	0.17	-0.30	0.18	0.20	0.16	-0.05	0.14	-0.16	0.15	0.35	0.17
Cu	-0.12	0.14	-0.10	0.15	-0.05	0.12	-0.11	0.14	-0.12	0.14	-0.05	0.15	-0.11	0.14	-0.01	0.12
Cr	0.05	0.06	0.08	0.06	0.08	0.07	0.07	0.06	0.00	0.07	0.07	0.07	0.04	0.06	0.04	0.07
Pb	0.23	0.20	0.32	0.17	0.30	0.17	0.03	0.18	0.19	0.17	0.05	0.18	0.22	0.18	0.29	0.19
Zn	-0.15	0.65	-0.70	0.61	0.70	0.63	0.56	0.55	0.62	0.56	0.65	0.55	-0.28	0.41	0.39	0.36
Fe	0.72	0.16	0.87	0.15	1.33	0.16	0.51	0.14	0.58	0.13	0.72	0.13	1.04	0.15	0.68	0.14
TOT	92.28		86.54		88.04		88.70		87.12		86.30		84.92		91.03	
	Unreacted cement phases		CSH													

Sample b

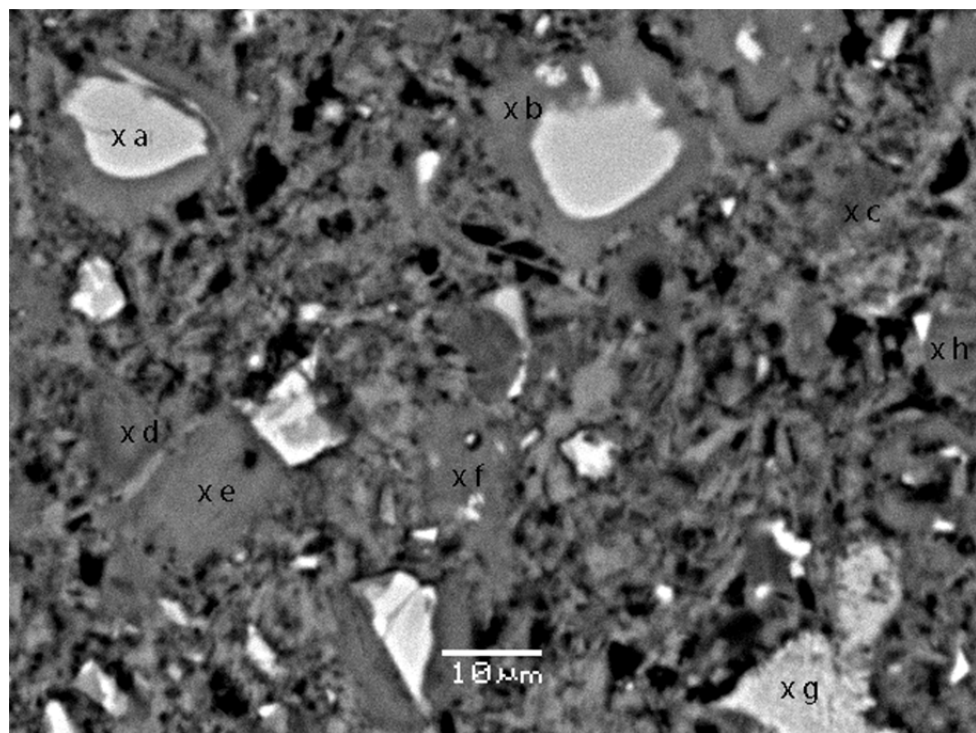
	a		b		c		d		e		f		g		h	
	Element %	σ	Element %	σ	Element %	σ	Element %	σ	Element %	σ	Element %	σ	Element %	σ	Element %	σ
O	39.31	0.13	25.88	0.12	27.94	0.16	25.03	0.19	39.64	0.17	37.37	0.11	38.58	0.13	41.31	0.17
Na	-0.23	0.09	0.73	0.14	-0.02	0.12	-0.21	0.12	-0.06	0.11	-0.01	0.11	-0.01	0.11	-0.26	0.11
Mg	0.24	0.07	0.72	0.12	0.34	0.09	0.32	0.09	0.28	0.08	0.57	0.09	0.25	0.08	0.31	0.08
Al	0.66	0.07	10.88	0.15	0.73	0.09	1.08	0.09	0.80	0.08	1.08	0.09	1.16	0.08	0.71	0.08
Si	11.20	0.13	3.90	0.12	11.82	0.14	11.19	0.14	11.42	0.14	10.25	0.13	10.40	0.13	11.02	0.14
S	0.68	0.07	0.60	0.08	0.11	0.07	0.22	0.07	0.69	0.08	0.99	0.08	0.90	0.08	0.91	0.08
K	0.03	0.06	-0.03	0.07	0.02	0.04	0.09	0.05	0.11	0.07	0.10	0.07	0.09	0.07	0.08	0.07
Ca	34.74	0.27	37.60	0.29	52.36	0.35	52.84	0.35	34.49	0.29	33.51	0.28	32.76	0.28	35.81	0.29
Cd	-0.06	0.17	0.31	0.18	-0.10	0.16	-0.19	0.19	-0.08	0.16	-0.21	0.19	-0.06	0.18	-0.32	0.17
Cu	-0.03	0.13	-0.06	0.15	-0.04	0.13	-0.12	0.12	-0.08	0.12	-0.01	0.13	-0.02	0.12	-0.06	0.15
Cr	0.08	0.07	0.05	0.06	0.06	0.06	0.05	0.07	0.08	0.07	0.08	0.06	0.04	0.07	0.03	0.07
Pb	0.23	0.20	0.21	0.18	0.16	0.17	0.15	0.19	0.21	0.17	0.05	0.17	0.28	0.19	0.08	0.17
Zn	-0.68	0.38	0.42	0.43	-0.53	0.43	-0.33	0.62	-0.54	0.46	-0.15	0.69	0.56	0.45	-0.34	0.42
Fe	0.54	0.13	8.50	0.27	0.57	0.15	1.08	0.16	1.05	0.15	0.57	0.14	1.00	0.15	0.89	0.15
TOT	86.71		89.71		93.42		91.20		88.01		84.19		85.93		90.17	
	CSH		Unreacted cement phases		Unreacted cement phases		Unreacted cement phases		CSH		CSH		CSH		CSH	

SEM-EDS analysis of carbonated cement-based s/s zinc doped sample

Sample a



Sample b



Sample a

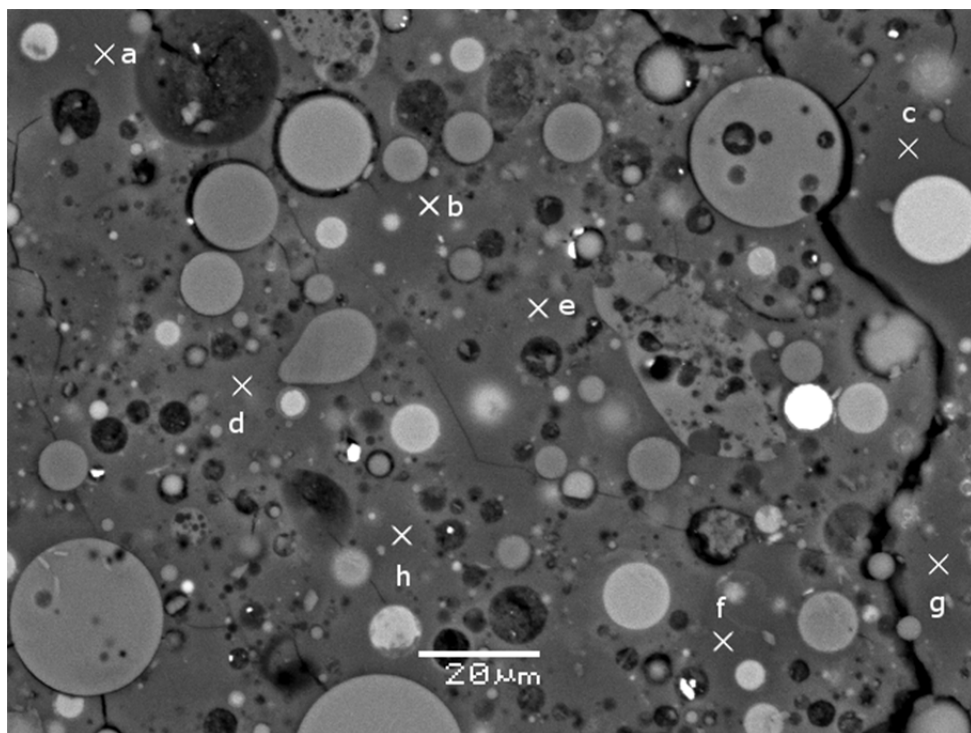
	a		b		c		d		e		f		g		h	
	Element %	σ	Element %	σ	Element %	σ	Element %	σ	Element %	σ	Element %	σ	Element %	σ	Element %	σ
O	24.38	0.13	37.75	0.14	38.95	0.14	39.14	0.17	39.79	0.17	25.35	0.15	26.74	0.17	51.25	0.13
Na	1.03	0.13	-0.10	0.11	-0.04	0.11	0.02	0.13	-0.17	0.11	0.53	0.15	-0.01	0.16	-0.20	0.12
Mg	0.93	0.11	0.26	0.08	0.36	0.09	0.28	0.09	0.24	0.08	0.68	0.13	1.17	0.14	0.66	0.09
Al	12.66	0.16	1.19	0.09	1.82	0.09	0.67	0.08	1.11	0.08	12.07	0.17	10.59	0.17	0.08	0.07
Si	2.23	0.11	9.43	0.14	10.07	0.14	2.10	0.09	10.56	0.14	2.13	0.12	1.01	0.11	0.16	0.06
S	0.21	0.07	1.07	0.09	0.70	0.08	0.68	0.07	0.98	0.08	0.15	0.08	0.23	0.08	-0.01	0.06
K	0.00	0.05	0.13	0.07	0.06	0.07	0.09	0.07	0.08	0.06	0.04	0.06	-0.02	0.08	0.07	0.06
Ca	38.13	0.28	32.75	0.29	35.13	0.29	45.29	0.32	33.24	0.28	38.75	0.31	34.94	0.29	37.43	0.29
Cd	0.11	0.14	0.16	0.15	0.01	0.14	-0.35	0.15	0.12	0.18	-0.01	0.15	-0.03	0.16	-0.13	0.19
Cu	-0.01	0.14	-0.10	0.14	-0.07	0.15	-0.02	0.13	-0.03	0.14	-0.02	0.15	-0.03	0.14	-0.03	0.14
Cr	0.03	0.07	0.07	0.07	0.02	0.06	0.00	0.07	-0.01	0.07	0.01	0.06	0.04	0.06	0.07	0.07
Pb	0.22	0.19	0.05	0.20	0.29	0.18	0.07	0.17	0.05	0.17	0.08	0.20	0.25	0.17	0.19	0.19
Zn	0.52	0.38	-0.74	0.53	-0.20	0.34	-0.08	0.35	-0.50	0.60	0.59	0.57	0.56	0.47	-0.65	0.35
Fe	10.20	0.28	1.21	0.14	1.05	0.16	0.77	0.15	0.73	0.14	10.08	0.30	18.31	0.37	0.10	0.13
TOT	90.64		83.13		88.15		88.66		86.19		90.43		93.75		88.99	
	Unreacted cement phases		CSH		CSH		CaCO ₃		CSH		Unreacted cement phases		Unreacted cement phases		CaCO ₃	

Sample b

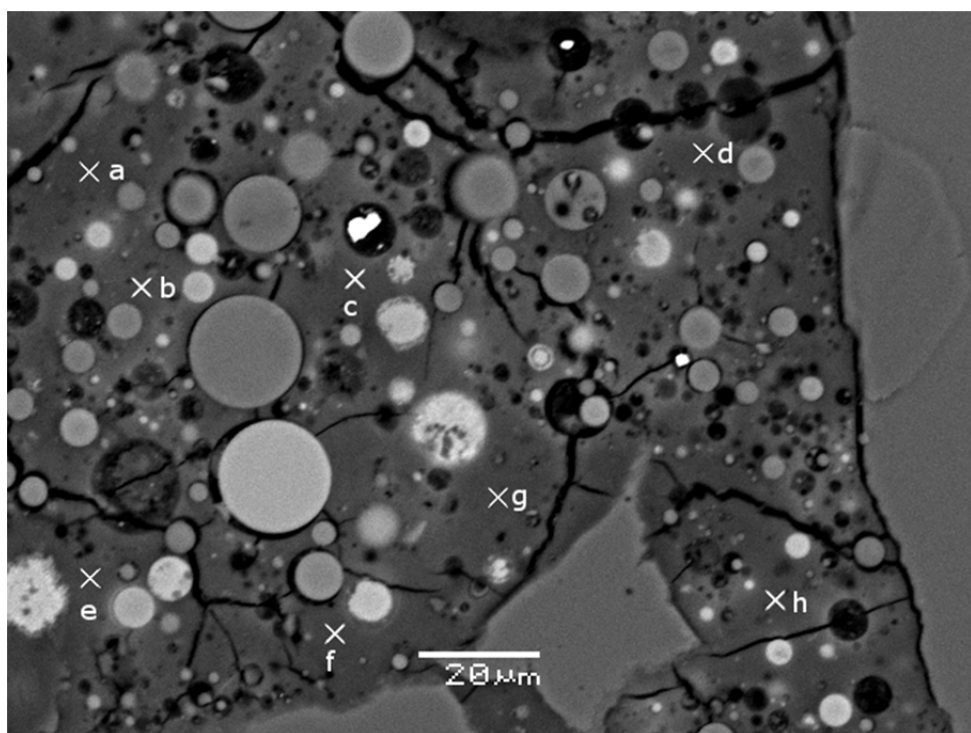
	a		b		c		d		e		f		g		h	
	Element %	σ	Element %	σ	Element %	σ	Element %	σ	Element %	σ	Element %	σ	Element %	σ	Element %	σ
O	26.83	0.12	39.97	0.10	40.51	0.14	39.57	0.14	38.98	0.14	39.49	0.12	27.00	0.14	39.75	0.19
Na	0.08	0.12	-0.14	0.11	0.10	0.11	-0.17	0.11	-0.18	0.13	-0.17	0.12	0.07	0.35	-0.19	0.13
Mg	0.24	0.09	0.28	0.09	0.33	0.08	0.42	0.09	0.40	0.09	0.55	0.08	0.25	0.08	0.46	0.09
Al	0.84	0.09	2.81	0.10	0.89	0.08	0.96	0.09	0.21	0.07	0.61	0.07	0.82	0.07	0.61	0.07
Si	11.51	0.14	8.51	0.13	9.99	0.13	9.98	0.13	1.71	0.06	1.79	0.08	11.53	0.14	1.19	0.07
S	0.04	0.07	1.33	0.09	0.83	0.08	1.01	0.08	0.23	0.06	0.27	0.06	0.03	0.09	0.38	0.07
K	0.17	0.08	0.10	0.07	0.05	0.07	0.15	0.07	0.07	0.04	-0.03	0.06	0.05	0.04	0.03	0.06
Ca	52.33	0.35	32.30	0.28	33.37	0.28	34.27	0.29	40.59	0.31	45.26	0.30	52.34	0.09	37.92	0.32
Cd	0.26	0.15	-0.02	0.17	-0.25	0.14	0.02	0.17	-0.20	0.18	0.14	0.18	0.24	0.14	-0.32	0.15
Cu	-0.04	0.15	-0.04	0.14	-0.03	0.12	-0.07	0.14	-0.04	0.12	-0.12	0.15	-0.09	0.12	-0.11	0.13
Cr	0.07	0.07	0.05	0.07	0.02	0.06	0.00	0.07	0.02	0.06	0.09	0.07	0.07	0.07	0.02	0.06
Pb	0.27	0.19	0.02	0.18	0.09	0.17	0.00	0.19	0.15	0.19	0.12	0.18	0.14	0.20	0.15	0.19
Zn	-0.45	0.58	-0.75	0.53	0.49	0.34	-0.35	0.66	-0.77	0.34	-0.66	0.40	-0.02	0.45	-0.72	0.56
Fe	0.49	0.16	1.67	0.18	0.49	0.14	0.61	0.14	0.51	0.14	0.20	0.15	0.47	0.18	0.51	0.13
TOT	92.64		86.09		86.88		86.40		81.68		87.54		92.90		79.68	
	Unreacted cement phases		CSH		CSH		CSH		CaCO ₃		CaCO ₃		Unreacted cement phases		CaCO ₃	

SEM-EDS analysis of non-carbonated geopolymers-based s/s control sample

Sample a



Sample b



Sample a

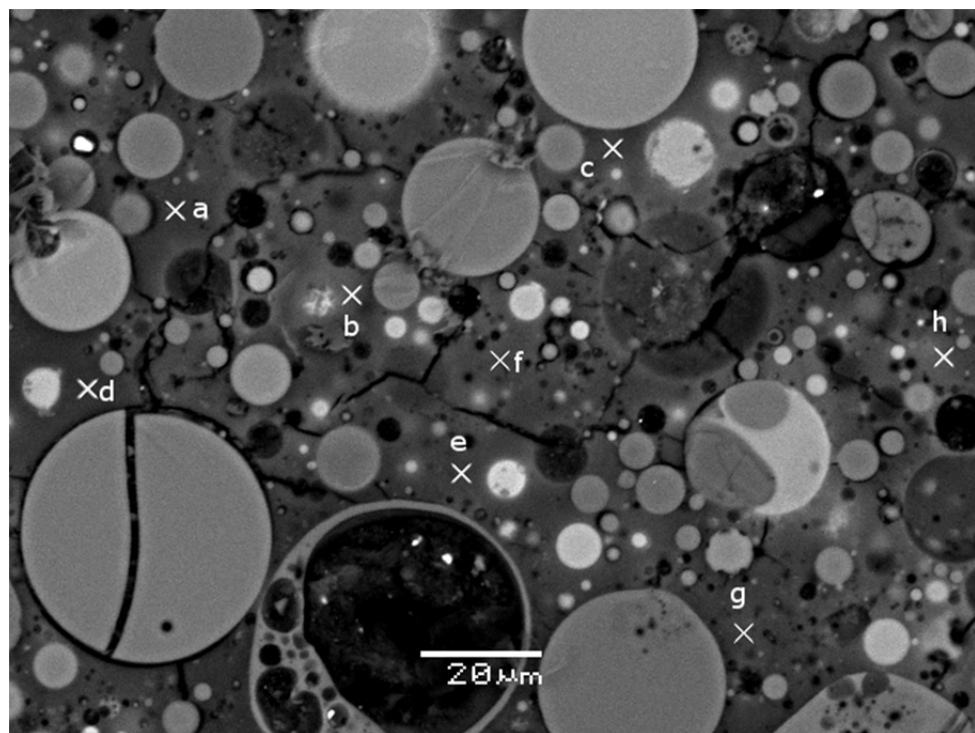
	a		b		c		d		e		f		g		h	
	Element %	σ														
O	37.62	1.35	39.82	1.41	44.74	0.90	41.83	0.97	37.84	1.24	41.95	1.29	43.82	1.33	42.17	1.04
Na	9.03	-0.20	7.67	-0.18	9.23	-0.18	7.83	-0.18	8.42	-0.19	8.92	-0.17	8.06	-0.19	8.47	-0.17
Mg	0.81	0.09	0.92	0.07	0.92	0.07	0.86	0.11	0.80	0.09	0.85	0.06	0.92	0.08	0.93	0.08
Al	6.18	0.10	6.86	0.13	6.19	0.10	6.55	0.09	6.22	0.10	6.61	0.07	6.05	0.07	5.96	0.13
Si	21.19	0.09	19.74	0.09	19.26	0.13	21.45	0.06	19.77	0.11	19.91	0.12	20.84	0.06	20.83	0.06
K	0.35	0.06	0.33	0.07	0.38	0.05	0.38	0.05	0.37	0.04	0.32	0.07	0.35	0.07	0.38	0.07
Ca	7.94	0.23	7.03	0.20	8.14	0.29	8.08	0.19	7.54	0.24	8.35	0.21	7.27	0.29	8.21	0.24
Cd	-0.24	0.14	-0.27	0.17	-0.18	0.16	0.27	0.16	-0.07	0.17	-0.23	0.15	0.12	0.18	-0.03	0.14
Cu	-0.08	0.14	-0.10	0.15	-0.10	0.12	-0.10	0.15	-0.10	0.13	-0.04	0.14	-0.06	0.14	-0.03	0.13
Cr	0.08	0.06	0.05	0.07	-0.01	0.06	0.05	0.07	0.05	0.07	0.04	0.06	0.02	0.06	0.00	0.07
Pb	0.02	0.17	0.26	0.20	0.05	0.19	0.27	0.17	0.09	0.17	0.27	0.20	0.22	0.20	0.36	0.20
Zn	-0.10	0.61	0.21	0.41	0.09	0.58	-0.28	0.64	0.13	0.55	0.64	0.44	-0.10	0.44	0.48	0.64
Fe	1.77	0.19	1.85	0.19	1.60	0.25	1.70	0.24	1.61	0.20	1.59	0.19	1.58	0.16	1.64	0.21
TOT	84.57		84.37		90.31		88.89		82.67		89.18		89.09		89.37	

Sample b

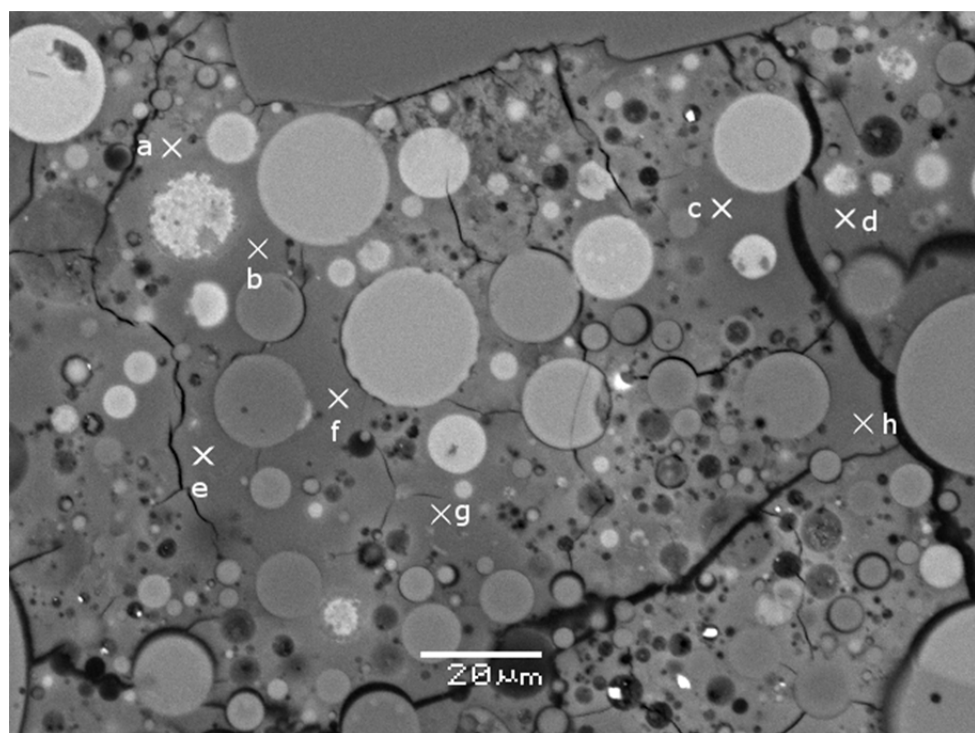
	a		b		c		d		e		f		g		h	
	Element %	σ														
O	39.72	1.22	45.69	1.32	40.76	1.31	37.79	1.09	40.33	1.24	43.76	1.02	39.31	1.20	45.19	0.96
Na	8.89	-0.19	8.76	-0.17	8.35	-0.18	9.14	-0.20	8.15	-0.18	8.98	-0.19	7.63	-0.20	8.32	-0.18
Mg	0.90	0.06	0.94	0.10	0.86	0.05	0.87	0.10	0.84	0.06	0.78	0.06	0.84	0.07	0.81	0.05
Al	6.67	0.10	6.12	0.10	6.12	0.09	6.78	0.09	6.03	0.11	5.85	0.13	6.65	0.08	6.74	0.11
Si	21.97	0.05	19.23	0.06	20.82	0.06	20.57	0.13	22.76	0.08	23.16	0.07	23.33	0.12	20.81	0.10
K	0.32	0.06	0.33	0.05	0.32	0.04	0.32	0.05	0.35	0.05	0.32	0.07	0.35	0.04	0.35	0.07
Ca	7.51	0.23	7.60	0.23	7.61	0.27	7.45	0.21	8.13	0.18	7.08	0.19	7.04	0.22	7.46	0.18
Cd	0.29	0.15	0.21	0.15	-0.05	0.16	-0.15	0.19	0.16	0.15	0.16	0.17	-0.07	0.18	0.28	0.18
Cu	-0.09	0.15	-0.01	0.13	-0.08	0.12	-0.10	0.13	-0.04	0.12	-0.11	0.12	-0.10	0.15	-0.08	0.12
Cr	0.02	0.07	0.09	0.07	0.08	0.06	0.03	0.06	0.03	0.07	0.06	0.07	0.08	0.07	0.08	0.07
Pb	0.31	0.17	0.13	0.18	0.32	0.19	0.21	0.18	0.35	0.19	0.04	0.18	0.04	0.18	0.04	0.19
Zn	-0.38	0.38	-0.30	0.62	-0.21	0.51	0.13	0.59	-0.75	0.37	-0.65	0.44	0.50	0.59	-0.36	0.69
Fe	1.61	0.25	1.86	0.12	1.66	0.25	1.61	0.23	1.55	0.19	1.61	0.18	1.59	0.11	1.72	0.17
TOT	87.74		90.65		86.56		84.65		87.89		91.04		87.19		91.36	

SEM-EDS analysis of non-carbonated geopolymers-based s/s cadmium sample

Sample a



Sample b



Sample a

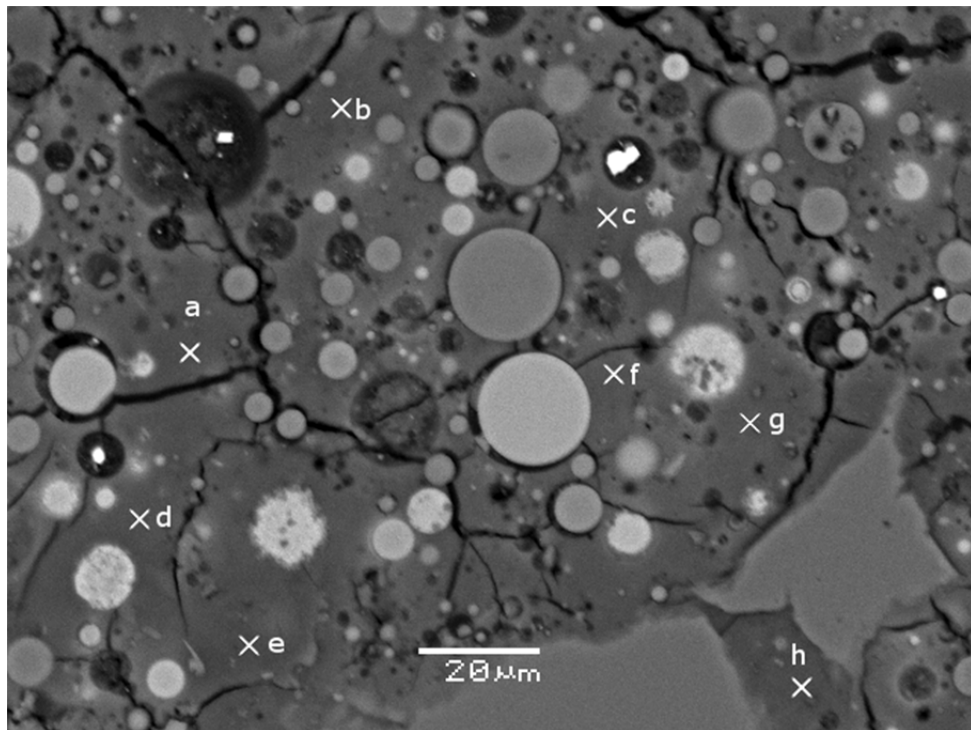
	a		b		c		d		e		f		g		h	
	Element %	σ														
O	41.09	1.27	42.76	1.27	40.54	1.19	43.44	1.35	44.71	1.23	41.39	1.03	45.32	1.31	40.81	1.33
Na	9.20	-0.17	9.20	-0.20	8.96	-0.19	8.26	-0.18	7.62	-0.17	8.09	-0.18	8.02	-0.19	8.29	-0.18
Mg	0.90	0.06	0.79	0.06	0.93	0.06	0.78	0.06	0.90	0.11	0.83	0.10	0.87	0.06	0.88	0.09
Al	6.12	0.06	5.91	0.09	5.93	0.06	6.56	0.10	5.89	0.09	6.69	0.10	6.79	0.08	6.84	0.12
Si	22.42	0.11	21.80	0.12	21.73	0.12	21.06	0.08	20.94	0.13	22.53	0.12	19.62	0.10	19.17	0.06
K	0.37	0.06	0.36	0.05	0.34	0.07	0.32	0.07	0.37	0.04	0.37	0.07	0.37	0.07	0.35	0.06
Ca	8.16	0.22	8.47	0.22	7.20	0.18	8.39	0.26	8.11	0.27	7.96	0.29	7.28	0.29	7.17	0.28
Cd	-0.23	0.14	-0.12	0.18	-0.30	0.19	-0.25	0.19	0.13	0.19	-0.35	0.16	0.27	0.16	-0.22	0.17
Cu	-0.04	0.12	-0.01	0.14	-0.02	0.13	-0.05	0.14	-0.01	0.12	-0.02	0.13	-0.03	0.14	-0.12	0.14
Cr	0.08	0.06	0.03	0.07	-0.01	0.07	0.07	0.06	0.00	0.07	0.08	0.07	0.08	0.06	0.05	0.07
Pb	0.21	0.19	0.15	0.18	0.04	0.20	0.11	0.20	0.24	0.20	0.29	0.20	0.00	0.20	0.16	0.18
Zn	-0.45	0.62	0.18	0.65	0.36	0.45	-0.48	0.57	-0.43	0.62	-0.53	0.44	0.18	0.43	-0.24	0.43
Fe	1.76	0.19	1.62	0.25	1.77	0.11	1.85	0.24	1.85	0.10	1.81	0.20	1.57	0.15	1.82	0.18
TOT	89.59		91.14		87.47		90.06		90.32		89.14		90.34		84.96	

Sample b

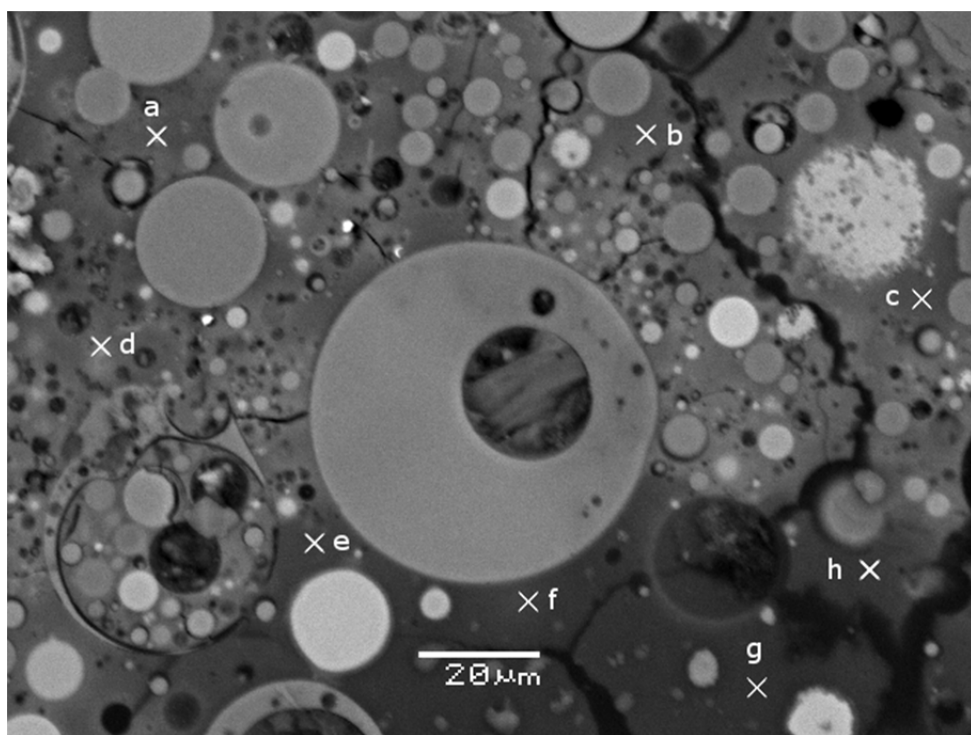
	a		b		c		d		e		f		g		h	
	Element %	σ														
O	44.24	1.29	42.02	1.24	40.24	1.34	38.60	1.30	39.54	0.87	44.91	1.36	44.91	1.40	41.45	1.21
Na	8.48	-0.17	7.70	-0.18	8.12	-0.19	7.72	-0.18	7.80	-0.20	8.97	-0.19	8.29	-0.20	8.37	-0.20
Mg	0.94	0.09	0.92	0.05	0.83	0.11	0.91	0.09	0.85	0.09	0.84	0.10	0.78	0.05	0.85	0.07
Al	6.72	0.13	6.80	0.10	6.68	0.07	5.78	0.13	6.17	0.08	6.35	0.11	5.72	0.06	5.80	0.13
Si	20.49	0.11	19.13	0.05	22.20	0.12	21.15	0.11	20.22	0.12	23.30	0.08	20.16	0.05	20.94	0.06
K	0.32	0.07	0.35	0.07	0.34	0.05	0.35	0.07	0.32	0.06	0.33	0.07	0.33	0.04	0.34	0.06
Ca	7.84	0.27	8.14	0.19	7.39	0.30	7.10	0.29	8.51	0.19	7.49	0.20	7.64	0.26	7.51	0.25
Cd	0.32	0.18	-0.08	0.15	0.06	0.19	0.32	0.14	-0.23	0.17	-0.16	0.19	0.14	0.15	-0.15	0.19
Cu	-0.01	0.13	-0.09	0.13	-0.12	0.12	-0.11	0.12	-0.12	0.15	-0.08	0.14	-0.05	0.15	-0.03	0.13
Cr	0.07	0.07	0.01	0.07	0.08	0.06	0.09	0.07	0.01	0.07	0.03	0.07	0.04	0.06	0.04	0.07
Pb	0.32	0.17	0.11	0.18	0.00	0.19	0.33	0.17	0.08	0.20	0.00	0.17	0.22	0.18	0.09	0.17
Zn	-0.48	0.65	-0.66	0.61	-0.60	0.68	-0.26	0.56	-0.34	0.35	-0.59	0.46	-0.40	0.42	-0.63	0.59
Fe	1.83	0.22	1.81	0.20	1.75	0.25	1.62	0.17	1.86	0.17	1.71	0.23	1.77	0.24	1.59	0.16
TOT	91.08		86.16		86.97		83.60		84.67		93.10		89.55		86.17	

SEM-EDS analysis of non-carbonated geopolymers-based s/s chromium (III) sample

Sample a



Sample b



Sample a

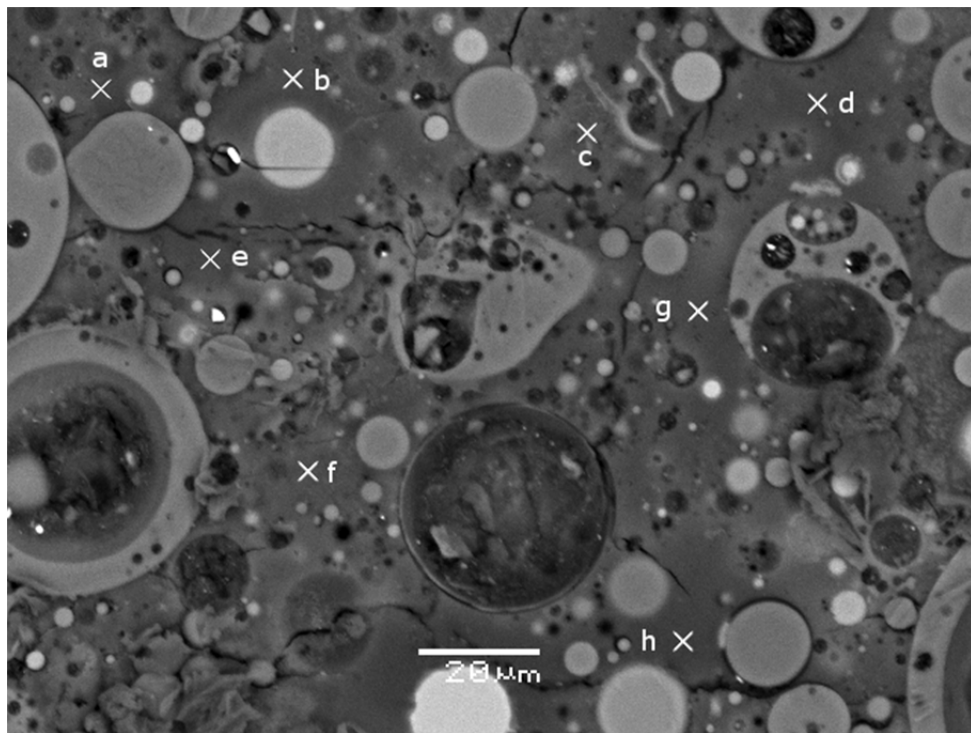
	a		b		c		d		e		f		g		h	
	Element %	σ														
O	42.67	1.24	38.33	1.32	41.40	1.34	45.00	1.12	43.73	0.94	37.66	1.16	40.94	1.19	45.32	1.44
Na	8.06	-0.18	8.75	-0.20	8.65	-0.19	7.84	-0.20	9.06	-0.17	7.93	-0.18	8.80	-0.17	8.08	-0.19
Mg	0.94	0.08	0.93	0.05	0.87	0.07	0.80	0.10	0.93	0.11	0.84	0.06	0.88	0.05	0.91	0.10
Al	6.61	0.10	6.45	0.11	6.04	0.08	6.49	0.06	6.29	0.07	6.61	0.11	6.39	0.09	6.14	0.09
Si	22.01	0.07	22.43	0.07	20.96	0.13	21.39	0.07	19.13	0.05	21.94	0.11	22.12	0.08	22.37	0.10
K	0.32	0.06	0.33	0.05	0.38	0.07	0.34	0.07	0.37	0.04	0.33	0.05	0.36	0.05	0.37	0.06
Ca	7.83	0.28	7.17	0.18	7.27	0.22	7.99	0.18	7.97	0.29	8.18	0.21	8.42	0.24	8.23	0.25
Cd	0.30	0.14	-0.35	0.19	0.00	0.16	0.06	0.18	-0.16	0.16	0.08	0.17	-0.35	0.18	-0.01	0.14
Cu	-0.04	0.14	-0.11	0.14	-0.08	0.13	-0.05	0.13	-0.01	0.14	-0.12	0.14	-0.03	0.14	-0.03	0.13
Cr	0.03	0.06	0.04	0.06	0.01	0.06	0.02	0.06	0.07	0.06	0.02	0.06	0.05	0.06	-0.01	0.06
Pb	0.18	0.17	0.15	0.18	0.05	0.17	0.15	0.18	0.15	0.20	0.01	0.19	0.05	0.20	0.09	0.20
Zn	-0.34	0.39	0.17	0.67	-0.61	0.46	-0.46	0.57	0.37	0.49	0.68	0.59	-0.01	0.55	-0.76	0.56
Fe	1.79	0.22	1.63	0.11	1.78	0.10	1.60	0.12	1.68	0.22	1.72	0.14	1.61	0.21	1.55	0.11
TOT	90.36		85.92		86.72		91.17		89.58		85.88		89.23		92.25	

Sample b

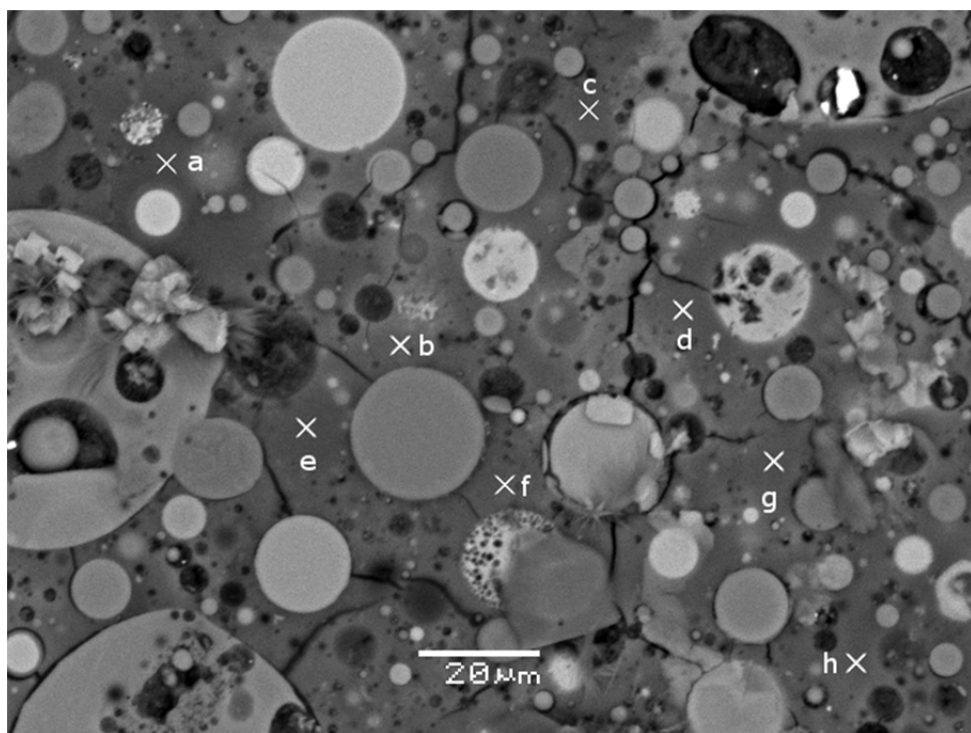
	a		b		c		d		e		f		g		h	
	Element %	σ														
O	38.17	1.17	41.06	1.25	38.69	1.36	42.42	0.88	42.73	1.29	44.41	1.01	42.27	1.14	37.51	1.01
Na	8.60	-0.19	7.90	-0.17	7.61	-0.18	9.19	-0.20	8.83	-0.18	8.01	-0.18	8.56	-0.17	8.44	-0.19
Mg	0.85	0.11	0.84	0.06	0.87	0.10	0.90	0.06	0.83	0.05	0.83	0.06	0.79	0.05	0.91	0.05
Al	6.94	0.09	5.71	0.07	6.59	0.12	6.61	0.12	6.16	0.06	6.68	0.09	5.84	0.11	6.86	0.11
Si	21.36	0.07	20.21	0.06	19.26	0.12	20.78	0.13	22.90	0.13	22.96	0.06	20.81	0.13	21.29	0.06
K	0.35	0.07	0.33	0.06	0.32	0.06	0.33	0.07	0.35	0.05	0.34	0.07	0.35	0.06	0.34	0.07
Ca	7.09	0.23	7.42	0.18	8.08	0.21	8.11	0.22	7.11	0.18	7.88	0.24	8.27	0.30	7.32	0.22
Cd	-0.27	0.15	-0.07	0.17	-0.19	0.14	-0.17	0.14	0.18	0.18	-0.31	0.14	0.29	0.16	0.33	0.19
Cu	-0.06	0.15	-0.09	0.12	-0.01	0.12	-0.04	0.15	-0.04	0.13	-0.10	0.13	-0.09	0.14	-0.05	0.13
Cr	0.06	0.06	0.06	0.06	0.04	0.06	0.08	0.07	0.09	0.06	0.09	0.07	0.05	0.06	0.09	0.06
Pb	0.07	0.17	0.27	0.17	0.14	0.20	0.09	0.20	0.23	0.19	0.07	0.20	0.03	0.19	0.05	0.20
Zn	-0.10	0.35	0.37	0.51	-0.41	0.40	-0.10	0.54	-0.09	0.49	-0.33	0.47	0.63	0.58	0.39	0.45
Fe	1.65	0.20	1.78	0.15	1.59	0.21	1.65	0.18	1.82	0.23	1.83	0.16	1.79	0.11	1.68	0.16
TOT	84.71		85.79		82.58		89.85		91.10		92.36		89.59		85.16	

SEM-EDS analysis of non-carbonated geopolymers-based s/s chromium (VI) sample

Sample a



Sample b



Sample a

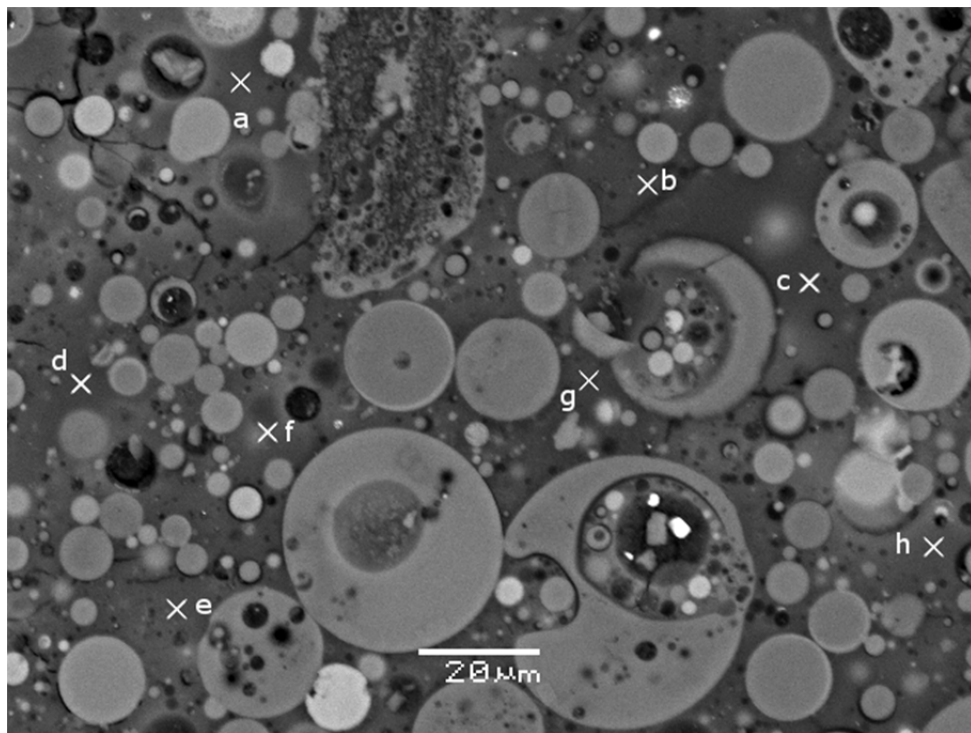
	a		b		c		d		e		f		g		h	
	Element %	σ														
O	44.79	0.87	41.05	1.36	44.83	1.24	44.91	1.08	39.16	0.99	44.85	1.41	42.81	1.36	44.52	1.08
Na	7.84	-0.19	8.59	-0.17	8.44	-0.18	8.22	-0.18	7.88	-0.18	8.66	-0.18	8.55	-0.17	9.12	-0.17
Mg	0.80	0.07	0.91	0.05	0.79	0.10	0.87	0.09	0.80	0.07	0.81	0.11	0.83	0.10	0.92	0.07
Al	5.94	0.11	6.28	0.07	6.61	0.12	6.59	0.09	6.25	0.12	6.42	0.06	6.45	0.10	6.81	0.10
Si	21.75	0.12	20.29	0.10	22.93	0.12	19.43	0.11	21.28	0.06	22.95	0.08	22.82	0.11	20.20	0.06
K	0.34	0.05	0.38	0.06	0.36	0.06	0.32	0.07	0.36	0.04	0.37	0.07	0.36	0.06	0.32	0.07
Ca	8.46	0.29	7.19	0.24	7.59	0.20	7.91	0.18	8.22	0.23	7.74	0.27	8.30	0.23	7.37	0.22
Cd	0.14	0.18	-0.32	0.17	0.26	0.17	0.32	0.17	0.24	0.18	0.08	0.16	0.11	0.17	-0.28	0.14
Cu	-0.04	0.12	-0.02	0.14	-0.06	0.15	-0.09	0.13	-0.04	0.13	-0.10	0.15	-0.12	0.13	-0.06	0.13
Cr	0.00	0.07	0.06	0.07	0.06	0.07	0.04	0.07	0.05	0.06	0.00	0.06	0.09	0.06	0.07	0.07
Pb	0.12	0.20	0.09	0.18	0.08	0.20	0.37	0.17	0.26	0.20	0.33	0.19	0.21	0.17	0.36	0.19
Zn	-0.01	0.36	-0.15	0.70	0.42	0.49	0.31	0.40	0.32	0.56	-0.36	0.36	0.55	0.39	-0.70	0.52
Fe	1.70	0.15	1.66	0.11	1.84	0.18	1.81	0.19	1.63	0.21	1.61	0.14	1.76	0.19	1.86	0.14
TOT	91.83		86.01		94.15		91.01		86.41		93.36		92.72		90.51	

Sample b

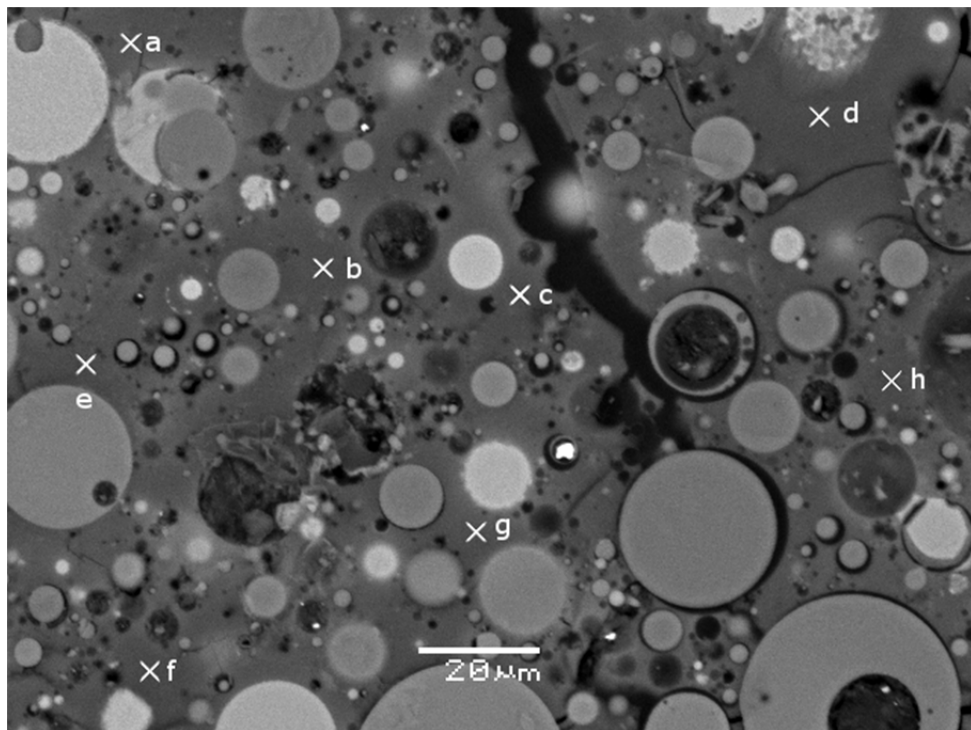
	a		b		c		d		e		f		g		h	
	Element %	σ														
O	42.43	0.87	43.93	1.44	45.81	1.12	42.66	0.96	42.33	1.39	39.30	1.41	41.20	0.94	40.85	1.10
Na	8.76	-0.17	9.26	-0.19	8.96	-0.17	8.69	-0.19	8.43	-0.19	7.61	-0.17	8.37	-0.18	8.26	-0.19
Mg	0.83	0.07	0.83	0.05	0.82	0.07	0.81	0.06	0.87	0.05	0.92	0.09	0.91	0.07	0.90	0.06
Al	6.42	0.06	6.46	0.11	6.52	0.10	6.35	0.10	6.73	0.06	6.04	0.10	6.90	0.09	6.32	0.08
Si	21.30	0.12	19.84	0.06	21.45	0.09	22.32	0.13	21.84	0.10	19.53	0.12	22.16	0.05	22.79	0.12
K	0.38	0.07	0.35	0.07	0.32	0.06	0.38	0.06	0.32	0.06	0.36	0.07	0.37	0.04	0.32	0.07
Ca	7.95	0.28	7.37	0.23	8.15	0.20	8.21	0.26	8.28	0.22	8.35	0.29	7.64	0.18	7.93	0.26
Cd	0.11	0.17	-0.10	0.19	-0.02	0.14	-0.31	0.18	0.01	0.15	0.04	0.14	0.06	0.15	0.18	0.19
Cu	-0.01	0.13	-0.08	0.15	-0.01	0.15	-0.10	0.12	-0.12	0.14	-0.09	0.13	-0.08	0.13	-0.10	0.15
Cr	0.00	0.07	0.04	0.07	0.01	0.06	0.08	0.07	0.06	0.07	-0.01	0.07	0.00	0.07	0.06	0.06
Pb	0.09	0.17	0.11	0.17	0.14	0.17	0.23	0.19	0.11	0.20	0.25	0.20	0.18	0.20	0.03	0.17
Zn	-0.25	0.70	0.46	0.62	0.08	0.48	0.68	0.39	0.55	0.44	0.36	0.54	0.22	0.36	-0.37	0.34
Fe	1.55	0.14	1.66	0.25	1.83	0.25	1.53	0.16	1.69	0.14	1.82	0.12	1.69	0.15	1.70	0.18
TOT	89.56		90.13		94.06		91.53		91.10		84.48		89.62		88.87	

SEM-EDS analysis of non-carbonated geopolymers-based s/s copper sample

Sample a



Sample b



Sample a

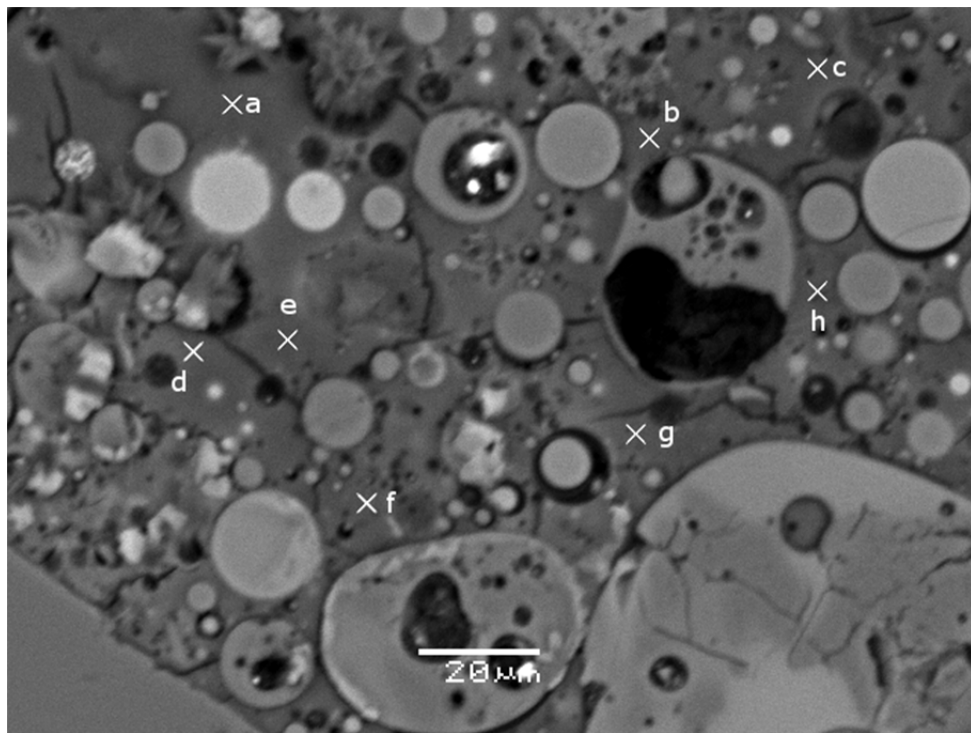
	a		b		c		d		e		f		g		h	
	Element %	σ														
O	44.67	0.97	44.78	0.91	45.19	0.87	44.63	1.26	39.22	1.35	42.69	0.92	38.90	0.90	38.56	1.35
Na	8.18	-0.18	8.04	-0.19	7.74	-0.17	7.94	-0.17	8.93	-0.18	7.93	-0.18	7.59	-0.19	8.66	-0.20
Mg	0.87	0.11	0.94	0.05	0.85	0.11	0.83	0.06	0.88	0.05	0.83	0.05	0.89	0.09	0.92	0.08
Al	6.49	0.11	6.67	0.09	6.84	0.11	6.37	0.07	6.55	0.10	6.61	0.07	6.87	0.06	5.70	0.09
Si	19.77	0.07	23.18	0.06	22.12	0.09	21.37	0.05	19.68	0.05	20.09	0.07	21.45	0.05	21.13	0.10
K	0.33	0.06	0.38	0.05	0.36	0.05	0.37	0.06	0.34	0.06	0.36	0.04	0.35	0.04	0.37	0.07
Ca	7.74	0.29	8.22	0.27	8.13	0.21	8.50	0.18	7.42	0.29	8.48	0.20	8.36	0.18	7.93	0.18
Cd	0.05	0.19	0.26	0.16	-0.03	0.19	-0.33	0.16	0.28	0.14	0.00	0.16	0.01	0.14	0.15	0.15
Cu	-0.09	0.15	-0.09	0.15	-0.08	0.13	-0.01	0.15	-0.09	0.13	-0.10	0.12	-0.01	0.13	-0.10	0.15
Cr	0.07	0.06	0.09	0.06	0.09	0.07	-0.01	0.07	0.06	0.06	0.00	0.06	0.04	0.06	0.01	0.07
Pb	0.33	0.19	0.38	0.18	0.35	0.19	0.17	0.19	0.08	0.20	0.17	0.17	0.28	0.19	0.19	0.18
Zn	-0.11	0.47	0.56	0.54	0.65	0.57	-0.04	0.40	-0.39	0.52	0.19	0.56	0.12	0.44	0.26	0.34
Fe	1.71	0.24	1.64	0.16	1.64	0.20	1.78	0.18	1.76	0.12	1.75	0.20	1.53	0.14	1.54	0.17
TOT	90.01		95.05		93.85		91.57		84.72		89.00		86.38		85.32	

Sample b

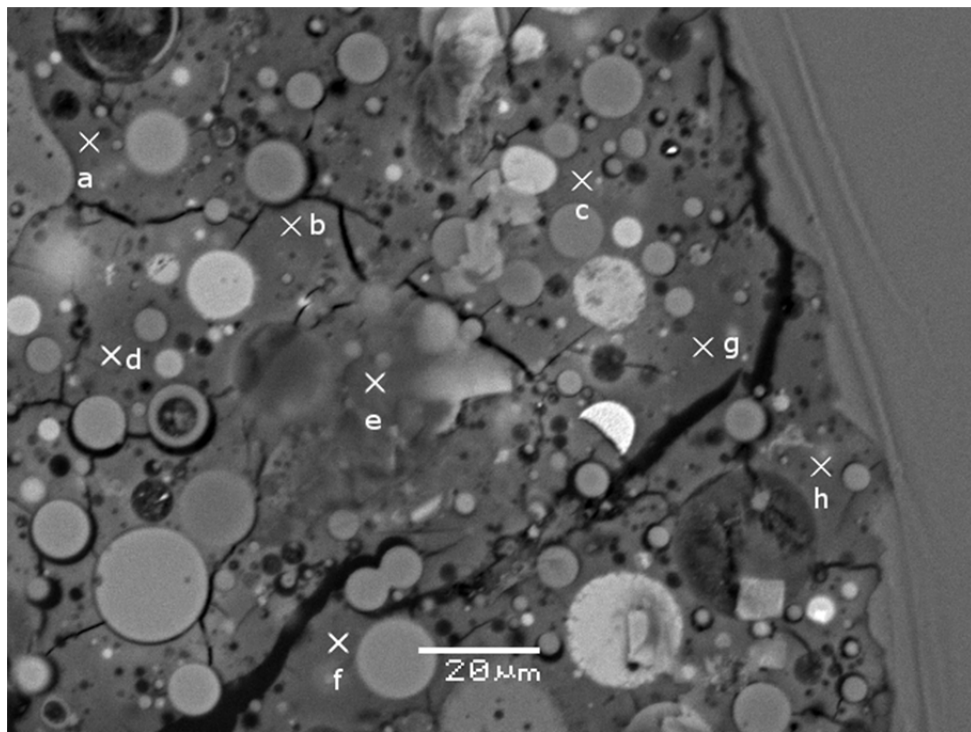
	a		b		c		d		e		f		g		h	
	Element %	σ														
O	40.69	0.96	37.70	1.32	40.78	1.20	43.34	1.40	44.69	1.00	39.18	1.29	45.65	1.15	44.03	1.44
Na	8.59	-0.20	8.92	-0.19	8.27	-0.20	8.73	-0.17	7.87	-0.20	8.30	-0.17	7.87	-0.19	9.17	-0.17
Mg	0.93	0.05	0.85	0.09	0.88	0.07	0.78	0.11	0.83	0.08	0.79	0.09	0.84	0.07	0.90	0.11
Al	6.43	0.07	6.67	0.11	6.65	0.11	5.72	0.09	6.70	0.07	5.95	0.11	6.60	0.08	5.96	0.06
Si	20.46	0.13	20.28	0.05	21.49	0.05	23.00	0.08	19.68	0.13	19.61	0.13	21.35	0.10	22.31	0.12
K	0.32	0.06	0.35	0.04	0.38	0.07	0.38	0.07	0.32	0.06	0.34	0.06	0.35	0.04	0.33	0.07
Ca	7.31	0.20	7.45	0.18	7.96	0.26	8.56	0.24	7.02	0.23	8.24	0.22	7.11	0.30	7.19	0.27
Cd	0.25	0.14	0.27	0.17	-0.06	0.15	0.25	0.19	0.13	0.14	-0.34	0.16	-0.28	0.19	0.31	0.15
Cu	-0.09	0.13	-0.03	0.12	-0.03	0.13	-0.11	0.14	-0.03	0.12	-0.07	0.12	-0.09	0.15	-0.07	0.14
Cr	0.05	0.07	0.05	0.06	0.05	0.06	0.04	0.06	0.05	0.06	0.08	0.07	0.07	0.07	-0.01	0.06
Pb	0.21	0.20	0.36	0.20	0.06	0.18	0.10	0.18	0.31	0.20	0.10	0.17	0.13	0.19	0.38	0.17
Zn	-0.14	0.34	-0.41	0.56	-0.77	0.38	0.40	0.51	0.12	0.67	-0.61	0.39	0.35	0.62	-0.41	0.34
Fe	1.83	0.13	1.76	0.11	1.80	0.11	1.76	0.22	1.80	0.18	1.87	0.15	1.53	0.11	1.78	0.16
TOT	86.84		84.22		87.46		92.95		89.49		83.44		91.48		91.87	

SEM-EDS analysis of non-carbonated geopolymers-based s/s lead sample

Sample a



Sample b



Sample a

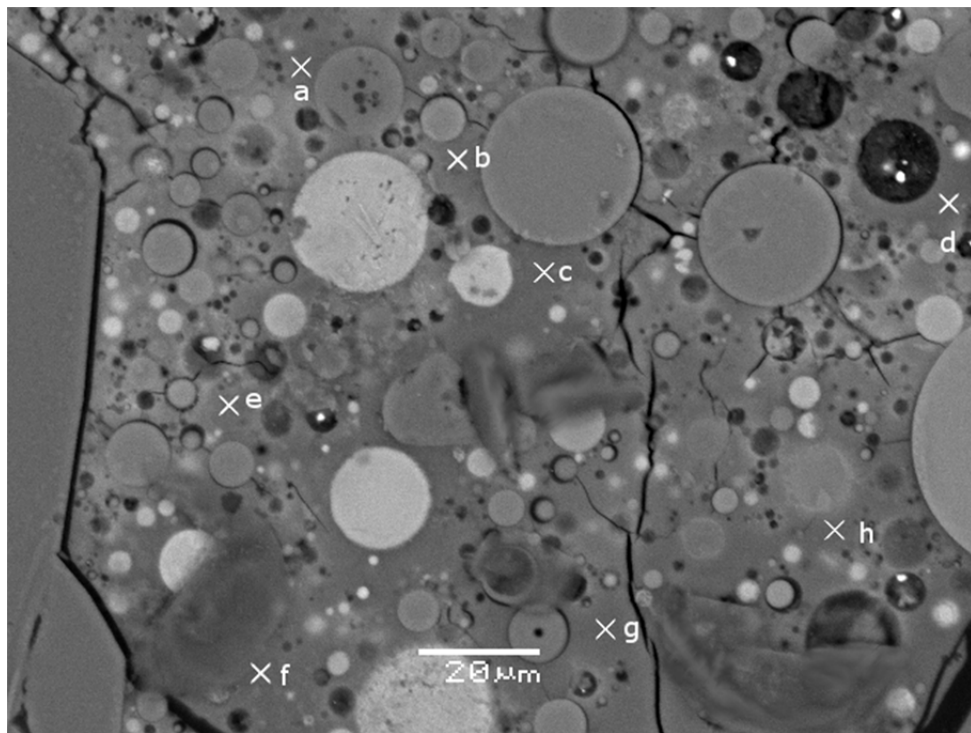
	a		b		c		d		e		f		g		h	
	Element %	σ														
O	41.23	1.06	39.32	1.33	39.80	0.96	38.01	1.09	45.63	1.00	43.14	0.92	38.34	1.07	40.40	1.15
Na	8.44	-0.18	8.42	-0.20	7.89	-0.17	7.70	-0.17	9.01	-0.19	8.84	-0.20	7.86	-0.17	8.55	-0.20
Mg	0.93	0.06	0.86	0.10	0.83	0.10	0.92	0.07	0.82	0.05	0.84	0.05	0.81	0.07	0.82	0.09
Al	6.20	0.12	5.84	0.08	5.94	0.13	5.85	0.06	5.74	0.10	6.52	0.06	5.90	0.06	5.98	0.08
Si	19.93	0.05	19.75	0.05	19.72	0.09	22.84	0.07	19.25	0.09	19.15	0.13	20.39	0.11	19.26	0.08
K	0.36	0.05	0.33	0.04	0.36	0.04	0.38	0.06	0.38	0.07	0.34	0.07	0.32	0.06	0.34	0.07
Ca	7.70	0.26	7.60	0.24	7.45	0.22	7.88	0.21	7.85	0.25	7.50	0.21	8.44	0.26	7.31	0.18
Cd	-0.30	0.17	0.09	0.19	0.14	0.14	0.35	0.15	0.24	0.18	0.12	0.17	-0.16	0.18	-0.29	0.18
Cu	-0.09	0.14	-0.11	0.14	-0.04	0.14	-0.02	0.12	-0.07	0.15	-0.09	0.13	-0.02	0.15	-0.06	0.14
Cr	0.03	0.06	0.03	0.06	0.01	0.06	0.05	0.06	0.08	0.06	0.01	0.06	-0.01	0.07	0.07	0.06
Pb	0.20	0.17	0.06	0.19	0.12	0.19	0.21	0.18	0.14	0.20	0.01	0.20	0.34	0.17	0.10	0.20
Zn	-0.07	0.57	-0.23	0.70	0.28	0.50	0.02	0.60	-0.49	0.65	-0.40	0.38	0.42	0.44	-0.26	0.55
Fe	1.80	0.24	1.63	0.23	1.83	0.10	1.71	0.15	1.86	0.16	1.72	0.12	1.54	0.18	1.57	0.20
TOT	86.36		83.59		84.33		85.90		90.44		87.70		84.17		83.79	

Sample b

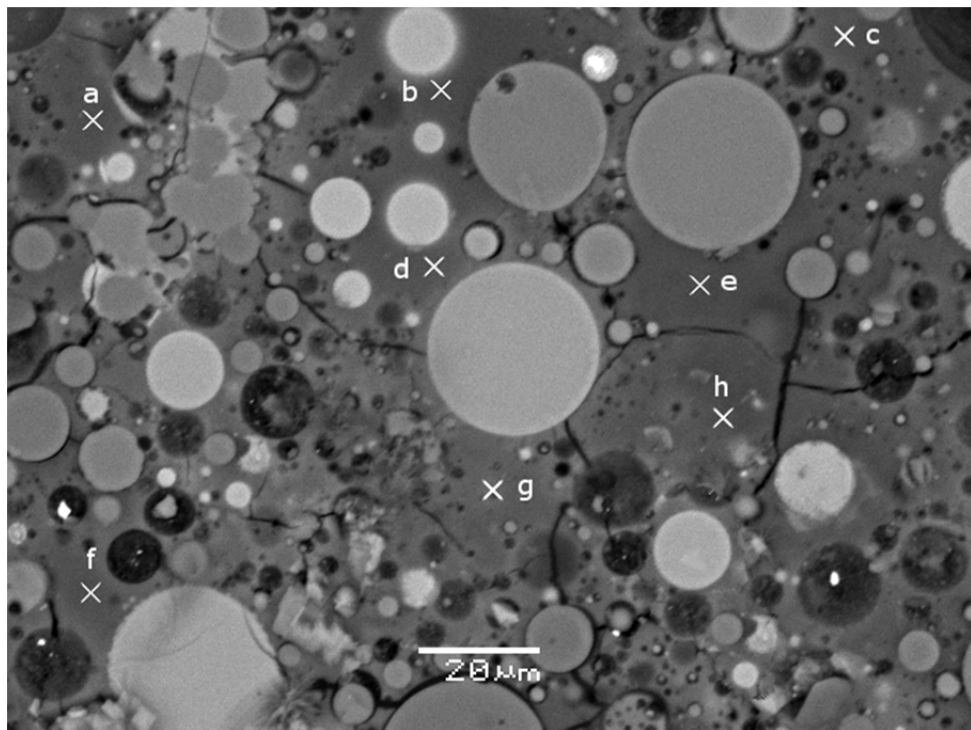
	a		b		c		d		e		f		g		h	
	Element %	σ														
O	41.36	1.06	37.86	1.21	44.05	1.05	42.74	1.19	39.21	1.15	40.57	1.15	38.17	1.14	38.57	0.98
Na	7.59	-0.17	8.12	-0.18	8.02	-0.17	8.33	-0.17	8.22	-0.19	8.83	-0.17	8.96	-0.17	8.73	-0.18
Mg	0.89	0.08	0.93	0.07	0.93	0.06	0.80	0.08	0.92	0.08	0.80	0.11	0.79	0.06	0.82	0.11
Al	6.32	0.12	6.00	0.13	6.56	0.11	5.80	0.11	6.24	0.12	6.47	0.06	5.91	0.07	6.70	0.10
Si	20.12	0.10	19.49	0.07	21.63	0.06	22.30	0.05	21.73	0.13	21.50	0.08	21.05	0.13	19.62	0.05
K	0.32	0.04	0.33	0.07	0.35	0.05	0.32	0.05	0.37	0.07	0.32	0.06	0.38	0.04	0.33	0.07
Ca	7.53	0.18	8.37	0.19	8.08	0.22	7.72	0.21	8.33	0.22	8.52	0.20	7.29	0.30	7.50	0.22
Cd	-0.23	0.19	-0.26	0.15	-0.09	0.15	0.28	0.14	-0.25	0.17	-0.20	0.18	-0.09	0.19	0.04	0.19
Cu	-0.05	0.15	-0.03	0.14	-0.04	0.13	-0.09	0.12	-0.07	0.13	-0.04	0.12	-0.05	0.15	-0.11	0.12
Cr	0.01	0.06	0.03	0.06	0.04	0.07	0.05	0.06	0.07	0.06	0.05	0.06	0.05	0.06	0.02	0.07
Pb	0.06	0.19	0.07	0.18	0.10	0.19	0.02	0.18	0.16	0.17	0.20	0.18	0.09	0.19	0.17	0.17
Zn	-0.67	0.48	-0.33	0.68	0.44	0.68	-0.53	0.56	0.21	0.42	0.65	0.62	-0.29	0.64	-0.49	0.52
Fe	1.58	0.18	1.77	0.19	1.65	0.22	1.84	0.15	1.76	0.22	1.83	0.11	1.70	0.14	1.65	0.15
TOT	84.83		82.35		91.72		89.58		86.90		89.50		83.96		83.55	

SEM-EDS analysis of non-carbonated geopolymers-based s/s zinc sample

Sample a



Sample b



Sample a

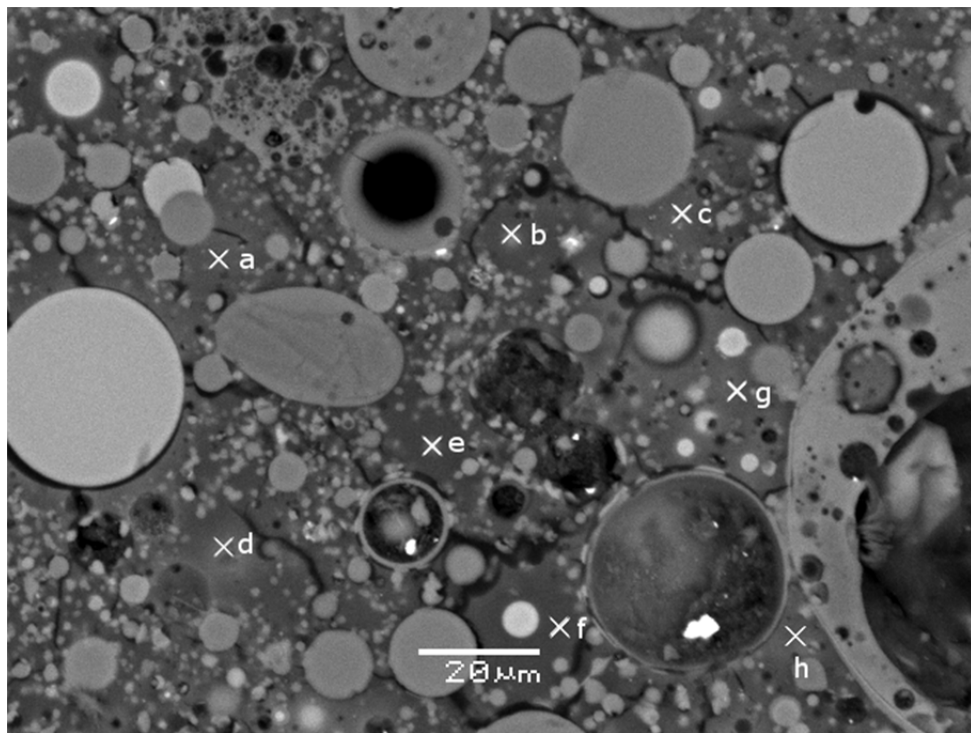
	a		b		c		d		e		f		g		h	
	Element %	σ														
O	42.60	1.20	43.03	1.14	45.28	0.98	39.95	0.99	40.78	0.96	43.69	1.35	43.65	1.23	43.30	0.99
Na	8.19	-0.18	7.63	-0.20	8.44	-0.20	8.51	-0.19	8.03	-0.18	9.02	-0.20	7.88	-0.19	8.59	-0.17
Mg	0.89	0.07	0.82	0.11	0.81	0.06	0.79	0.10	0.92	0.08	0.87	0.10	0.79	0.11	0.92	0.10
Al	6.69	0.09	5.98	0.11	5.88	0.11	6.64	0.07	6.51	0.08	6.66	0.10	6.79	0.08	6.35	0.06
Si	20.78	0.10	20.68	0.13	19.56	0.07	21.72	0.13	23.17	0.05	21.42	0.05	19.96	0.08	20.56	0.13
K	0.35	0.05	0.33	0.06	0.38	0.07	0.33	0.07	0.38	0.05	0.38	0.05	0.33	0.07	0.34	0.05
Ca	8.20	0.21	7.43	0.20	7.45	0.21	7.62	0.29	7.77	0.26	8.27	0.25	7.02	0.18	7.64	0.26
Cd	0.15	0.17	-0.06	0.18	0.06	0.14	0.08	0.14	-0.33	0.14	0.13	0.19	0.17	0.18	-0.15	0.16
Cu	-0.05	0.13	-0.04	0.15	-0.04	0.15	-0.11	0.12	-0.02	0.12	-0.09	0.15	-0.04	0.13	-0.05	0.12
Cr	-0.01	0.07	0.00	0.07	0.07	0.07	0.06	0.07	0.08	0.07	0.03	0.06	0.00	0.06	0.01	0.07
Pb	0.15	0.18	0.34	0.18	0.36	0.18	0.17	0.19	0.14	0.19	0.13	0.18	0.37	0.18	0.24	0.17
Zn	-0.39	0.70	0.60	0.38	-0.70	0.48	0.16	0.60	-0.25	0.43	-0.04	0.65	0.07	0.58	0.50	0.61
Fe	1.67	0.12	1.55	0.20	1.62	0.14	1.69	0.20	1.68	0.10	1.67	0.14	1.84	0.10	1.58	0.24
TOT	89.22		88.29		89.17		87.61		88.86		92.14		88.83		89.83	

Sample b

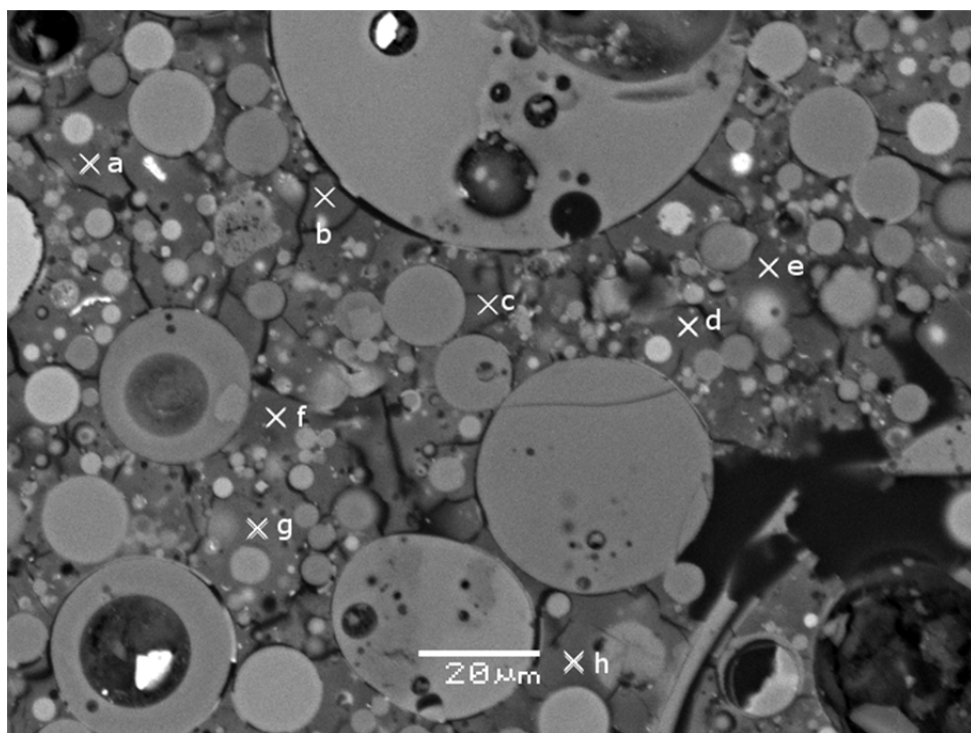
	a		b		c		d		e		f		g		h	
	Element %	σ														
O	42.74	1.39	43.11	1.21	38.85	0.93	43.43	1.14	45.44	1.41	39.16	1.23	39.16	1.14	40.85	1.34
Na	7.79	-0.18	8.79	-0.20	8.57	-0.17	9.02	-0.20	9.25	-0.20	9.20	-0.18	8.82	-0.17	8.70	-0.17
Mg	0.80	0.05	0.93	0.10	0.89	0.06	0.85	0.05	0.80	0.05	0.83	0.11	0.84	0.06	0.83	0.09
Al	6.22	0.07	6.18	0.13	5.82	0.07	6.61	0.12	5.82	0.10	6.45	0.08	6.42	0.12	6.74	0.11
Si	20.04	0.09	23.21	0.06	23.18	0.07	22.12	0.13	22.52	0.07	19.63	0.10	21.24	0.13	19.52	0.07
K	0.35	0.06	0.32	0.05	0.33	0.04	0.36	0.06	0.37	0.04	0.36	0.05	0.32	0.06	0.34	0.05
Ca	7.92	0.28	8.19	0.28	8.00	0.25	8.55	0.24	7.05	0.21	7.39	0.24	7.98	0.27	7.38	0.25
Cd	0.27	0.15	0.13	0.15	0.08	0.19	-0.21	0.15	0.16	0.15	-0.02	0.18	0.19	0.18	-0.07	0.17
Cu	-0.03	0.12	-0.05	0.12	-0.06	0.13	-0.04	0.12	-0.06	0.14	-0.12	0.15	-0.01	0.12	-0.07	0.14
Cr	0.00	0.07	0.00	0.07	0.07	0.06	0.00	0.06	0.03	0.06	0.09	0.06	0.07	0.06	0.01	0.06
Pb	0.26	0.20	0.36	0.20	0.02	0.20	0.05	0.17	0.04	0.19	0.09	0.18	0.37	0.18	0.02	0.17
Zn	-0.74	0.63	-0.26	0.36	-0.30	0.51	0.36	0.44	0.59	0.40	-0.46	0.52	0.57	0.40	-0.59	0.38
Fe	1.64	0.15	1.71	0.14	1.87	0.11	1.74	0.12	1.61	0.13	1.55	0.19	1.87	0.13	1.74	0.25
TOT	87.26		92.62		87.32		92.84		93.62		84.15		87.84		85.40	

SEM-EDS analysis of carbonated geopolymers-based s/s control sample

Sample a



Sample b



Sample a

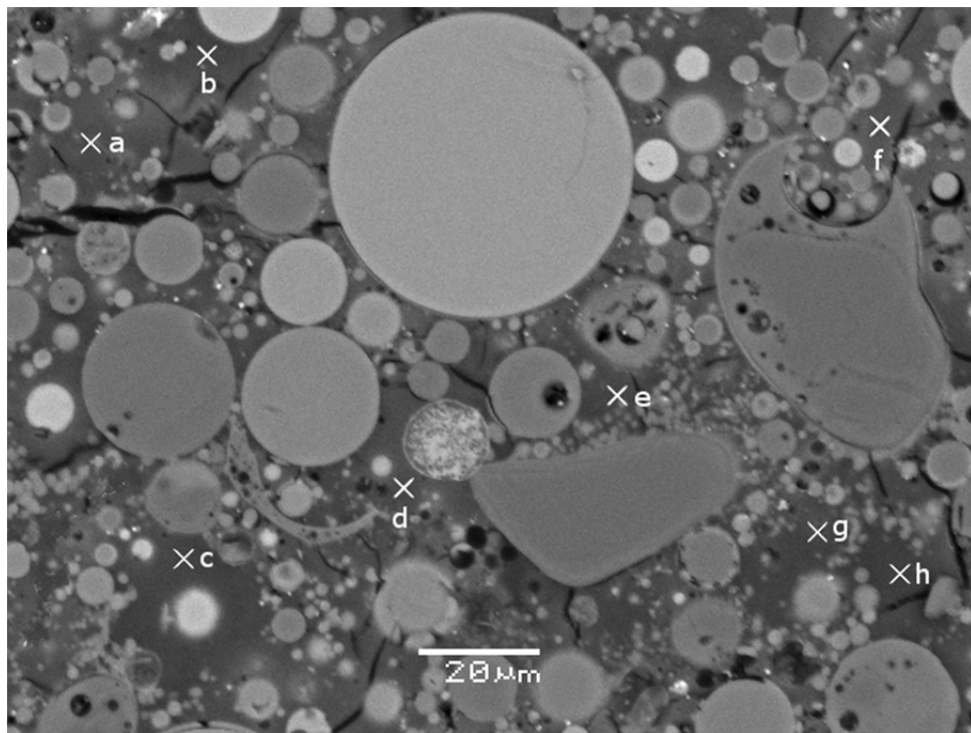
	a		b		c		d		e		f		g		h	
	Element %	σ														
O	34.98	0.91	37.24	1.36	34.34	1.22	34.86	0.87	36.98	1.31	37.18	0.97	39.24	1.29	39.44	1.03
Na	6.61	-0.18	7.62	-0.20	7.53	-0.18	7.04	-0.18	7.51	-0.19	7.37	-0.18	6.62	-0.19	6.55	-0.20
Mg	0.80	0.06	0.82	0.09	0.86	0.07	0.83	0.09	0.93	0.07	0.79	0.11	0.85	0.11	0.84	0.09
Al	6.29	0.08	6.25	0.07	6.06	0.12	6.99	0.07	6.59	0.10	6.52	0.09	6.83	0.13	6.42	0.08
Si	19.76	0.09	19.98	0.08	18.57	0.07	19.82	0.11	21.33	0.09	17.96	0.11	18.39	0.07	20.08	0.09
K	0.28	0.04	0.24	0.07	0.28	0.06	0.25	0.06	0.28	0.07	0.27	0.05	0.25	0.04	0.25	0.06
Ca	8.24	0.26	6.84	0.22	7.59	0.25	7.59	0.29	7.02	0.21	8.04	0.28	7.41	0.28	6.99	0.24
Cd	0.26	0.14	0.35	0.18	-0.05	0.14	-0.29	0.17	0.33	0.19	-0.20	0.17	0.24	0.15	0.01	0.14
Cu	-0.06	0.13	-0.12	0.13	-0.10	0.14	-0.10	0.13	-0.05	0.12	-0.12	0.15	-0.07	0.15	-0.09	0.14
Cr	0.00	0.06	0.00	0.06	0.09	0.06	0.03	0.07	0.00	0.07	0.04	0.07	0.08	0.07	0.04	0.06
Pb	0.03	0.18	0.03	0.19	0.31	0.17	0.02	0.17	0.35	0.20	0.17	0.17	0.28	0.20	0.06	0.19
Zn	-0.52	0.44	-0.26	0.69	0.12	0.45	-0.47	0.37	-0.29	0.69	0.24	0.36	0.35	0.44	-0.58	0.45
Fe	1.44	0.25	1.44	0.23	1.60	0.21	1.48	0.11	1.44	0.25	1.46	0.11	1.48	0.19	1.55	0.15
TOT	78.11		80.43		77.20		78.05		82.42		79.72		81.95		81.56	

Sample b

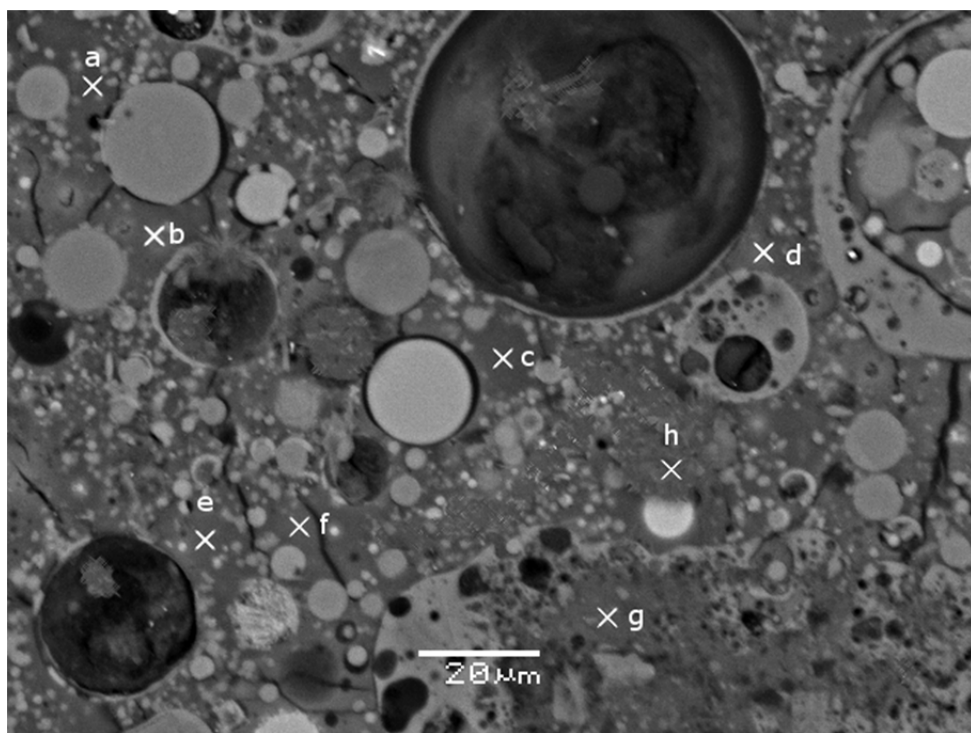
	a		b		c		d		e		f		g		h	
	Element %	σ														
O	39.74	1.22	36.12	1.41	34.15	0.88	37.14	1.02	35.73	0.94	39.35	1.04	35.57	0.94	39.44	0.91
Na	7.16	-0.19	6.47	-0.19	6.93	-0.20	6.67	-0.19	7.38	-0.17	7.02	-0.20	6.57	-0.19	7.40	-0.17
Mg	0.93	0.10	0.80	0.07	0.91	0.10	0.85	0.07	0.85	0.08	0.86	0.09	0.80	0.06	0.86	0.09
Al	6.29	0.11	6.90	0.13	6.05	0.08	6.27	0.08	7.12	0.07	6.88	0.13	6.86	0.10	6.34	0.07
Si	19.92	0.09	18.30	0.06	20.57	0.05	20.14	0.08	21.03	0.06	19.73	0.07	18.33	0.10	20.14	0.12
K	0.27	0.06	0.25	0.06	0.24	0.05	0.24	0.06	0.28	0.06	0.28	0.06	0.27	0.07	0.26	0.06
Ca	7.24	0.28	7.53	0.29	8.26	0.21	7.68	0.25	7.86	0.29	8.24	0.18	8.07	0.18	7.84	0.21
Cd	0.17	0.19	-0.14	0.17	-0.16	0.16	-0.20	0.18	-0.13	0.16	0.01	0.19	-0.08	0.14	-0.21	0.18
Cu	-0.01	0.13	-0.08	0.15	-0.11	0.13	-0.07	0.13	-0.09	0.13	-0.12	0.12	-0.02	0.12	-0.10	0.12
Cr	0.07	0.06	0.04	0.06	0.08	0.07	0.05	0.06	-0.01	0.06	0.03	0.06	-0.01	0.06	0.05	0.06
Pb	0.14	0.20	0.29	0.17	0.09	0.18	0.24	0.18	0.03	0.19	0.05	0.19	0.18	0.19	0.20	0.20
Zn	-0.56	0.42	-0.32	0.37	-0.56	0.43	0.55	0.49	-0.15	0.67	0.13	0.52	0.48	0.36	0.39	0.52
Fe	1.42	0.22	1.53	0.15	1.39	0.23	1.53	0.12	1.43	0.10	1.50	0.10	1.42	0.13	1.42	0.22
TOT	82.78		77.69		77.84		81.09		81.33		83.96		78.44		84.03	

SEM-EDS analysis of carbonated geopolymers-based s/s cadmium sample

Sample a



Sample b



Sample a

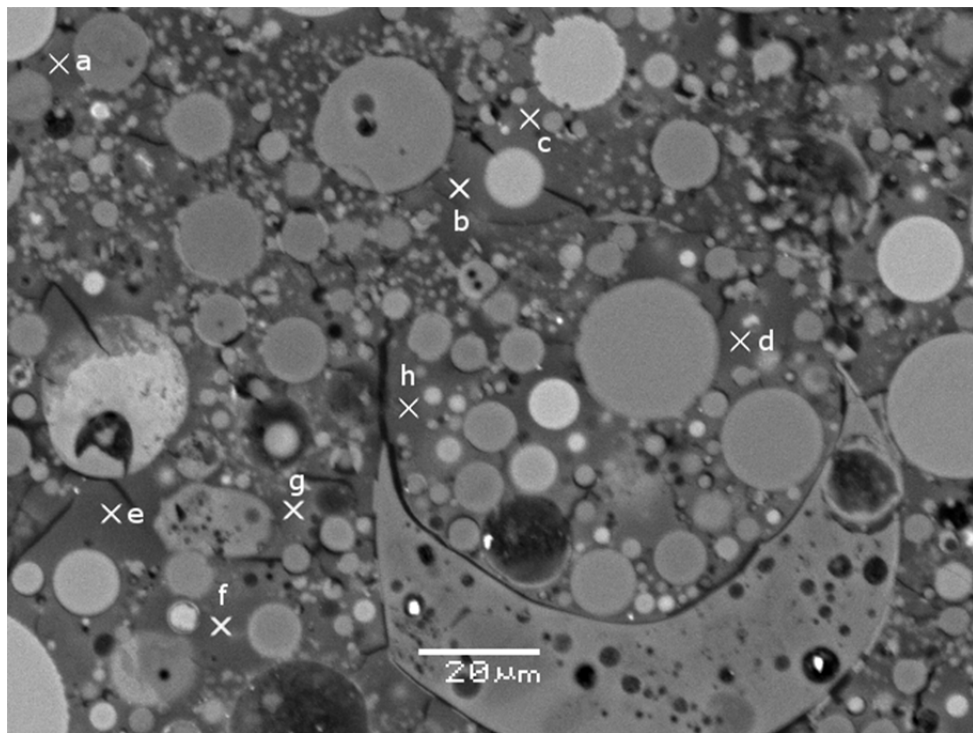
	a		b		c		d		e		f		g		h	
	Element %	σ														
O	35.22	1.33	38.86	1.14	36.18	1.04	34.20	1.06	36.11	0.92	34.83	1.25	40.30	1.09	35.60	1.16
Na	6.85	-0.18	7.46	-0.17	7.21	-0.20	6.75	-0.19	7.50	-0.20	7.21	-0.17	7.41	-0.17	7.33	-0.19
Mg	0.94	0.06	0.87	0.11	0.93	0.06	0.88	0.10	0.93	0.09	0.81	0.10	0.89	0.11	0.84	0.05
Al	7.17	0.10	6.95	0.12	6.29	0.07	6.43	0.07	6.75	0.12	6.83	0.13	6.14	0.13	6.99	0.06
Si	18.38	0.12	21.37	0.07	18.65	0.08	18.12	0.05	19.44	0.08	18.80	0.13	17.95	0.11	20.78	0.07
K	0.24	0.06	0.26	0.06	0.24	0.05	0.27	0.07	0.27	0.06	0.24	0.04	0.28	0.04	0.28	0.04
Ca	7.20	0.21	7.77	0.25	7.36	0.24	7.55	0.25	8.03	0.23	7.44	0.27	7.08	0.19	7.96	0.25
Cd	0.12	0.15	-0.16	0.16	0.17	0.15	0.32	0.14	-0.13	0.19	-0.04	0.19	0.16	0.15	-0.25	0.14
Cu	-0.12	0.15	-0.12	0.12	-0.05	0.12	-0.07	0.13	-0.12	0.15	-0.01	0.13	-0.06	0.15	-0.12	0.13
Cr	0.08	0.07	0.09	0.07	0.00	0.06	0.08	0.06	0.06	0.06	0.07	0.07	0.09	0.06	0.07	0.07
Pb	0.19	0.20	0.01	0.20	0.28	0.19	0.37	0.18	0.21	0.18	0.26	0.18	0.30	0.17	0.00	0.19
Zn	0.12	0.52	-0.73	0.41	0.10	0.43	-0.18	0.67	0.68	0.47	-0.28	0.59	0.07	0.65	-0.43	0.54
Fe	1.54	0.24	1.50	0.12	1.60	0.24	1.62	0.14	1.36	0.10	1.50	0.11	1.41	0.19	1.39	0.13
TOT	77.93		84.13		78.96		76.34		81.09		77.66		82.02		80.44	

Sample b

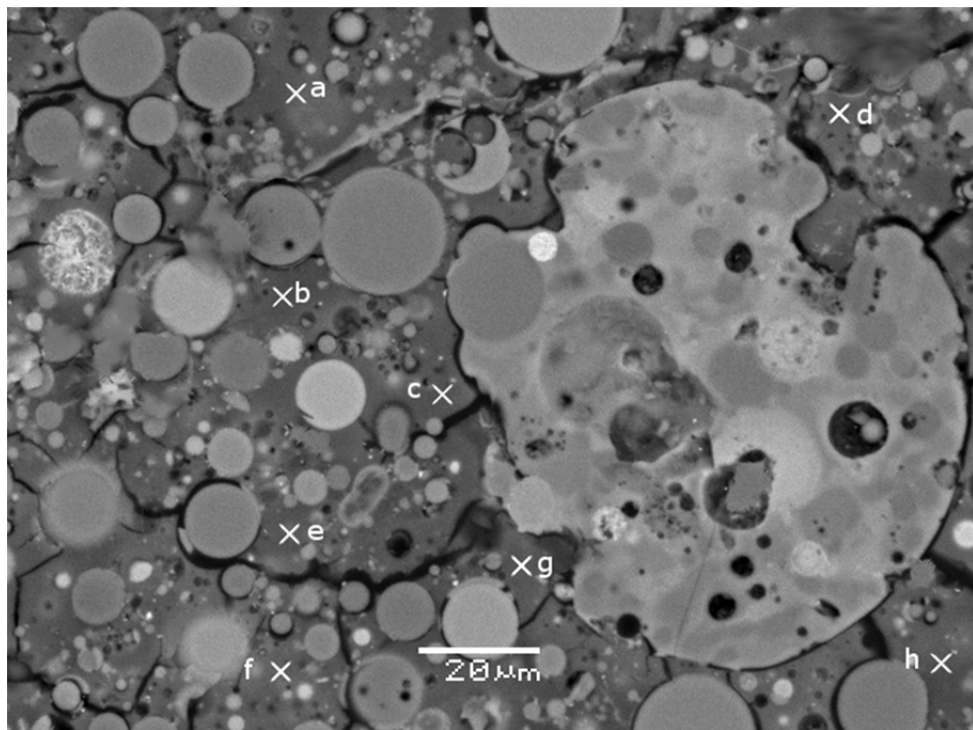
	a		b		c		d		e		f		g		h	
	Element %	σ														
O	34.23	1.04	40.32	1.07	40.74	1.37	40.00	1.15	40.43	1.26	34.45	1.31	39.22	0.90	35.76	1.27
Na	6.87	-0.20	7.57	-0.17	6.81	-0.20	7.28	-0.20	7.75	-0.20	6.46	-0.18	7.74	-0.17	6.84	-0.17
Mg	0.93	0.06	0.89	0.06	0.82	0.07	0.85	0.05	0.87	0.11	0.93	0.07	0.88	0.11	0.81	0.07
Al	7.06	0.09	6.19	0.08	6.09	0.12	5.97	0.06	6.90	0.08	6.19	0.10	6.06	0.10	6.82	0.10
Si	19.05	0.05	21.43	0.10	18.53	0.13	18.74	0.10	19.52	0.10	20.91	0.09	19.61	0.11	20.03	0.08
K	0.27	0.04	0.25	0.06	0.24	0.04	0.27	0.06	0.27	0.04	0.25	0.06	0.25	0.07	0.28	0.07
Ca	7.01	0.21	6.82	0.20	7.62	0.23	7.16	0.20	7.57	0.26	7.47	0.28	7.60	0.20	7.30	0.30
Cd	-0.04	0.14	0.10	0.19	-0.13	0.19	-0.11	0.14	-0.30	0.19	-0.09	0.15	-0.15	0.14	0.31	0.18
Cu	-0.12	0.15	-0.08	0.12	-0.06	0.13	-0.12	0.12	-0.01	0.15	-0.10	0.13	-0.12	0.14	-0.01	0.13
Cr	0.04	0.06	0.00	0.06	0.04	0.07	0.08	0.07	0.00	0.07	0.06	0.07	0.04	0.06	0.00	0.06
Pb	0.29	0.19	0.23	0.17	0.19	0.19	0.26	0.17	0.16	0.18	0.04	0.20	0.03	0.17	0.04	0.17
Zn	0.08	0.63	0.17	0.63	-0.03	0.44	-0.78	0.66	0.59	0.46	-0.67	0.66	-0.37	0.51	0.03	0.50
Fe	1.40	0.18	1.41	0.25	1.38	0.13	1.41	0.24	1.58	0.18	1.48	0.11	1.36	0.18	1.41	0.16
TOT	77.07		85.30		82.24		81.01		85.33		77.38		82.15		79.62	

SEM-EDS analysis of carbonated geopolymers-based s/s chromium (III) sample

Sample a



Sample b



Sample a

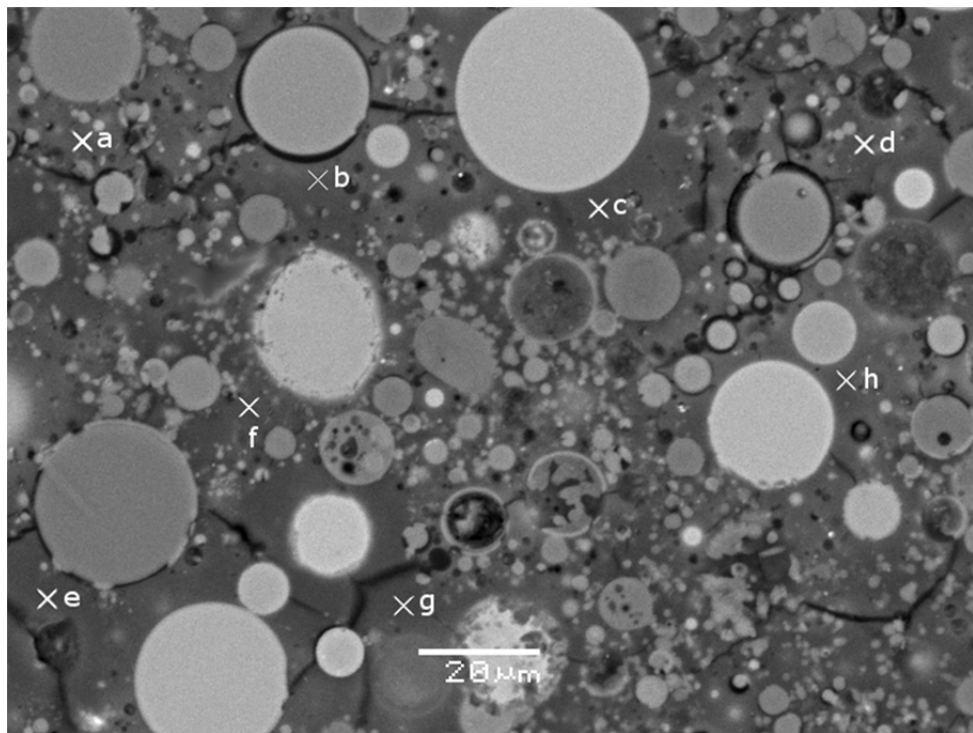
	a		b		c		d		e		f		g		h	
	Element %	σ														
O	40.43	0.90	40.10	1.08	34.52	0.91	34.98	0.99	35.85	1.34	34.49	1.42	39.19	1.32	35.42	1.05
Na	7.62	-0.20	6.68	-0.20	7.63	-0.20	7.65	-0.20	6.70	-0.19	6.68	-0.19	6.97	-0.17	7.43	-0.17
Mg	0.83	0.05	0.94	0.08	0.90	0.10	0.94	0.06	0.94	0.10	0.91	0.05	0.80	0.05	0.81	0.08
Al	7.20	0.13	7.17	0.12	6.59	0.08	6.62	0.10	6.98	0.08	7.03	0.08	6.44	0.07	7.15	0.12
Si	20.78	0.12	21.08	0.13	17.72	0.10	17.82	0.11	20.97	0.07	21.16	0.13	20.95	0.13	18.08	0.11
K	0.24	0.06	0.24	0.06	0.27	0.05	0.28	0.05	0.28	0.06	0.27	0.04	0.27	0.05	0.27	0.05
Ca	8.28	0.26	7.44	0.27	8.15	0.19	7.91	0.28	7.51	0.23	7.08	0.25	7.11	0.23	8.21	0.18
Cd	-0.07	0.18	0.04	0.16	0.05	0.19	-0.27	0.19	0.34	0.15	-0.02	0.18	0.21	0.18	-0.11	0.14
Cu	-0.12	0.15	-0.01	0.14	-0.06	0.12	-0.05	0.12	-0.01	0.13	-0.06	0.15	-0.09	0.12	-0.03	0.13
Cr	0.04	0.07	0.00	0.07	0.00	0.06	0.06	0.07	0.05	0.06	0.05	0.06	0.08	0.07	0.05	0.06
Pb	0.14	0.18	0.16	0.20	0.06	0.20	0.32	0.17	0.12	0.18	0.19	0.17	0.12	0.17	0.38	0.19
Zn	-0.53	0.36	-0.15	0.64	0.55	0.51	0.51	0.55	0.11	0.53	-0.40	0.66	-0.35	0.51	0.10	0.36
Fe	1.37	0.12	1.51	0.20	1.44	0.22	1.57	0.14	1.34	0.10	1.55	0.17	1.38	0.25	1.56	0.15
TOT	86.21		85.20		77.82		78.34		81.18		78.93		83.08		79.32	

Sample b

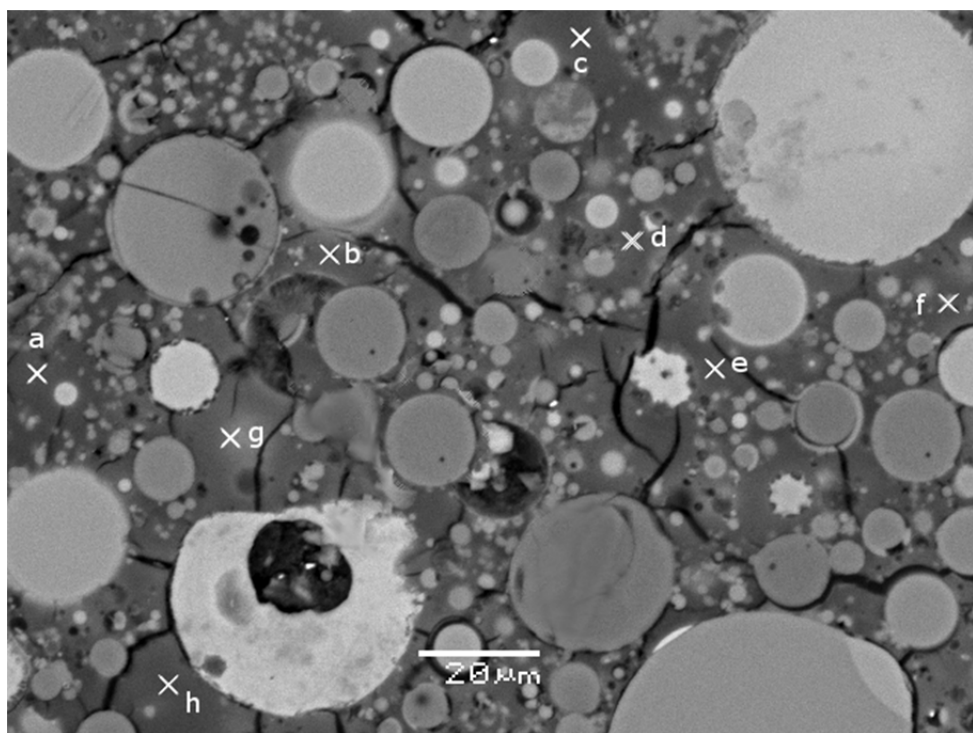
	a		b		c		d		e		f		g		h	
	Element %	σ														
O	38.17	0.89	34.50	1.23	41.59	1.31	35.50	1.41	35.42	1.27	39.47	0.90	40.67	1.18	38.39	0.93
Na	7.09	-0.19	7.58	-0.17	7.35	-0.19	7.46	-0.18	7.65	-0.18	7.47	-0.18	6.64	-0.19	6.77	-0.19
Mg	0.88	0.08	0.81	0.08	0.88	0.07	0.78	0.06	0.93	0.05	0.84	0.10	0.94	0.10	0.87	0.10
Al	6.19	0.11	6.79	0.06	6.14	0.09	6.75	0.13	6.78	0.10	6.48	0.11	6.28	0.06	6.14	0.08
Si	18.08	0.06	19.19	0.11	19.36	0.10	20.40	0.05	19.41	0.08	20.90	0.07	17.89	0.11	20.03	0.09
K	0.26	0.05	0.28	0.07	0.24	0.07	0.24	0.07	0.25	0.07	0.25	0.07	0.26	0.05	0.26	0.06
Ca	7.33	0.28	7.47	0.28	7.98	0.27	8.15	0.26	7.18	0.25	8.00	0.28	6.94	0.19	8.14	0.29
Cd	0.23	0.15	-0.16	0.17	0.10	0.19	0.14	0.16	-0.26	0.16	-0.05	0.17	-0.13	0.16	-0.19	0.14
Cu	-0.02	0.13	-0.07	0.14	-0.04	0.14	-0.11	0.14	-0.06	0.12	-0.08	0.13	-0.01	0.14	-0.01	0.14
Cr	0.04	0.06	0.01	0.06	0.00	0.07	0.06	0.07	0.09	0.07	0.06	0.07	0.05	0.07	0.06	0.06
Pb	0.14	0.20	0.30	0.18	0.16	0.18	0.25	0.20	0.35	0.19	0.06	0.18	0.35	0.17	0.33	0.17
Zn	0.10	0.42	0.00	0.44	-0.22	0.61	0.65	0.67	0.39	0.69	-0.39	0.51	-0.49	0.55	-0.74	0.63
Fe	1.54	0.17	1.60	0.19	1.40	0.21	1.47	0.18	1.41	0.19	1.52	0.11	1.54	0.23	1.41	0.22
TOT	80.03		78.30		84.94		81.74		79.54		84.53		80.93		81.46	

SEM-EDS analysis of carbonated geopolymers-based s/s chromium (VI) sample

Sample a



Sample b



Sample a

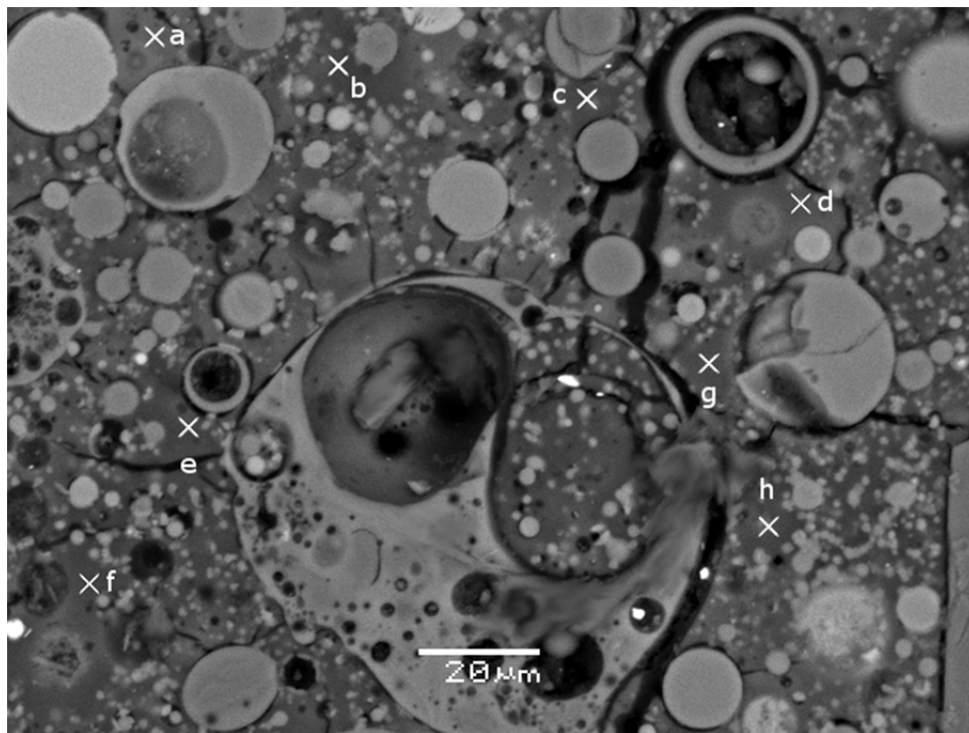
	a		b		c		d		e		f		g		h	
	Element %	σ														
O	41.18	1.24	34.66	0.94	41.37	0.90	36.18	1.39	34.63	0.87	39.28	0.86	35.51	1.39	36.35	1.08
Na	6.80	-0.20	7.05	-0.18	6.93	-0.20	6.68	-0.20	7.59	-0.20	7.18	-0.17	6.62	-0.18	7.20	-0.17
Mg	0.83	0.06	0.84	0.07	0.93	0.09	0.80	0.10	0.92	0.09	0.85	0.11	0.94	0.07	0.82	0.09
Al	6.32	0.07	6.73	0.12	6.51	0.08	6.65	0.11	6.81	0.11	7.07	0.13	6.12	0.09	6.27	0.13
Si	19.98	0.05	18.52	0.05	18.34	0.07	20.22	0.13	17.98	0.05	21.35	0.08	20.94	0.10	18.15	0.09
K	0.28	0.07	0.24	0.07	0.24	0.05	0.24	0.04	0.28	0.05	0.25	0.06	0.27	0.05	0.27	0.07
Ca	7.66	0.24	6.96	0.26	7.25	0.22	7.91	0.30	7.91	0.25	6.81	0.23	8.10	0.24	8.26	0.28
Cd	0.31	0.16	0.06	0.16	-0.24	0.14	0.06	0.18	-0.18	0.19	-0.13	0.15	0.03	0.16	-0.12	0.16
Cu	-0.11	0.14	-0.01	0.14	-0.07	0.12	-0.12	0.13	-0.01	0.15	-0.04	0.15	-0.08	0.13	-0.04	0.13
Cr	0.09	0.06	0.08	0.07	0.01	0.07	0.08	0.06	0.03	0.06	0.00	0.06	0.01	0.07	0.02	0.06
Pb	0.21	0.17	0.38	0.20	0.12	0.18	0.25	0.17	0.25	0.18	0.06	0.18	0.05	0.20	0.23	0.17
Zn	-0.21	0.49	0.58	0.57	-0.60	0.42	-0.59	0.51	-0.12	0.38	-0.65	0.64	0.65	0.53	-0.10	0.48
Fe	1.59	0.23	1.57	0.10	1.60	0.25	1.38	0.21	1.34	0.19	1.61	0.13	1.49	0.18	1.39	0.14
TOT	84.93		77.66		82.39		79.74		77.43		83.64		80.65		78.70	

Sample b

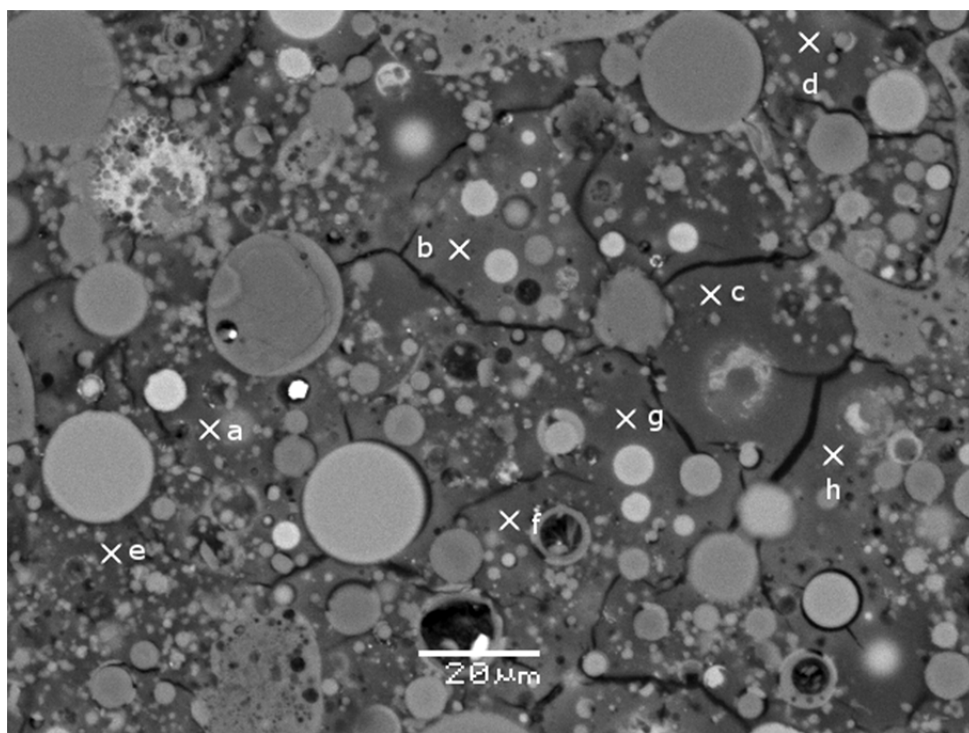
	a		b		c		d		e		f		g		h	
	Element %	σ														
O	41.67	0.92	35.57	1.30	34.72	1.35	34.92	1.38	40.32	1.01	36.50	1.09	39.41	1.38	37.72	1.06
Na	6.50	-0.19	6.73	-0.18	6.69	-0.20	7.36	-0.18	7.65	-0.18	7.41	-0.20	6.97	-0.19	7.54	-0.18
Mg	0.94	0.07	0.93	0.05	0.84	0.11	0.93	0.09	0.93	0.05	0.92	0.11	0.79	0.09	0.87	0.08
Al	6.74	0.11	6.06	0.08	6.46	0.11	6.22	0.13	6.65	0.11	6.68	0.11	6.87	0.13	6.80	0.13
Si	20.69	0.06	18.89	0.06	18.54	0.08	19.51	0.13	21.19	0.11	20.41	0.08	20.45	0.13	19.98	0.10
K	0.27	0.07	0.25	0.07	0.28	0.05	0.26	0.04	0.26	0.07	0.24	0.06	0.26	0.06	0.26	0.06
Ca	7.50	0.18	6.86	0.18	8.28	0.26	7.50	0.24	6.89	0.22	8.29	0.19	7.49	0.22	8.09	0.24
Cd	-0.18	0.14	-0.15	0.16	0.12	0.16	-0.01	0.15	0.21	0.14	-0.32	0.17	0.06	0.19	0.16	0.17
Cu	-0.03	0.14	-0.11	0.13	-0.12	0.14	-0.07	0.13	-0.11	0.14	-0.05	0.14	-0.10	0.12	-0.03	0.13
Cr	0.00	0.07	0.07	0.07	0.08	0.06	0.01	0.07	0.04	0.06	0.05	0.06	0.05	0.06	0.08	0.07
Pb	0.34	0.18	0.28	0.17	0.27	0.18	0.10	0.20	0.38	0.18	0.06	0.17	0.31	0.17	0.09	0.18
Zn	0.15	0.64	-0.44	0.60	-0.17	0.61	0.47	0.57	0.41	0.63	-0.23	0.62	-0.26	0.37	-0.20	0.42
Fe	1.58	0.14	1.38	0.22	1.58	0.23	1.37	0.12	1.57	0.20	1.39	0.22	1.59	0.20	1.52	0.13
TOT	86.17		76.32		77.57		78.57		86.39		81.35		83.89		82.88	

SEM-EDS analysis of carbonated geopolymers-based s/s copper sample

Sample a



Sample b



Sample a

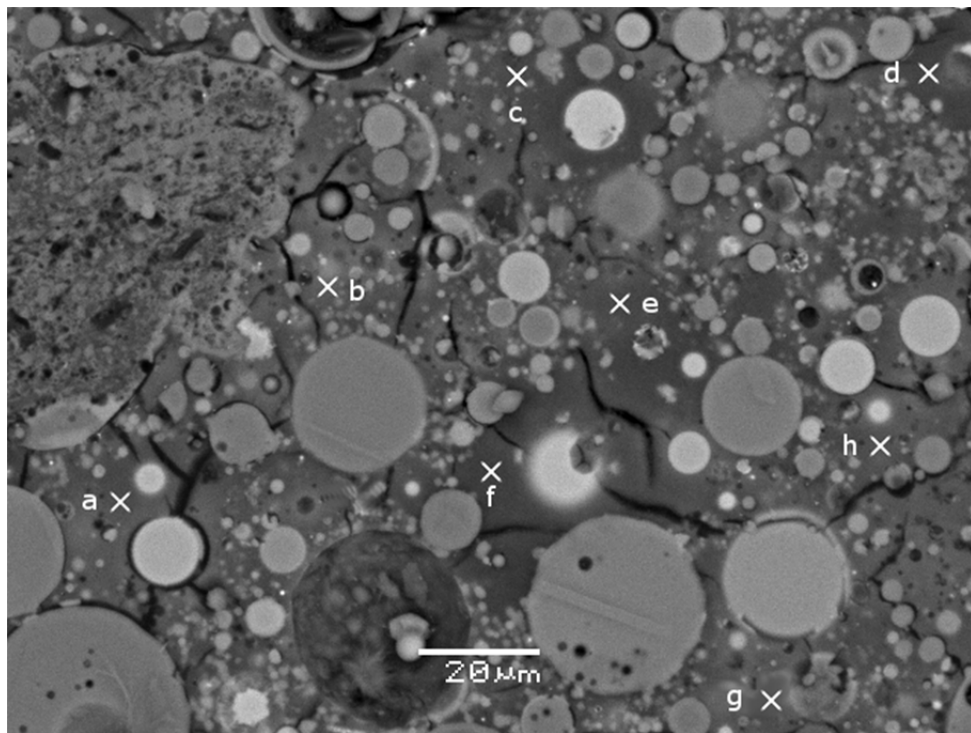
	a		b		c		d		e		f		g		h	
	Element %	σ														
O	41.08	0.98	34.15	1.31	40.86	1.19	40.85	1.09	39.68	1.11	35.44	0.98	35.20	1.10	41.31	1.16
Na	7.67	-0.17	7.67	-0.19	6.42	-0.18	7.05	-0.20	6.50	-0.17	7.18	-0.18	6.65	-0.17	6.51	-0.19
Mg	0.84	0.08	0.94	0.08	0.83	0.07	0.89	0.08	0.80	0.11	0.85	0.06	0.80	0.08	0.80	0.10
Al	6.55	0.06	7.17	0.07	6.61	0.06	6.67	0.10	7.04	0.12	5.92	0.12	7.21	0.07	6.75	0.08
Si	19.31	0.05	17.95	0.06	20.81	0.05	17.94	0.08	21.34	0.08	19.55	0.12	20.30	0.11	17.96	0.12
K	0.24	0.05	0.28	0.07	0.27	0.07	0.24	0.07	0.24	0.06	0.24	0.05	0.26	0.04	0.26	0.06
Ca	7.77	0.30	8.21	0.21	7.27	0.28	7.29	0.29	7.51	0.22	7.04	0.27	7.45	0.25	6.95	0.25
Cd	-0.03	0.19	0.12	0.16	0.28	0.18	-0.14	0.16	0.28	0.15	-0.03	0.16	0.10	0.16	-0.08	0.16
Cu	-0.12	0.15	-0.03	0.14	-0.08	0.12	-0.09	0.12	-0.11	0.12	-0.11	0.15	-0.12	0.14	-0.01	0.12
Cr	0.04	0.06	0.00	0.06	0.06	0.06	0.06	0.06	0.05	0.07	0.08	0.07	0.00	0.07	0.06	0.07
Pb	0.00	0.18	0.01	0.18	0.18	0.18	0.12	0.17	0.05	0.18	0.23	0.18	0.14	0.18	0.19	0.18
Zn	0.20	0.69	0.35	0.55	-0.16	0.42	0.49	0.45	-0.29	0.42	-0.12	0.39	0.08	0.67	0.16	0.53
Fe	1.53	0.25	1.60	0.17	1.49	0.10	1.38	0.24	1.39	0.23	1.46	0.16	1.56	0.11	1.57	0.15
TOT	85.08		78.42		84.84		82.75		84.48		77.73		79.63		82.43	

Sample b

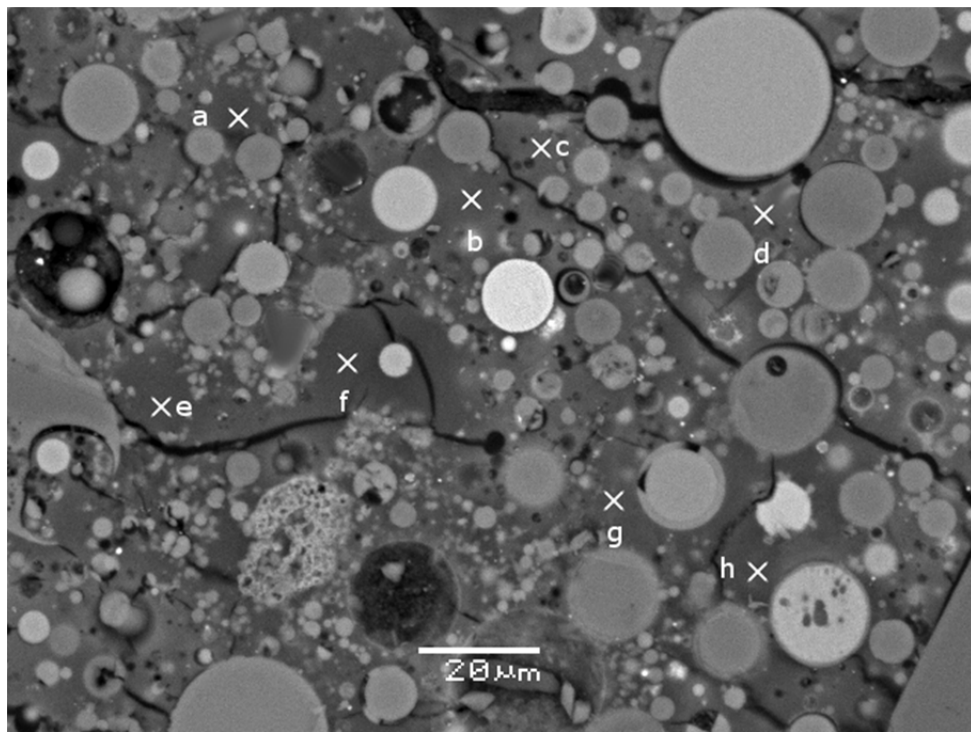
	a		b		c		d		e		f		g		h	
	Element %	σ														
O	34.49	1.31	41.27	1.24	38.97	1.43	37.15	1.25	40.68	1.20	35.01	1.18	40.00	1.30	37.50	1.18
Na	7.10	-0.17	7.13	-0.20	6.99	-0.20	7.30	-0.18	7.40	-0.18	6.82	-0.17	7.62	-0.20	7.49	-0.20
Mg	0.81	0.06	0.79	0.08	0.81	0.11	0.88	0.08	0.87	0.06	0.83	0.06	0.81	0.09	0.93	0.09
Al	6.48	0.10	6.92	0.10	7.09	0.13	7.21	0.06	7.09	0.06	5.98	0.13	7.06	0.06	5.93	0.10
Si	18.58	0.13	20.98	0.10	19.79	0.08	18.90	0.07	21.56	0.06	20.78	0.09	21.57	0.13	19.37	0.10
K	0.28	0.05	0.24	0.06	0.26	0.05	0.28	0.05	0.26	0.04	0.24	0.04	0.28	0.07	0.24	0.06
Ca	6.94	0.18	7.28	0.30	7.48	0.18	7.03	0.22	7.24	0.28	7.85	0.23	7.50	0.28	7.43	0.27
Cd	0.32	0.18	0.25	0.19	-0.08	0.16	0.12	0.16	-0.33	0.14	0.12	0.19	0.19	0.18	0.10	0.19
Cu	-0.07	0.12	-0.01	0.12	-0.02	0.15	-0.09	0.13	-0.10	0.13	-0.08	0.13	-0.04	0.13	-0.08	0.15
Cr	-0.01	0.07	0.06	0.07	0.09	0.07	0.04	0.06	0.01	0.07	0.04	0.07	0.00	0.07	0.01	0.06
Pb	0.24	0.17	0.33	0.17	0.34	0.19	0.30	0.19	0.31	0.20	0.00	0.18	0.28	0.18	0.01	0.20
Zn	-0.53	0.36	0.60	0.47	0.65	0.43	-0.64	0.55	0.35	0.61	-0.40	0.56	0.34	0.65	0.04	0.45
Fe	1.47	0.20	1.56	0.14	1.57	0.21	1.52	0.25	1.59	0.17	1.58	0.22	1.38	0.12	1.41	0.10
TOT	76.10		87.40		83.94		80.00		86.93		78.77		86.99		80.38	

SEM-EDS analysis of carbonated geopolymers-based s/s lead sample

Sample a



Sample b



Sample a

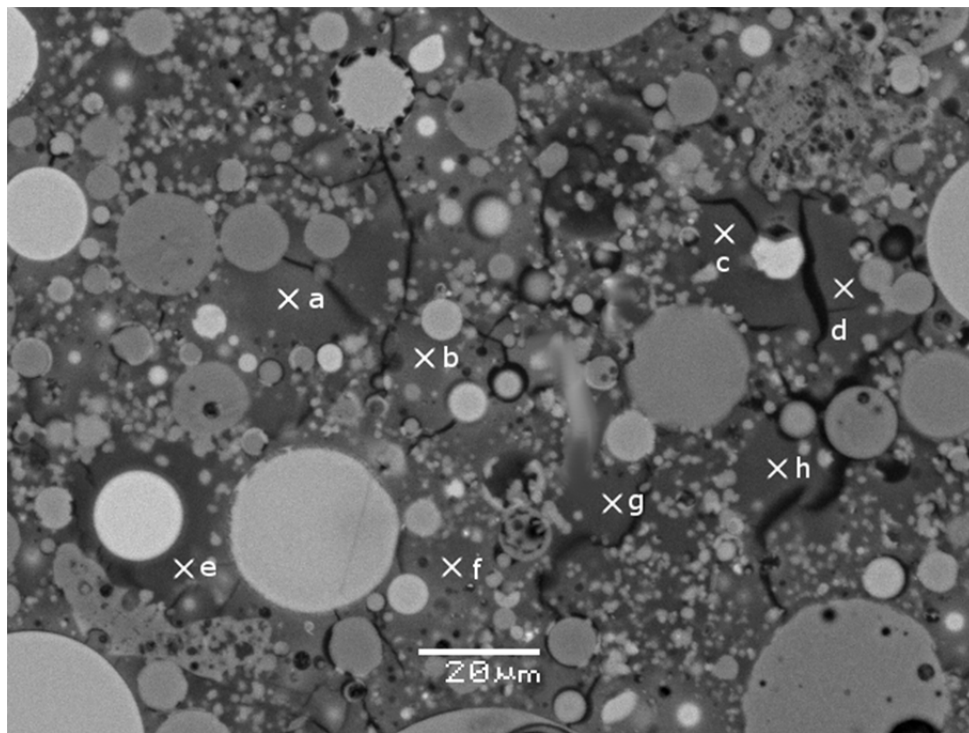
	a		b		c		d		e		f		g		h	
	Element %	σ														
O	38.23	1.31	39.40	1.04	37.98	1.31	37.59	1.08	41.11	1.02	38.30	1.30	34.20	1.19	36.05	1.16
Na	7.39	-0.19	7.41	-0.19	6.84	-0.18	6.54	-0.20	6.71	-0.20	6.89	-0.17	6.88	-0.20	7.74	-0.17
Mg	0.81	0.06	0.88	0.05	0.94	0.10	0.94	0.09	0.86	0.05	0.94	0.07	0.94	0.06	0.93	0.07
Al	6.25	0.10	6.54	0.13	7.17	0.07	6.42	0.10	6.92	0.06	6.13	0.06	6.62	0.09	6.96	0.07
Si	17.70	0.07	21.39	0.12	20.33	0.07	19.77	0.06	18.89	0.09	20.71	0.13	21.56	0.12	19.27	0.12
K	0.28	0.05	0.26	0.07	0.27	0.06	0.28	0.04	0.27	0.05	0.24	0.04	0.27	0.05	0.27	0.06
Ca	7.48	0.29	8.20	0.20	6.90	0.24	7.49	0.22	7.44	0.23	7.23	0.30	7.81	0.24	7.19	0.20
Cd	0.07	0.16	0.03	0.16	0.18	0.17	0.04	0.15	-0.14	0.16	-0.34	0.16	-0.31	0.18	0.05	0.16
Cu	-0.05	0.14	-0.03	0.14	-0.07	0.14	-0.11	0.14	-0.12	0.12	-0.10	0.13	-0.09	0.15	-0.06	0.13
Cr	-0.01	0.06	-0.01	0.06	0.09	0.07	0.00	0.07	0.03	0.06	0.09	0.07	0.03	0.07	0.09	0.06
Pb	0.19	0.17	0.32	0.19	0.18	0.20	0.16	0.20	0.24	0.20	0.12	0.19	0.19	0.20	0.29	0.17
Zn	-0.73	0.43	0.57	0.40	-0.37	0.69	0.37	0.46	0.57	0.66	0.65	0.49	0.57	0.46	0.32	0.49
Fe	1.43	0.15	1.48	0.15	1.38	0.16	1.52	0.23	1.35	0.11	1.43	0.25	1.39	0.18	1.58	0.13
TOT	79.04		86.44		81.82		81.01		84.13		82.29		80.06		80.68	

Sample b

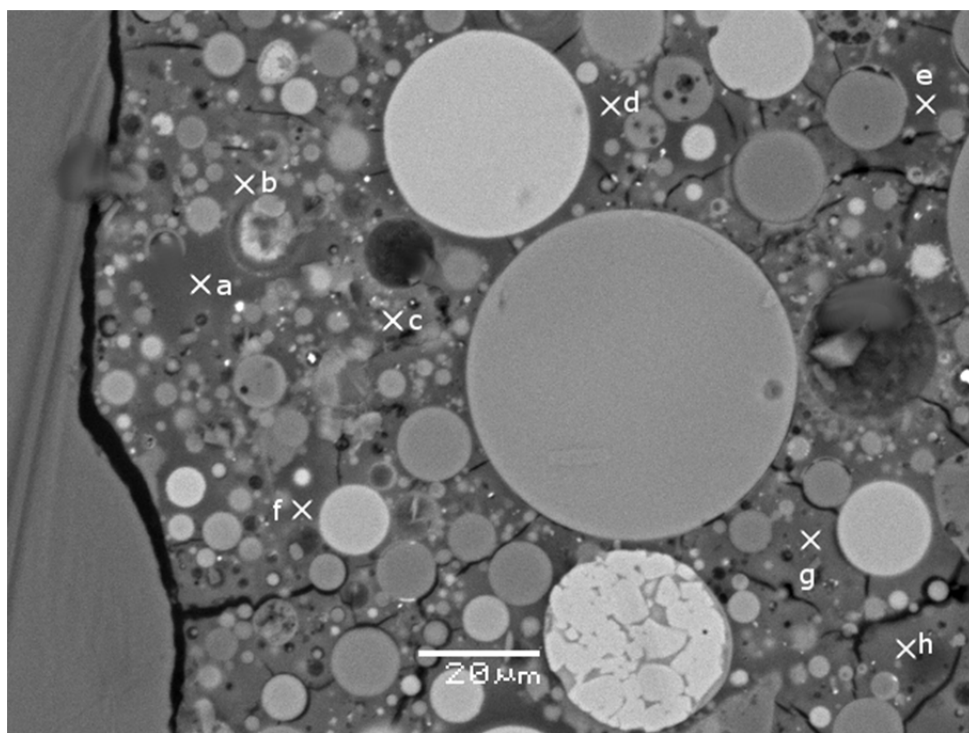
	a		b		c		d		e		f		g		h	
	Element %	σ														
O	39.93	1.10	40.32	1.21	38.22	1.17	37.19	1.08	37.10	0.88	35.79	1.21	36.80	1.35	36.29	0.92
Na	7.03	-0.17	7.09	-0.20	7.37	-0.17	7.49	-0.18	7.10	-0.20	7.71	-0.20	7.55	-0.19	7.45	-0.19
Mg	0.81	0.07	0.80	0.05	0.92	0.05	0.82	0.07	0.80	0.08	0.83	0.07	0.90	0.05	0.90	0.09
Al	7.18	0.09	7.07	0.12	6.28	0.08	7.17	0.09	6.42	0.12	6.14	0.13	6.68	0.10	6.87	0.06
Si	20.55	0.11	18.93	0.10	18.86	0.10	20.54	0.05	20.42	0.07	18.72	0.12	18.31	0.05	21.57	0.09
K	0.24	0.06	0.27	0.07	0.28	0.06	0.27	0.05	0.28	0.06	0.27	0.07	0.27	0.07	0.27	0.05
Ca	7.88	0.24	7.32	0.24	7.72	0.21	7.23	0.26	7.28	0.29	7.00	0.22	8.05	0.30	7.59	0.21
Cd	0.08	0.18	0.31	0.16	0.08	0.18	0.31	0.18	0.20	0.15	0.05	0.16	0.33	0.19	0.02	0.18
Cu	-0.06	0.12	-0.12	0.12	-0.11	0.15	-0.10	0.13	-0.08	0.14	-0.12	0.14	-0.11	0.12	-0.10	0.12
Cr	0.04	0.07	0.02	0.07	0.02	0.07	0.09	0.06	0.03	0.07	0.01	0.06	0.09	0.07	0.07	0.07
Pb	0.35	0.18	0.29	0.20	0.20	0.19	0.33	0.18	0.17	0.20	0.09	0.20	0.01	0.19	0.12	0.20
Zn	0.17	0.65	-0.17	0.58	-0.70	0.41	-0.20	0.51	0.61	0.67	0.65	0.67	0.31	0.50	-0.12	0.55
Fe	1.57	0.12	1.47	0.12	1.39	0.19	1.51	0.20	1.41	0.20	1.47	0.23	1.41	0.14	1.55	0.16
TOT	85.77		83.60		80.53		82.65		81.74		78.61		80.60		82.48	

SEM-EDS analysis of carbonated geopolymers-based s/s zinc sample

Sample a



Sample b



Sample a

	a		b		c		d		e		f		g		h	
	Element %	σ														
O	39.72	1.09	41.54	1.01	40.00	0.89	35.02	0.94	40.02	1.09	35.13	1.22	34.69	1.10	35.66	1.32
Na	7.74	-0.19	7.13	-0.19	7.29	-0.19	7.26	-0.19	7.13	-0.19	6.76	-0.20	7.02	-0.20	7.03	-0.18
Mg	0.92	0.05	0.80	0.07	0.93	0.10	0.92	0.11	0.82	0.11	0.84	0.10	0.88	0.11	0.85	0.05
Al	6.58	0.11	6.15	0.06	6.77	0.07	6.10	0.09	7.08	0.08	6.24	0.07	5.91	0.10	7.16	0.08
Si	20.01	0.06	20.47	0.12	21.28	0.08	21.54	0.11	19.54	0.12	19.59	0.09	18.70	0.05	19.84	0.13
K	0.27	0.06	0.25	0.06	0.25	0.06	0.28	0.07	0.24	0.06	0.25	0.04	0.25	0.05	0.28	0.05
Ca	7.39	0.18	7.63	0.29	7.40	0.23	7.65	0.27	7.56	0.19	8.21	0.21	8.05	0.29	6.85	0.21
Cd	0.21	0.14	-0.28	0.19	-0.09	0.14	0.14	0.18	-0.29	0.16	-0.07	0.15	0.08	0.16	0.16	0.14
Cu	-0.11	0.13	-0.01	0.13	-0.04	0.12	-0.09	0.14	-0.08	0.14	-0.08	0.15	-0.07	0.15	-0.12	0.15
Cr	0.04	0.06	0.08	0.07	0.08	0.07	-0.01	0.06	0.05	0.07	-0.01	0.07	0.08	0.07	0.09	0.06
Pb	0.18	0.18	0.05	0.20	0.20	0.19	0.13	0.17	0.33	0.19	0.01	0.17	0.08	0.19	0.21	0.20
Zn	-0.47	0.61	-0.54	0.44	-0.39	0.69	0.10	0.51	0.07	0.36	0.04	0.59	-0.60	0.68	0.15	0.64
Fe	1.56	0.18	1.53	0.15	1.58	0.13	1.37	0.13	1.50	0.24	1.47	0.15	1.49	0.22	1.45	0.13
TOT	84.04		84.80		85.26		80.41		83.97		78.38		76.56		79.61	

Sample b

	a		b		c		d		e		f		g		h	
	Element %	σ														
O	35.54	1.05	37.32	1.44	34.99	0.87	39.19	1.06	40.46	1.28	39.31	0.95	40.49	1.04	40.03	1.31
Na	6.46	-0.20	7.66	-0.19	6.58	-0.20	7.58	-0.18	7.48	-0.18	7.46	-0.19	7.04	-0.17	7.51	-0.20
Mg	0.84	0.05	0.94	0.05	0.79	0.05	0.80	0.05	0.83	0.08	0.89	0.07	0.78	0.11	0.79	0.05
Al	6.62	0.13	6.82	0.07	5.92	0.12	7.12	0.13	6.58	0.06	6.59	0.13	6.84	0.07	6.34	0.08
Si	19.58	0.13	21.56	0.10	18.91	0.08	20.04	0.06	18.42	0.11	19.73	0.07	20.87	0.12	19.22	0.08
K	0.24	0.04	0.28	0.06	0.25	0.05	0.24	0.04	0.25	0.07	0.25	0.07	0.26	0.04	0.26	0.06
Ca	6.85	0.30	7.24	0.24	8.28	0.23	7.43	0.21	8.14	0.22	7.08	0.25	8.23	0.24	8.10	0.19
Cd	0.00	0.14	-0.20	0.15	0.19	0.14	-0.20	0.18	-0.03	0.17	0.33	0.14	0.35	0.15	0.11	0.14
Cu	-0.08	0.13	-0.04	0.14	-0.09	0.12	-0.07	0.14	-0.12	0.13	-0.04	0.14	-0.02	0.13	-0.05	0.14
Cr	0.05	0.07	0.07	0.07	0.09	0.07	0.04	0.07	0.04	0.06	0.08	0.06	0.04	0.06	0.02	0.06
Pb	0.21	0.20	0.18	0.20	0.18	0.17	0.23	0.17	0.07	0.20	0.19	0.20	0.13	0.18	0.15	0.20
Zn	0.51	0.38	0.24	0.47	-0.33	0.39	0.11	0.62	-0.37	0.48	-0.36	0.70	-0.75	0.46	0.11	0.41
Fe	1.34	0.24	1.56	0.16	1.35	0.19	1.37	0.12	1.60	0.15	1.37	0.20	1.42	0.25	1.57	0.21
TOT	78.16		83.63		77.11		83.88		83.35		82.88		85.68		84.16	

Appendix III – Geochemical Equilibrium Modeling Results

The following tables show the solubility of metal hydroxides, oxides, and carbonates as a function of pH calculated from geochemical equilibrium model Visual MINTEQ. The temperature in the calculations was set at 23°C.

Cadmium concentration in leachates with calculated solubilities of various cadmium minerals

versus pH

pH	Cd(OH) ₂	Otavite CdCO ₃ in Carbonated Cement	Otavite CdCO ₃ in Carbonated Geopolymer
4.0	1.450	1.4500	1.4500
4.5	1.450	0.3405	1.4500
5.0	1.450	0.0770	0.3639
5.5	1.450	0.0248	0.0433
6.0	1.450	0.0077	0.0077
6.5	1.450	0.0028	0.0028
7.0	1.450	0.0012	0.0012
7.5	1.450	0.0006	0.0006
8.0	1.450	0.0003	0.0003
8.5	0.685	0.0002	0.0002
9.0	0.064	0.0001	0.0001
9.5	0.007	0.0001	0.0001
10.0	0.001	0.0001	0.0001
10.5	0.000	0.0002	0.0002
11.0	0.000	0.0011	0.0011
11.5	0.000	0.0087	0.0089
12.0	0.000	0.0622	0.0634
12.5	0.000	0.3192	0.3247
13.0	0.001	1.4500	1.4500

Chromium (III) concentration in leachates with calculated solubilities of various chromium (III)

minerals versus pH

pH	Cr(OH) ₃ (am)	Cr ₂ O ₃ (c)
4.0	1.4499	1.4499
4.5	1.4500	1.2002
5.0	0.1095	0.0707
5.5	0.0111	0.0073
6.0	0.0016	0.0010
6.5	0.0004	0.0003
7.0	0.0002	0.0002
7.5	0.0002	0.0001
8.0	0.0002	0.0001
8.5	0.0002	0.0001
9.0	0.0002	0.0001
9.5	0.0002	0.0001
10.0	0.0002	0.0001
10.5	0.0002	0.0001
11.0	0.0003	0.0002
11.5	0.0004	0.0003
12.0	0.0009	0.0006
12.5	0.0026	0.0017
13.0	0.0085	0.0056

Chromium (VI) concentration in leachates with calculated solubilities of various chromium (VI)

minerals versus pH

pH	CrO ₃	Cr(VI) ettringite in non-carbonated cement	Cr(VI) Ettringite in Carbonated cement	CaCrO ₄ in non-carbonated cement	Cr(VI) ettringite in non-carbonated geopolymers	Cr(VI) ettringite in Carbonated geopolymers
4.0	1.4499	1.4499	1.4490	1.4499	1.4490	1.4490
4.5	1.4500	1.4499	1.4490	1.4499	1.4490	1.4490
5.0	1.4500	1.4499	1.4490	1.4499	1.4490	1.4490
5.5	1.4500	1.4499	1.4490	1.4499	1.4490	1.4490
6.0	1.4500	1.4499	1.4490	1.4499	1.4490	1.4490
6.5	1.4500	1.4499	1.4490	1.4499	1.4490	1.4490
7.0	1.4500	1.4499	1.4490	1.4499	1.4490	1.4490
7.5	1.4500	1.4499	1.4490	1.4499	1.4490	1.4490
8.0	1.4500	1.4499	1.4490	1.4499	1.4490	1.4490
8.5	1.4500	1.4499	1.4491	1.4499	1.4490	1.4491
9.0	1.4500	1.4500	1.4490	1.4499	1.4490	1.4490
9.5	1.4500	1.4499	1.4490	1.4499	1.4490	1.4490
10.0	1.4500	1.2793	1.4490	1.4499	1.4490	1.4490
10.5	1.4500	0.5115	1.4490	1.4499	1.4490	1.4490
11.0	1.4500	0.2050	1.4490	1.4499	1.0113	1.4490
11.5	1.4500	0.0831	1.4490	1.4499	0.4131	1.4490
12.0	1.4500	0.0658	1.2597	1.4499	0.1743	1.2098
12.5	1.4501	0.1335	0.9632	1.4499	0.1371	0.9298
13.0	1.4500	0.5869	0.9270	1.4499	0.6000	0.8988

Copper concentration in leachates with calculated solubilities of various copper minerals versus pH

pH	Cu(OH) ₂	CuCO ₃ in carbonated cement	CuCO ₃ in carbonated geopolymer	Malachite Cu ₂ (OH) ₂ CO ₃ in carbonated cement	Malachite Cu ₂ (OH) ₂ CO ₃ in Carbonated geopolymer	Tenorite(am) CuO	Tenorite(c) CuO
4.0	1.4500	1.4500	1.4500	1.4500	1.4500	1.4500	1.4500
4.5	1.4500	1.2031	1.4500	1.4501	1.4500	1.4500	1.4500
5.0	1.4500	0.2950	1.2053	0.3904	0.5804	1.4500	1.4500
5.5	1.4499	0.1073	0.1673	0.0737	0.0741	1.4499	0.6155
6.0	1.4500	0.0462	0.0462	0.0153	0.0152	0.4401	0.0564
6.5	0.3061	0.0288	0.0288	0.0044	0.0044	0.0426	0.0058
7.0	0.0332	0.0236	0.0236	0.0016	0.0016	0.0049	0.0007
7.5	0.0048	0.0223	0.0223	0.0006	0.0006	0.0007	0.0001
8.0	0.0010	0.0234	0.0235	0.0003	0.0003	0.0002	0.0000
8.5	0.0003	0.0319	0.0323	0.0001	0.0001	0.0001	0.0000
9.0	0.0002	0.0975	0.1000	0.0001	0.0001	0.0000	0.0000
9.5	0.0001	0.2844	0.2890	0.0001	0.0001	0.0000	0.0000
10.0	0.0002	0.5677	0.5754	0.0003	0.0003	0.0000	0.0000
10.5	0.0003	1.3772	1.3976	0.0011	0.0012	0.0000	0.0000
11.0	0.0006	1.4500	1.4500	0.0073	0.0074	0.0001	0.0000
11.5	0.0018	1.4500	1.4500	0.0573	0.0586	0.0003	0.0000
12.0	0.0060	1.4500	1.4500	0.3950	0.4029	0.0010	0.0001
12.5	0.0228	1.4501	1.4501	1.4501	1.4501	0.0037	0.0005
13.0	0.1208	1.4500	1.4500	1.4500	1.4500	0.0198	0.0028

Lead concentration in leachates with calculated solubilities of various lead minerals versus pH

pH	Pb(OH) ₂	Cerrusite PbCO ₃ in Carbonated Cement	Cerrusite PbCO ₃ in Carbonated Geopolymer	Hydrocerrusite Pb ₃ (OH) ₂ (CO ₃) ₂ in Carbonated Cement	Litharge PbO	Massicot PbO
4.0	1.4500	0.3339	1.4500	1.4499	1.4500	1.4500
4.5	1.4500	0.0651	0.2628	1.2258	1.4500	1.4500
5.0	1.4500	0.0192	0.0367	0.2938	1.4500	1.4500
5.5	1.4500	0.0061	0.0071	0.0603	1.4500	1.4500
6.0	1.4500	0.0020	0.0020	0.0120	1.4500	1.4500
6.5	1.4499	0.0008	0.0008	0.0028	1.4499	1.4499
7.0	0.2213	0.0004	0.0004	0.0009	1.4500	1.4500
7.5	0.0297	0.0003	0.0003	0.0004	1.4500	1.4500
8.0	0.0057	0.0003	0.0003	0.0002	1.4500	1.4500
8.5	0.0015	0.0003	0.0003	0.0001	1.4499	1.4499
9.0	0.0005	0.0004	0.0004	0.0001	0.8337	1.4500
9.5	0.0003	0.0007	0.0007	0.0001	0.1528	0.3938
10.0	0.0002	0.0023	0.0024	0.0001	0.0719	0.1288
10.5	0.0002	0.0145	0.0149	0.0005	0.0674	0.1088
11.0	0.0003	0.1007	0.1027	0.0030	0.0973	0.1550
11.5	0.0006	0.5316	0.5416	0.0255	0.2044	0.3253
12.0	0.0016	1.4500	1.4500	0.2059	0.5591	0.8902
12.5	0.0049	1.4500	1.4500	1.2397	1.4500	1.4500
13.0	0.0166	1.4500	1.4500	1.4499	1.4501	1.4501

Lead concentration in leachates with calculated solubilities of various lead minerals versus pH

(continued)

pH	Pb ₂ O(OH) ₂	PbO:0.3H ₂ O	Pb ₂ OCO ₃ in Carbonated Cement	Pb ₁₀ (OH) ₆ O(CO ₃) ₆ in Carbonated Cement	Pb ₃ O ₂ CO ₃ in Carbonated Cement
4.0	1.4500	1.4500	1.4500	1.4500	1.4499
4.5	1.4500	1.4500	1.4501	1.4501	1.4500
5.0	1.4500	1.4500	1.4500	1.4500	1.4499
5.5	1.4500	1.4500	1.4500	1.4500	1.4499
6.0	1.4500	1.4500	1.4500	1.4500	1.4499
6.5	1.4499	1.4499	1.4499	1.4499	1.4499
7.0	1.4500	1.4500	0.4011	1.4500	1.4499
7.5	1.4500	1.4500	0.1269	1.4500	0.4089
8.0	1.4500	1.4500	0.0494	1.4500	0.1204
8.5	1.4499	1.4499	0.0223	1.4500	0.0408
9.0	1.4500	1.4500	0.0119	1.2746	0.0163
9.5	0.8012	0.4174	0.0087	1.1779	0.0089
10.0	0.1976	0.1334	0.0114	1.2625	0.0085
10.5	0.1479	0.1116	0.0272	1.4500	0.0150
11.0	0.2074	0.1589	0.0994	1.4500	0.0426
11.5	0.4349	0.3336	0.4232	1.4500	0.1707
12.0	1.1907	0.9129	1.4500	1.4500	0.7576
12.5	1.4500	1.4500	1.4500	1.4500	1.4499
13.0	1.4501	1.4501	1.4500	1.4500	1.4499

Zinc concentration in leachates with calculated solubilities of various zinc minerals versus pH

pH	Zn(OH) ₂ (am)	Zincite ZnO	Hydrozincite Zn ₅ (CO ₃) ₂ (OH) ₆ in Carbonated Cement	Hydrozincite Zn ₅ (CO ₃) ₂ (OH) ₆ in Carbonated Geopolymer	Zn(OH)2 (beta)	Zn(OH)2 (delta)
4.0	1.4500	1.4500	1.4500	1.4500	1.4500	1.4500
4.5	1.4500	1.4500	1.4501	1.4500	1.4500	1.4500
5.0	1.4500	1.4500	1.4500	1.4500	1.4500	1.4500
5.5	1.4500	1.4500	1.4500	1.4500	1.4500	1.4500
6.0	1.4500	1.4500	1.4499	1.4500	1.4500	1.4500
6.5	1.4500	1.4500	0.5083	0.5007	1.4500	1.4500
7.0	1.4500	1.4500	0.0838	0.0825	1.4500	1.4500
7.5	1.4500	0.2484	0.0156	0.0154	0.8843	0.8659
8.0	0.5113	0.0270	0.0035	0.0034	0.0907	0.0889
8.5	0.0977	0.0056	0.0013	0.0013	0.0183	0.0180
9.0	0.0553	0.0032	0.0012	0.0012	0.0105	0.0103
9.5	0.0499	0.0029	0.0021	0.0022	0.0094	0.0093
10.0	0.0499	0.0029	0.0045	0.0045	0.0094	0.0093
10.5	0.0530	0.0031	0.0104	0.0105	0.0100	0.0098
11.0	0.0640	0.0037	0.0289	0.0293	0.0121	0.0119
11.5	0.1013	0.0058	0.1030	0.1046	0.0192	0.0188
12.0	0.2455	0.0141	0.4695	0.4779	0.0464	0.0455
12.5	1.0044	0.0575	1.4501	1.4501	0.1889	0.1852
13.0	1.4500	0.4254	1.4500	1.4500	1.4067	1.3796

Zinc concentration in leachates with calculated solubilities of various zinc minerals versus pH

(continued)

pH	Zn(OH) ₂ (epsilon)	Zn(OH) ₂ (gamma)	ZnCO ₃ in Carbonated Cement	Smithsonite ZnCO ₃ in Carbonated Geopolymer	ZnCO ₃ :1H ₂ O in Carbonated Cement	Zn-Al LDH (s)
4.0	1.4500	1.4500	1.4500	1.4500	1.4500	1.4500
4.5	1.4500	1.4500	1.4501	1.4500	1.4501	1.4500
5.0	1.4500	1.4500	1.2465	1.4500	1.4500	1.4500
5.5	1.4500	1.4500	0.4019	0.5533	1.4065	1.4500
6.0	1.4500	1.4500	0.1249	0.0992	0.4371	1.4499
6.5	1.4500	1.4500	0.0454	0.0361	0.1589	0.1734
7.0	1.4500	1.4500	0.0201	0.0160	0.0703	0.0361
7.5	0.5050	0.8377	0.0104	0.0083	0.0365	0.0137
8.0	0.0534	0.0862	0.0065	0.0052	0.0229	0.0061
8.5	0.0109	0.0174	0.0068	0.0055	0.0237	0.0038
9.0	0.0062	0.0099	0.0186	0.0152	0.0613	0.0046
9.5	0.0056	0.0090	0.0780	0.0657	0.1995	0.0081
10.0	0.0056	0.0090	0.2400	0.2128	0.4800	0.0160
10.5	0.0060	0.0096	0.6327	0.5689	1.2169	0.0339
11.0	0.0072	0.0115	1.4500	1.4500	1.4500	0.0795
11.5	0.0114	0.0182	1.4500	1.4500	1.4500	0.2223
12.0	0.0276	0.0442	1.4500	1.4500	1.4500	0.7850
12.5	0.1123	0.1797	1.4501	1.4501	1.4501	1.4501
13.0	0.8338	1.3378	1.4500	1.4500	1.4500	1.4500

Appendix IV – Strength and Percentage Carbonation Measurements

The following table contains individual unconfined compressive strength and percentage carbonation measurements of the geopolymers and cement-based s/s cubes. The instrument used for unconfined compressive strength measurement was an MTS 311.21 analyzer (MTS Systems Corp., Eden Prairie, MN, USA).

Sample		Cement (MPa)			Geopolymer (MPa)		
		Non-carbonated	Carbonated	% Carbonation	Non-carbonated	Carbonated	% Carbonation
Control	1	54.2	77.4	96.4	50.8	45.7	79.5
	2	63.1	77.5	90.0	50.6	49.1	83.1
	3	54.3	69.3	89.9	53.6	47.1	78.5
	4	63.6	71.8	96.1	54.5	43.3	84.5
Cd	1	50.0	64.0	95.2	54.3	37.2	89.1
	2	55.5	68.8	89.6	54.2	36.9	86.0
	3	51.2	64.3	91.7	54.3	39.9	82.9
	4	56.4	69.3	93.9	54.3	43.6	81.2
Cr (III)	1	47.1	59.2	90.4	43.1	35.9	80.0
	2	51.0	56.9	94.9	41.0	27.7	80.1
	3	44.6	60.8	93.3	41.6	26.6	80.0
	4	52.5	57.5	89.8	31.9	46.6	80.0
Cr (VI)	1	43.9	44.7	94.0	40.9	42.2	86.2
	2	39.3	45.0	93.2	45.1	40.0	79.3
	3	45.4	55.2	89.3	42.4	40.9	78.4
	4	39.8	53.1	88.7	44.0	42.9	85.7
Cu	1	43.6	53.9	96.3	43.0	36.0	84.3
	2	42.2	55.7	91.6	53.6	43.8	85.3
	3	38.2	52.8	94.1	49.8	44.8	87.6
	4	38.8	51.2	90.0	41.2	38.2	82.0
Pb	1	45.2	55.5	92.4	66.1	48.8	87.2
	2	45.9	54.7	92.0	56.2	47.5	87.9
	3	37.8	49.5	95.0	45.5	42.2	87.8
	4	41.9	60.7	97.4	40.6	43.9	79.5
Zn	1	42.0	55.8	88.4	36.8	42.0	81.6
	2	50.2	53.8	96.5	48.8	41.8	84.5
	3	50.6	59.0	95.3	42.7	43.9	88.3
	4	40.6	61.0	87.8	48.9	39.2	88.8